TECHNICAL REPORT 1862
February 2002

Thermal and Nuclear Aspects of the Pd/D_20 System

Volume 2: Simulation of the Electrochemical Cell (ICARUS) Calorimetry

S. Szpak
P. A. Mosier–Boss
Editors

SSC San Diego
San Diego, CA 92152-5001

SSC SAN DIEGO
San Diego, California 92152-5001

P. A. Miller, CAPT, USN
Commanding Officer

R. C. Kolb
Executive Director

ADMINISTRATIVE INFORMATION

The work described in this report was performed for the Office of Naval Research through the collaboration of Space and Naval Warfare Systems Center, San Diego (SSC San Diego); the Naval Air Warfare Center, Weapons Division, China Lake; and the Naval Research Laboratory (NRL).

FOREWORD

The calorimetry of any electrochemical cell involves two type of activities: data collection and data evaluation. The required data are the cell potential–time and cell temperature–time series. The evaluation is based on conservation laws subject to constraints dictated by cell design and the adapted experimental procedure.

Volume 2 of this report deals with the modeling and simulation of the Dewar-type calorimeter. It was written by Professor Fleischmann to provide an authoritative discussion of the calorimetry of electrochemical cells. The emphasis is on the interpretation of data and the accuracy of the determination of the excess enthalpy generation via the appropriate selection of heat transfer coefficients. The discussion of the calorimetry of the Dewar-type cells is presented in the form of technical report for a number of reasons, among them: (i) its length would likely prohibit publication in topical journals, (ii) to clarify misunderstandings regarding the principles of calorimetry as applied to electrochemical cell in general and to the cell employed by Fleischmann and his collaborators, in particular.

S. Szpak and P.A. Mosier–Boss, eds.

TABLE OF CONTENTS

INTRODUCTION

Apart from some fragmentary investigations, primarily related to the study of the self-discharge of batteries, there exists no well defined set of studies in the field of the electrochemical calorimetry. We note that such studies would allow the investigation of the thermal behavior of a wide range of reactions, especially irreversible processes. Thus, the establishment of an accurate model of an experiment is very important. However, as this aspect is not generally understood, we felt it necessary to produce this document.

In spite of its length, this volume only covers the analysis of a data set generated by calculation and one measurement cycle for a "blank experiment." We believe that it is very important to produce a detailed analysis and account (as far as is possible at this stage) of the methodology which we adopted. This is especially important in view of the misleading comments which have been made about the calorimetry of the Pd/D system. Taken at face value, one must believe that the workers concerned do not understand the difference between differential and integral coefficients, the disadvantages of differentiating "noisy" data as compared to integrating such data, the differences between the precision and accuracy of data evaluations, the recognition of "negative" and "positive feedback," the analysis of cooling curves, etc. They do not understand relaxation nor recognize the presence of strange attractors and the way in which the effects of such complications can be circumvented.[1]

It is relevant here to reflect on the precision and accuracy of the experiments. Of course, if the precision is high, then there will be no difficulty in interpreting changes in the rates of excess enthalpy generation as small as 1 mW at the 10 σ

[1] Of course, it is possible that the researchers concerned do not understand any of these matters, but what is so remarkable is that they have failed to understand these topics even when they have been described to them.

level.[2] Of course, the question of the magnitude of the errors raises three further important questions: (i) what error limits are required so as to be able to detect excess enthalpy generation at an adequate level of statistical significance? (ii) what is the difference (if any) between the experiments carried out with ICARUS systems and ICARUS look-alikes and with other types of calorimetry? (iii) how can one assess the error limits of a given piece of instrumentation?

The answer is that one simply stops the development of the methodology when one is able to make an adequate set of measurements. We note here that this particular specification is itself dependent on the physical size of the systems being investigated as well as the chosen operating conditions. In our particular investigation the limit was certainly reached when the errors had been reduced to the 0.01% level. Naturally, the first question impacts on the second and we note that it is the use of less precise and accurate calorimetric methods which has bedeviled so much of the research in this field. The reason is that with the use of less precise/accurate methods, it becomes impossible to monitor the build-up of excess enthalpy generation. This then brings us to the third question and the answer to this is exactly with the methods outlined in this document, at least as far as isoperibolic calorimetry is concerned (although it is not very difficult to specify improvements in those methods!).[3] It is relevant that although errors had undoubtedly been made in setting up these experiments, the detailed data analyses had also shown the way in which such errors could be allowed for.[4]

To reiterate, we considered it necessary to produce this document for the following reasons: Firstly, it is always essential to determine the Instrument Function (or of a parameter or sets of parameters which define the Instrument Function) and to validate the methods of data analysis. Such validation is best done using simulated/calculated data. Secondly, one needs to see the extent to which "blank" experiments conform to expectations. Thirdly, one needs to investigate the ways in which methods of data analysis may fail.

[2]However, the high precision of the instrumentation (relative errors below 0.01%) has been converted into a 10% error by the group at NHE. It is hard to see how anybody can make such an assertion while still keeping a straight face. If the errors were as high as this, then it would be impossible to say anything sensible about calorimetry – for that matter, it would remove one of the main planks of scientific methodology.

[3]The answer to this question brings us to very interesting further lines of enquiry which can be summarized by the question: "why is it that NHE have never made any sets of raw data for blank experiments available for further analysis?" If one considers this question in a naive way, then one would say that there can hardly be any reason for not releasing data sets which do not show any generation of excess enthalpy!

[4]Instead of seeking to establish the correct way(s) of calibrating the systems, the group at NHE used the procedure leading to $(k'^{,0}_R)_{362}$, probably coupled to timing errors in the calibration pulse which they did not allow for. Needless to say, this produced nonsensical results which they used as a justification for substituting an invalid method of data analysis. Moreover, this invalid method of data analysis was applied to just two experiments, regarded as being typical, although the fact that there were malfunctions in these experiments has also been pointed out.

SYMBOLS USED

C – heat capacitance. [J(gMole)$^{-1}$K^{-1}]
$E_c(t)$ – cell voltage at time t. [V]
$E_{th,b}$ – thermoneutral potential at bath temperature. [V]
F – Faraday constant. [coulombs(gMole)^{1}]
ΔH – rate of enthalpy input. [W]
ΔH_{ev} – rate of evaporative cooling. [W]
$\Delta H_{net}(t)$ – rate of net enthalpy input at time t. [W]
k – heat transfer coefficient. [WK^{-4}]
L – latent heat of evaporation. [J(gMole)$^{-1}$]
M – number of moles of D_2O at $t = 0$.
P – vapor pressure at the cell temperature. [bar]
P^* – atmospheric pressure. [bar]
$Q_f(t)$ – rate of generation of excess enthalpy in the cell at time t. [W]
t – time. [s]
α – defined in Eq. (27).
γ – related to time dependence of the (k) coefficient defined in Eq. (20).
λ – defined in Eq. (35).
Λ – defined in Eq. (36).
τ – time. [s]
θ – bath temperature. [K]
$\Delta\theta$ – temperature difference between the cell and the water bath. [K]

SECTION 1: THE EVOLUTION OF THE ICARUS DATA EVALUATION STRATEGIES.

We have in the past used a variety of strategies to evaluate the experimentally determined temperature–time and cell potential–time series. These strategies can be described (at least in part) by the heat transfer coefficients which govern the "Black Box" representing the calorimeters. We will confine attention here to the particular forms of the heat transfer coefficients which were important for the evolution of the data evaluation strategies used with the ICARUS Systems. There is a considerable amount of material which needs to be considered even if we pose this restriction.

The specification of the ICARUS Data Evaluation Strategies [1] (as modified in part in [2]) was based mainly on the analysis of temperature–time and input enthalpy–time series generated by simulations based on the differential equations representing the models of the calorimeters as well as on the evaluation of suitable "blank experiments" (principally using Pt cathodes polarized in 0.1 M $LiOD/D_2O$), compare [3–6]). For the first of these sets of tests, the validity (or otherwise) of the methods used was judged by the recovery of the parameters used in the simulations at adequately high levels of statistical significance. These tests have now been reconstructed and are described in Section 5 where it will be seen that they were sufficient for the specification of the ICARUS data processing strategies (as well as for the specification of some of the shortcomings of the various methodologies).

The validity (or otherwise) of the methods defined in the first set of tests was then further evaluated by using data for "blank experiments." This validity was then assessed principally by investigating the degree of conformity with the predictions based on the first set of tests as well as by the statistical significance of the methodologies; by determining the degree of correspondence of the "true"

and "lower bound" heat transfer coefficients and, related to this, the observation of a "zero" rate of excess enthalpy generation [4]; by checking the relationship between the various forms of the heat transfer coefficient [3–6]; and by determining whether the experimentally observed relaxations of the temperature–time series conform to predictions based on simplified models of the calorimeters [4]. One such set of tests for a "blank" experiment carried out using an ICARUS-2 system is described in Section 6 (but excluding the test of the relaxation behavior). The conclusions drawn from tests such as those described in Sections 5 and 6 are summarized in Section 7, where they are compared with the specifications of the experimental protocols and data evaluation strategies contained in the Handbook for the ICARUS-1 Systems [1].

It is perhaps not surprising that most of this material has never been published. We could not imagine that any paper written on this topic would ever be accepted by a scientific journal and believed that it would be sufficient for us to specify the protocols and data evaluation strategies to be used with the ICARUS Systems [1]. It is the deviation of the NHE group from the recommended protocols and their use of inaccurate and/or invalid methods of data evaluation [7] which makes it necessary to reconsider the background material for the ICARUS-1 systems. Unfortunately, such a reconsideration makes it necessary to give a more closely defined description for some of the heat transfer coefficients than has hitherto been used. This is contained in Section 2. We will use the designation $(k'_R)_{i,j,l}$, where $i = 1, 2, 3$ denotes "differential", "backward integration" and "forward integration" respectively; j is defined in Section 2 and $l = 1, 2$ denotes "lower bound" and "true" respectively. We had hoped to circumvent the need for such an extended description so as to avoid overburdening our accounts with redundant symbolism. Evidently, we were mistaken with our descriptions.

Section 4 describes the method used in the simulations of the data evaluated in Section 5. It will be seen that the first set of tests were incomplete although they were sufficient for the specification of the second set of tests (Section 6) and, in turn, for the specification of the ICARUS protocols and data processing strategies [1].

SECTION 2: DEFINITION OF THE HEAT TRANSFER COEFFICIENTS.

It is convenient to consider the form of the cell temperature–time series generated by the simulation described in Section 3, Fig. 1. As will be shown in that Section, the data have been generated using Eq. (31) in which the heat transfer from the cell is described as being pseudo - conductive while the effects of "negative feedback" are taken into account by writing the input enthalpy as

$$\text{input enthalpy} = (\mathrm{E} - \lambda\Delta\theta)\mathrm{I}, \tag{1}$$

where

$$E = E_c(t = 0) - E_{th,b} \tag{2}$$

and

$$\Delta\theta(t) = \theta(t) - \theta_b. \tag{3}$$

However, in order to prepare the way for the consideration of the "blank experiment", Section 5 as well as the later sections, the heat transfer coefficients are defined by describing the heat transfer as being pseudo-radiative, Eq. (21), giving the "temperature function"

$$f_1(\theta) = [\theta_b + \Delta\theta(t)]^4 - \theta_b^4. \tag{4}$$

For the case of the description of heat transfer being pseudo-conductive, we need to replace the temperature function by $\Delta\theta$,

$$f_1(\theta) = \Delta\theta. \tag{5}$$

We can then define a "lower bound heat transfer coefficient" (i.e., a coefficient which assumes that the rate of excess enthalpy generation is zero) for any part

of the measurement cycle, Fig. 1,

$$(k'_R)_{11} = \frac{[E_c(t) - E_{th,b}]I - \Delta H_{ev}(t) - C_pM(d\Delta\theta/dt)}{f_1(\theta)}. \tag{6}$$

In our early work we evaluated this coefficient just before the start of the calibration pulse and designated this particular value as $(k'_R)_4$ (see [8]), a matter which was evidently not understood [9] although the calculation scheme was set out in Appendix 4 of [8]. The special value of $(k'_R)_{11}$ just before the end of the calibration pulse had originally been designated as $(k'_R)_1$. (Together with $(k'_R)_2$ described below, these were the first two coefficients which we used in the data analysis, hence their designation with the suffixes 1 and 2). It was our investigation of the "Harwell Data Sets" [10] which convinced us that the "lower bound heat transfer coefficient" is more useful than just the two special values $(k'_R)_1$ and $(k'_R)_4$ leading to $(k'_R)_{11}$ as derived in the "ICARUS $(k\prime_R)_{11}$–spreadsheets," see Section 6.

Having obtained $(k'_R)_{11}$, we frequently wish to establish the 11-point averages $(\overline{k'_R})_{11}$ so as to decrease the "noise." This gives us *ca* 26 values for measurement cycles lasting 1 day or, better *ca* 52 values for the recommended 2-day cycles. In turn it is useful to evaluate the 6-point averages of $(\overline{k'_R})_{11}$ which we have designated as $(\overline{\overline{k'_R}})_{11}$. It is not useful to extend this averaging beyond 6 points because any such extension makes the systematic errors (due to the residual decrease of $(k'_R)_{11}$ with time) larger than the random errors, that is, if the systems are behaving sensibly.

It will become apparent that we need accurate values of C_pM to make $(k'_R)_{11}$ generally useful but, if we exclude regions where the temperature is varying rapidly with time, then "guesstimates" of C_pM are quite adequate. We note that if we rearrange Eq.(6) to the straight line form

$$y = mx + c, \tag{7}$$

i.e.,

$$\frac{[E_c(t) - E_{th,b}]I - \Delta H_{ev}(t)}{f_1(\theta)} = \frac{C_pM(d\Delta\theta/dt)}{f_1(\theta)} + (k'_R)_{1,j,1}, \tag{8}$$

then approximate values of C_pM can be obtained from the slopes of the plots derived for regions where the temperature is varying relatively rapidly with time. We can distinguish four such plots which we have designated by the relevant derived heat transfer coefficients: $(k'^{,0}_R)_{151}$, $(k'^{,0}_R)_{161}$, $(k'^{,0}_R)_{171}$ and $(k'^{,0}_R)_{181}$ according to whether the fitting of Eq. (8) is carried at at times somewhat above the origin, at times somewhat above t_1 (the time of application of the calibration pulse), at times somewhat above t_2 (the time of cessation of the calibration pulse) or by the combination of the last two time regions, Fig. 1. However, we

note that there is a measure of ambiguity about the interpretation of the values of$(k'_R)_{1,j,1}$ derived, which will be discussed in Sections 5 and 6.

We note here that separate investigations showed that $(d\Delta\theta(t)/dt)$ is best estimated by using the second order central differences (i.e., the chords of the curves) when using "real" data (i.e., experimental rather than simulated data). More accurate values could be derived in principle by using higher order differences. However, in practice, the repeated differentiation of the experimental data leads to an increase in "noise" if we use differences higher than the second order. This use of the central difference is of some importance when we consider the integration processes required for the derivation of the heat transfer coefficients based on the forward integration of the experimental data (see below).

We note also that objections have often been raised to the procedures which we have adopted based on the fact that we have not "binned the data," i.e., we have not signal averaged before the data analysis. However, "binning of the data" must always be approached with great caution: one should only "bin data" or "bin coefficients" if these data or coefficients can be expected to be constant over the averaging interval. This is not the case for $(k'_R)_{11}$ unless the effects of the term $C_pM(d\Delta\theta(t)/dt)$ have been taken into account. Once this is done, we can, of course, bin the data as we have done in deriving $(\overline{k'_R})_{11}$ and $(\overline{\overline{k'_R}})_{11}$.

In the case of the interpretation of data derived with calorimeters relying on radiative cooling, the position is further complicated by the fact that the differential equation representing the calorimeters, Eq. (20), is both nonlinear and inhomogeneous. It does not follow therefore that coefficients derived by averaging the data are the same as averages of the coefficients derived by using the raw data. However, we did confirm in 1992 (when this whole saga was first investigated) that we do in fact obtain an equivalence, provided we restrict attention to regions where $(d\Delta\theta(t)/dt)$ is adequately small. We concluded that in such regions the differential Eq. (20) could be sufficiently linearized and that second order small differences were sufficiently small to allow such averaging. However, as the values of $(\overline{k'_R})_{11}$ obtained in this way were identical to those obtained following the procedure outlined above, there was evidently no justification in pursuing the matter further (nor to complicate the instrumentation!).

We will refer to the averaging procedures further below when discussing the heat transfer coefficients based on the forward and backward integration procedures. It is next necessary to evaluate the "true heat transfer coefficients." The value $(k'_R)_2$ near the end of the calibration period is obtained by including the calibration pulse, ΔQ:

$$(k'_R)_2 = \frac{\Delta Q + [E_c(\Delta\theta_2, t_2) - E_c(\Delta\theta_1, t_1]I - \Delta H_{ev}(\Delta\theta_2, t_2) + \Delta H_{ev}(\Delta\theta_1, t_1)}{f_2(\theta)}$$

$$- \frac{C_p M[(d\Delta\theta/dt)_{\Delta\theta_{2,t_2}} - d(\Delta\theta/dt)_{\Delta\theta_{1,t_2}}]}{f_2(\theta)}, \tag{9}$$

where we now have

$$f_2(\theta) = [\theta_b + (\Delta\theta_{2,t_2})]^4 - [\theta_b + (\Delta\theta_{1,t_2}]^4. \tag{10}$$

In order to carry out this evaluation, it is useful to construct A4– or A3– sized plots (European notation); see Sections 5 and 6, and then to obtain appropriate averages using a transparent ruler. This type of analysis used to be a generally accepted approach but then fell into disrepute. However, it is now again accepted as giving so-called "robust estimates."

We note that the errors in $(k'_R)_2$ are measures of the accuracy of the "true heat transfer coefficient" as the estimate is made in terms of the known Joule enthalpy input to the calibration heater. Errors in $(k'_R)_1$ or $(k'_R)_{11}$ are measures of the precision of the "lower bound heat transfer coefficients" as there is no independent calibration and there may be excess enthalpy generation in the system. It is important that $(k'_R)_{11}$ and $(k'_R)_2$ are the least precise and least accurate coefficients, which can be obtained from the raw data.[5]

We have always insisted that the construction and evaluation of plots of the raw data is an essential prerequisite of the more elaborate data evaluation procedures. For one thing, it shows whether the "noise levels" in the experiments were sufficiently low to justify more detailed evaluations and also points to malfunctions in the operation of the experiments. It is very important therefore to establish whether the group at NHE ever followed this particular instruction and, if they did, what conclusions they may have drawn from any such plots.

Having obtained the "true heat transfer coefficient" at a single point (usually near the end of the calibration pulse), it is important to ask: "what is the true heat transfer coefficient $(k'_R)_{12}$ at any other time?" We can make such an evaluation within the duration $t_1 < t < t_2$ of the calibration pulse simply by using Eq. (9), giving $(k'_R)_{12}$ rather than $(k'_R)_2$. Note also that Eq. (9) can be rearranged to the straight line form

[5] Any statements that the errors are larger than this (as has been made, for example, in the paper from the group at NHE [7]) simply show that mistakes have been made in the data analysis procedures and/or the execution of the experiments.

$$\frac{\Delta Q + [E_c(\Delta\theta_2, t) - E_c(\Delta\theta_1, t)]I - \Delta H_{ev}(\Delta\theta_2, t) + \Delta H_{ev}(\Delta\theta_1, t)}{f_2(\theta)}$$

$$= \frac{C_p M[(d\Delta\theta/dt)_{\Delta\theta_{2,t}} - (d\Delta\theta/dt)_{\Delta\theta_{1,t}}]}{f_2(\theta)} + (k'^{,0}_R)_{162}, \qquad (11)$$

which is applicable to times close to and above t_1. It is evident, therefore, that such data derived from the experiments can also be used to obtain estimates of C_pM, but the accuracy of such values is inevitably much lower than of those obtained by the application of the corresponding expression for the "lower bound heat transfer coefficient," $(k'^{,0}_R)_{161}$, Eq. (8). Nevertheless, Eq. (11) is useful because it allows the removal of the effects of the water equivalent on the "true heat transfer coefficient," $(k'^{,0}_R)_{162}$, simply by extrapolating to zero value of the abscissa.

In the regions in which there is no application of the heater pulse, i.e., for $0 < t < t_1$ and $t_2 < t < T$, the "true heat transfer coefficient" can only be obtained from the "heating" and "cooling curves," i.e., the "driving force" is the change in the enthalpy content of the calorimeters rather than ΔQ. It is now sensible to cast Eq. (9) in the form

$$\frac{C_p M[(d\Delta\theta/dt)_{\Delta\theta_{2,t}} - (d\Delta\theta/dt)_{\Delta\theta_{1,t}}]}{f_2(\theta)} = -(k'^{,0}_R)_{152}$$

$$+ \frac{[E_c(\Delta\theta_2, t) - E_c(\Delta\theta_1, t)]I - \Delta H_{ev}(\Delta\theta_2, t) + \Delta H_{ev}(\Delta\theta_1, t)}{f_2(\theta)}. \qquad (12)$$

If the system is functioning correctly, then it will be found that the L.H.S. of Eq. (12) is essentially constant (although this constancy can only be probed over a short time range). The second term on the R.H.S. of Eq. (12) will be much smaller than the term on the L.H.S., i.e., it is in the nature of a correction term to give the "point-by-point" values of $(k'^{,0}_R)_{152}$ or $(k'^{,0}_R)_{172}$. It will be evident that the accuracy of these versions of the "true heat transfer coefficient" is limited by the accuracy of our estimates of C_pM. This particular part of the methodology is therefore only useful to serve as a check on the operation of the cells and methods of data evaluation.[6] The importance of Eqs. (11) and (12) lies partly in the fact that these equations lead to the interpretation of what we have classified as Cases 1 and 2 of the phenomenon of "Heat after Death"[3] (and to other related versions of these Cases).

The assumption underlying this part of the account is that we can only determine $(k'_R)_{12}$ within the duration of application of the calibration pulse,

[6]It is not possible to combine the data in the regions just above t_1 and t_2 to give a simple equation leading to $(k'^{,0}_R)_{182}$, at least we should say that we have not been able to specify a simple data processing strategy!

$t_1 < t < t_2$, Fig 1, and at lower accuracy, $(k'^{,0}_R)_{152}$ and $(k'^{,0}_R)_{172}$, in regions adjacent to the origin and for times adjacent and above t_2. However, this conclusion is incorrect. We need to make the additional assumption that the rate of any excess enthalpy generation is constant during any particular calibration period in order to determine $(k'_R)_{12}$. This means that we can only obtain a single value of this heat transfer coefficient per calibration period and, consequently, a single value of $(k'_R)_{12} - (k'_R)_{11}$. Two important points follow from this conclusion. In the first place, the precision of $(k'_R)_{12}$ must be very nearly equal to the precision of $(k'_R)_{11}$ (this is discussed further in Section 6). Secondly, if we extend the assumption that the rate of excess enthalpy generation is constant during the period $t_1 < t < t_2$ to saying that it is constant during the period $0 < t < T$, then it is immediately possible to derive $(k'_R)_{12}$ over the whole of the measurement cycle. The values obtained can be compared to the special values of $(k'^{,0}_R)_{152}$ and $(k'^{,0}_R)_{172}$ in the relevant time regions.

Having obtained the local (differential) values of the "lower bound" and "true heat transfer coefficient," we naturally cast around for methods which would increase their precision and accuracy. The reason for the limited precision and accuracy is mainly due to the need to differentiate the noisy experimental data sets. In our early work, we overcame this particular difficulty by using $(k'_R)_4$ and $(k'_R)_2$ as starting values for the nonlinear regression procedure leading to the heat transfer coefficient $(k'_R)_5$. Here, we fitted the numerical integrals of the differential equation governing the behavior of the calorimeters to the data sets for complete measurements cycles. The relative errors in $(k'_R)_5$ which we could achieve in this way were below 0.1%, even when using the unsatisfactory early version of our calorimeters (i.e., those not silvered in their top portions).

The use of nonlinear regression procedure had the further distinct advantage that we could adjust the integration interval in regions where the temperature was varying rapidly with time so as to achieve the required accuracy in the integrals. This is not possible for the methods which we will discuss below (and which were part of the ICARUS data processing strategy) because the intervals for the data acquisition were fixed. As a matter of fact, the interval 300 s was chosen because such an interval does not degrade the evaluation of any of the series $(k'_R)_{21}$, $(k'_R)_{22}$, $(k'^{,0}_R)_{251}$, $(k'^{,0}_R)_{252}$, $(k'^{,0}_R)_{261}$, $(k'^{,0}_R)_{262}$, $(k'^{,0}_R)_{271}$, and $(k'^{,0}_R)_{272}$. However, it does degrade the evaluation of $(k'_R)_{31}$, $(k'^{,0}_R)_{351}$, $(k'^{,0_R})_{361}$, and $(k'^{,0}_R)_{371}$ to some extent, and leads to a marked degradation of $(k'_R)_{32}$, $(k'^{,0}_R)_{352}$, $(k'^{,0}_R)_{362}$, and $(k'^{,0}_R)_{372}$. The fact that the data acquisition interval was too long for straightforward estimations of the $(k'_R)_{3,j,l}$ series of heat transfer coefficients was already pointed out to NHE in the ICARUS-1 Handbook [1]. These matters will be considered further in Sections 5 and 6.

We have pointed out on other occasions that the reason we opted for using nonlinear regression fitting in our early work was because the pressure of events

did not allow us to go through the logical sequence of using linear regression, multilinear regression and nonlinear regression (in fact, we had to opt for a "catch–all" methodology). However, as we could not make nonlinear regression "user friendly" with the computing power then available to us, so in 1991–92, we investigated the application of linear regression, which became part and parcel of the ICARUS-1 methodology.[7]

Attention has been drawn to some of these details because it would certainly be possible to reimplement parts of these projects provided one could gain access to the data sets. If one wishes to avoid the numerical differentiation of the experimental data sets, then one can rely instead on the numerical integrations of these data and compare these to the integrals of the differential equation representing the model of the calorimeters. For the backward integrals starting from the end of the measurement cycles at $t = T$, we obtain

$$(k'_R)_{21} = \frac{\int_T^t \Delta H_{net}(\tau)d\tau}{\int_T^t f_1(\theta)d\tau} - \frac{C_p M[\Delta\theta(t) - \Delta\theta(T)]}{\int_T^t f_1(\theta)d\tau} \tag{13}$$

while the corresponding equation for forward integration from the start of the measurement cycle is

$$(k'_R)_{32} = \frac{\int_0^t \Delta H_{net}(\tau)d\tau}{\int_0^t f_1(\theta)d\tau} - \frac{C_p M[\Delta\theta(t) - \Delta\theta(0)]}{\int_0^t f_1(\theta)d\tau}. \tag{14}$$

Here, the suffices 21 and 31 denote respectively "backward integration, lower bound" and "forward integration, lower bound." $(k'_R)_{21}$ and $(k'_R)_{31}$ are the corresponding integral heat transfer coefficients defined at the time t.

We note here that care is needed when integrating the term [net enthalpy input, $\Delta H_{net}(\tau)$] around the discontinuities at $t = t_1$ and $t = t_2$. This is a matter which will be considered further in Sections 5 and 6. In our work we have at various times used the trapezium rule, Simpson's rule, or the mid-point rule to carry out the integrations. Of these rules, only the mid-point rule is strictly

[7]While dealing with these "historical aspects," we note also that in 1990-92 we investigated the use of Kalman filtering (leading to an heat transfer coefficient labelled as $(k'_R)_6$ and we also investigated the use of other filtering methods. Some of this was rather promising especially that designed to extract information about "positive feedback," but these projects had to be abandoned. As part of these projects we also investigated the use of averaging techniques other than the "square-box" version, which gives $(\overline{k'_R})_{11}$ from $k'_R)_{11}$ and $(\overline{\overline{k'_R}})_{11}$ from $(\overline{k'_R})_{11}$. These projects were also promising, but again had to be abandoned. Finally, in 1994, the change of the ICARUS systems to hardware based switching was investigated with a view to allowing changes in the data acquisition intervals (thereby putting the $(k'_R)_{3,j,l}$ strategies on a sounder basis). However, these switching systems were not incorporated in the ICARUS–2 systems.

speaking correct in that it agrees with the mathematical definition of an integral. It is quite generally assumed that integrations carried out using the trapezium or Simpson's rule will converge onto the "correct" algebraic result if the integration interval is made adequately small, but this does not necessarily follow. It is a matter which needs to be investigated for each particular case.

The merits of the particular integration procedures coupled to the adequacy of the chosen integration interval is revealed more clearly when we come to the use of Eqs. (13) and (14) to determine C_pM and to carry out extrapolations to remove the effects of the second term on the R.H.S. of Eqs. (13) and (14) on the corresponding heat transfer coefficients. We will follow here the procedure laid down in the ICARUS-1 Handbook [1] where the integrations were restricted to the region of application of the heater calibration pulse. For backward integration, we obtain

$$\frac{\int_{t_2}^{t} \Delta H_{net}(\tau)d\tau}{\int_{t_2}^{t} f_1(\theta)d\tau} = \frac{C_pM[\Delta\theta(t) - \Delta\theta(t_2)]}{\int_{t_2}^{t} f_1(\theta)d\tau} + (k_R^{\prime,0})_{261} \tag{15}$$

while for the forward integration we have

$$\frac{\int_{t_1}^{t} \Delta H_{net}(\tau)d\tau}{\int_{t_1}^{t} f_1(\theta)d\tau} = \frac{C_pM[\Delta\theta(t) - \Delta\theta(t_2)}{\int_{t_1}^{t} f_1(\theta)d\tau} + (k_R^{\prime,0})_{361}. \tag{16}$$

It will be seen in Sections 5 and 6 (more especially in Section 6) that Eq. (15) can be used to derive accurate values of C_pM while there is some minor degradation when using the forward integration, Eq. (16). The application of Eq. (15) to the data sets was the "target methodology" of the ICARUS systems and the derived "lower bound heat transfer coefficient," $(k_R^{\prime,0})_{261}$ was described as $(k_R^{\prime})_{21}$ in the Handbook [1] and the associated correspondence. The same types of equation may be used to derive $(k_R^{\prime,0})_{251}$, $(k_R^{\prime,0})_{271}$, and $(k_R^{\prime,0})_{281}$ as well as $(k_R^{\prime,0})_{351}$, $(k_R^{\prime,0})_{371}$, and $(k_R^{\prime,0})_{381}$; it is only necessary to start the interpretation from the appropriate times, which also give the starting values of θ for the R.H.S. of the relevant equations. Of these sets of estimates, that leading to $(k_R^{\prime,0})_{281}$ is especially useful and this particular fit also gives a good estimate of C_pM.

In order to obtain the "true heat transfer coefficients" it is necessary to combine the integrals of the enthalpy inputs in Eqs. (15) and (16) with thermal balances made at one or a series of points.[8] We will confine attention here to the procedure originally suggested in the Handbook for the ICARUS-1 system[1]. We make a

[8]This can be done in a number of ways and it is important that this part of the evaluation was changed during the summer of 1994 following the receipt of the first two sets of data collected by NHE.

thermal balance just before the application of the calibration pulse and, if the system has relaxed adequately and, if $d\theta/dt = 0$, then if we consider $(k'_R)_{32}$,

$$0 = [\Delta H_{net}(t_1)][t - t_1] + Q_f[t - t_1] - (k'_R)_{32}[(\theta_b + \Delta\theta(t_1))^4 - \theta_b^4][t - t_1] \quad (17)$$

Combination with Eq. (14) eliminates the unknown rate of excess enthalpy generation, Q_f. We obtain

$$(k'_R)_{32} = \frac{\int_{t_1}^{t} \Delta H_{net}(\tau)d\tau - [\Delta H_{net}(t_1)][t - t_1]}{\int_{t_1}^{t} f_2(\theta)d\tau} - \frac{C_pM[\Delta\theta(t) - \Delta\theta(t_1)]}{\int_{t_1}^{t} f_2(\theta)d\tau}. \quad (18)$$

The corresponding equation for $(k'_R)_{22}$ follows from Eq. (18) on replacing t_1 by t_2.[9]

The corresponding equation for $(k'_R)_{22}$, based on the backward integration of the data sets, follows from Eq. (18) on replacing t_1 by t_2. It is also convenient to rewrite the derived equation in the straight line form:

$$\frac{\int_{t_2}^{t} \Delta H_{net}(\tau)d\tau - [\Delta H_{net}(t_2)][t - t_2]}{\int_{t_2}^{t} f_2(\theta)d\tau} = \frac{C_pM[\Delta\theta(t) - \Delta\theta(t_2)]}{\int_{t_2}^{t} f_2(\theta)d\tau} + (k'^{,0}_R)_{262}. \quad (19)$$

$(k'^{,0}_R)_{262}$ was the version of $(k'_R)_{22}$, which we used in our investigations prior to the construction of the ICARUS-1 system. As we did not want to discuss the differences between these two versions, we also labelled $(k'^{,0}_R)_{262}$ with the suffices 22. It should be noted that Eq. (19) is soundly based (in a mathematical sense) in that the extrapolation to $[\Delta\theta(t) - \Delta\theta(t_2)] = 0$ gives the value of $(k'^{,0}_R)_{262}$ at a well defined time, $t = t_2$. This extrapolation automatically removes the effect of the term $C_pM[(\theta(t) - \theta(t_2)]/\int_{t_2}^{t} f_2(\theta)d\tau$ on the heat transfer coefficient. This was one objective for our methodology because C_pM is the, least accurate parameter in the analysis; the application of Eq. (19) to the data sets was the "target methodology" for evaluating the "true heat transfer coefficients."

While it is also possible to write Eq. (18) in the form (19) to give $(k'^{,0}_R)_{362}$, this method of analysis is not useful as the range of the extrapolation required is too long as will be shown in Sections 5 and 6. For this reason we recommended in the Handbook [1] that $(k'_R)_{32}$ be evaluated at times close to $t = t_2$ using Eq. (18). However, in view of the errors in the determination of C_pM, these values of $(k'_R)_{32}$ are inevitably less accurate than those of $(k'^{,0}_R)_{262}$.

[9]We note that NHE did not follow the instruction in the ICARUS-1 Handbook [1] to use 2-day measurement cycles and, for the reduced time scales of 1-day cycles in particular, it is necessary to include the term $C_pM(d\Delta\theta/dt)$ in the thermal balances, Eq. (17). However, NHE continued to use the original form of the equation. They also did not follow the instruction to evaluate $(k'_R)_{32}$ at times close to t_2.

We note here also that one must be somewhat careful in carrying out the required linear regression fitting procedures, a matter which is considered further in Sections 5 and 6.

SECTION 3: DIFFERENTIAL EQUATIONS GOVERNING THE BEHAVIOR OF THE CALORIMETERS: SIMULATIONS OF THE TEMPERATURE–TIME SERIES.

It has been established that at low to intermediate cell temperatures (say, $30 < \theta < 80^0C$) the behavior of the calorimeters is modelled adequately by the differential equation

$$C_pM(d\Delta\theta/dt) = [E_c(t) - E_{th,b}]I + Q_f(t) + [\Delta QH(t-t_1) - \Delta QH(t-t_2)]$$
$$-(3I/4F)\left[(P/P^* - P)\right]\left[(C_{p,D_2O,g} - C_{p,D_2O,l})\Delta\theta + L\right]$$
$$-(k_R^0)\theta_b^3\left[1-\gamma t\right]\left[f_1(\theta)/\theta_b^3 + 4\phi\Delta\theta\right]. \qquad (20)$$

With the calorimeters used in the ICARUS-type investigations, the conductive contribution to heat transfer is small. We have therefore assumed that this term can be "lumped" into the radiative term by allowing a small increase in the radiative heat transfer coefficient:

$$\text{radiative heat transfer} = (k_R'^{,0})\left[1-\gamma t\right]\left[(\theta_b + \Delta\theta)^4 - \theta_b^4\right]. \qquad (21)$$

If the time dependence of the heat transfer coefficient is not included explicitly in this equation, then

$$\text{radiative heat transfer} = (\mathrm{k_R'})[(\theta_\mathrm{b} + \Delta\theta)^4 - \theta_\mathrm{b}]^4], \qquad (22)$$

where the radiative heat transfer coefficient (k_R') now shows a weak time dependence.

In calculating the rate of enthalpy removal by the gas stream,

$$(3I/4F)[P/(P^* - P)][(C_{p,D_2O,g} - C_{p,D_2O,l})\Delta\theta + L], \qquad (23)$$

we have always assumed that the partial pressure of D_2O (or H_2O) in this gas stream can be calculated using the Clausius-Clapeyron equation with the

latent heat of evaporation, L, being that at the boiling point. Evaporative cooling only becomes a major term at temperatures close to the boiling point (say, at $\Delta\theta > 70^0C$) where these two assumptions are justified. At low to intermediate temperatures, $\Delta H_{ev}(t)$ is a minor correction term so that errors due to the two assumptions introduce second order small quantities (for a further approximation, see below).

In carrying out simulations to be analyzed by the methods outlined in Section 2, we have further usually assumed that the rate of excess enthalpy generation is zero,

$$Q_f(t) = 0, \tag{24}$$

and that the radiative heat transfer term can be linearized: rate of heat transfer,

$$4(k'_R)\theta_b^3\Delta\theta = (k'_c)\Delta\theta, \tag{25}$$

i.e., that the heat transfer is now pseudo-conductive. This is an assumption which we also used (with several restrictions) in our original investigation [8]. We note here that the heat transfer coefficients for the Dewar cells used at that time were up to twice those which are calculated from the Stefan-Boltzmann coefficient and the radiative surface area so that we had to assume that the conductive contribution was appreciable. We attributed this conductive contribution to conduction across the nominal vacuum gap due to inadequate evacuation/baking of the Dewars. It was therefore not clear whether the heat transfer term should be described as being pseudo-radiative or pseudo-conductive and the experiments had to be carried out in such a way that the errors due to the limiting assumptions were below those of the experiment. In our later work (including that carried out with the ICARUS systems), we ensured that the vacuum in the Dewars was sufficiently hard so that the radiative heat transfer coefficient was now given by the product of the Stefan-Boltzmann coefficient and the radiative surface area. However, it is evident that the vacuum in some of the cells used in the NHE investigations had become rather soft.

The correct description of heat transfer from the cell is a matter which requires further investigation. While the limiting assumptions introduce small errors, we can ensure that these errors are less than those due to the experiment. It is therefore better to use these assumptions rather than to attempt to separate this term into the radiative and conductive contributions. However, a better approach might well be that we should calculate the radiative term and then derive the conductive contribution from the calibrations [3]. This would ensure that we do not introduce an additional parameter into the modeling of the cells. It should be noted that such a methodology would automatically ensure the linearization of Eq. (20). In carrying out such modified procedures, we should weight the radiative contribution appropriately (say 95% of the total) rather than using the 50:50 split of the original analysis [3].

The use of the descriptions and assumptions outlined above gives us the differential equation

$$C_p M^0 (d\Delta\theta/dt) = [E_c(t) - E_{th,b}]I + Q_f(t) + \Delta QH(t - t_1) - \Delta QH(t - t_2) -$$
$$\Delta H_{ev}(t) - (k'^0_R)[1 - \gamma t][(\theta_b + \Delta\theta)^4 - \theta_b^4]. \quad (26)$$

In order to calculate the $\Delta\theta - t$ series we have to deal with a further difficulty in that the function $E_c(t)$ is unknown. However, it is evident from the experimental $\Delta\theta(t) - t$ and $E_c(t) - t$ series that we can always observe "negative feedback," i.e., that E_c decreases with $\Delta\theta$. If we assume that this is the only cause of the variation of E_c with t, then

$$E_c(t) = E_c(0) - \alpha(\Delta\theta - \Delta\theta^0) = E'_c - \alpha\Delta\theta \quad (27)$$

(i.e., we neglect any variation of the activation overpotentials with time) and

$$C_p M (d\Delta\theta/dt) = [E'_c - E_{th,b} - \alpha\Delta\theta]I + Q_f(t) + [\Delta QH(t - t_1) - \Delta QH(t - t_2)]$$
$$-\Delta H_{ev}(t) - (k'^0_R)(1 - \gamma t)[(\theta_b + \Delta\theta_b)^4 - \theta_b^4]. \quad (28)$$

It was not clear during 1991-92 whether we should change our data processing strategy to that later incorporated into the ICARUS systems or whether we should continue to use nonlinear regression fitting. At that time, we therefore investigated further the possibility of obtaining an analytic solution of Eq. (27) so as to speed up the latter procedure. Such a solution was derived and it was shown that the numerical integration of Eq. (28) agreed with this solution to better than 0.1%, the target figure for our data analyses (these solutions required the assumption $Q_f(t) =$ constant, which is in any event necessary so as to achieve calibrations of the systems). We believe that the residual discrepancy is due to deficiencies in the numerical techniques, i.e., that the analytic solutions are exact. This program of work was discontinued when it became clear that satisfactory data analysis could be achieved by using linear regression procedures. However, it may well be that this particular aspect of the data analysis procedures should be restarted if we wish to develop a general investigation of existing data sets.

At that time, we also investigated the application of various data evaluation procedures to simulated data sets. Attention was confined to linearized versions of Eq. (28) with the additional assumptions,

$$Q_f(t) = 0 \quad (29)$$

$$\Delta H_{ev}(t) = 0, \quad (30)$$

giving the equation,

$$C_pM(d\Delta\theta/dt) = E_c'I + [\Delta QH(t-t_1) - \Delta QH(t-t_2)]$$
$$-(k_c'^{,0})[1-\gamma t]\Delta\theta - \alpha I\Delta\theta. \quad (31)$$

With the additional assumption that the pseudo-conductive heat transfer coefficient is independent of time we have

$$C_pM(d\Delta\theta/dt) = E_c'I + [\Delta QH(t-t_1) - \Delta QH(t-t_2)] - (k_c'^{,0} + \alpha I)\Delta\theta. \quad (32)$$

Parts of these investigations have now been repeated. The integrations of (32) follow immediately. For the initial condition

$$\Delta\theta = \Delta\theta_i, \quad t = 0, \quad (33)$$

we obtain

$$\Delta\theta = \Delta\theta_i e^{-\lambda t} + \Lambda_1(1 - e^{-\lambda t}) \quad (34)$$

where

$$\lambda = (k_c'^{,0} + \alpha I)/C_pM \quad (35)$$

and

$$\Lambda_1 = E_c'/(k_c'^{,0} + \alpha I) \quad (36)$$

i.e., in the region $0 < t < t_1$. We assume

$$C_pM^0 = 330JK^{-1} \quad (37)$$

$$k_c'^{,0} = 0.073WK^{-1} \quad (38)$$

$$\gamma I = 0.007WK^{-1} \quad (39)$$

$$\Delta\theta_i = 11.75^0C \quad (40)$$

$$E'I = \gamma I\Delta\theta_i = 1W. \quad (41)$$

With the exception of the rather low value of $\Delta\theta_i$, these parameters are close to those which we would derive for the blank experiment discussed in Section 6. The reason why $\Delta\theta_i$ has been set artificially low is so as to allow an examination of the region close to $t = 0$. With (36) through (40), we obtain from Eq. (34)

$$\Delta\theta = 13.528125 - 1.778125e^{[-0.000(24.)t]} \quad (42)$$

while the enthalpy input is given by

$$\text{input enthalpy} = 0.987553 + 0.012447\text{exp}[-0.000(24.)\text{t}]. \quad (43)$$

Here (24.) denotes the recurrence of the number group 24.

We next use (41) to give the value of $\Delta\theta_1$ at $t = t_1 = 43{,}200$s

$$\Delta\theta_1 = 13.528075^0C \; at \; t = 43,200s. \tag{44}$$

This value is adequately close to 13.528125^0C, which applies to complete thermal relaxation. We use this value together with

$$\Delta Q = 0.2W, \quad t_1 < t < t_2 \tag{45}$$

for the next step of the integration. With

$$\Lambda_2 = (E_c' I + \Delta Q)/(k_c'^{,0} + \alpha I) \tag{46}$$

$$\begin{aligned} \Delta\theta &= \Delta\theta_1 e^{-\lambda(t-t_1)} + \Lambda_2[1 - e^{-\lambda(t-t_1)}] \\ &= 16.028125 - 2.500050e^{[-0.000(24.)(t-t_1)]}. \end{aligned} \tag{47}$$

and

$$\text{input enthalpy} = 0.970053 + 0.017500\text{e}^{[-0.000(24.)(\text{t}-\text{t}_1)]} \tag{48}$$

Equation (47) can be used in turn to derive

$$\Delta\theta_2 = 16.028049^0C \quad at \quad (t_2 - t_1) = 42,900s, \tag{49}$$

which is used as the initial value for the final step in the integration. We obtain

$$\begin{aligned} \Delta\theta &= \Delta\theta_2 e^{-\lambda(t-t_2)} + \Lambda_1[1 - e^{-\lambda(t-t_2)}] \\ &= 13.528125 + 2.499924e^{[-0{,}000(24.)(t-t_2)]} \end{aligned} \tag{50}$$

and

$$\text{input enthalpy} = 0.987553 - 0.017499\text{e}^{[-0.000(24.)(\text{t}-\text{t}_2)]}. \tag{51}$$

The "raw data" calculated using Eqs. (42), (43), (47), (48), (50), and (51) are given in the ICARUS $(k_c'^{,0})_{11}$ spreadsheet, spreadsheet 1. These data are analyzed in Section 5 using the methodologies outlined in Section 3. It will be seen that simulations of this kind are adequate for demonstrating the advantages and shortcomings of the various possible methods. It will also be clear that such simulations are deficient in several important respects. In the first place the residual time dependence of the heat transfer coefficient has not been taken into account. However, it was confirmed in 1992 that a data set generated with approximate solutions which include this effect does indeed generate the key features observed when using "real experimental data," see Section 6. We note here that data sets have never yet been generated using the full analytic solution described above. Secondly, the effects of "noise" having defined characteristics (i.e., defined power spectral densities as well as the effects of quantization of the

measurements) on the methods of data evaluation has never yet been investigated. Instead, we have relied on a comparison of the analysis of simulated data, Section 5, with those for "blank" experiments, Section 6. If the question of the effects of "noise" ever becomes an important issue, then we would suggest that the "noise" characteristics of $E_c(t)$ and $\Delta\theta(t)$ be first determined and that data be then generated using the full analytic solution with addition of the correct "noise" characteristics.

SECTION 4: SPECIFICATION OF THE ICARUS–1 EXPERIMENTAL PROTOCOLS AND DATA EVALUATION PROCEDURES.

Before dealing with the analysis of the simulated data, Section 5, and the analysis of data for a "blank" experiment, Section 6, we will outline the experimental protocols and data evaluation strategies specified for experiments with the ICARUS systems. The key elements were as follows:

(i) the measurement cycles should be lengthened to 48 hours. Following the replenishment of the D_2O (or H_2O) in the cells to make up for losses due to electrolysis, the relaxation of the systems was to be followed for 12 hours followed by the application of a Joule heating pulse for a further 12 hours (when this calibration was required) in turn followed by a final relaxation for a further 24-hour period.

(ii) the protocols were to be:
(a) two measurement cycles without calibration pulses;
(b) ten measurement cycles with calibration pulses;
(c) two measurement cycles without calibration pulses;
(d) ten measurement cycles with calibration pulses.

It will be seen that a total experiment duration of 48 days was specified;

(iii) several "blank experiments" were to be carried out (at least one for each cell in use; the use of Pt cathodes in 0.1M $LiOD/D_2O$ was recommended). The protocol **(ii)** was to be followed.

(iv) the execution of the "blank experiments" was to be followed by experiments using cathodes made of Johnson Matthey Material Type A. The protocol **(ii)**

was again to be followed;

(v) the first step in the data evaluation was to be the plotting of A3- or A4-sized graphs of the raw data. The heat transfer coefficients $(k'_R)_1$ and $(k'_R)_2$ were to be derived for each measurement cycle.

(vi) the next step was to be the construction of $(k'_R)_{11}$–type spreadsheets coupled to the determination and interpretation of $(k'_R)_{11}$, $(\overline{k'_R})_{11}$ and $(\overline{\overline{k'_R}})_{11}$. The further evaluation of these spreadsheets was not specified in 1993; this was a matter which was to be decided by a collaborative program between NHE and IMRA Europe.

(vii) after the execution of **(vi)**, the $(k'_R)_{21}$-type spreadsheets were to be prepared and values of $(k'^{,0}_R)_{261}$ and $(k'^{,0}_R)_{361}$ and the associated values of C_pM were to be determined. These values of C_pM were to be used both to correct the evaluations in **(vi)** and to determine the "true" heat transfer coefficients $(k'_R)_{32}$ at times close to the end of the calibration period, $t = t_2$;

(viii) it was envisaged that, following the completion of this initial stage of the investigation, the ICARUS program would move on to the examination of materials variables as well as the production of ICARUS-2. This second part was intended to deal with the effects of increasing the current density, the analysis of data close to the boiling point (including the boiling episodes), and "Heat after Death."

After the receipt of the data for the first set of experiments carried out in the NHE Laboratories, it became apparent that there were timing errors in the ICARUS-1 system installed in Sapporo [1]. The most self–evident error was in the timing of the application and cessation of the calibration pulses (t_1 and t_2), which degraded somewhat the estimation of $(k'_R)_{31}$ and caused a serious degradation of the evaluation of $(k'_R)_{32}$. The estimations of $(k'_R)_{21}$ and $(k'_R)_{22}$ were not affected by these errors (as had been the case for the experiments carried out prior to the construction of the ICARUS-1 system). It was therefore recommended [16] that **(vii)** be modified and that the "true heat transfer coefficient" be estimated using $(k'_R)_{22}$ evaluated at times close to t_1 and by $(k'^{,0}_R)_{262}$ (rather than by $(k'_R)_{32}$ estimated at times close to t_2 as recommended in the Handbook for the ICARUS-1 system [1]).

This set of objectives and instructions will be reconsidered in Section 7 in the light of the evaluation of the simulated data, Section 5, and of a "blank" experiment, Section 6.

SECTION 5: EVALUATION OF THE "RAW DATA" GENERATED USING THE SIMULATION DESCRIBED IN SECTION 4.

(a) We start by plotting the "raw data" generated by the simulation Eqs. (42), (43), (47), (48), (50), and (51) described in Section 3; see the ICARUS $(k_c')_{11}$-spreadsheet, spreadsheet 1. The plots of the temperature–time and input enthalpy–time series are shown in Fig. 2 (the data are the same as in Fig. 1). We evaluate $(k_c')_1$ and $(k_c')_2$ using the graphical method and obtain

$$(k_c')_1 = 0.07294 W K^{-1} \tag{52}$$

$$(k_c')_2 = 0.07280 W K^{-1}. \tag{53}$$

It should be noted that the scale of the y-axis in Fig. 2 is markedly reduced compared to that used in the evaluation of experimental data, e.g., Fig. 38. The reasons for this are the rather low value of $\Delta\theta_i$ used in the simulation (Eq. (39)) which increases the excursion of the temperature–time series coupled to use of landscape rather than portrait format so as to allow the presentation of the whole of the measurement cycle. In view of this compressed scale, the accuracies of $(k_c')_1$ and $(k_c')_2$ are somewhat reduced compared to those normally achieved. This effect is to some extent counteracted by the absence of "noise" in the simulated data.

At this stage, we have also always prepared a diagram on a much larger scale of the regions straddling the times t_1 and t_2 such as that shown in Fig. 3. There are several reasons for preparing such diagrams. First of all, when dealing with experimental data collected with the ICARUS systems (and their precursors), it is important to determine the exact times of application and cessation of the calibration pulses. It was the preparation of such diagrams which showed that there were timing errors in the ICARUS-1 system which could be easily allowed for by deriving the exact values of t_1 and t_2. As has already been stated on

other occasions there was no point in changing the hardware to correct for these effects as the times of data acquisition were known with sufficient accuracy.

Of course, when dealing with the simulated data, t_1 and t_2 are known exactly and these times should also be known accurately for experimental data collected with the ICARUS-2 system. However, we believe that this assumption/prediction will turn out to be incorrect!

The second reason for investigating the temperature–time series in these time regions is to define the time series required for the integrations of the input enthalpy to be used in the $(k'_R)_{21}$–spreadsheets. This definition is in turn dependent on the methods to be used for the numerical integrations. Here, we will assume here that we have decided to use the trapezium or sum rules for the integrations (these methods are related because the values given by the trapezium rule are those derived by the sum rule less one half the terms at the extremes of the range multiplied by the integration interval). For these rules, we need to insert an additional point into the experimental data at t_1 and t_2 if these times correspond to the data acquisition intervals. If t_1 and t_2 do not correspond to these intervals, we need to insert two additional points at each of t_1 and t_2.

We note here that the trapezium and sum rules can be used in a straightforward way to integrate around the discontinuities at t_1 and t_2. The mid-point and Simpson's rule cannot be used in this way: in particular, it is necessary to use much more complicated procedures if we wish to use the mathematically exact central difference methods. For this reason, we have always relied on the trapezium or sum rules except if the integrations are confined to regions $0 < t < t_1$, $t_1 < t < t_2$ or $t_2 < t < T$.[10]

(b) The next step is to carry out a detailed examination of the $(k'_c)_{11}$– spreadsheet, spreadsheet 1 and this examination itself falls into several parts. We first of all plot the lower bound heat transfer coefficient, $(k'_c)_{11}$, against time (here given by the measurement interval) where we use the assumed value of C_pM, Fig. 4. Of course, for the case of the interpretation of the simulated data, we know the value of C_pM used in the simulation. The deviation of $(k'_c)_{11}$ from the value 0.073000 WK^{-1} used in the simulation is therefore an indication of

[10]We believe that these integrations have been carried out incorrectly by the ICARUS-2 software. It would be important to check this particular point if we can reimplement the software. The reason is not only that incorrect integrations will lead to incorrect values of the "true heat transfer coefficient," a matter which will be illustrated below, but also that we will calculate an incorrect value of the excess enthalpy for each measurement cycle even if we should have a correct value for the heat transfer coefficient! If we cannot reimplement the software, then we will be able to make some sort of overall check of the ICARUS-2 software by carrying out correct and detailed checks of the measurement cycles for which NHE have given values of the "true heat transfer coefficient" evaluated by their methodology. This should automatically reveal the method(s) they actually used to arrive at their conclusions.

the errors in $d\Delta\theta/dt$ produced by using the second order central difference when using a 300 s measurement interval. We can see that we can obtain reasonable values of $(k'_c)_{11}$ provided we exclude, say, the first six hours following any change in the operating conditions of the cells.

Of course, in the case of the evaluation of spreadsheets derived for experimental measurements, our first evaluation will be based on a "guesstimate" of C_pM. It will therefore be necessary to amend the spreadsheet once an accurate value of C_pM has been derived.[11] It is important that under such conditions the further average $(\overline{k'_c})_{11}$ cannot be derived and $(\overline{\overline{k'_c}})_{11}$ is quite meaningless. It is therefore impossible to carry out these important averaging methods which reduce the effects of random errors. These difficulties could have been avoided if the experiments had been carried out using the stipulated 48-hour measurement cycles.

We note that the error of 0.04% in the "lower bound heat transfer coefficient" is above that which was specified for the ICARUS-1 system (0.01%). An alternative approach to removing the errors due to incorrect estimates of C_pM is to use the evaluations of $(k'^{,0}_c)_{151}$, $(k'^{,0}_c)_{161}$, $k'^{,0}_c)_{171}$, and $(k'^{,0}_c)_{181}$, Figs. 5 through 8. These extrapolations automatically give us values of C_pM and the relevant values of the "lower bound heat transfer coefficients" are shown on Fig. 4.

This particular approach was de-emphasized in setting up the ICARUS-1 system because the extrapolations in Figs. 5 trough 8 are to a point where $d\Delta\theta/dt = 0$. While this condition is satisfied for the simulations, it will not be observed for experiments carried out with a 24-hour measurement cycle. If a 48-hour cycle is used, then there will be two times at which this condition will hold (one within the period $0 < t < t_1$, and one within $t_1 < t < t_2$; see Section 6). However, it has never been established that the plots in Figs. 5, 6 and 8 extrapolate to these points. This is a matter which should be investigated using data generated by more elaborate simulations.

(c) The next step is to investigate the "true heat transfer coefficient", $(k'_c)_{12}$. In the region $t_1 < t < t_2$, we can apply Eq. (9) at any chosen point. This is straightforward for the data derived by simulation because the thermal balance in the absence of the calibration pulse is known exactly. For experimental data, the relevant values can be obtained from the plots of the temperature–time and cell potential–time series such as those shown in Fig. 38, Section 6. Figure 9 gives the relevant values using the data on the $(k'_c)_{11}$-spreadsheet, spreadsheet 1.

[11]The little which we have seen of the NHE evaluations leads us to think that this further step was never carried out. If this is correct, then the values of C_pM used would have been in error by between 10 and 20%. This error would in turn have produced an error of – 0.04% in the "lower bound heat transfer coefficients" under the most favorable conditions of estimating this coefficient at the end of the relevant 6-hour periods.

The deviations from the known value ($(k'_c)_{12} = 0.073000\,\mathrm{WK}^{-1}$) shown in Fig. 9 as well as the component parts of this heat transfer coefficient (the ordinates and abscissae shown in spreadsheet 1) show that the effects of errors in the estimates of $(d\Delta\theta/dt)$ are now more serious than is the case for the calculation of $(k'_c)_{11}$. This is to be expected mainly in view of the relative magnitudes of $f_1(\theta)$ and $f_2(\theta)$, Eqs. (9) and (10). However, we can see from spreadsheet 2 that we would be able to derive values of $(k'_c)_{12}$ accurate to 0.01% if measurement cycles lasting 48 hours were used. It is possible to apply averaging procedures leading to $(\overline{k'_c})_{12}$ and $(\overline{\overline{k'_c}})_{12}$ for the last 6 hours of calibration periods lasting 12 hours, thereby, markedly reducing the effects of "noise" in the experimental temperature– and cell potential–time series. The benefits of this type of averaging are, indeed, foreshadowed by the accurate determination of $(k'_c)_2$, Fig. 2.

The restrictions which should be placed on the determination of the "differential true heat transfer coefficients" are also illustrated by the determination of $(k'^{,0}_c)_{162}$, Fig. 10. It can be seen from this figure and/or spreadsheet 2 that the range of the extrapolation required to remove (nominally) the effects of C_pM on the derived heat transfer coefficient is much longer than for the equivalent determination of $(k'^{,0}_c)_{161}$. The abscissae are still *ca* 10% of the ordinates even at the end of the region which can sensibly be used for the determination of $(k'^{,0}_c)_{162}$ (say, 3 hours after the application of the calibration pulse). It follows that a 20% error in C_pM will lead to at least a 2% error in $(k'^{,0}_c)_{162}$. Of course, such effects are not apparent when using data produced by simulations free of "noise" but we would predict that procedures based on making thermal balances close to $t = t_1$ will not give accurate "true heat transfer coefficients" and that we should instead rely on evaluating $(k'_c)_{12}$ (and of related coefficients) at times close to $t = t_2$. This point, which will be further illustrated in Section 6, was of key importance to the specification of the ICARUS procedures [1].

The value of $(k'^{,0}_c)_{162}$ obtained from Fig. 10 is also shown on Fig. 9. Although this value agrees with those described by methods judged to be satisfactory, it should be noted that this agreement is largely due to the use of data free from all ambiguities (absence of "noise," time dependence of the heat transfer coefficients, timing errors). The use of experimental data leads to a marked degradation of the evaluation, see Section 6. A major reason for this degradation is that the data points having the highest statistical weight are also the ones which have the lowest accuracy, Fig. 10 and spreadsheet 1. It is possible, however, that the use of statistical weighting procedures would allow satisfactory estimates of $(k'^{,0}_c)_{162}$ to be made.

Figure 9 also shows the values of $(k'^{,0}_c)_{152}$ and $(k'^{,0}_c)_{172}$ derived from spreadsheet 1 by using Eq. (12). The form of this equation shows that the derivation of these versions of the heat transfer coefficient is, in fact, dependent on the interpretation of cooling (or heating) curves, i.e., the driving force is now the enthalpy content

of the calorimeters rather than the heater calibration pulse, ΔQ (these methods were developed largely as part of a program of work on the interpretation of phenomena linked to "Heat after Death"). As would be expected, the accuracy of these estimates of the heat transfer coefficient is limited even when using data free from all ambiguities. The accuracy of estimates of $(k_c'^0)_{152}$ and $(k_c'^0)_{162}$ can never be greater than that of C_pM when using real experimental data. This accuracy is further degraded by the fact that the estimates are dependent on the derivation of $(d\Delta\theta/dt)$ in regions where the accuracy of this gradient is limited by the length of the data acquisition interval.

Although Fig. 9 shows three data points for each of these estimates of the "true heat transfer coefficient," we would expect that only one such data point could be derived when using experimental data in view of the need to estimate $(d\Delta\theta/dt)$.

d) In this sub-section, we are also including a second set of evaluations which exactly follow the set described above, Figs. 4 through 10, except that $d\Delta\theta/dt$ has been estimated using the first order backward difference. Comparison of Figs. 11 and 4 shows that the errors in $(k_c')_{11}$ are now markedly increased in regions where $(d\Delta\theta/dt)$ is large: as expected, the errors in $(d\Delta\theta/dt)$ based on the first order differences are much larger than those based on the second order differences. Nevertheless, satisfactory values of $(k_c')_{11}$ can be obtained provided measurement cycles of 48-hour durations are used.

Figure 11 also includes values of $(k_c'^0)_{151}$, $k_c'^0)_{161}$, $k_c'^0)_{171}$ and $(k_c'^0)_{181}$ determined by using the relevant extrapolations, Fig. 12 through 15. It can be seen that these values of the heat transfer coefficient can again be estimated satisfactorily. However, the slopes of the regression lines are markedly reduced (due to the incorrect estimation of $(d\Delta\theta/dt)$) so that the values of C_pM are now also too low. Of course, application of this methodology to "real experimental data" would then lead to erroneous estimates of $(k_c')_{11}$. Figure 16 gives the plot of $(k_c')_{12}$ versus time again based on the first order backward differences while Fig. 17 illustrates the estimation of $(k_c'^0)_{162}$. Comparison of Figs. 16 and 9 shows that $(k_c')_{12}$ is now markedly in error in the time region adjacent to t_1: it is necessary to extend measurements to at least 7 hours in order to ensure that the errors due to the incorrect estimation of $(d\Delta\theta/dt)$ fall below 0.1% (the target specification for ICARUS-1). Of course, this situation if aggravated when using "real experimental data" in view of errors in estimation of C_pM. Figure 17 shows that satisfactory values of $(k_c'^0)_{162}$ can still be obtained when using such incorrect estimates of $(d\Delta\theta/dt)$. This would be expected because the extrapolation procedure removes the effects of C_pM. Needless to say, the value of C_pM derived is markedly in error. Comparison of Fig. 17 with spreadsheet 2 leads to a further important conclusion. We can see that satisfactory extrapolations can be obtained even though the "point-by-point" values are totally in error at short

times. As has already been noted, such long extrapolations are to be avoided when evaluating experimental data.

Figure 16 also includes some values of $(k_c'^{,0})_{152}$ and $(k_c'^{,0})_{172}$ derived from spreadsheet 2. It can be seen that these values are markedly in error even when using the correct value of C_pM. However, we note that values close to 0.073000 WK^{-1} (the value in the simulation) would be obtained if the incorrect estimate of the water equivalent (318.1 JK^{-1}) derived in Fig. 17 were used to calculate the "point-by-point" values of $(k_c'^{,0})_{152}$ and $(k'^{,0}c)_{172}$. It follows that the estimates of C_pM and of $(k_c'^{,0})_{152}$, $(k_c'^{,0})_{162}$ and $(k_c'^{,0})_{172}$ are internally consistent even through the component parts deviate from the true values. The procedures used to calculate these values of the "true heat transfer coefficients" must therefore be used with due care – in fact it is best to avoid such methodologies.

(e) We will consider next the derivation of the various versions of the integral heat transfer coefficients. The $(k_c'^{,0})_{21}$ spreadsheet, spreadsheet 3, gives the integrals required for the evaluation of $(k_c')_{21}$ and $(k_c')_{31}$ and Fig. 13 gives the plots of these two heat transfer coefficients against the time. It can be seen that except for small deviations of $(k_c')_{31}$ from the value 0.073000 WK^{-1} used in the calculation of the "raw data," the two estimates of the heat transfer coefficient agree with this value. The reason for the small deviations of $(k_c')_{21}$ at short times are immediately evident. The term

$$C_pM(\theta - \theta_0)/\int_{t_2}^{t} f(\theta)d\tau$$

is negligibly small for the estimation of $(k_c')_{21}$ because $(\theta - \theta_0)$ is itself small for the backward integration. On the other hand, the term

$$C_pM(\theta - \theta_0)/\int_{t_1}^{t} f(\theta)d\tau$$

is initially more than 10% of $(k_c')_{31}$ for the forward integration procedure. The deficiencies of using the trapezium rule coupled to the use of an inadequately long data acquisition interval are therefore immediately apparent. It should be noted that the plots of $(k_c')_{21}$ and $(k_c')_{31}$ versus time do not show any effect due to the discontinuities at $t = t_1$ and $t = t_2$, provided the integral of the enthalpy input has been correctly estimated at these points. The reason for this suppression of the effects of the discontinuities is simply that the magnitudes of the integrals are now sufficiently large so that errors due to the use of the trapezium rule coupled to the use of an inadequate long measurement interval are no longer detectable.

These effects (and noneffects!) due to errors in the estimation of the integrals were of key importance to the evolution of the ICARUS-1 data processing strat-

egy in particular the preference for the methods leading to $(k_c'^0)_{2,j,2}$ rather than for $(k_c'^0)_{3,j,2}$.

Figure 19 and spreadsheet 4 give comparisons of $(k_c')_{21}$ and $(k_c')_{22}$. It can be seen that the evaluation of the "true heat transfer coefficient, $(k_c')_{22}$, is satisfactory under all conditions. This is also brought out very clearly by considering the extrapolation procedures, Figs. 20 and 21. In particular, in the estimation of $(k_c'^0)_{262}$, the term

$$C_pM(\theta - \theta_0)/\int_{t_2}^{t} f_2(\theta)d\tau$$

never exceeds 10% of the term

$$\int_{t_2}^{t} \Delta H d\tau / \int_{t_2}^{t} f_2(\theta)d\tau.$$

The situation is radically different for the evaluation of $(k_c'^0)_{362}$, spreadsheet 5. While the extrapolation procedure for obtaining $(k_c'^0)_{361}$, Fig 22, is still reasonably satisfactory, provided the points immediately adjacent to t_1 are excluded (the abscissae never exceed 15% of the ordinates, spreadsheet 5), that for $(k_c'^0)_{362}$, Fig. 23, is unsatisfactory because the range of the extrapolation required is very long (note the magnitudes of the ordinates and abscissae in spreadsheet 5 and the fact that the abscissae are almost equal to the ordinates at short times). Such evaluations will also be markedly degraded by the "noise" of real experimental data. Furthermore, even the borderline fits obtained must be to some extent fortuitous because the replacement of integrations using the trapezium rule by the mathematically sound mid-point rule, Figs. 24 and especially Fig. 25, gives less satisfactory results than those obtained in Fig. 23. (Note especially the erroneous values of C_pM.)

The conflicting effects of changes in the integration methods and data acquisition interval have never yet been resolved. In view of this situation, it was recommended in the Handbook for the ICARUS-1 system [1] that $(k_c')_{32}$ be evaluated at times close to t_2 where the effects of the term

$$C_pM(\theta - \theta_0)/\int_{t_1}^{t} f_2(\theta)d\tau$$

on the overall value of$(k_c')_{32}$ are reduced. However, following the receipt of the first set of data from the NHE Laboratory [11], it became clear that the Group would never achieve satisfactory evaluations of this version of the "true heat transfer coefficient." As $(k_c'^0)_{262}$ could be evaluated satisfactorily under all conditions, it was recommended that future evaluations should be based on this version of the "true heat transfer coefficient."

This recommendation was also influenced by a consideration of the effects of timing errors. As has already been explained, the times of application and cessation of the heater calibration pulses did not coincide exactly with the data acquisition points in the pre-ICARUS phase of the investigation. Furthermore, there were evident timing errors in the ICARUS-1 systems. These timing errors did not affect the determination of $(k_c'^{,0})_{262}$ as the times of the data acquisition points were known exactly. Nevertheless we investigated the effects of gross errors in the estimation of $\int \Delta H d\tau$ on the evaluation of $(k_c'^{,0})_{261}$ and $(k_c'^{,0})_{262}$. See Figs. 26 through 29 and spreadsheet 4. It can be seen that such gross errors lead to a maximum error of 0.5% in $(k_c'^{,0})_{262}$.

Such evaluations are therefore reasonably satisfactory. On the other hand, evaluations of $(k_c'^{,0})_{361}$ and $(k'^{,0}c)_{362}$ fail almost completely. Thus, Figs. 30 and 31 (spreadsheets 5) show that erroneous values of both the "lower bound heat transfer coefficients" and of the water equivalent are obtained if there are errors in $\int \Delta H d\tau$. Nevertheless, the values of $(k_c')_{31}$ at long times are still within the acceptable range as specified in the ICARUS-1 Handbook [1]. The extrapolations required for $(k_c'^{,0})_{362}$ fail completely (and the estimates of C_pM vary widely) as shown by Figs. 32 through 37. Examination of the sets Figs. 32 through 34 and Figs. 35 through 37 shows that the values of $(k_c'^{,0})_{362}$ and C_pM deduced depend on the range of the regression lines fitted. This is just the sort of behavior which was detected in the limited information available about the experiments carried out by NHE. We believe therefore that the malfunctions which they have reported are in large measure due to the combination of estimating the "true heat transfer coefficients" by using $(k_R'^{,0})_{362}$ without any correction of the effects due to timing errors.

SECTION 6: EVALUATION OF A MEASUREMENT CYCLE FOR A "BLANK EXPERIMENT" (Pt cathode polarized in 0.1M LiOD/D_20) USING AN ICARUS-2 SYSTEM.

It has been explained elsewhere the reasons why we have very few data sets collected with the ICARUS-1 and -2 systems. However, some of the "raw data" for parts of a "blank experiment" carried out during the summer of 1995 using an ICARUS-2 system installed at IMRA Europe are available. This experiment used a Pt cathode polarized in 0.1 M LiOD/D_2O in an ICARUS–2 cell (having an extended length of silvering in the upper portion of the cell). This measurement cycle belongs to one set of calibrations of the ICARUS-2 systems carried out at that time. Unfortunately, these calibrations were terminated in 1995 and most of the data collected at that time are no longer available.

This data set can be regarded as being satisfactory except in one regard. At that time, the cells had been wired to the "switching boxes" using thin wire. This was to be replaced by thick wire, but, unfortunately, the wiring of the calibration heaters was not changed. The power delivered to these heaters therefore has to be corrected for voltage losses external to the cell. This correction is *ca* 2% of the nominal power delivered to the cell and can be made to better than 0.1% of the 2% level. The possible error in the calibration power is therefore well below the target value for obtaining the "true heat transfer coefficients" with errors below 0.1%. The power delivered to the calibration heater was 0.23025W and the cell current was 0.20306A.

(a) We again start by plotting the "raw data," this time of the cell temperature and cell potential versus time, Fig. 38, and by constructing the relevant $(k'_R)_{11}$ spreadsheet, spreadsheet 6. Here, we have used the third measurement cycle so as to be consistent with later evaluations (to follow). It can be seen that such measurements for "blank systems" do not show any anomalies. In particular,

the initial temperature perturbation due to the refilling of the cell (to make up for the losses of D_2O due to electrolysis) relaxes within, say, 7 hours; in view of the much larger amplitude of the temperature perturbation due to the application and cessation of the heater calibration pulse, we need to allow at least 8.5 hours to "eye-ball" the relaxations in the regions $t_1 < t < t_2$ and $t_2 < t < T$. One reason for the specification of the 48-hour long measurement cycles will be apparent immediately; such measurement cycles allow us to make the durations of $t_1 - t_0$ and $t_2 - t_1$ equal to 12 hours.

It will also be evident that the temperature following the cessation of the calibration pulse relaxes to the sloping base line. Furthermore, it will be clear that the system normally shows "negative feedback" in that increases of the cell temperature lead to a lowering of the enthalpy input (and vice versa). Tests of this "negative feedback" will be discussed in later sections.[12]

If we accept data sets such as those in Fig. 38 as being "reasonably normal," we can evaluate the "lower bound" and "true heat transfer coefficients" at a time close to t_2 by using the graphical methods. We obtain

$$(k'_R)_{11} = 0.61844 \times 10^{-9} WK^{-4} \text{ with } E_{th,b} = 1.54V \tag{54}$$

$$(k'_R)_{11} = 0.62006 \times 10^{-9} WK^{-4} \text{ with } \mathrm{E_{th,b}} = 1.527\mathrm{V} \tag{55}$$

$$(k'_R)_2 = 0.62027 \times 10^{-9} \mathrm{WK^{-4}}. \tag{56}$$

The close agreement of Eqs. (54) and (56) is almost certainly fortuitous because we expect the errors in $(k'_R)_2$ to be $ca \pm 0.002 \times 10^{-9}$ $\mathrm{WK^{-4}}$. If we accept the values given by Eqs. (55) and (56), then we deduce a rate of excess enthalpy generation of 0.00034W, a value which is comparable to those which we had observed previously for "blank experiments" [5, 6, 8]. As was noted previously, such low values are below those expected for the reduction of electrogenerated oxygen present in the solution. This can be explained by the degassing of the solution adjacent to the cathode by the electrogenerated deuterium.

In this preliminary assessment, we also prepare plots on an expanded scale of the temperature–time data in the regions adjacent to t_1 and t_2, Fig. 39 (compare Fig. 3). We can see that the times of application and cessation of the calibration

[12] As we have always explained, it is essential to produce such graphs of the raw data in order to check on the normality (or otherwise) of the experiments. The data shown in Fig. 38 are "reasonably normal," i.e., we can judge them as being suitable for further evaluation although it was apparent that the "noise levels" had increased compared to the data sets which had been collected in Salt Lake City and, subsequently, in the "old part" of the IMRA, Europe Building in Sophia Antipolis. This increase in the "noise levels" caused some degradation in the evaluations compared to those which we could achieve previously up to the end of 1992. This was already apparent in 1994 at which time we tried to find the causes for the increases in "noise." Unfortunately, the attempts to do so were stopped.

pulse are adequately synchronized with the data acquisition points (although such extrapolations for "real" experimental data are inevitably less certain than those for simulation, Fig. 3). It follows that it is sufficient to insert single additional points at t_1 and t_2 in the preparation of the $(k'_R)_{21}$-spreadsheet.

The evaluation of $(k'_R)_{11}$ (at a point close to $t = t_2$) and of $(k'_R)_2$ is important for the evolution of the research program as well as for the assessment of the validity of other methods of data evaluation. We note in the first place that these "lower bound" and "true heat transfer coefficients" are, respectively, the least precise and least accurate values which can be obtained from the experimental data. Any conclusion that the precisions and accuracies of other methods of data evaluation are lower than this (as determined by repeated calibrations for "blank experiments") show that either the experiments have been carried out incorrectly or that the methods of data evaluation are invalid. We note, secondly, that the Second Law of Thermodynamics requires that $(k'_R)_2 > (k'_R)_{11}$ (at the same point in time). Any conclusion that $(k'_R)_{11} > (k'_R)_2$ can only be explained by either errors in the execution of the experiments or the presence of variable sources of excess enthalpy. If the latter statement is true, it is then impossible to calibrate any conceivable calorimetric system and, in that eventuality, we need to rely on separate calibrations of the calorimeters.

(b) We next carry out a detailed examination of the $(k'_R)_{11}$ spreadsheet, spreadsheet 6. We first of all prepare a plot of $(\overline{k'_R})_{11}$ versus time, Fig. 40 (compare Fig. 4) on which we also show the derived values of $(\overline{\overline{k'_R}})_{11}$. The error bars show $\pm\sigma$ of $(\overline{k'_R})_{11}$. The "lower bound heat transfer coefficient" shows the expected linear decrease with time and the relevant regression line is drawn on the plot.

We also examine the extrapolations required to obtain $(k'^{,0}_R)_{151}$, $(k'^{,0}_R)_{161}$, $(k'^{,0}_R)_{171}$, and $(k'^{,0}_R)_{181}$, Figs. 41 - 44 (compare Figs. 5 - 8, Section 6). Of these plots, Figs. 41 and 42 are probably soundly based in that the origin of the abscissae (where $d\Delta\theta/dt = 0$) can be defined on Fig. 38. The origin for Fig. 43 cannot be defined and this puts the mathematical validity of Fig. 44 in doubt as this requires a combination of the data used in Figs. 42 and 43. Here, we have said "probably soundly based" because the question of the origins for plots of this kind needs further investigation using appropriate simulations. Notwithstanding our reservations about the validity of Fig. 44, we regard this plot as the best way of estimating the "lower bound heat transfer coefficients" and the water equivalent of the cells in the vicinity of t_2. The water equivalent can also be estimated from a similar plot for $(k'^{,0}_R)_{281}$, see Fig. 55 below, and the compromise value of 330 JK^{-1} has been used to derive the $(k'_R)_{11}$ spreadsheet, spreadsheet 8. This spreadsheet is actually the first iteration in the calculation scheme.[13]

[13]As has already been noted in Section 6, we do not believe that this iteration has been carried out in the evaluations of the NHE data sets.

In view of the scatter of the points in Fig. 40, the values of $(k_R'^{,0})_{151}$, $(k_R'^{,0})_{161}$, $(k_R'^{,0})_{171}$ and $(k_R'^{,0})_{181}$ have not been added to this plot (contrast the plot of $(k_c')_{11}$ versus time, Fig. 4) but are given on a separate plot, Fig. 45, with respect to the regression line in Fig. 40. Figure 45 also includes the value of $(k_R')_{11}$ derived by the graphical method, Fig. 38.

(c) In the next step, we evaluate $(k_R')_{12}$ and $(\overline{k_R'})_{12}$ and plot these "true heat transfer coefficients" versus time in Fig. 46. In carrying out this evaluation, we estimate the values of E_c and θ at any given time within $t_1 < t < t_2$ by fitting regression lines through the data shown in Fig. 38 but excluding the region $t_1 < t < t_2$ and those plots where the temperature and cell potential relax following perturbations. It will be evident that the scatter of the values of $(\overline{k_R'})_{12}$ in Fig. 46 is much larger than that for $(\overline{k_R'})_{11}$ shown in Fig. 40 (the regression line for $(\overline{k_R'})_{11}$ is also shown in Fig. 46).

Figure 47 gives the evaluation for $(k_R'^{,0})_{162}$ and Fig. 48 shows values of $(k_R'^{,0})_{152}$, $(k_R'^{,0})_{162}$, $(k_R'^{,0})_{172}$ and $(k_R')_2$ again with respect to the regression line for the variation of $(\overline{k_R'})_{11}$ with time, Fig. 40. The increased scatter compared to the data in Fig. 45 will again be apparent. We conclude therefore that the evaluation of the "differential true heat transfer coefficients" will not be useful for calculating the rates of excess enthalpy generation. However, this does not mean that we cannot evaluate the differential rates – if we should wish to do so. The way in which we can circumvent the errors introduced by the determination of the "differential true heat transfer coefficients" is discussed in subsection of Section 6 **(f)** below.

(d) We will not describe/discuss the use of the first order backward difference in the evaluation of $(d\Delta\theta/dt)$ when considering the analysis of experimental data.

(e) We will consider next the derivation of the various versions of the integral heat transfer coefficients. The $(k_R')_{21}$-spreadsheet, spreadsheet 7, gives the integrals required for the evaluation of $(k_R')_{21}$ and $(k_R')_{31}$ and Fig. 49 gives the plots of these coefficients versus time. Figure 50 gives a comparison of $(k_R')_{21}$ with $(\overline{k_R'})_{11}$ and it can be seen that the use of the integral procedure leads to a marked reduction of the errors due to the differentiation of "noisy" experimental data (which is required for the evaluation of $(k_R')_{11}$ and the derived $(\overline{k_R'})_{11}$). Inevitably, the values of $(k_R')_{21}$ and $(\overline{k_R'})_{11}$ converge at long times where the definitions of the integral and differential heat transfer coefficients are equivalent. Equally the value of $(k_R')_{31}$ at short times (as given by the regression line through the points at long times) converges onto the value of $(\overline{k_R'})_{11}$ at short times as these values are again equivalent, Fig. 49.

It can be seen from Figs. 49 and 50 that the values of $(k'_R)_{21}$ at long times deviate somewhat from the regression line. The reason for these deviations is that it is necessary to carry out *ca* 100 integration steps in order to suppress the random errors in $f_1(\theta)$ and the enthalpy input. Of course, the integration procedure still leaves us with the random errors in $[\theta(t) - \theta_0]$. However, it can be seen from Figs. 49 and 50 that the further averaging to give $(\overline{k'_R})_{21}$ has a negligible effect on the errors of this heat transfer coefficient.

It can also be seen from Fig. 49 that the deviations of $(k'_R)_{31}$ at short times from the relevant regression line are much larger than those of $(k'_R)_{21}$ at long times. The major reason for this effect is that the use of the trapezium rule (coupled to a rather long measurement interval) introduces appreciable errors into the integration of $f_1(\theta)$ and the enthalpy input in regions where these two variables are changing rapidly with time. By contrast, the integrations required for $(k'_R)_{21}$ take place in an initial region where $f_1(\theta)$ and the enthalpy input are nearly constant with time. The curvatures of these variables with time at short times then have negligible effects on the integrals and the trapezium rule is perfectly adequate for the numerical integrations. This was the major reason for our preference for the use of $(k'_R)_{21}$ as compared to $(k'_R)_{31}$. There are, however, secondary reasons for this preference. These include the fact that $[\theta(t) - \theta_0]$ is appreciable for the initial region of the estimation of $(k'_R)_{31}$ whereas it is negligibly small for the evaluation of $(k'_R)_{21}$. Furthermore, the term

$$C_p M(\theta - \theta_0) \int f_1(\theta) dt$$

remains appreciable throughout the range of the evaluation (so that the values of $(k'_R)_{31}$ are subject to errors in C_pM) whereas one can find regions where

$$C_p M(\theta - \theta_0) \int f_1(\theta) dt$$

is zero (so that the values of $(k'_R)_{21}$ at these times are independent of C_pM).

It can be seen from Figs. 49 and 50 that the slope of the regression line for the variation of $(k'_R)_{11}$ with time is roughly twice that for the variations of $(k'_R)_{21}$ or $(k'_R)_{31}$ with time. This is to be expected. The time dependence of the heat transfer coefficients, Eq. (21), does not need to be taken into account when evaluating the differential version; it is then the variation of $(k'_R)_{11}$ with time which reveals this time dependence. This is just the term γt in Eq. (21) and we see that we can obtain a "good" value of γ from the slope of the regression line, Fig. 40. In the evaluations of $(k'_R)_{21}$ and $(k'_R)_{31}$ using Eqs. (13) and (14) we have usually defined $f_1(\theta)$ using Eq. (4) whereas our experience with the evaluations of $(k'_R)_{11}$ teaches us that we should use the definition Eq. (21). Integration of this equation gives

$$(k'^{,0}_R)[\int f_1(\theta) d\tau - \gamma t \int f_1(\theta) d\tau + \gamma \int \int f_1(\theta) d\tau d\tau]. \qquad (57)$$

If we now regard $f_1(\theta)$ as being constant throughout the measurement cycle (which is a rough approximation for the case of the "lower bound heat transfer coefficients"), then the integral becomes

$$(k'^{,0}_R) f_1(\theta) t[1 - \frac{\gamma t}{2}]. \tag{58}$$

It follows that the heat transfer coefficients given by Eqs. (13) and (14) are given by

$$(k'_R)_{21} = (k'^{,0}_R)_{21}[1 + \frac{\gamma(T-t)}{2}] \tag{59}$$

and

$$(k'_R)_{31} = (k'^{,0}_R)_{31}[1 - \frac{\gamma t}{2}] \tag{60}$$

within the limits of this approximation. $(k'^{,0}_R)_{21}$ and $(k'^{,0}_R)_{31}$ are respectively the values of $(k'_R)_{21}$ at $t = T$ and of $(k'_R)_{31}$ at $t = 0$. It follows that the slopes of the plots of $(k'_R)_{21}$ and $(k'_R)_{31}$ versus time are one half of the plot of $(k'_R)_{11}$ versus time.

Equation (57) also shows the way in which we can test whether the characteristics of the Dewar cells can be described by a single, time-independent heat transfer coefficient. Thus, evaluation of $(k'_R)_{21}$ according to Eq. (13) gives us the heat transfer coefficient

$$(k'_R)_{21} = (k'^{,0}_R)_{21} \left[1 - \gamma t + \gamma \int_T^t \int_T^t f_1(\theta) d\tau d\tau\right] / \int_T^t f_1(\theta) d\tau \tag{61}$$

so that the "time-independent" heat transfer coefficient $(k'^{,0}_R)_{21}$ is readily determined. Figure 51 shows this derived coefficient versus the measurement interval. We can see that if we exclude the region adjacent to T (where the methodology is unreliable) the values of $(k'^{,0}_R)_{21}$ are within $\pm 0.01\%$ of the mean of $(k'^{,0}_R)_{21}$ (the relative standard deviation is 0.0063%). This is the basis of our statement that the "integral lower bound heat transfer coefficient" can be determined with a precision given by a relative error of less than 0.01%. We note that the errors in $(k'^{,0}_R)_{21}$ shown in Fig. 51 are somewhat larger than those which we observed in the earlier work.

The success in deriving an unique value of $(k'^{,0}_R)_{21}$ brings in its train two further aspects. First of all, we need to assess the likely errors of the "point-by-point" values of $(k'_R)_{21}$ and $(k'_R)_{31}$. Examination of spreadsheet 10 shows that the "minor term"

$$C_p M(\theta - \theta_0) / \int_T^t f_1(\theta) d\tau$$

is maximally *ca* $\pm 1.4\%$ of the derived values of $(k'_R)_{21}$ (at the points $t = 0$ and $t = t_2$). On the other hand, this "minor term" rises to *ca* 25% of $(k'_R)_{31}$ within the calibration period $t_1 < t < t_2$ and is *ca* 7% of $(k'_R)_{31}$ at $t = 0$. Evidently,

the heat transfer coefficients based on the backward integration procedure are to be preferred to those based on forward integration. Secondly, we see that the preferred procedure would be to use extrapolation procedures to remove the effects of the water equivalent, which is the parameter subject to the greatest uncertainties.

Figures 52 through 55 show such extrapolation procedures for deriving $(k_R'^{,0})_{251}$, $(k_R'^{,0})_{261}$, $(k_R'^{,0})_{271}$, and $(k_R'^{,0})_{281}$, as well as the corresponding values of C_pM. The extrapolation in Fig. 52 will be to a point in the range $0 < t < t_1$ where the temperature is equal to that at the end of the measurement cycle (roughly at 6900s). As can be seen the values of $(k_R')_{21}$ and $(k_R'^{,0})_{251}$ show that this is indeed so. The extrapolations in Figs. 53 through 55 should all be to the end of the measurement cycle at $t = T$. However, the values of $(k_R'^{,0})_{261}$, $(k_R'^{,0})_{271}$ and $(k_R'^{,0})_{281}$ are somewhat larger than that of $(k_R')_{21}$ at that point (given the value read off from the regression line). In 1992/93, we concluded that this was due to the range of the extrapolation required being too long. In order to avoid this difficulty, we restricted the integrations to $t_1 < t < t_2$ and set the origin of the abscissa at a time close to $t = t_2$. The extrapolation, Fig. 62, will now be to the value of $(k_R')_{11}$ at this point and this is again the case (see also spreadsheet 8).

Figure 60 gives the "point-by-point" values of $(k_R')_{21}$ for the time range $t_1 < t < t_2$ and these are somewhat below the variation predicted based on the assumption in Eq. (59). We note that it has never been resolved whether the small discrepancies observed are due to using this assumption rather than Eq. (61) (however, they are at least due in part to the use of Eq. (59) rather than (61)). Instead, we have recommended the use of the extrapolation procedure shown in Fig. 62. In attempting to interpret the variation of (k_R') with time shown in Fig. 60, it should also be born in mind that the values of this heat transfer coefficient are unreliable for about the first 110 integration intervals adjacent to $t = t_2$.

Figure 60 also gives the corresponding data for $(k_R')_{32}$ while Fig. 63 shows that the extrapolation procedure required for deriving $(k_R'^{,0})_{361}$ is unreliable, even if the first 11 data points are excluded from the extrapolation. The main reason for this lack of reliability lies in the large values of the abscissae, which reach *ca* 30% of the value of $(k_R')_{31}$. (However, note that the extrapolations based on the integrals spanning the whole of the measurement cycle $0 < t < T$, Figs. 56 through 59, are somewhat more satisfactory; the procedure for deriving $(k_R'^{,0})_{361}$, Fig. 57, is reasonably sound). It was for this reason that this procedure was excluded in the Handbook for the ICARUS-1 systems [1]. We also see that the estimate of $(k_R')_{31}$ at times close to t_2 is somewhat lower than that predicted from Eq. (60). However, reference to spreadsheet 8 shows that the abscissae are still *ca* 2.3% of the ordinates for the evaluation of $(k_R')_{31}$ at this point (for the 24-hour measurement cycles used in the NHE investigations this ratio rises to

ca 4.4%). A 3% error in C_pM would therefore account for such discrepancies!

Figure 61 gives the values of the "true heat transfer coefficients" $(k'_R)_{22}$ and $(k'_R)_{32}$ over the restricted range $t_1 < t < t_2$ while Figs. 64 and 65 give the evaluations of $(k'^{,0}_R)_{262}$ and $(k'^{,0}_R)_{362}$. It can be seen that $(k'^{,0}_R)_{262}$ is close to the value of $(k'_R)_{11}$ at $t = t_2$ as given by the relevant regression line. On the other hand, $(k'^{,0}_R)_{362}$ deviates markedly from the value of $(k'_R)_{11}$ at $t = 0$, even if we once again exclude the first 11 points from the extrapolation. Spreadsheet 9 shows that the nominally "minor term" now reaches *ca* 100% of the value of the "major term" while the "minor term" is *ca* 2900% of $(k'_R)_{32}$. It goes without saying that it is not possible to evaluate $(k'_R)_{32}$ with this particular methodology. It was for this reason that the ICARUS-1 Handbook recommended that $(k'_R)_{32}$ should be evaluated "point-by-point" at times close to $t = t_2$. Spreadsheet 9 shows that the "minor term" in the evaluation of $(k'_R)_{32}$ is still *ca* 12% of the major term while for a 24-hour measurement cycle it would reach *ca* 25% of the major term. The accurate determination of $(k'_R)_{32}$ is therefore fraught with difficulties. These conclusions should be compared with those presented in the poster given at ICCF 7 [4].

Finally, Fig. 66 illustrates the determination of $(k'^{,0}_R)_{252}$, i.e., of the "true heat transfer coefficient" without making use of the calibration pulse. Whereas the determination of the differential coefficient $(k'^{,0}_R)_{152}$ fails (because of the inevitably large errors introduced by the differentiation of "noisy" experimental data), the determination of $(k'^{,0}_R)_{252}$ is reasonably successful. The evaluation of this version of the "true heat transfer coefficient" can therefore serve as a useful check on some of the more extreme statements which have been made about the validity of the ICARUS-1 evaluation procedures.

(f) We come now to the principal conclusions which we can draw from the detailed examination of "blank" experiments, taken in conjunction with the analysis of data generated by simulations, Section 5. The optimal methodology for the evaluation of the "lower bound heat transfer coefficient" is that based on the backward integration leading to $(k'_R)_{21}$, although that based on the forward integration leading to $(k'_R)_{31}$ can also be used. Furthermore, the differential form, $(k'_R)_{11}$, is also useful.

However, the only accurate method for the evaluation of the "true heat transfer coefficient" is that based on the backward integrals and, especially, the extrapolation procedure giving $(k'^{,0}_R)_{262}$, which was the methodology specified for the ICARUS-1 systems [1]. It is therefore sensible to combine such values of $(k'^{,0}_R)_{262}$ with the corresponding values of $(k'^{,0}_R)_{261}$. For the data set discussed here, we obtain from Figs. 60 and 61 (or Figs. 53 and 64, spreadsheets 8 and 9):

$$\Delta(k'_R) = (k'^{,0}_R)_{262} - (k'^{,0}_R)_{261} = 0.00043 \times 10^{-9}\mathrm{WK}^{-4}. \qquad (62)$$

This value is to be preferred to

$$\Delta(k'_R) = (k'_R)_2 - (k'_R)_{11} = 0.00021 \times 10^{-9}\mathrm{WK}^{-4}, \tag{63}$$

given by the graphical methods (Eu. (55)).

It should be noted that both of these methods give values of the heat transfer coefficients close to the mid-point of the measurement cycles (which was one reason for the specification of the time $t = t_2$). Furthermore, the difference in Eq. (62) is actually equal to

$$\Delta(k'_R) = (k'_R)_{12} - (k'_R)_{11} \tag{64}$$

at this point. This is of no particular consequence as far as the evaluation of the total excess enthalpy for the measurement cycle is concerned because the difference in Eq.(62) applies to any part of the cycle at the first level of approximation. It follows that

$$\text{Total excess enthalpy} = \Delta(\mathrm{k'_R}) \int_{\mathrm{T}}^{0} \mathrm{f}_1(\theta)\mathrm{d}\tau. \tag{65}$$

For the particular example used in the present illustration, we obtain

$$\text{Total excess enthalpy} = 102\mathrm{J}, \tag{66}$$

corresponding to a mean excess rate of 0.0006 W.

However, we note that the group at NHE have attempted to calculate the variation of the rate of excess enthalpy generation throughout the measurement cycles. At first sight, it would appear that we need to use the correct time-dependent values of $(k'_R)_{12}$, i.e., $[k'_R(t)]_{12}$. At the time of writing of the Handbook for the ICARUS-1 systems [1], it was not clear how this variation was to be established. It became clear subsequently that if the difference between the "true" and "lower bound heat transfer coefficients" could be established at any one time (say $\Delta(k'_R)_t$), then $[k'_R(t)]_{12}$ at any other time would be given by

$$[k'_R(t)]_{12} = [k'_R)(t)]_{11} + \Delta(k'_R)_{t_2} f_1(\theta)_{t_2}/f_1(\theta)_t. \tag{67}$$

The ratio $f_1(\theta)_{t_2}/f_1(\theta)_t$ is of order unity, which implies that the correction term is always close to that at the calibration point.

Any attempt to calculate the variation of rates of excess enthalpy generation within the measurement cycles must also pay due regard to the fact that it is not possible to calibrate the systems if the rate of excess enthalpy generation varies with time. If that is the case, then we must derive $\Delta(k'_R)$ from separate experiments.

Equation (67) also points to a further important conclusion. Again at the time of writing of the Handbook for the ICARUS-1 systems [1], we believed that the precision of $(k'_R)_{12}$ (and of other versions of the "true heat transfer coefficient") would always be given by the accuracy of that coefficient which is certainly lower than the precision of $(k'_R)_{11}$. Equation (67) shows that this is incorrect. The precision of $(k'_R)_{12}$ is nearly identical to the precision of $(k'_R)_{11}$. It follows that changes in the rates of excess enthalpy generation can be established at the same level of precision as that of $(k'_R)_{11}$, i.e., with relative errors *ca* 0.01%.

SECTION 7: ASSESSMENT OF THE SPECIFICATION OF THE ICARUS–1 EXPERIMENTAL PROTOCOLS AND DATA EVALUATION PROCEDURES.

The specification of the ICARUS-1 experimental protocols and data evaluation procedures has been outlined in Section 4. It is now important to assess the usefulness and validity of this specification in the light of its application to data generated by simulations (see Section 5) and by "blank" experiments (see Section 6). Of course, this procedure is "back-to-front": the specification, Section 4, was evolved from a consideration of the type of results outlined in Sections 5 and 6.

It is also important to consider the "raison-d'être" of this part of the research program and some comments on this are given at the end of this section. Furthermore, it is important to consider the causes of failures to achieve evaluations especially in the light of the well publicized publication from the group at NHE [5]. Finally, it is necessary to consider "short-cuts" to achieving satisfactory data evaluations.

In our view, the major results derived from Section 6 (backed up by the investigation in Section 5) are the comparisons of $(k'_R)_{21}$ and $(k'_R)_{11}$ in Fig. 50 and the reduction of $(k'_R)_{21}$ to a single, time-independent, lower bound heat transfer coefficient, Fig. 51. The comparison, Fig. 50, illustrates immediately the need to avoid the differentiation of "noisy" experimental data (required for the evaluation of $(k'_R)_{11}$ and the benefits of using instead the integration procedures in deriving $(k'_R)_{21}$); however, see further below. This was the basis for the specification of the construction of the $(k'_R)_{21}$ spreadsheets following on the construction of the $(k'_R)_{11}$ spreadsheets (see **(vi)** and **(vii)** of Section 4).

Results such as those illustrated in Fig. 50 show that it is possible to interpret the systematic variations with time of *ca* 0.4% of the "integral lower bound heat

transfer coefficient" while Fig. 51 shows that it is possible to reduce such data to a single, time-independent, heat transfer coefficient, $(k'^{,0}_R)_{21}$ with relative errors below 0.01%. This result is hardly surprising. The "physics" of the calorimeters are quite simple (they are "ideal well stirred tanks") and the errors are mainly due to those set by the temperature measurements. It is also relatively straightforward to specify the changes which would need to be made to reduce the errors – say, to 0.001% – if that should ever prove to be necessary or desirable.

The comparison of $(k'_R)_{21}$ with $(k'_R)_{31}$ in Fig. 50 as well as in spreadsheet 7 shows that the errors in $(k'_R)_{31}$ are inevitably larger than those of $(k'_R)_{21}$. This is mainly due to the larger contribution of the term

$$C_p M(\theta - \theta_0) / \int_0^t f_1)(\theta) d\tau$$

to $(k'_R)_{31}$ rather than the corresponding contribution of

$$C_p M(\theta - \theta_0) / \int_T^t f_1(\theta) d\tau$$

to $(k'_R)_{21}$. We can see immediately, that given the option of using forward or backward integration we should use the latter in order to achieve accurate evaluations. This restriction becomes much more important, however, when we consider the derivation of the "true heat transfer coefficients," $(k'_R)_{22}$ and $(k'_R)_{32}$, as well as of the likely effects of timing errors on the evaluations. Such evaluations must necessarily be mainly restricted to the duration of the calibration pulse, $t_1 < t < t_2$. Figures 60 and 61 and the associated spreadsheets 8 and 9 show that whereas an initial assessment might well be based on the use of $(k'_R)_{31}$, the evaluation and use of the "true heat transfer coefficient," $(k'_R)_{32}$, must follow strictly the instructions laid down in the ICARUS-1 Handbook [1] (see **(vii)** of Section 4) – and, even then, the errors are much larger than those of $(k'_R)_{22}$.

The optimum methodology for deriving the difference between the "true" and "lower bound heat transfer coefficients," i.e., $\Delta(k'_R)$, Eq. (62), is to estimate $(k'^{,0}_R)_{262}$ from plots such as that in Fig. 64 and $(k'^{,0}_R)_{261}$ from the corresponding plot in Fig. 62. Such evaluations automatically eliminate the contributions of the water equivalent on the estimates, a parameter which is subject to the greatest degree of uncertainty. The evaluation of the difference $\Delta(k'_R)$ allows us also to circumvent the errors in the evaluation of the "true differential heat transfer coefficient," $(k'_R)_{12}$, Fig. 46, because $\Delta(k'_R)$ applies equally to $(k'_R)_{12}$ and $(k'_R)_{11}$, Eq. (64), as to $(k'^{,0}_R)_{262}$ and $(k'^{,0}_R)_{261}$, Eq. (62). It follows. therefore that we can evaluate rates of excess enthalpy generation at the level of accuracy determined by $\Delta(k'_R)$ and precision of $(k'_R)_{11}$. However, we cannot see why we should ever wish to do so, given that we have had to evaluate the backward integrals to determine $\Delta(k'_R)$ so that the values of the total excess enthalpy in

a measurement cycle (or any given part of a measurement cycle) follow immediately as by the application of Eq. (65). If we evaluate instead the rates of excess enthalpy generation, then we must sum these rates (multiplied by the measurement interval) to obtain the total excess enthalpy [4] (more exactly, we need to apply an appropriate integration rule).

Sections 5 and 6 also illustrate the evaluations of the "time-independent" heat transfer coefficients $(k'^{,0}_R)_{151}$, $(k'^{,0}_R)_{161}$, $(k'^{,0}_R)_{171}$, $(k'^{,0}_R)_{181}$, $(k'^{,0}_R)_{152}$, $(k'^{,0}_R)_{162}$, $(k'^{,0}_R)_{172}$, $(k'^{,0}_R)_{251}$, $(k'^{,0}_R)_{261}$, $(k'^{,0}_R)_{271}$, $(k'^{,0}_R)_{281}$, $(k'^{,0}_R)_{252}$, $(k'^{,0}_R)_{262}$, $(k'^{,0}_R)_{272}$, $(k'^{,0}_R)_{351}$, $(k'^{,0}_R)_{361}$, $(k'^{,0}_R)_{371}$, $(k'^{,0}_R)_{381}$, $(k'^{,0}_R)_{352}$, $(k'^{,0}_R)_{362}$ and $(k'^{,0}_R)_{372}$. Of these, the evaluations of $(k'^{,0}_R)_{261}$ and $(k'_R)_{262}$, Figs. 62 and 64, were the methodologies specified for the ICARUS-1 system. The reduced precisions and accuracies of the series $(k'^{,0}_R)_{1,j,l}$ compared to those of $(k'^{,0}_R)_{2,j,l}$ will be apparent as will be the reduced precisions and accuracies of the series $(k'_R)_{3.j.l}$ compared to those of $(k'^{,0}_R)_{2,j,l}$. The evaluation of $(k'^{,0}_R)_{362}$, Fig. 65, is especially prone to error.[14]

The failure to achieve satisfactory calibrations of the cells using the procedures leading to $(k'_R)_{362}$ in the studies by the group at NHE coupled to the evident timing errors in the ICARUS-1 system installed in Sapporo, also prompted an investigation of the likely effects of such errors if these were not properly taken into account. Figs. 26-37 show the expected results. Whereas the "target evaluations" of $(k'^{,0}_R)_{261}$ and $(k'^{,0}_R)_{262}$ are relatively insensitive to the effects of such errors (Figs. 26-29), the evaluations of $(k'^{,0}_R)_{361}$ and $(k'^{,0}_R)_{362}$ are markedly degraded (Figs. 30-37). Moreover, the values of $(k'^{,0}_R)_{361}$ and $(k'^{,0}_R)_{362}$ (the intercepts of the plots) now depend on the time range of the regression fit (the discussion of these effects is beyond the scope of the present report). It is evidently critically important to avoid the effects of such timing errors because there are other reasons which preclude the achievement of satisfactory calibrations most notably the effects of changes in the rates of excess enthalpy generation especially those due to "positive feedback," e.g., see [4,12]. It is essential therefore that tests of the performance of the instrumentation be carried out using "blank experiments" (see Section 4 **(iii)**) in order to avoid the complications introduced by the study of the Pd-D_2O system.[15]

Sections 5 and 6 will also have illustrated the reasons for the need to use 48-hour measurement cycles [see Section 4 **(i)**] as well as the benefits of examining and evaluating plots of the raw data such as that in Fig. 38 [see Section 4 **(v)**].

[14] Unfortunately, such evaluations appear to have been a major part of the investigations carried out by NHE.

[15] We have never been able to obtain data for the study of any such "blank systems" which may have been carried out by NHE.

Finally, it is important to assess the usefulness of the calibration procedures described in this section as well as the preceding sections. It appears that this is a topic which has been misunderstood. It would hardly be possible to investigate all measurement cycles of all experiments at the level of detail set out in Section 6. The real purpose of developing precise and accurate methods of calibration is to gain an adequate understanding of the "instrument function" and then to use the calibration(s) to measure the rates of excess enthalpy generation. A secondary objective (related to the assessment of the calibrations) is to point the way towards necessary (or useful) improvements of the instrumentation. We note here that the original cells, which were not silvered in the top section, gave a flat temperature-time base line because changes in the heat transfer coefficient with time were compensated by changed in the enthalpy input. However, the heat transfer coefficients varied markedly with time and this complicated the methods of data analysis. The silvering in the top sections of the ICARUS-1 and -2 calorimeters has markedly reduced this time dependence of the heat transfer coefficients, but the effects (e.g., see Fig. 50) do still have to be taken into account.[16] In 1990/91, it appeared important that we should investigate a further modification of the calorimeter design designated as the ICARUS-4 version in 1993 (the ICARUS-3 designs were never constructed) but redesignated since that time as ICARUS-14, vol. I, Fig. 27. We believe that this design would give a flat base line for the heat transfer coefficient-time plot and that this would also make the heat transfer coefficient insensitive to the operating conditions.

An alternative approach would be to investigate the maintenance of constant electrolyte levels as has been done in the investigations carried out by the group at Grenobles [15]. It would be important to try to secure the release of data for "blank experiments" carried out by that group.

A secondary reason for carrying out repeated calibrations is to monitor the system behavior [4, 5] especially the effects of the onset of positive feedback. However, such investigations do not need to be carried out at the high levels of precision and accuracy required for the calibration of the calorimeters.

[16]We note that this has not been taken into account in the work carried out by the group at NHE.

REFERENCES.

1. "The ICARUS Systems: Isoperibolic Calorimetry Research and Utilities Systems. Version 1 Low Power Measuring System for Three Cells, Technova Inc., 13th Floor, Fukoku Science Bdg., 2–2–2 Uchisaivai–cho, Chiyodas–ku, Tokyo 100, Japan
2. "Second Report on the Experiments carried out under the NEDO/NHE Project at the Sapporo Laboratories", December 1994.
3. S. Pons and M. Fleischmann, Trans. Fusion Technology, 26 (1994) 87.
4. M. Fleischmann, "Illustrations of Evaluations of Calorimetric Data Sets", Poster given at I.C.C.F. 7, Vancouver, Canada, April (1998).
5. M. Fleischmann and S. Pons, Proceedings of ICCF–3 (1992) 47
6. M. Fleischmann and S. Pons, Physics Lett. **A 176**, 118 (1993)
7. Toshiya Saito, Masao Sumi, Naoto Asami and Hideo Ikegami, Proceedings of ICCF 5 (1995) 105.
8. M. Fleischmann, S. Pons, M.W. Anderson, L.J. Li and M. Hawkins. J. Electronal. Chem, 287 (1990) 293.
9. R.H. Wilson, J.W. Bray, P.G. Kosky, H.B. Vakil and F.G. Will, J. Electroanal. Chem, 332 (1992) 1.
10. D.E. Williams, D.J.S. Findley, D.W. Gaston, M.R. Sene, M. Bailey, S. Croft, B.W. Hooten, C.P. Jones, A.R.J. Kucernak, J.A. Mason and R.I. Taylor, Nature, 392 (1989) 375.
11. "Report on the First Set of Experiments carried out under the NEDO/NFIE Project at the Sapporo Laboratories", June 1994.
12. M. Fleischmann, Proceedings of ICCF 5, (1995) 152.
15. G. Lonchampt, L. Bonnetain and P. Hicter, Proceedings of I.C.C.F. 6 (1996) 113.
10. M. Fleischmann and S. Pons, J. Electroanal. Chem, 332 (1992) 33.

FIGURES

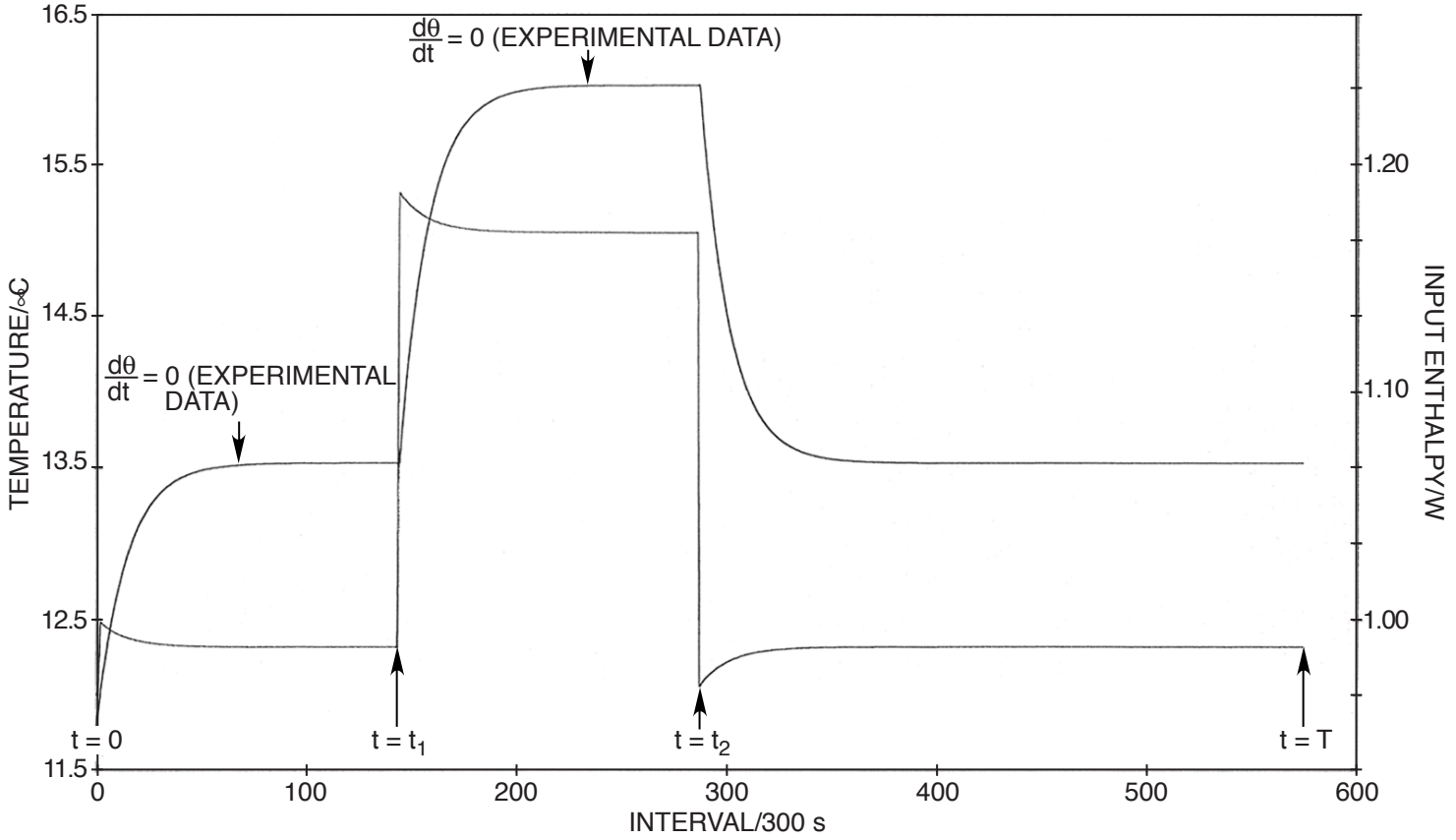

Fig. 1. ICARUS-2 simulation. Temperature-time and input enthalpy–time series.

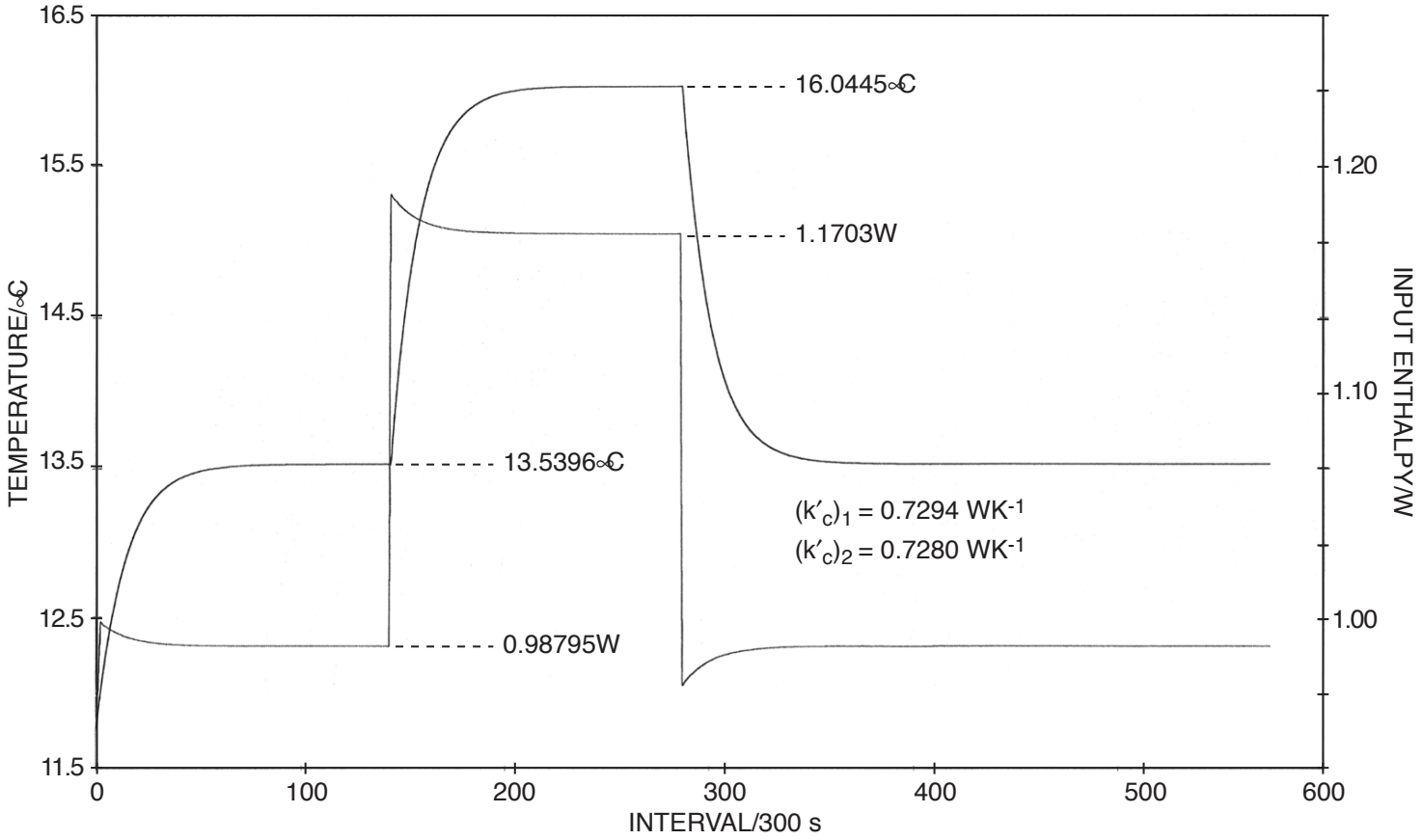

Fig. 2. ICARUS-2 simulation. Temperature-time and input enthalpy–time series.

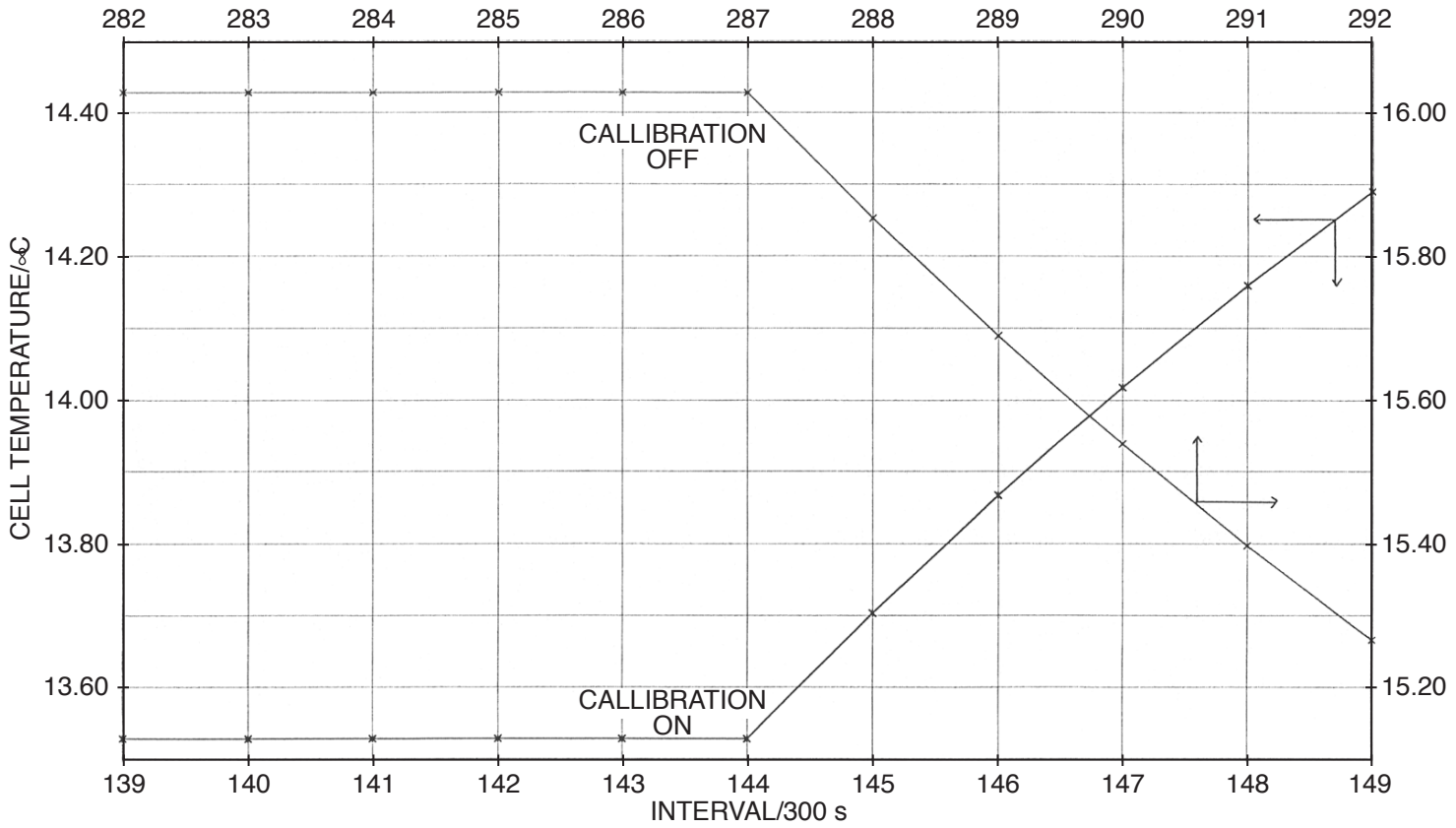

Fig. 3. ICARUS 2-simulation. Determination of "Start" and "Stop" of calibration pulse.

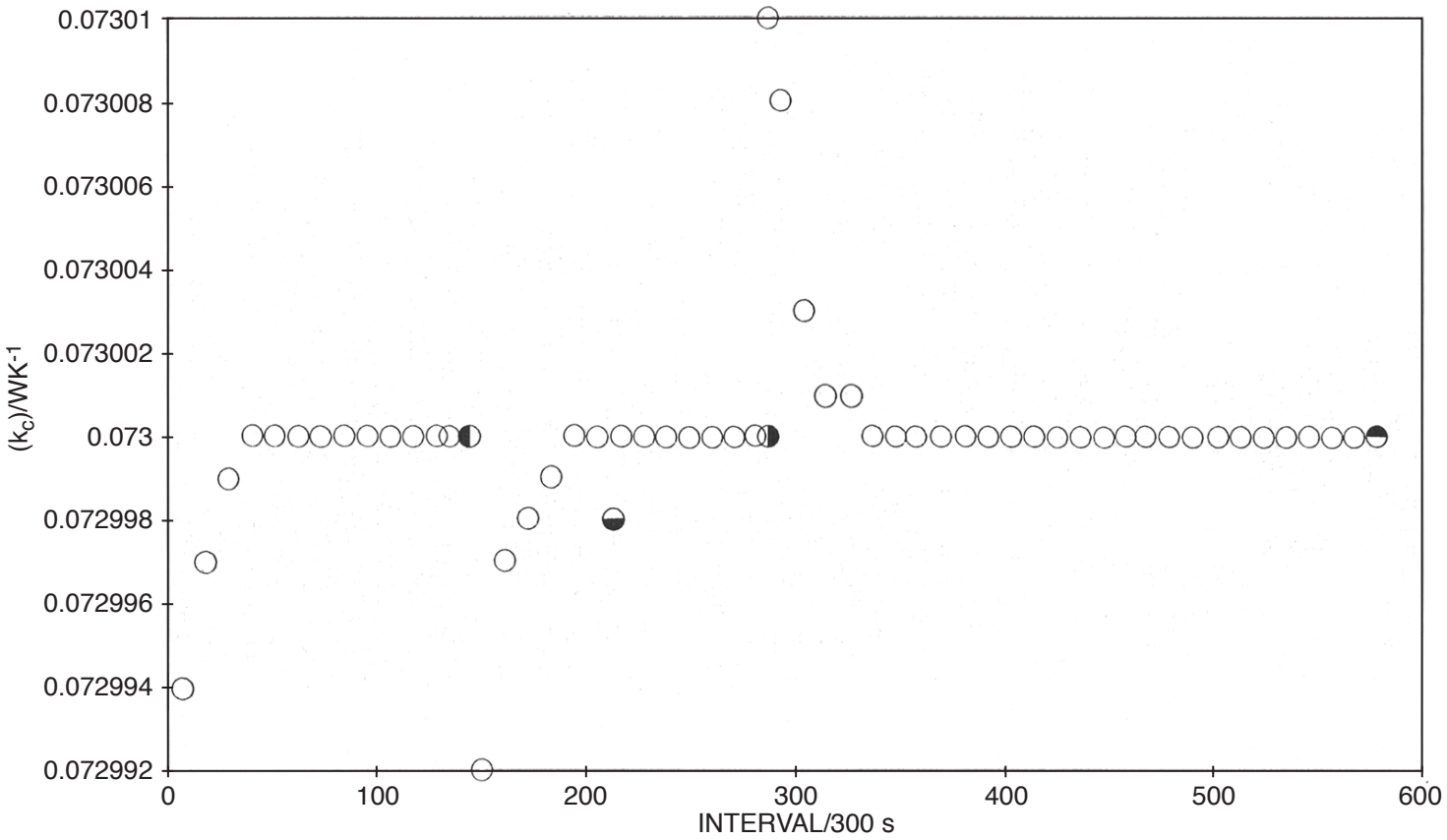

Fig. 4. ICARUS-2 simulation. $(k'_c)_{11}$, $(k'_c{}^o)_{151}$, $(k'_c{}^o)_{161}$, $(k'_c{}^o)_{171}$, and $(k'_c{}^o)_{181}$ versus time.

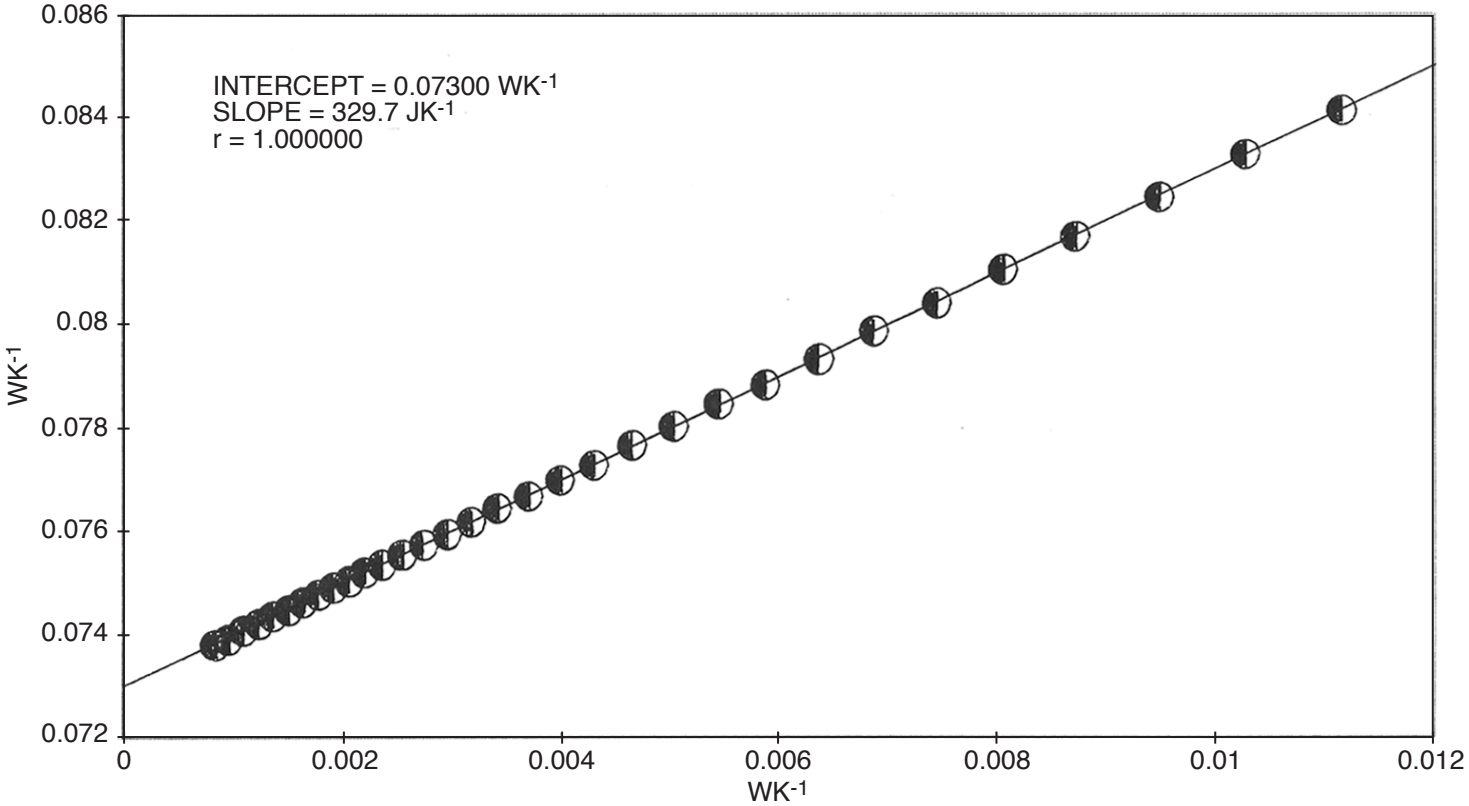

Fig. 5. ICARUS-2 simulation. Evaluation of $(k'_c{}^o)_{151}$.

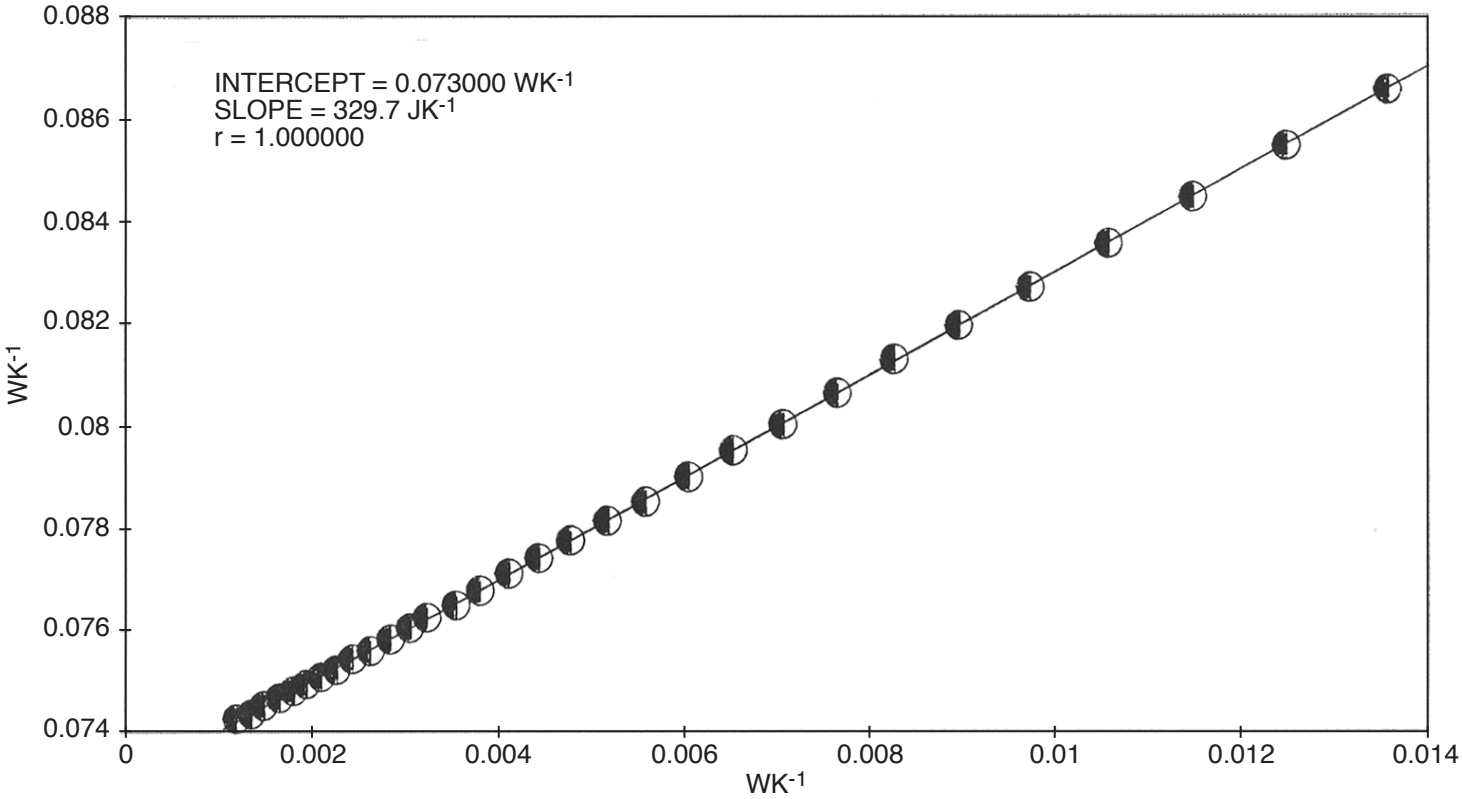

Fig. 6. ICARUS-2 simulation. Evaluation of $(k'_c{}^{o})_{161}$.

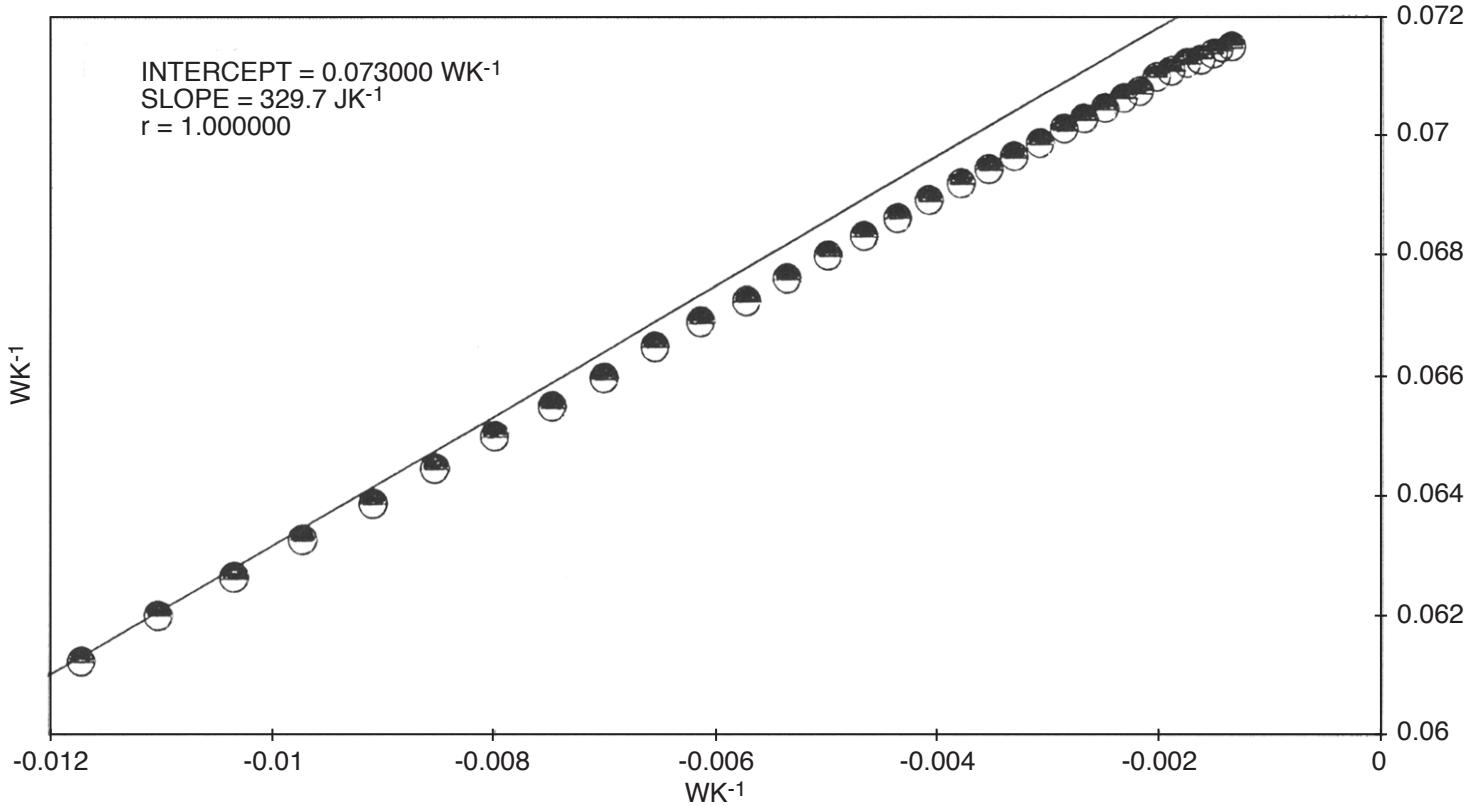

Fig. 7. ICARUS-2 simulation. Evaluation of $(k'_c{}^{o})_{171}$.

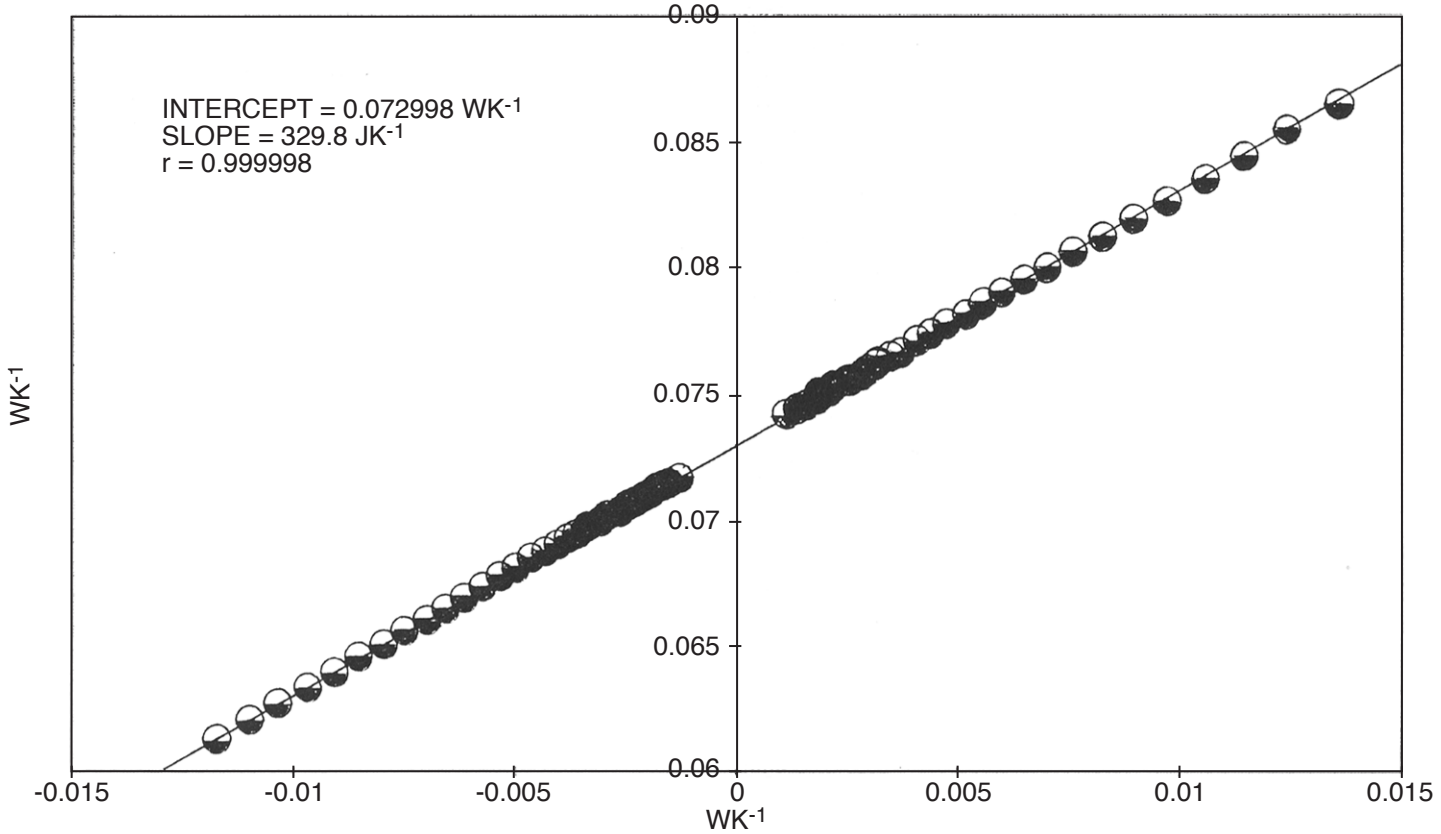

Fig. 8. ICARUS-2 simulation. Evaluation of $(k'_c{}^{o})_{181}$.

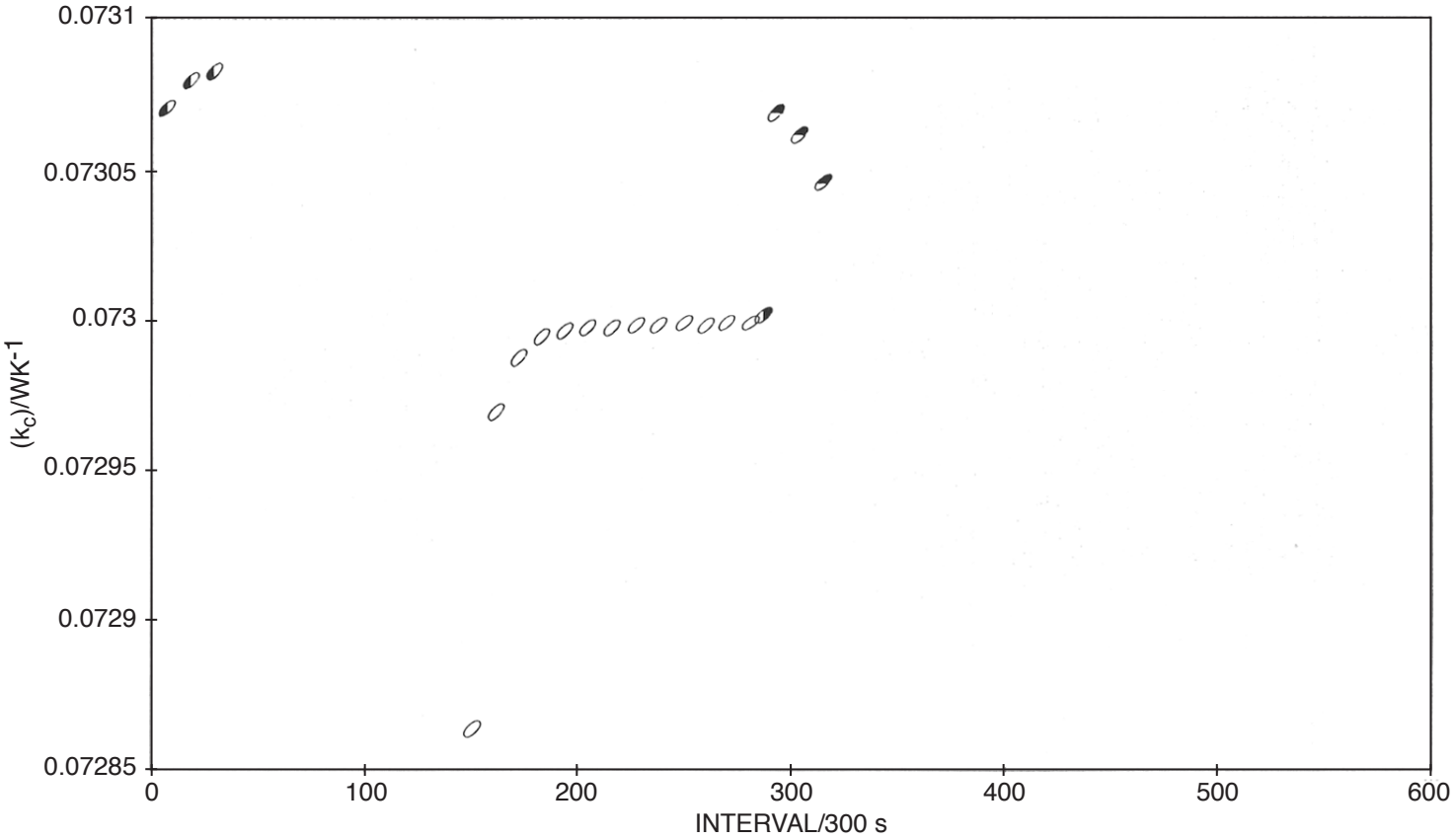

Fig. 9. ICARUS-2 simulation. $(k'_c)_{12}$, $(k'_c{}^o)_{152}$, $(k'_c{}^o)_{162}$, and $(k'_c{}^o)_{172}$ versus time.

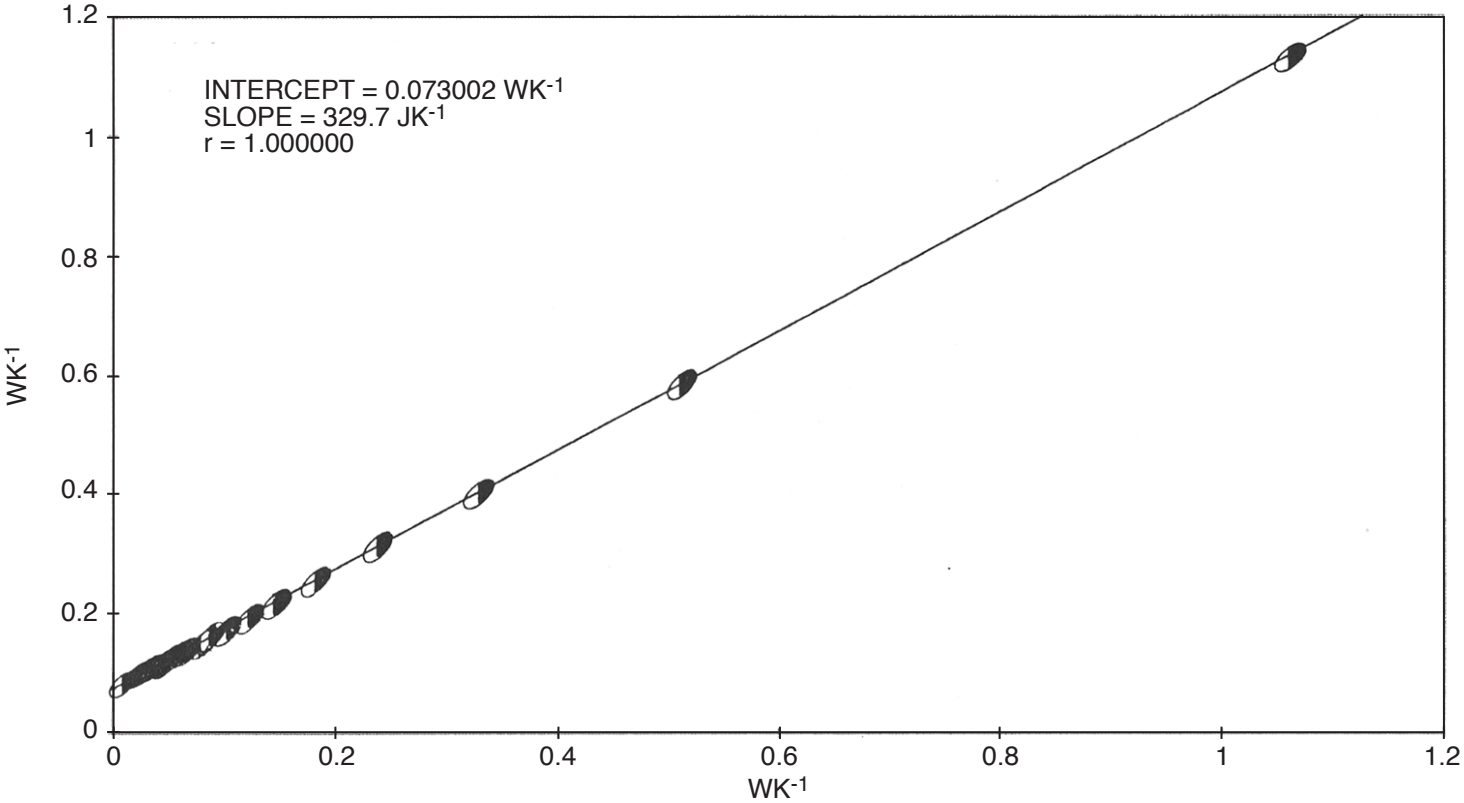

Fig. 10. ICARUS-2 simulation. Evaluation of $(k'_c{}^o)_{162}$.

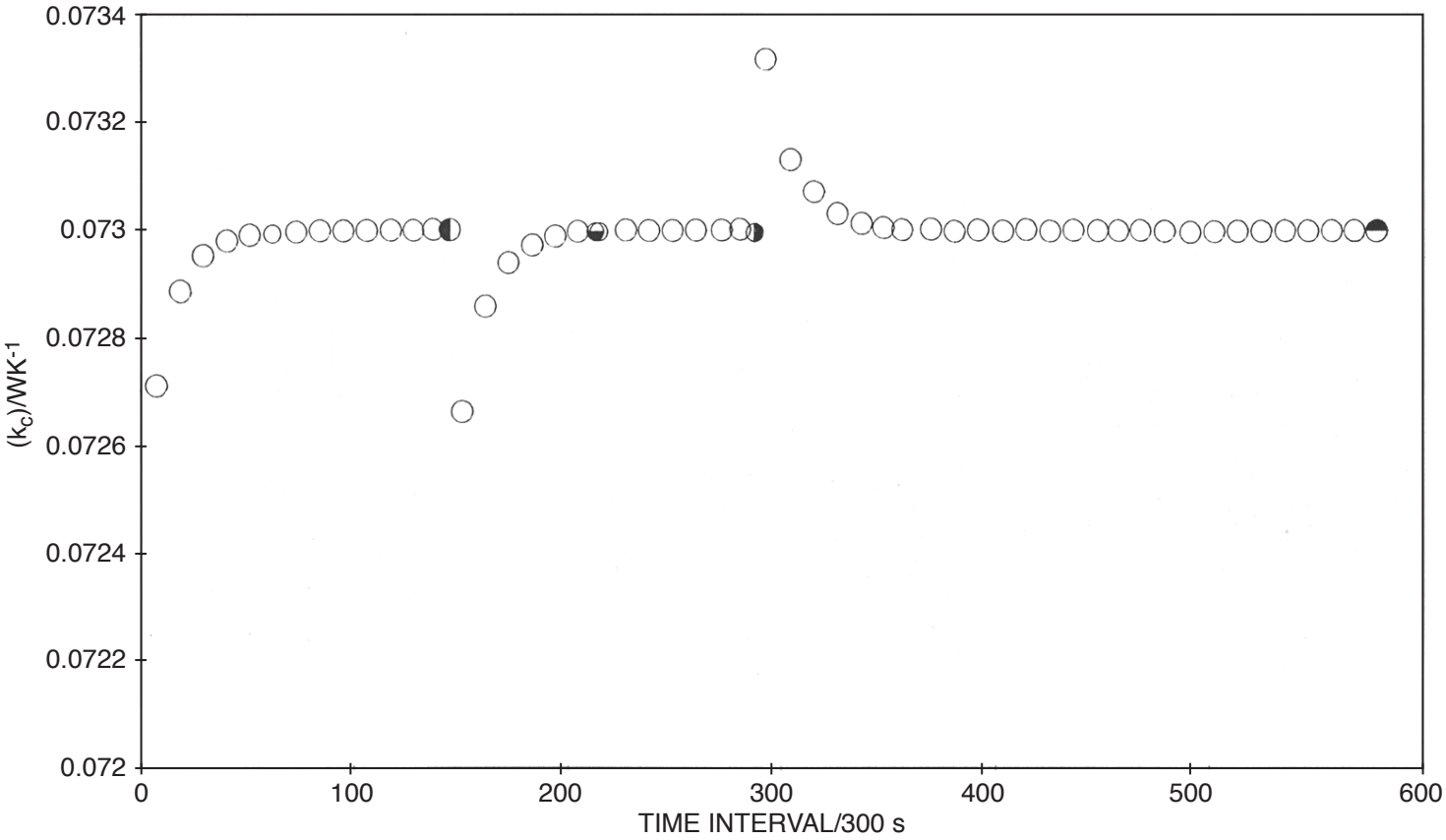

Fig. 11. ICARUS-2 simulation. $(k'_c)_{11}$, $(k'_c{}^o)_{151}$, $(k'_c{}^o)_{161}$, $(k'_c{}^o)_{171}$, and $(k'_c{}^o)_{181}$ versus time using first order differences.

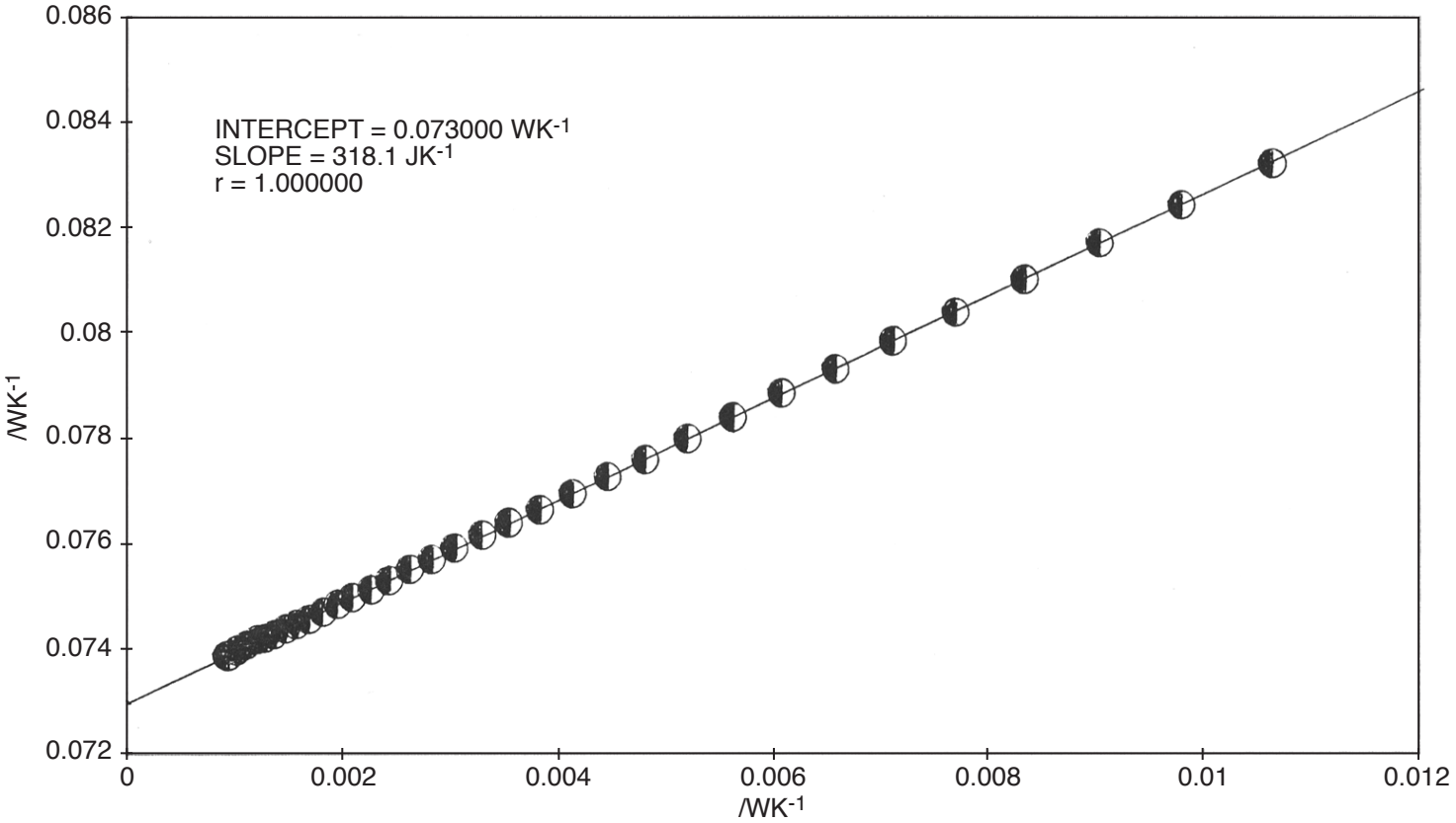

Fig. 12. ICARUS-2 simulation. Evaluation of $(k'^{o}_{c})_{151}$ using first order differences.

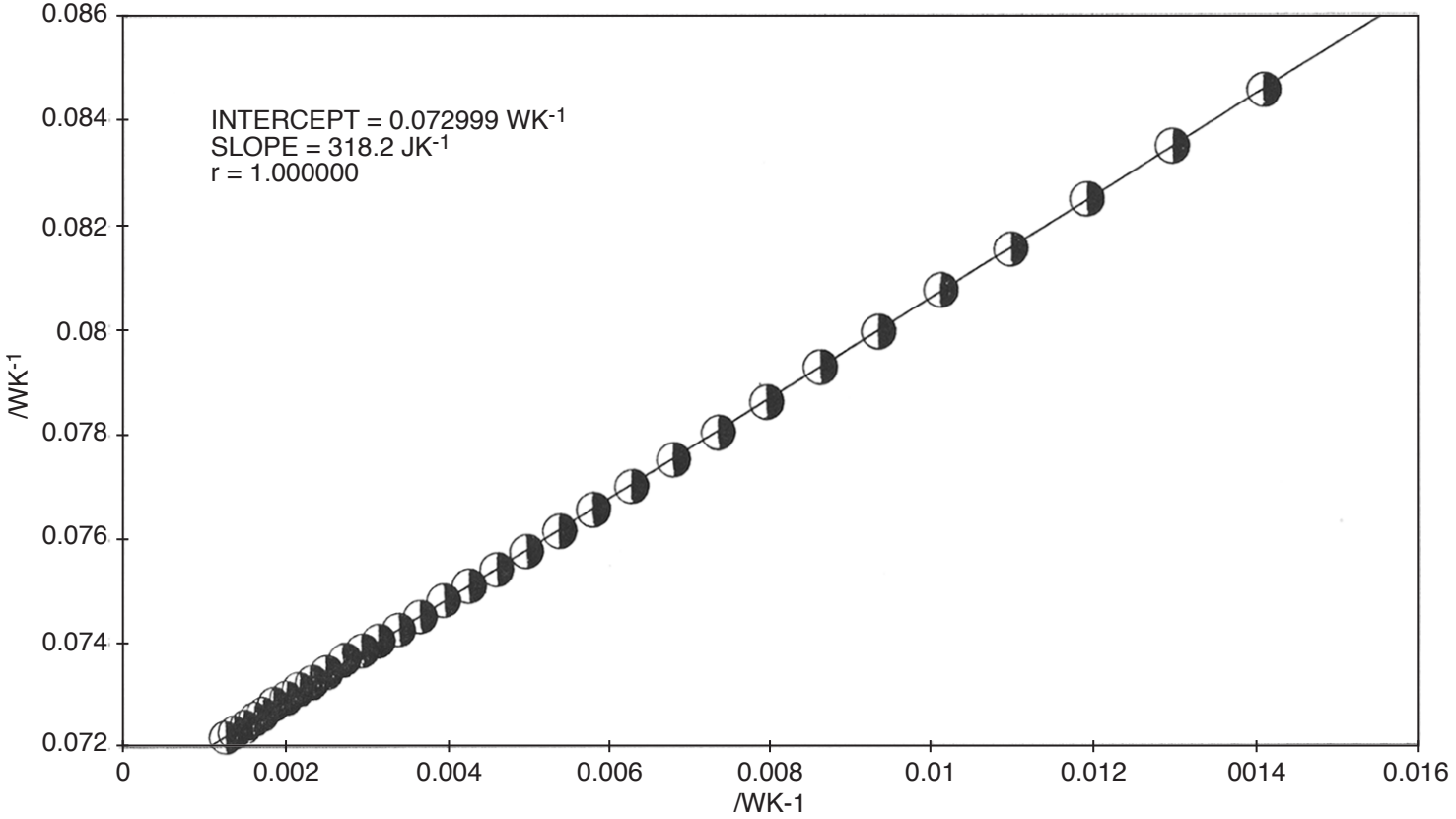

Fig. 13. ICARUS-2 simulation. Evaluation of $(k'_c{}^{o})_{161}$ using first order differences.

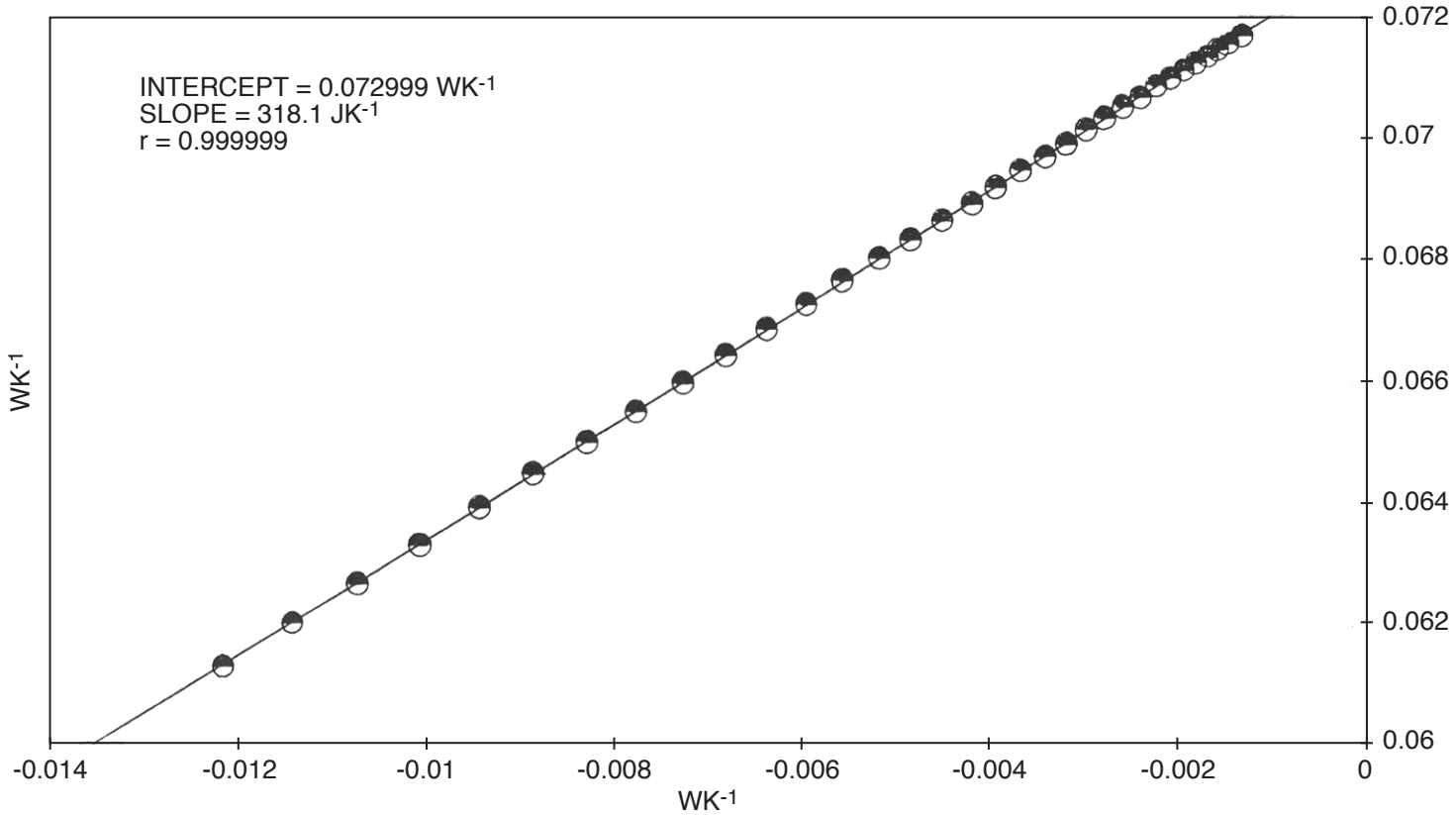

Fig. 14. ICARUS-2 simulation. Evaluation of $(k'_c{}^{o})_{171}$ using first order differences.

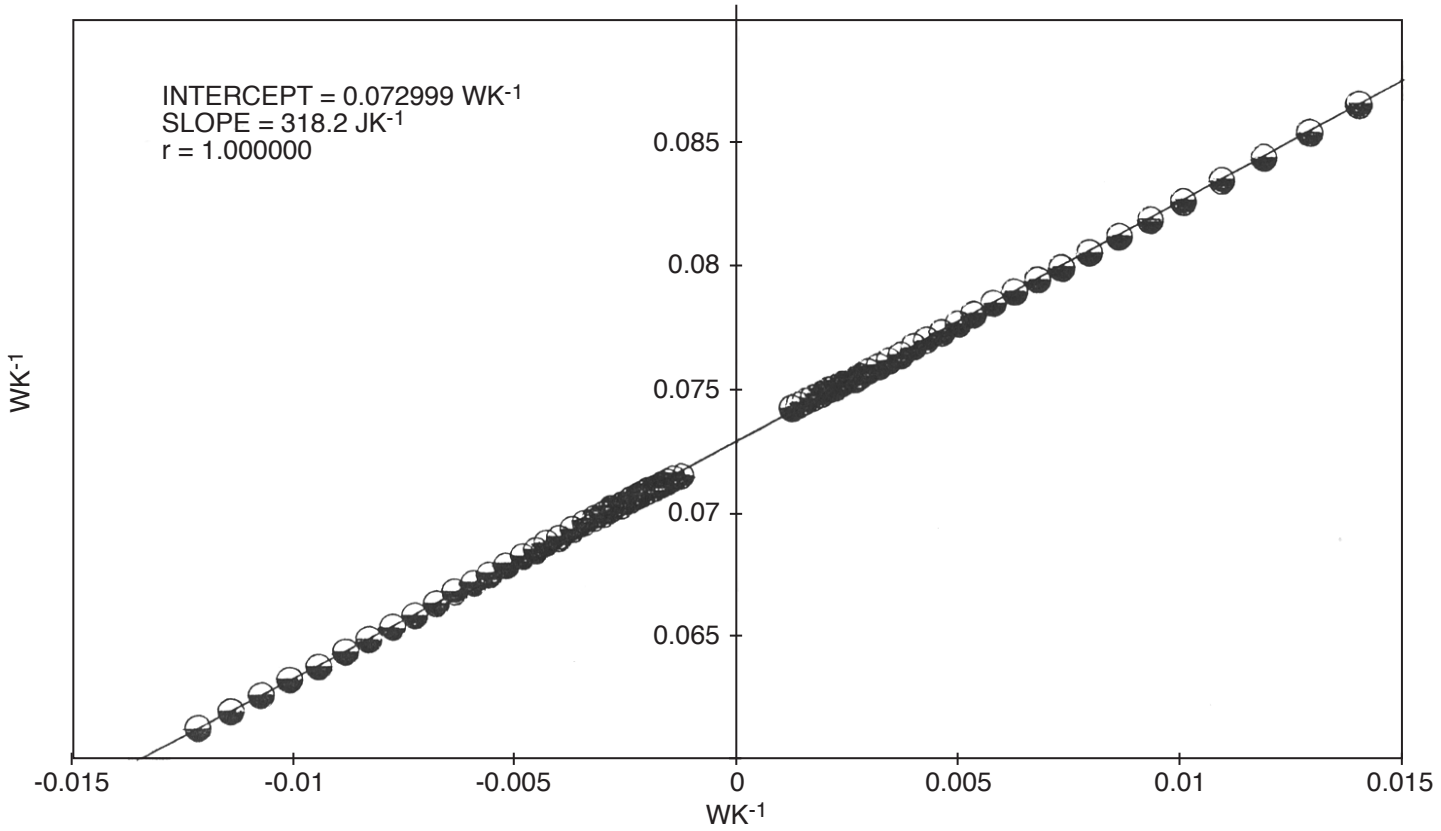

Fig. 15. ICARUS-2 simulation. Evaluation of $(k'_c{}^o)_{181}$.

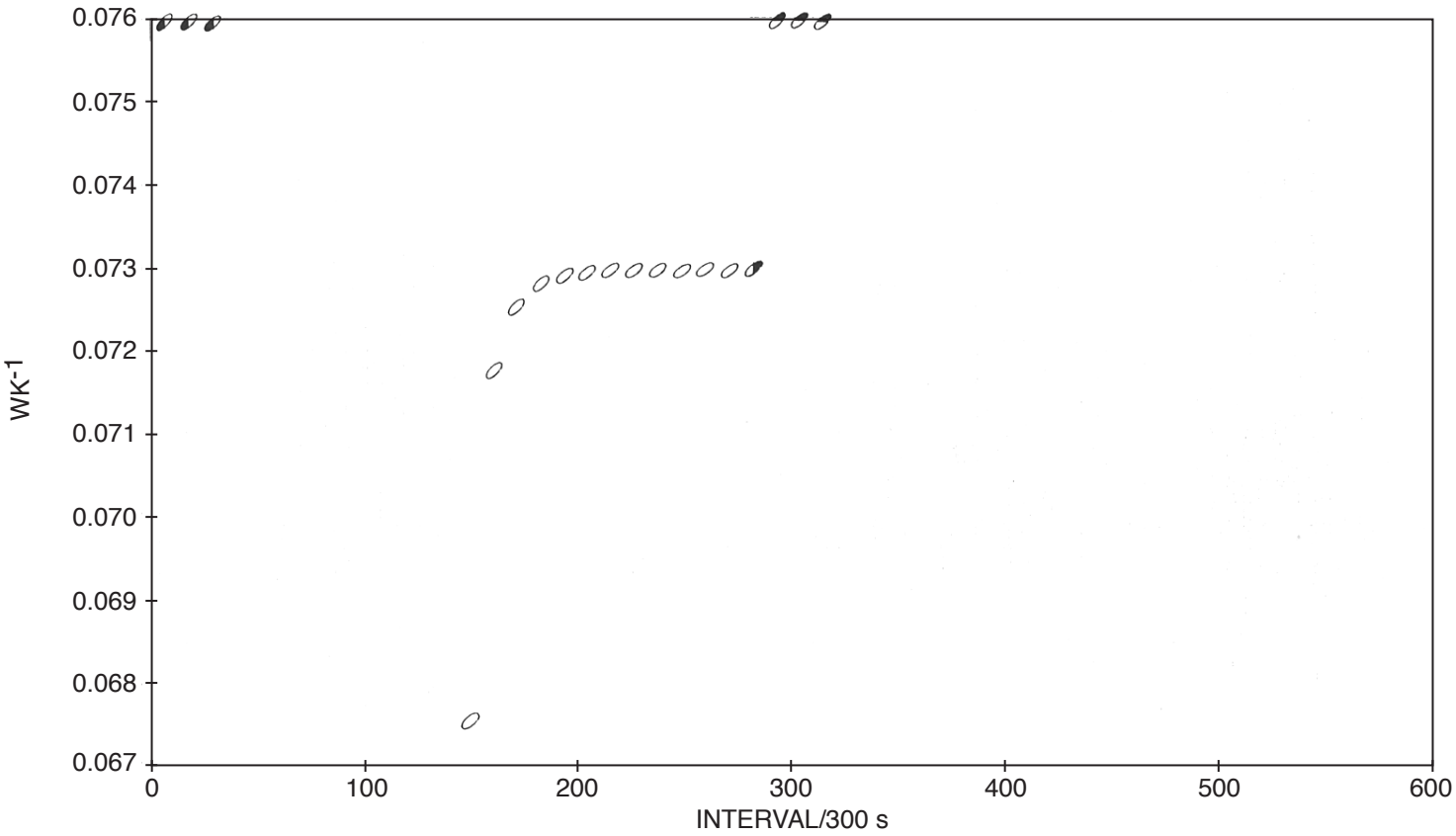

Fig. 16. ICARUS-2 simulation. $(k'_c)_{12}$, $(k'_c)_{152}$, $(k'_c{}^{o})_{162}$, and $(k'_c)_{172}$ versus time first order differences.

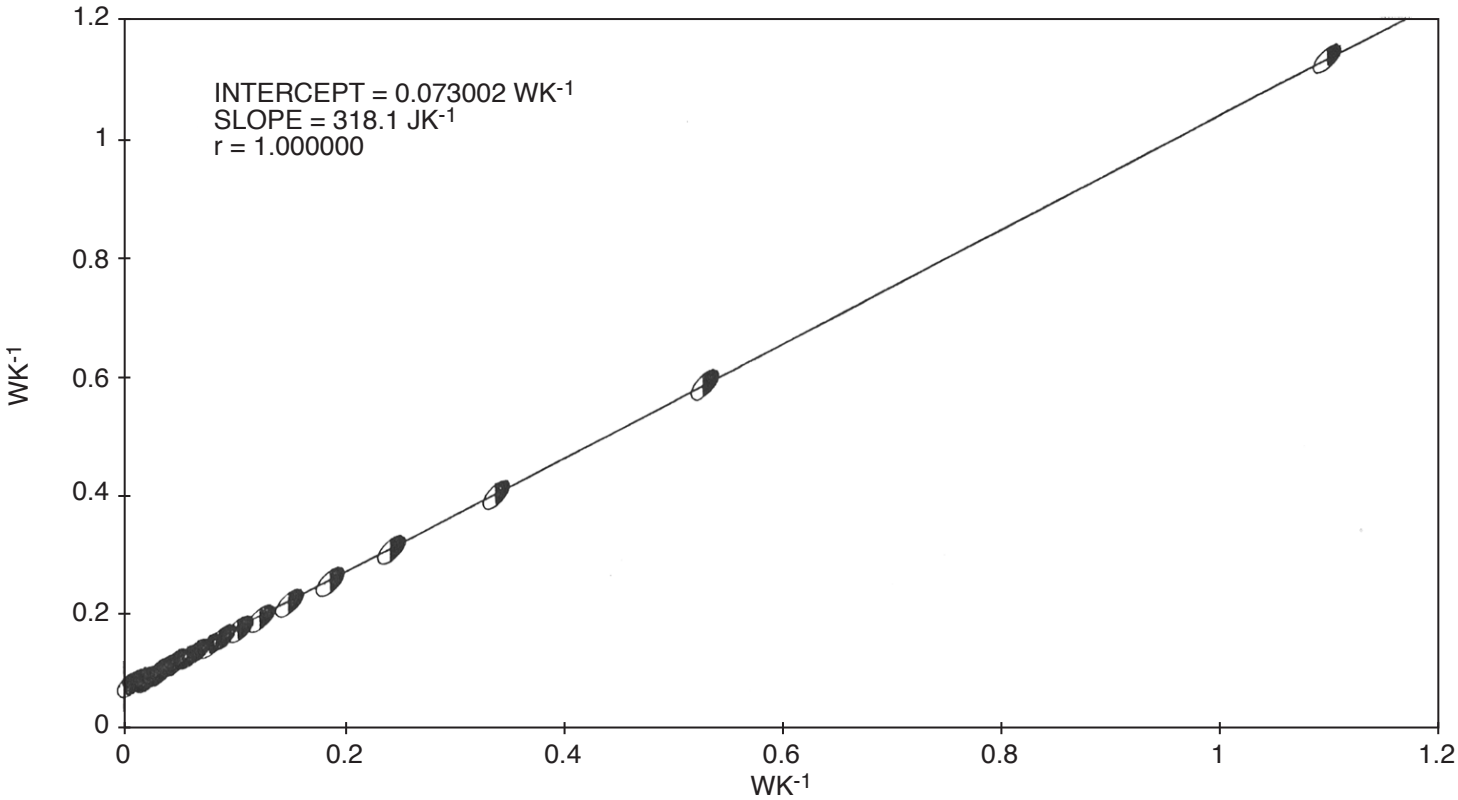

Fig. 17. ICARUS-2 simulation. Evaluation of $(k'^{o}_{c})_{162}$ using first order differences.

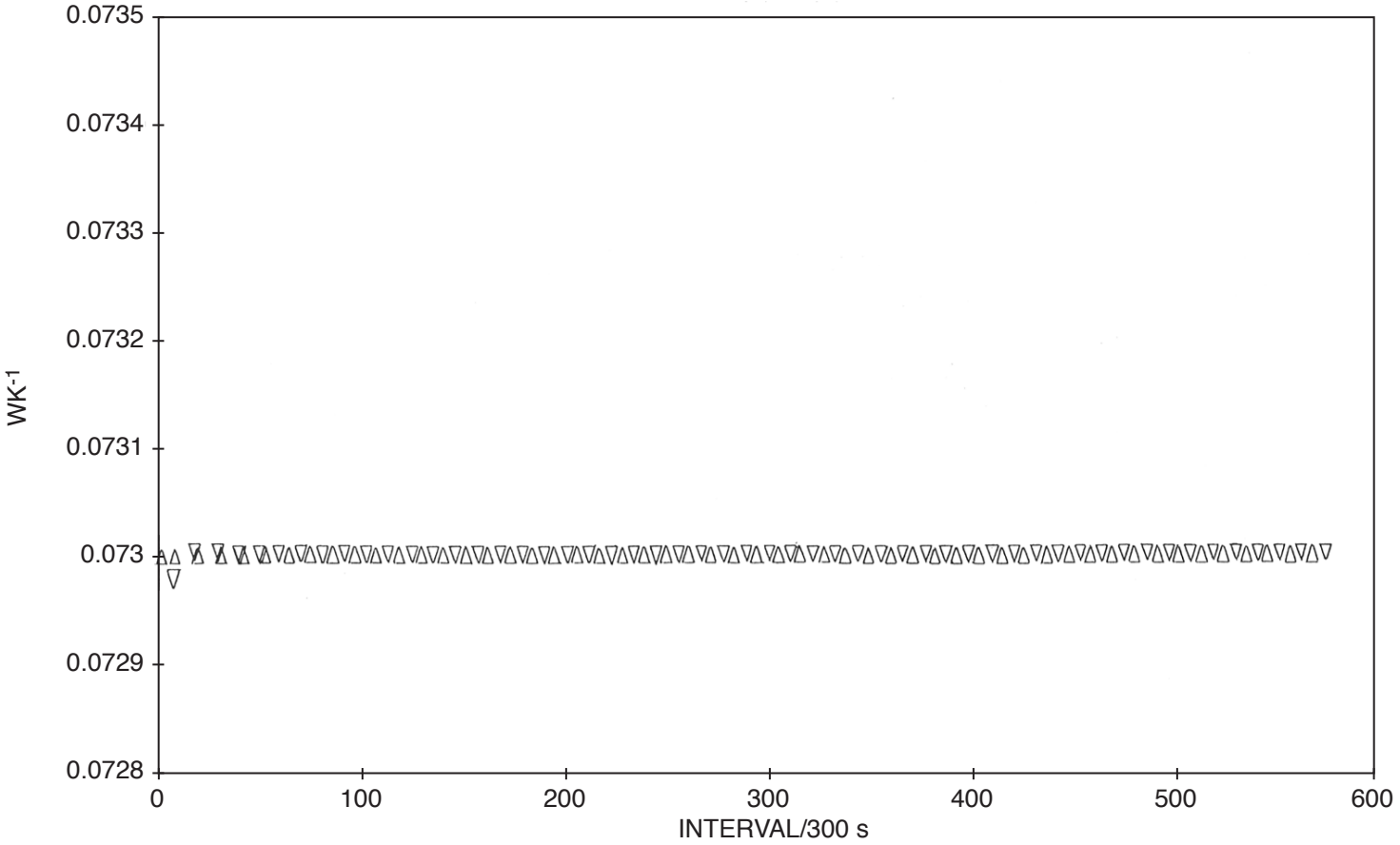

Fig. 18. ICARUS-2 simulation. $(k'_c)_{21}$ and $(k'_c)_{31}$ versus time.

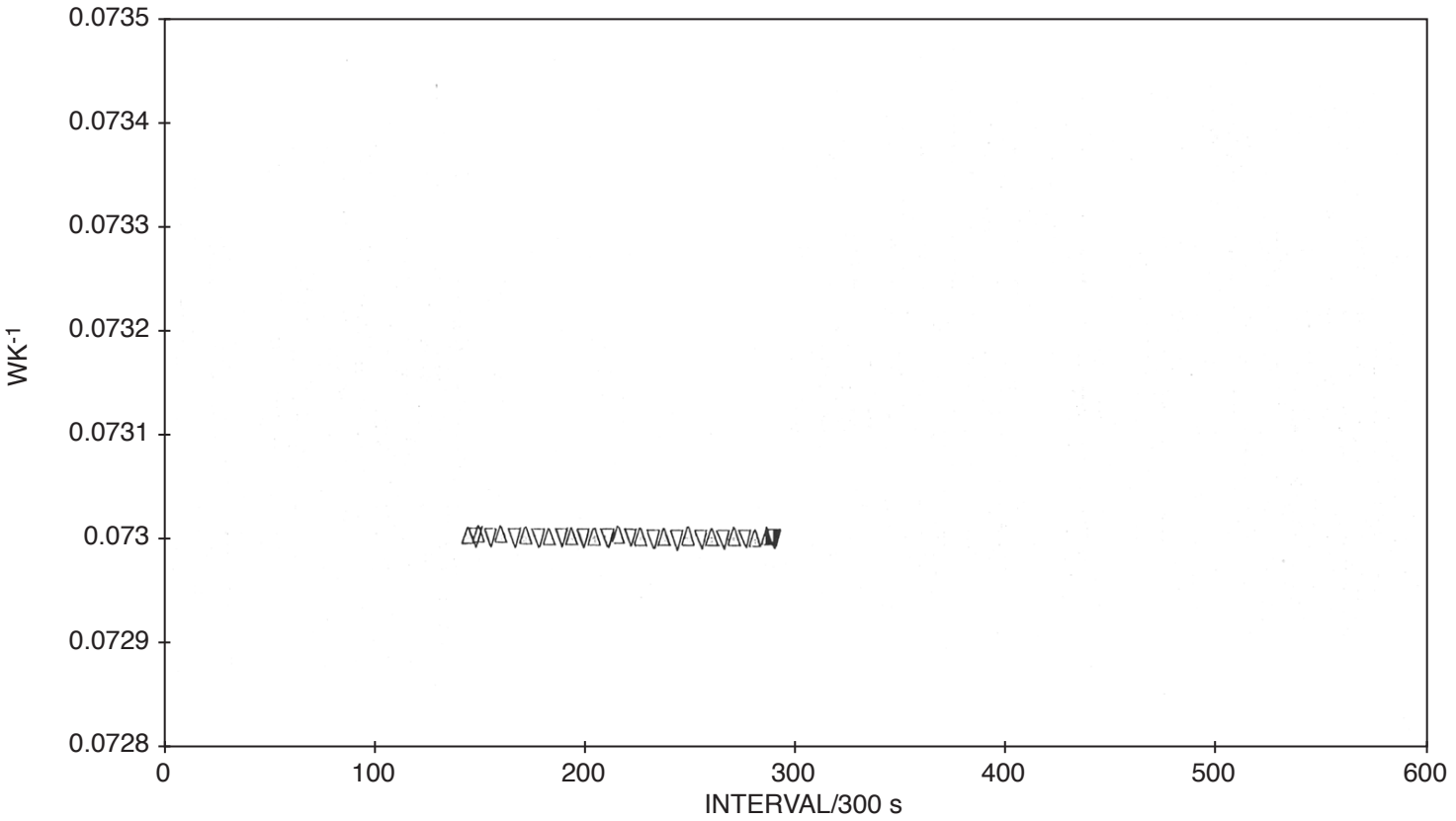

Fig.19. ICARUS-2 simulation. $(k'_c)_{21}$ and $(k'_c)_{22}$ versus time.

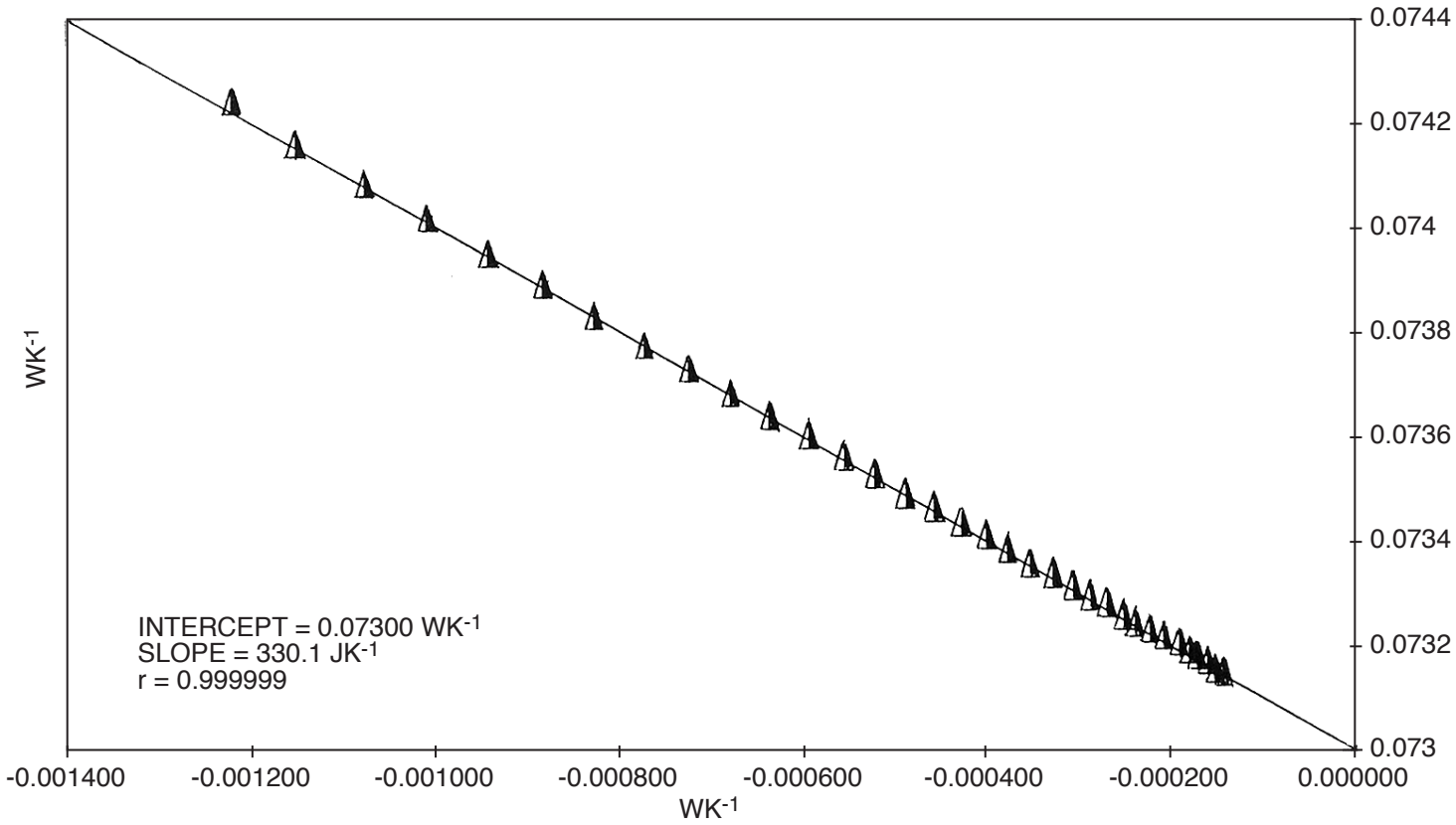

Fig. 20. ICARUS-2 simulation. Evaluation of $(k'_c)_{261}$.

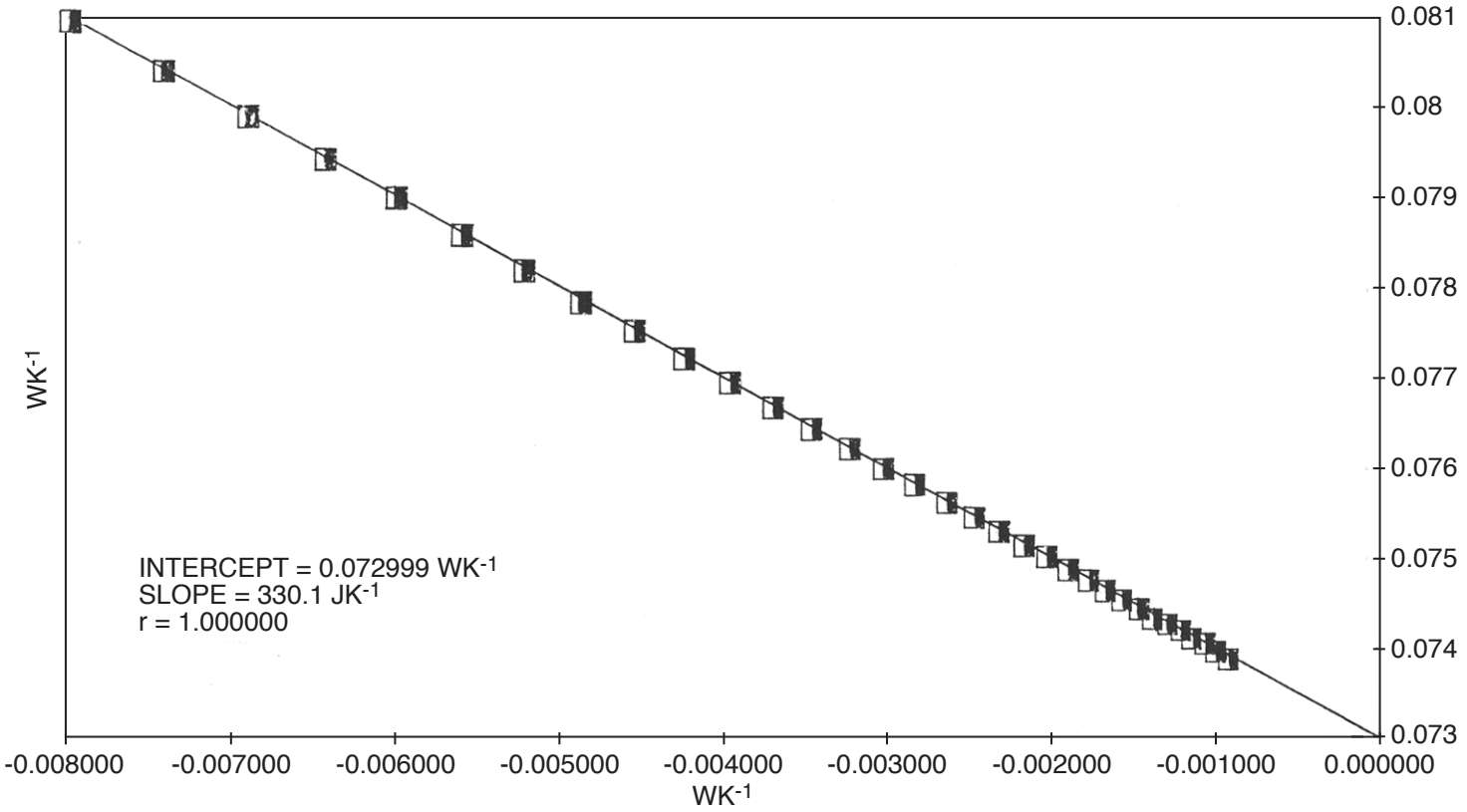

Fig. 21. ICARUS-2 simulation. Evaluation of $(k'_c{}^{o})_{262}$.

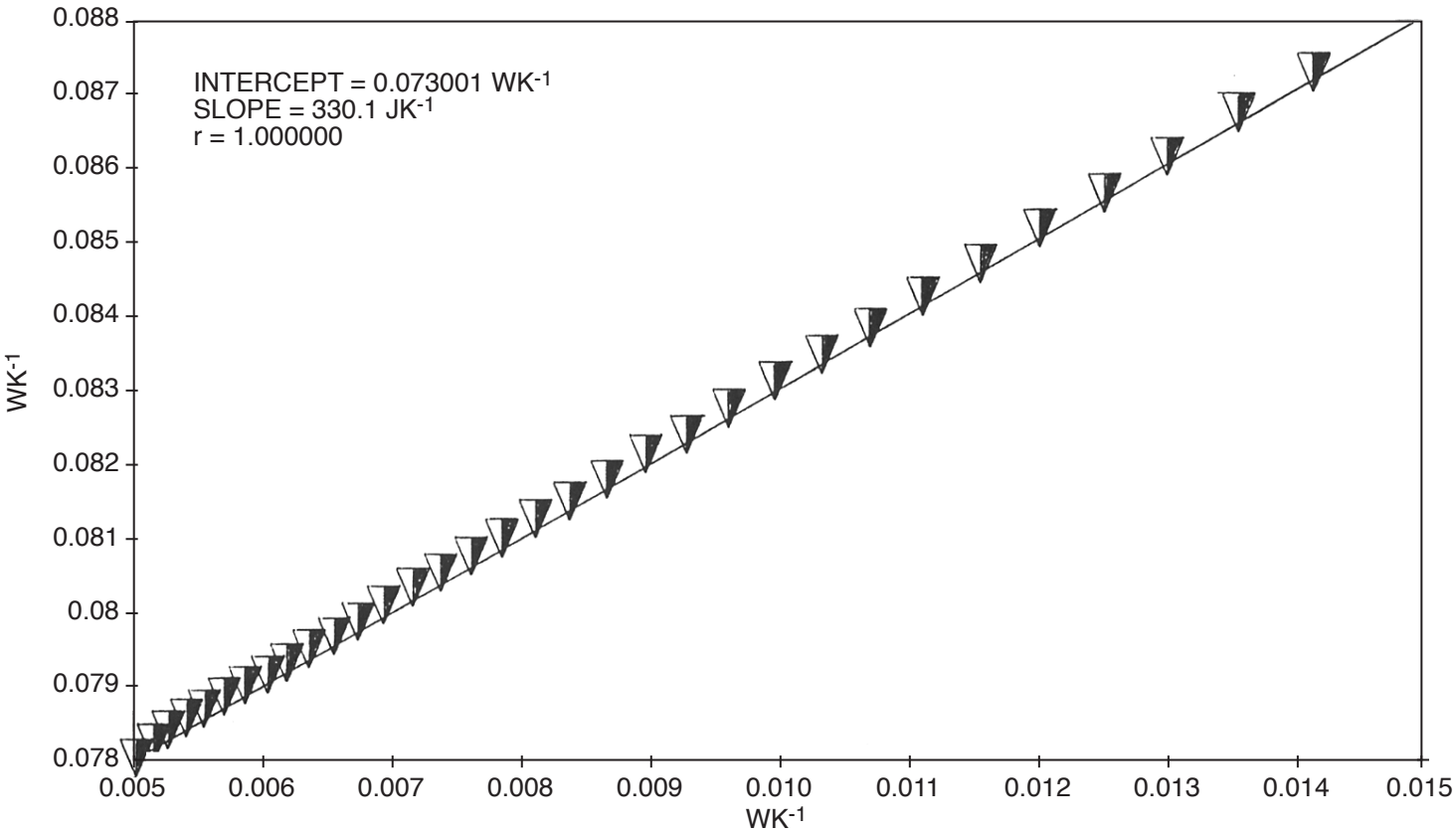

Fig. 22. ICARUS-2 simulation. Evaluation of $(k'_c{}^{o})_{361}$.

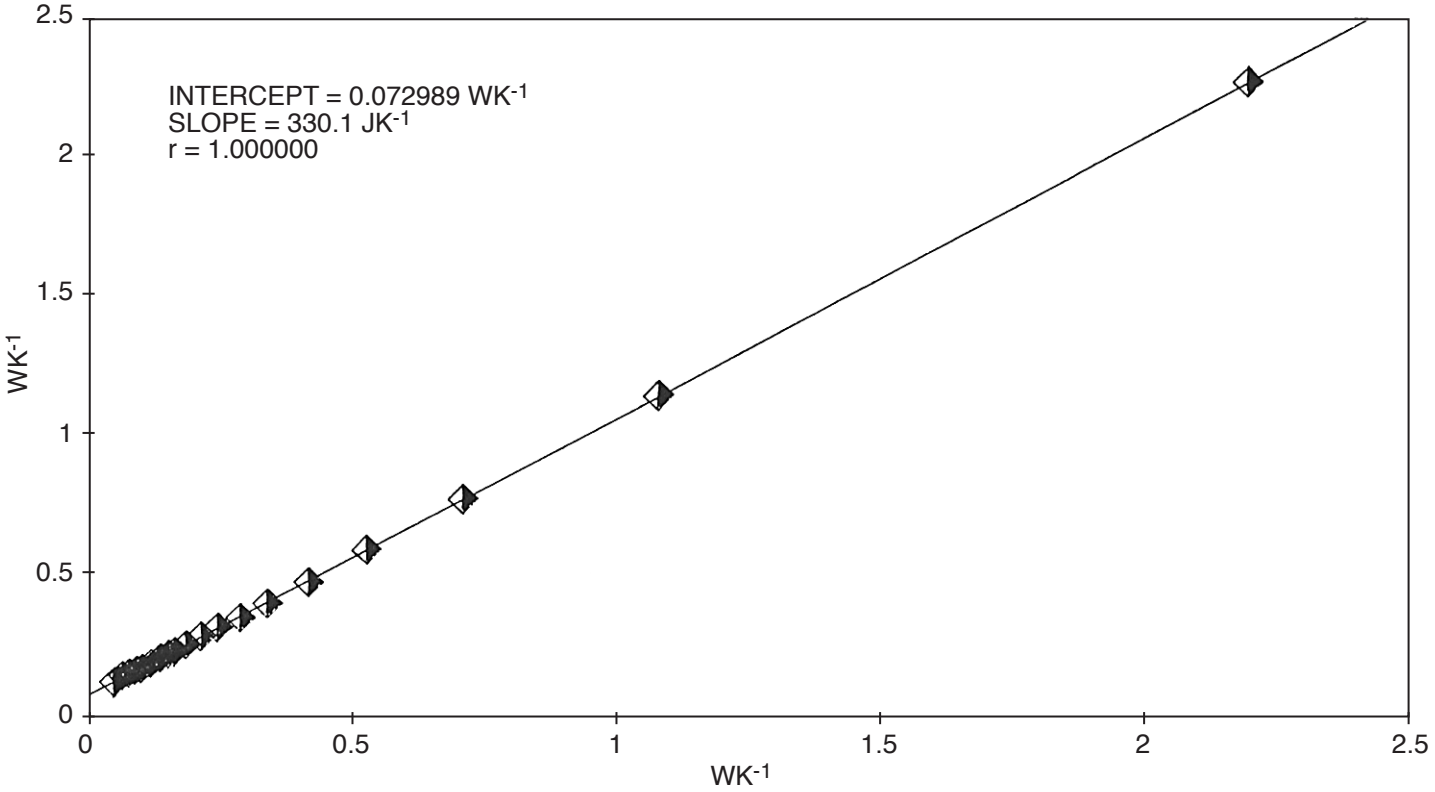

Fig. 23. ICARUS-2 simulation. Evaluation of $(k'_c{}^{o})_{362}$.

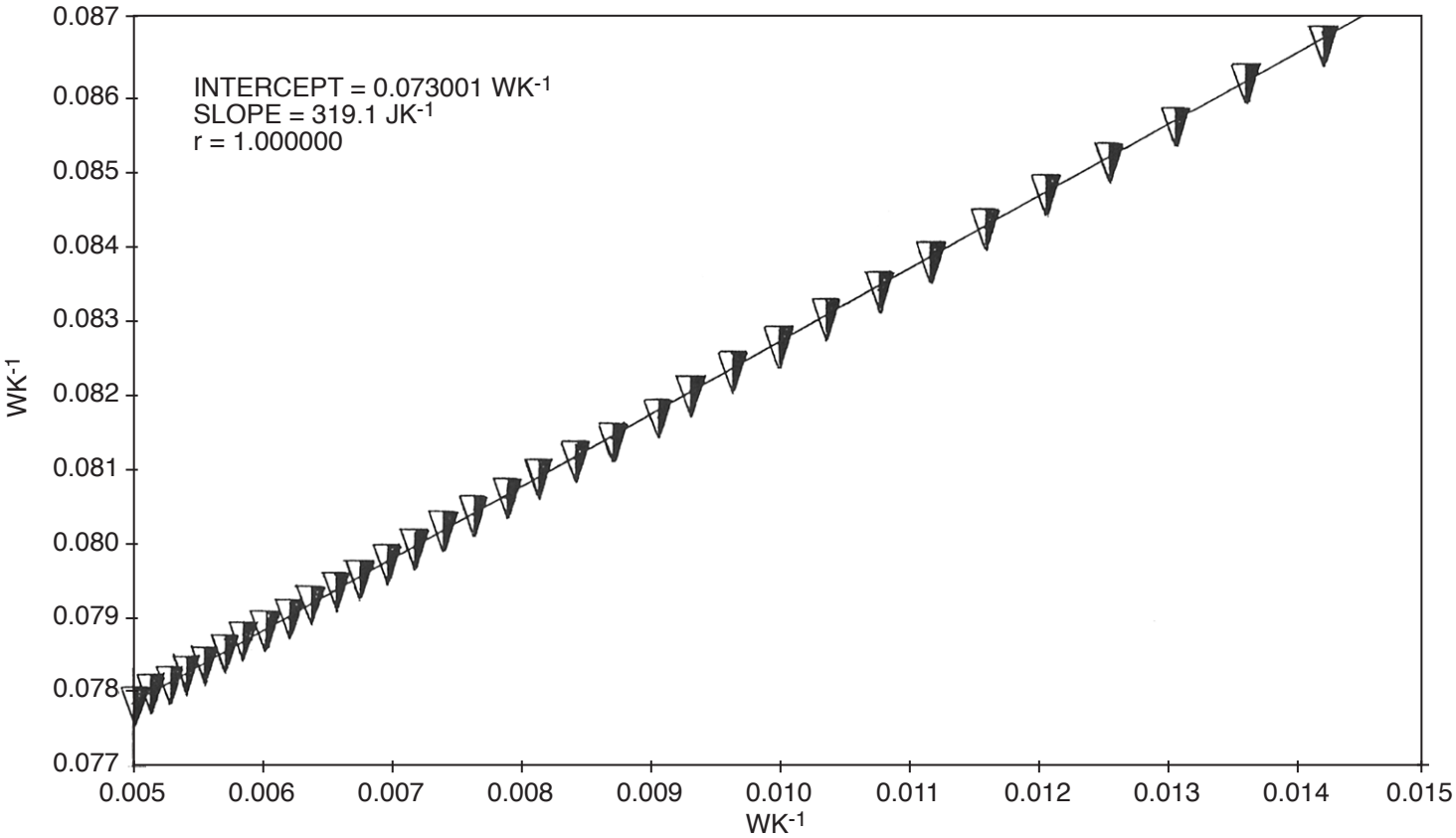

Fig. 24. ICARUS-2 simulation. Evaluation of $(k'_c{}^o)_{361}$ using mid-point integration rule.

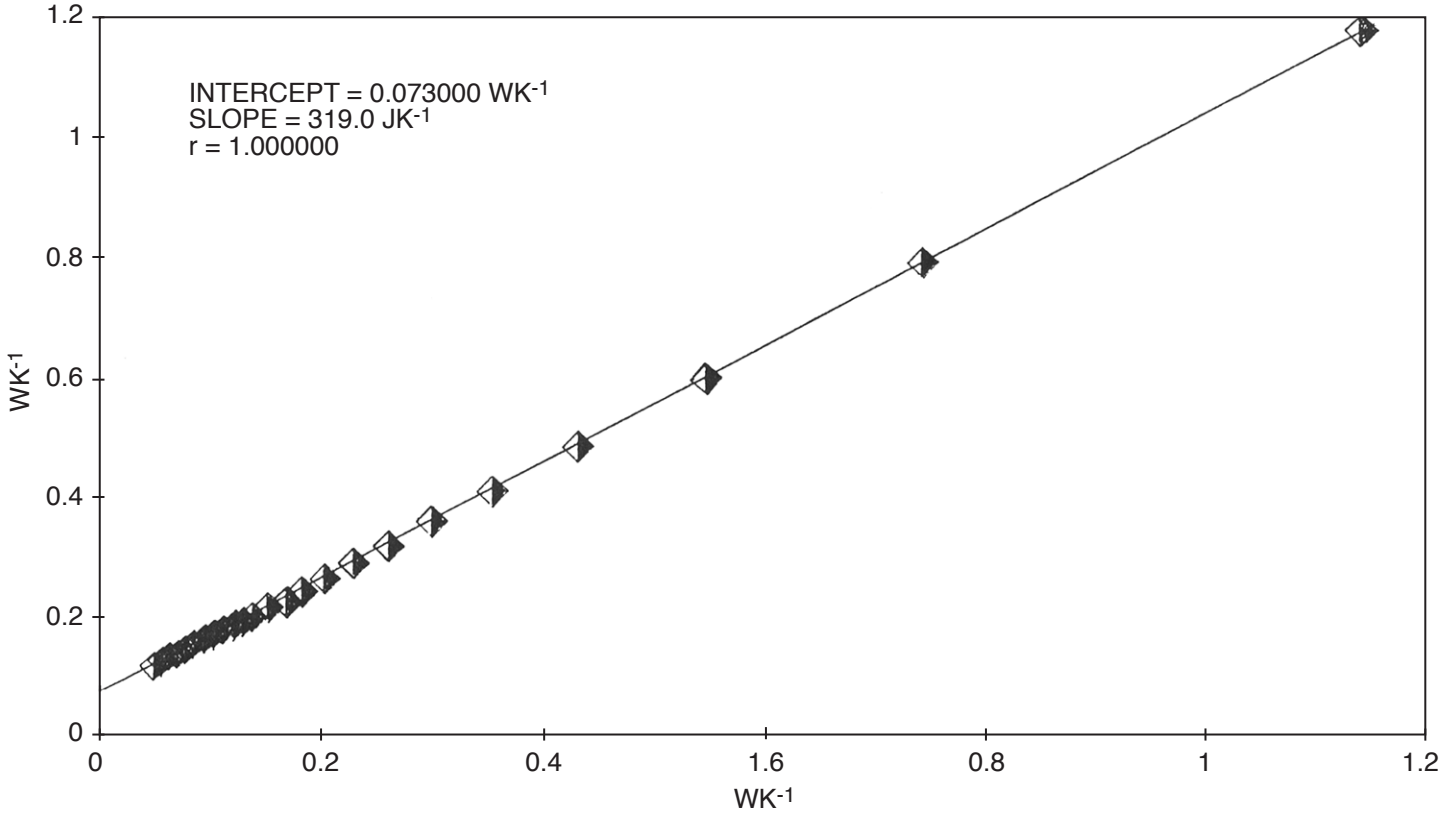

Fig. 25. ICARUS-2 simulation. Evaluation of $(k'_R{}^o)_{362}$ using mid-point integration rule.

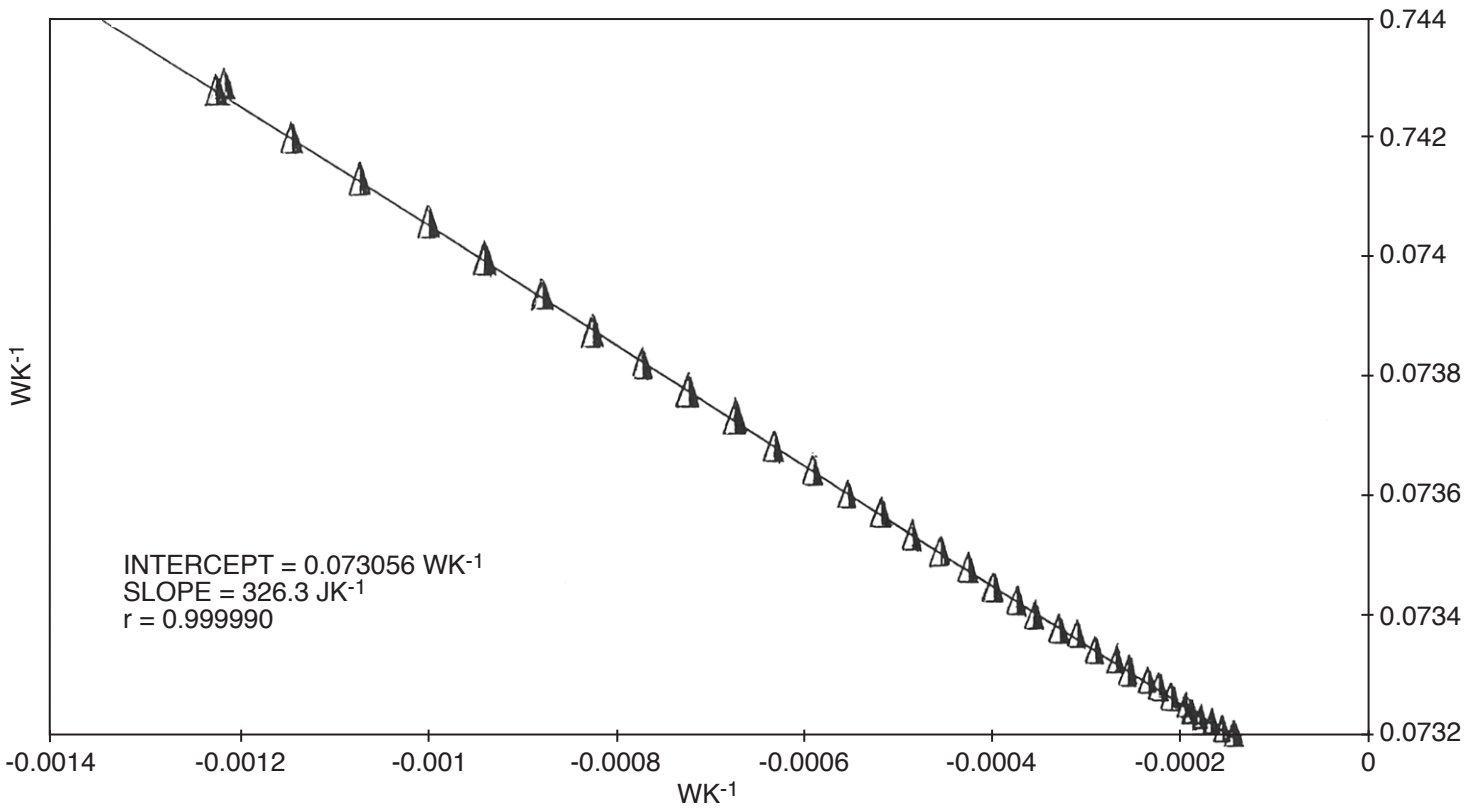

Fig. 26. ICARUS-2 simulation. Evaluation of $(k'_{R^o})_{261}$ with +30J error in input enthalpy.

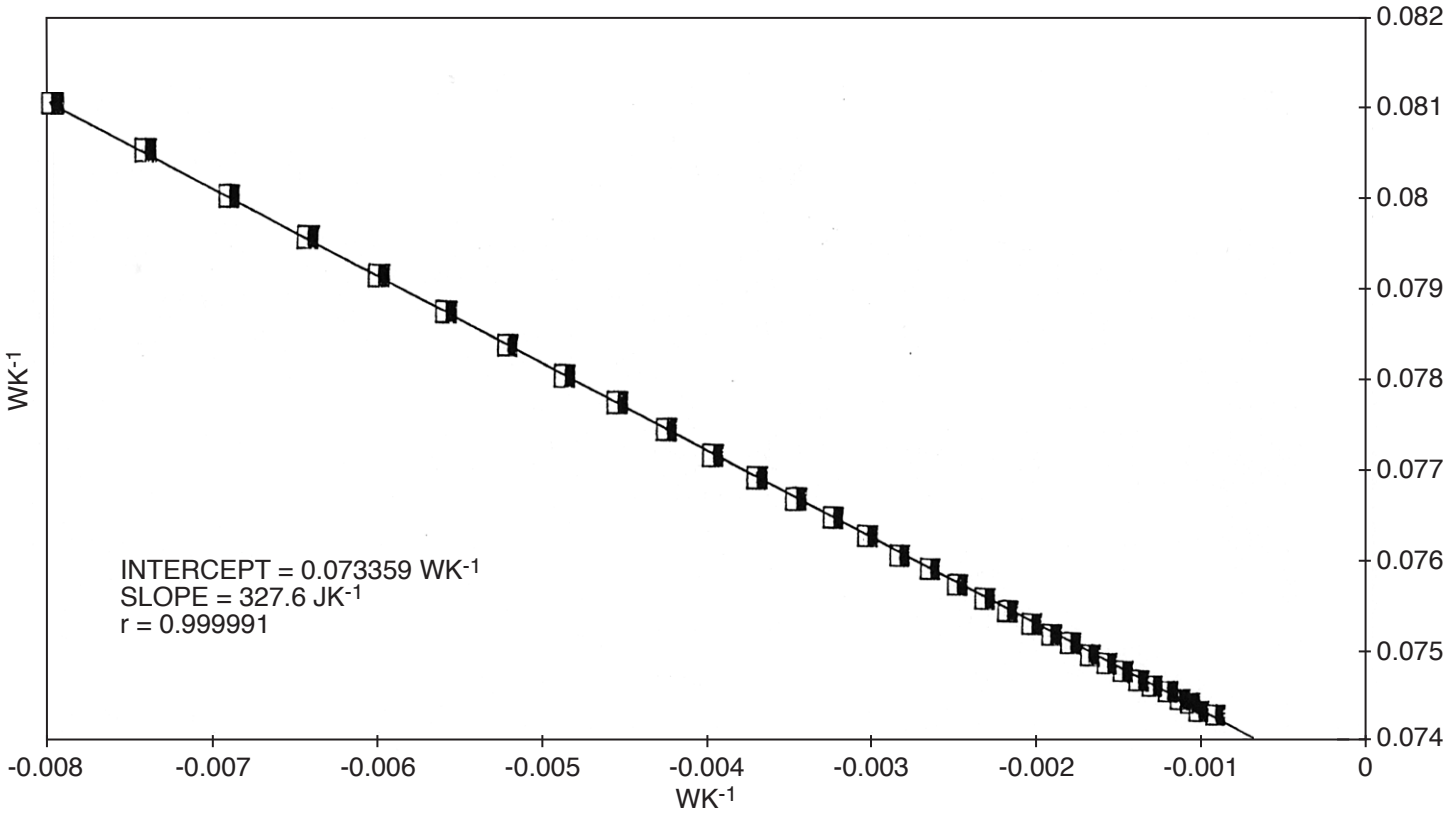

Fig. 27. ICARUS-2 simulation. Evaluation of $(k'_R{}^o)_{262}$ with +30J error in input enthalpy.

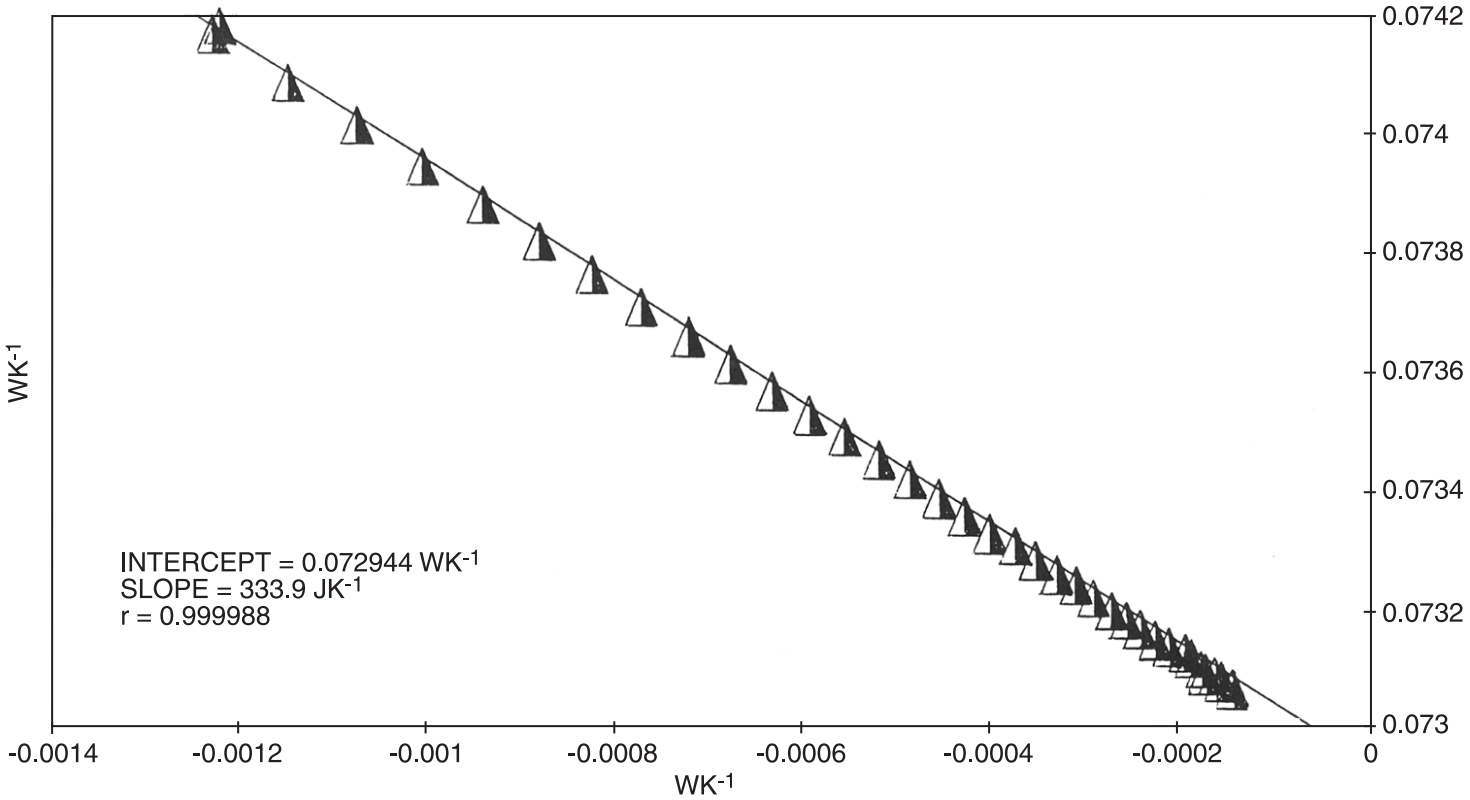

Fig. 28. ICARUS-2 simulation. Evaluation of $(k'_R{}^o)_{261}$ with +30J error in input enthalpy.

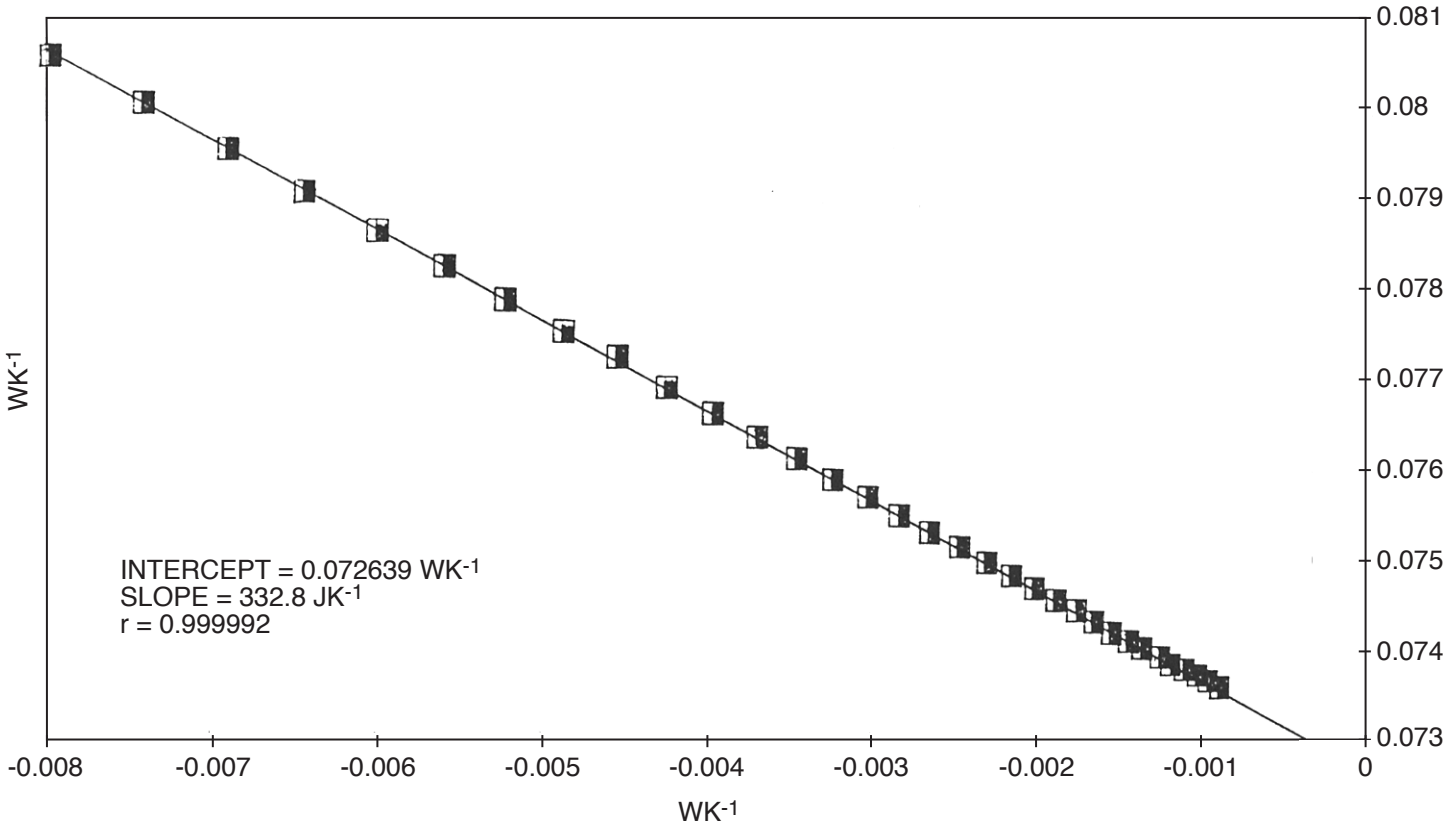

Fig. 29. ICARUS-2 simulation. Evaluation of $(k'_R{}^o)_{262}$ with -30J error in input enthalpy.

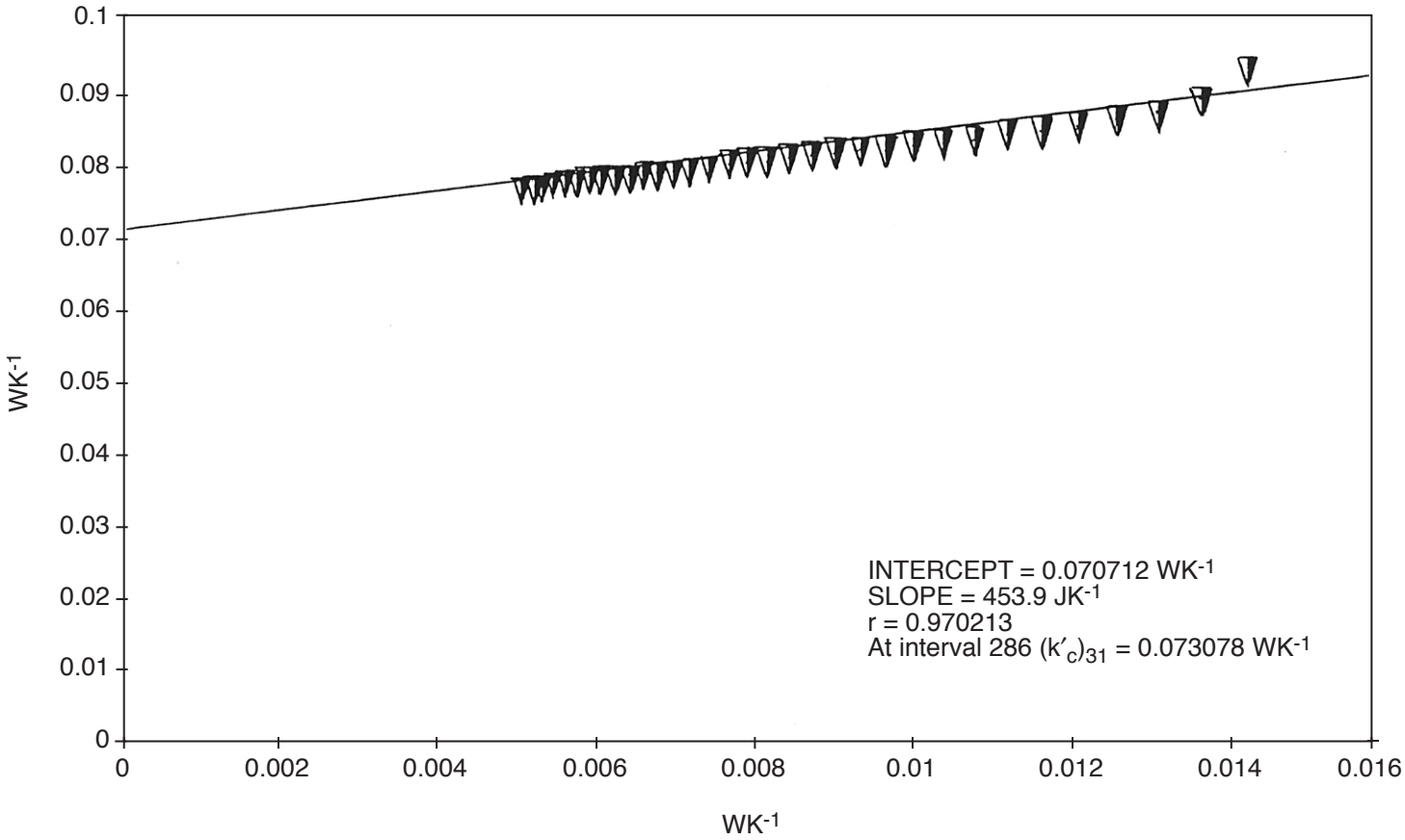

Fig. 30. ICARUS-2 simulation. Evaluation of $(k'_c{}^{o})_{361}$ +30J error in input enthalpy.

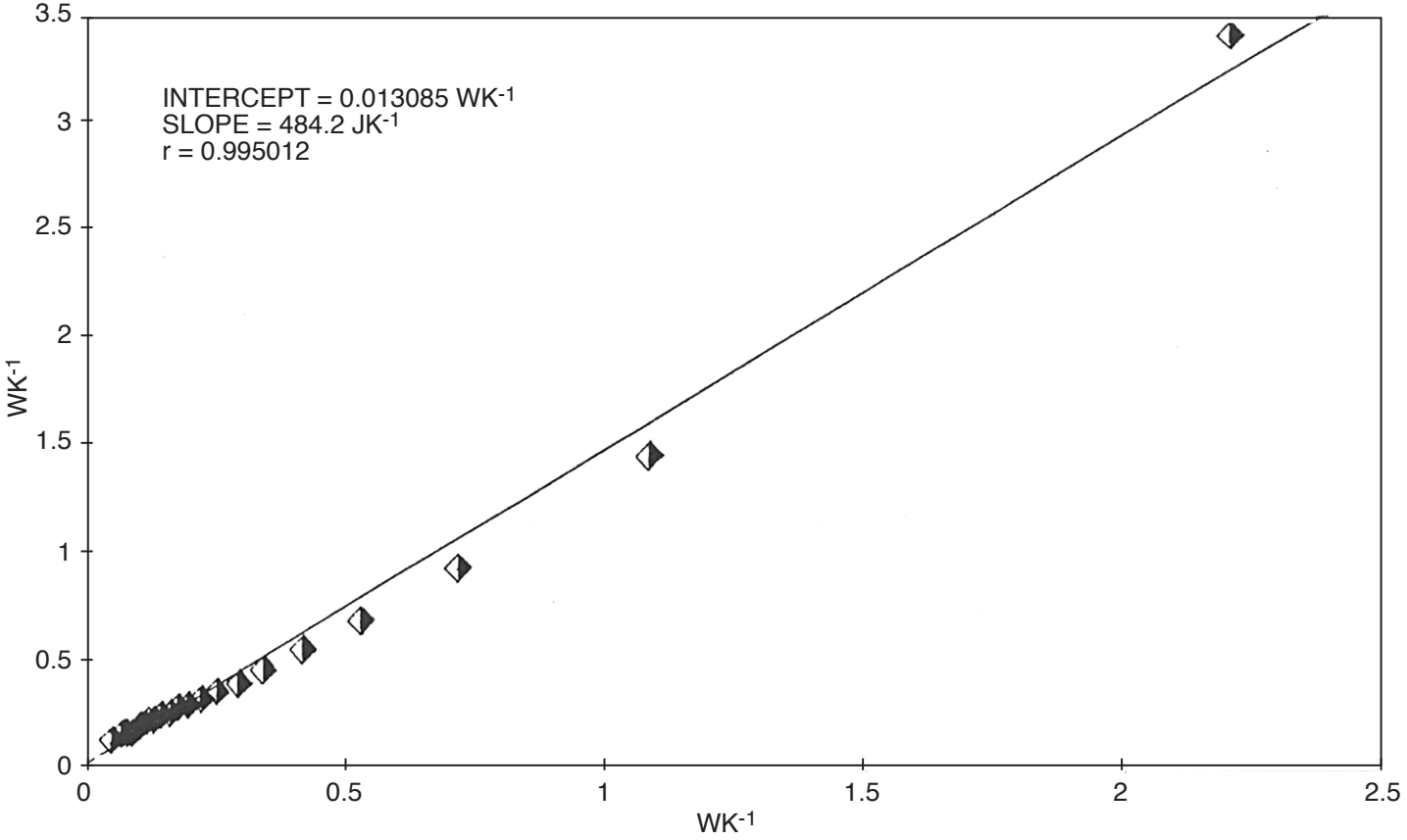

Fig. 31. ICARUS-2 simulation. Evaluation of $(k'_c{}^{o})_{362}$ with error +30J in input enthalpy and using intervals 145–177.

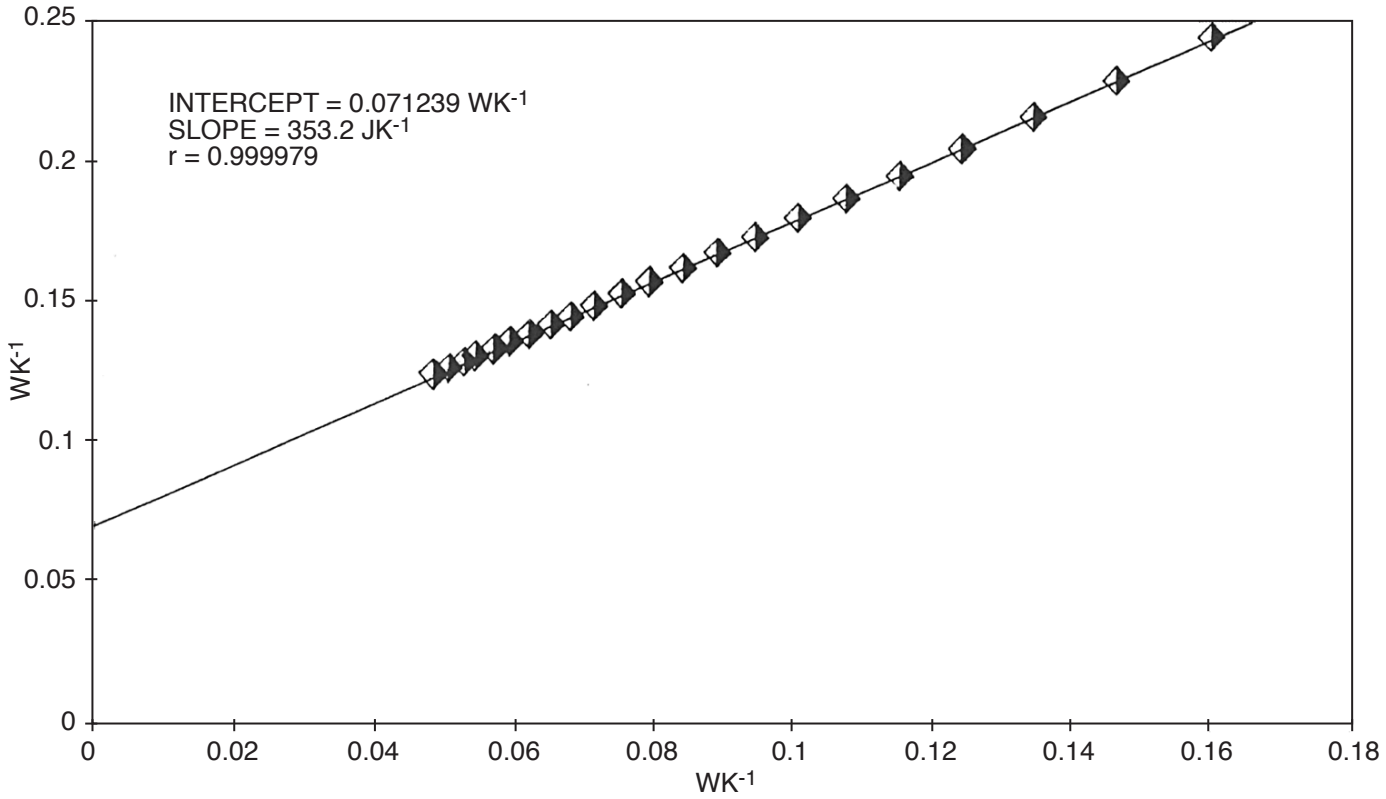

Fig. 32. ICARUS-2 simulation. Evaluation of $(k'_c{}^{o})_{362}$ with error +30J in input enthalpy and using intervals 156–177.

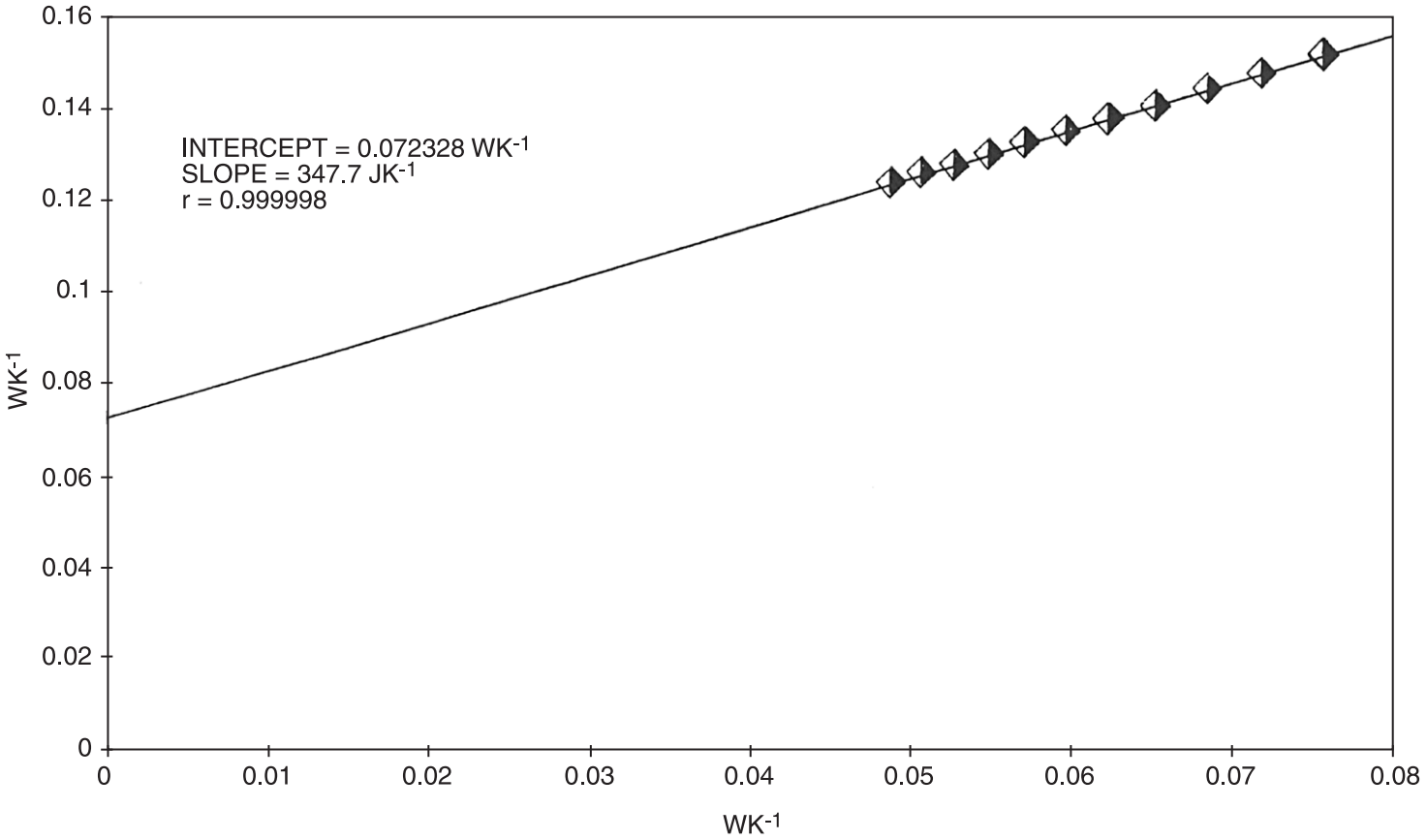

Fig. 33. ICARUS-2 simulation. Evaluation of $(k'_c{}^{o})_{362}$ with error +30J in input enthalpy and using intervals 167–177.

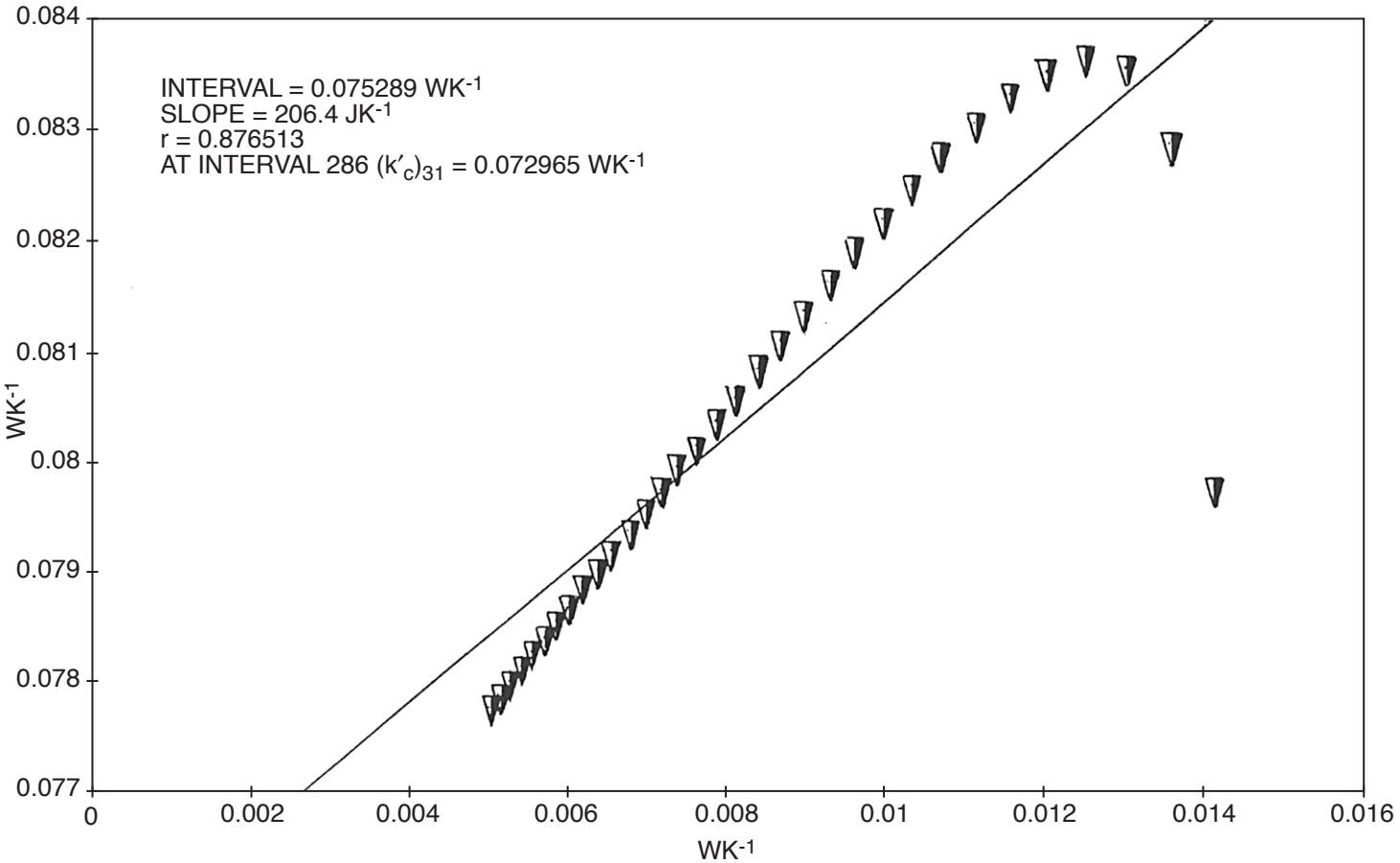

Fig. 34. ICARUS-2 simulation. Evaluation of $(k'_c{}^{o})_{361}$ with error +30J in input enthalpy.

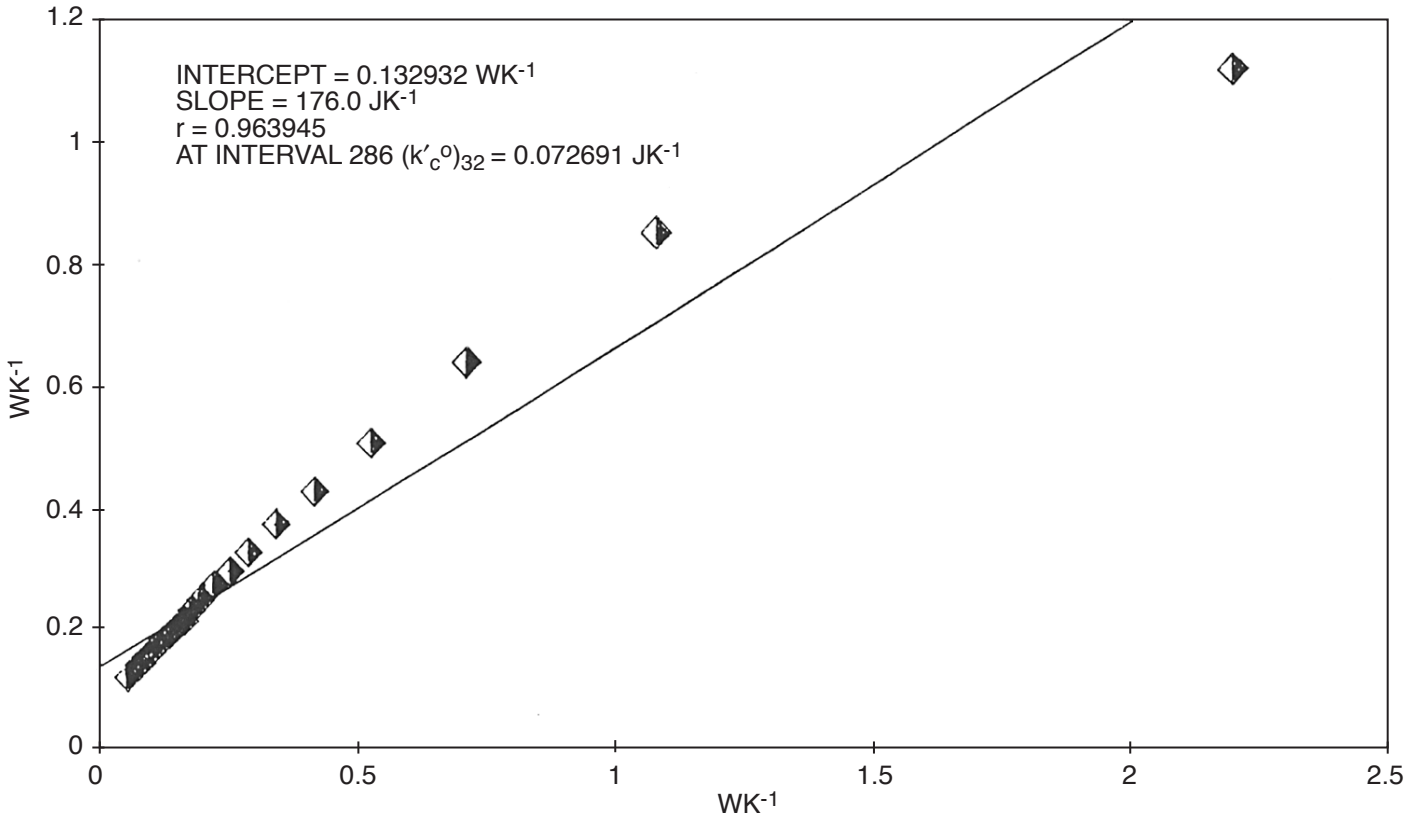

Fig. 35. ICARUS-2 simulation. Evaluation of $(k'_c{}^{o})_{362}$ with error -30J in input enthalpy and using intervals 145–177.

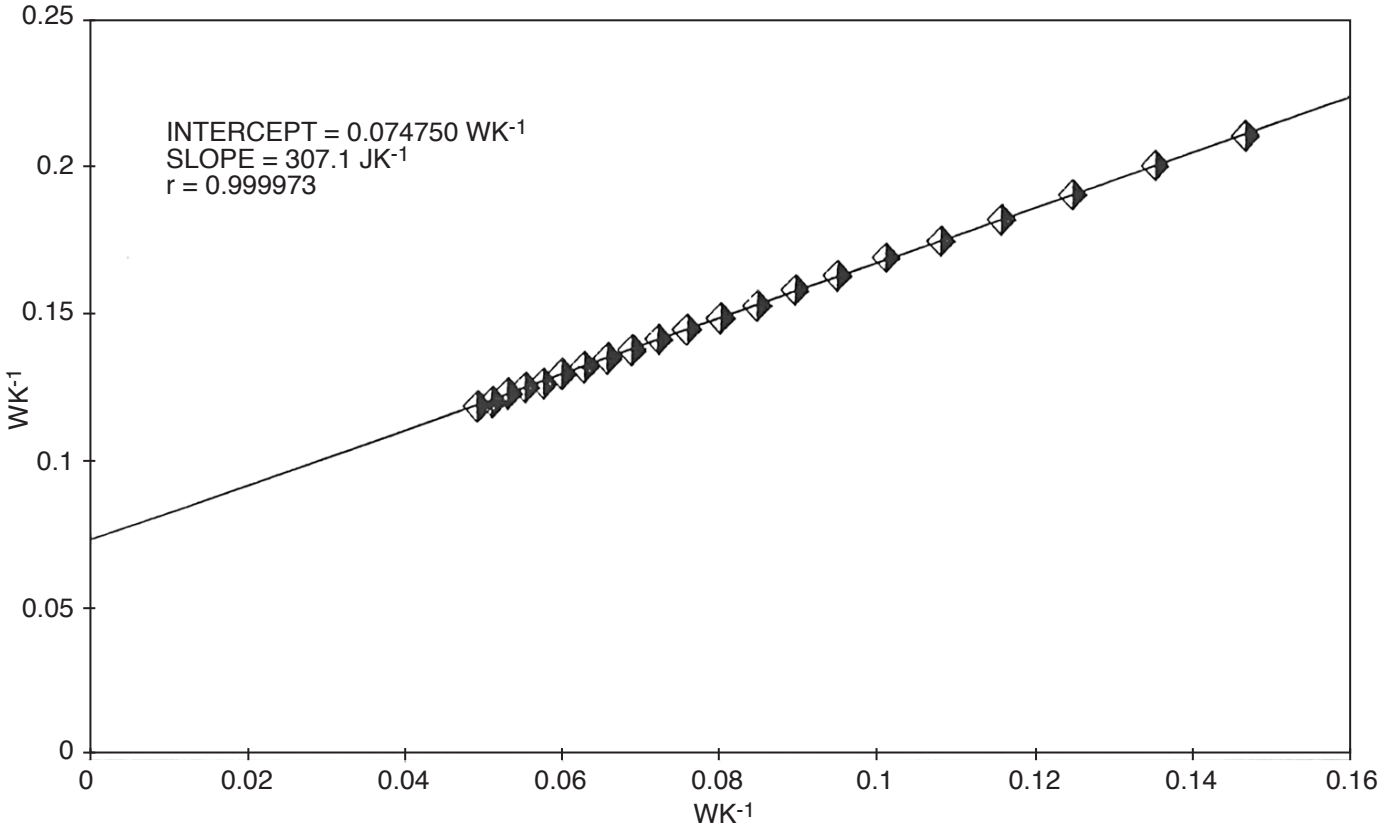

Fig. 36. ICARUS-2 simulation. Evaluation of $(k'_c{}^{o})_{362}$ with error +30J in input enthalpy and using intervals 156–177.

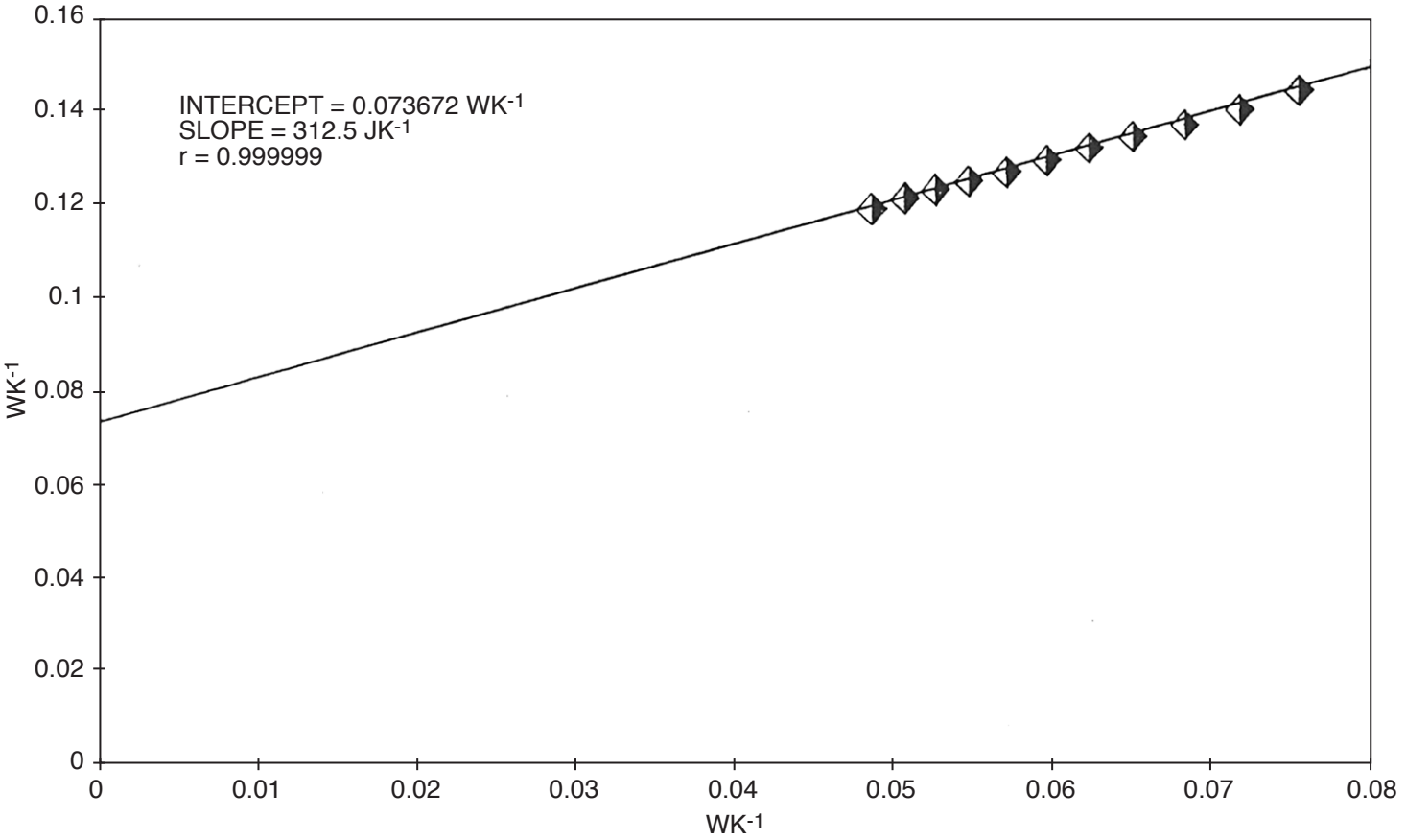

Fig. 37. ICARUS-2 simulation. Evaluation of $(k'_c{}^{o})_{362}$ with error +30J in input enthalpy and using intervals 167–177.

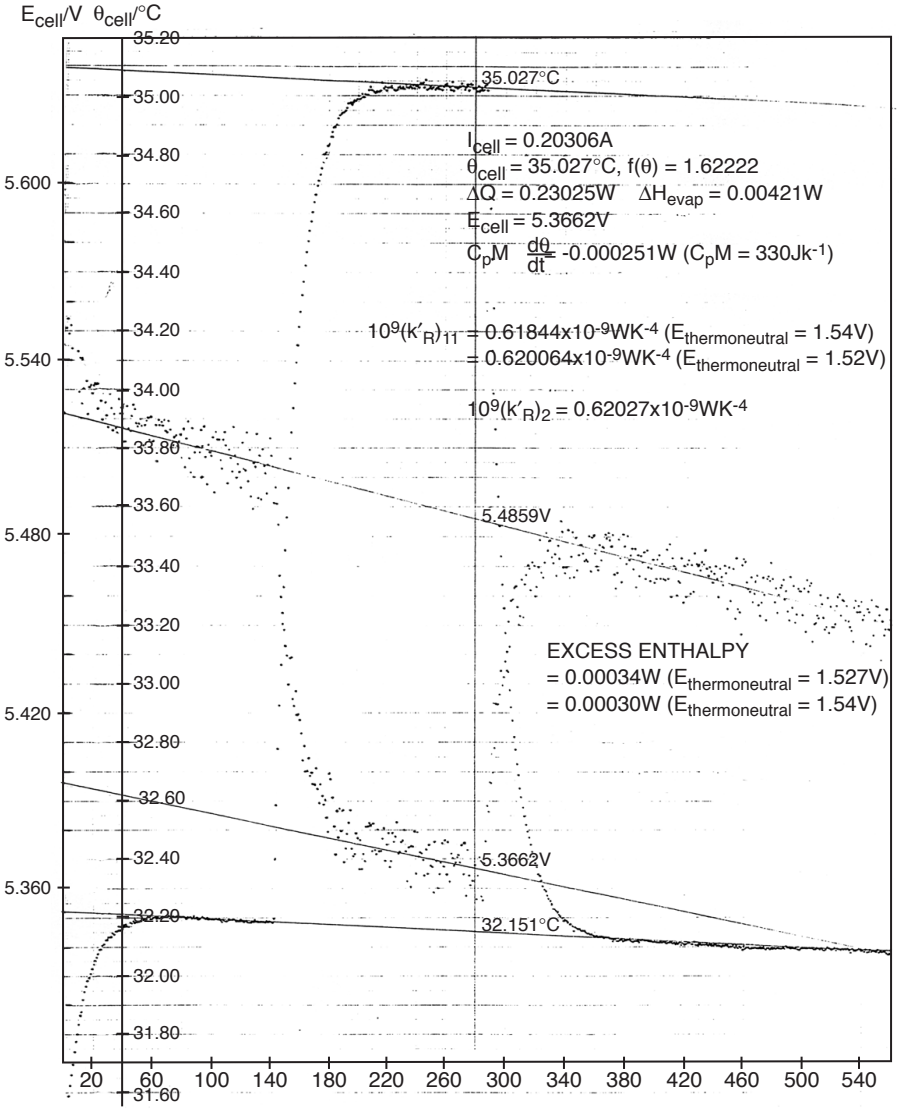

Fig. 38. The "raw data" for a blank experiment (Pt in 0.1M LiOD/D_2O) in an ICARUS-2 calorimeter. Third measurement cycle. Evaluation of $(k'_4)_{11}$ and $(k'_R)_2$ using the graphical method.

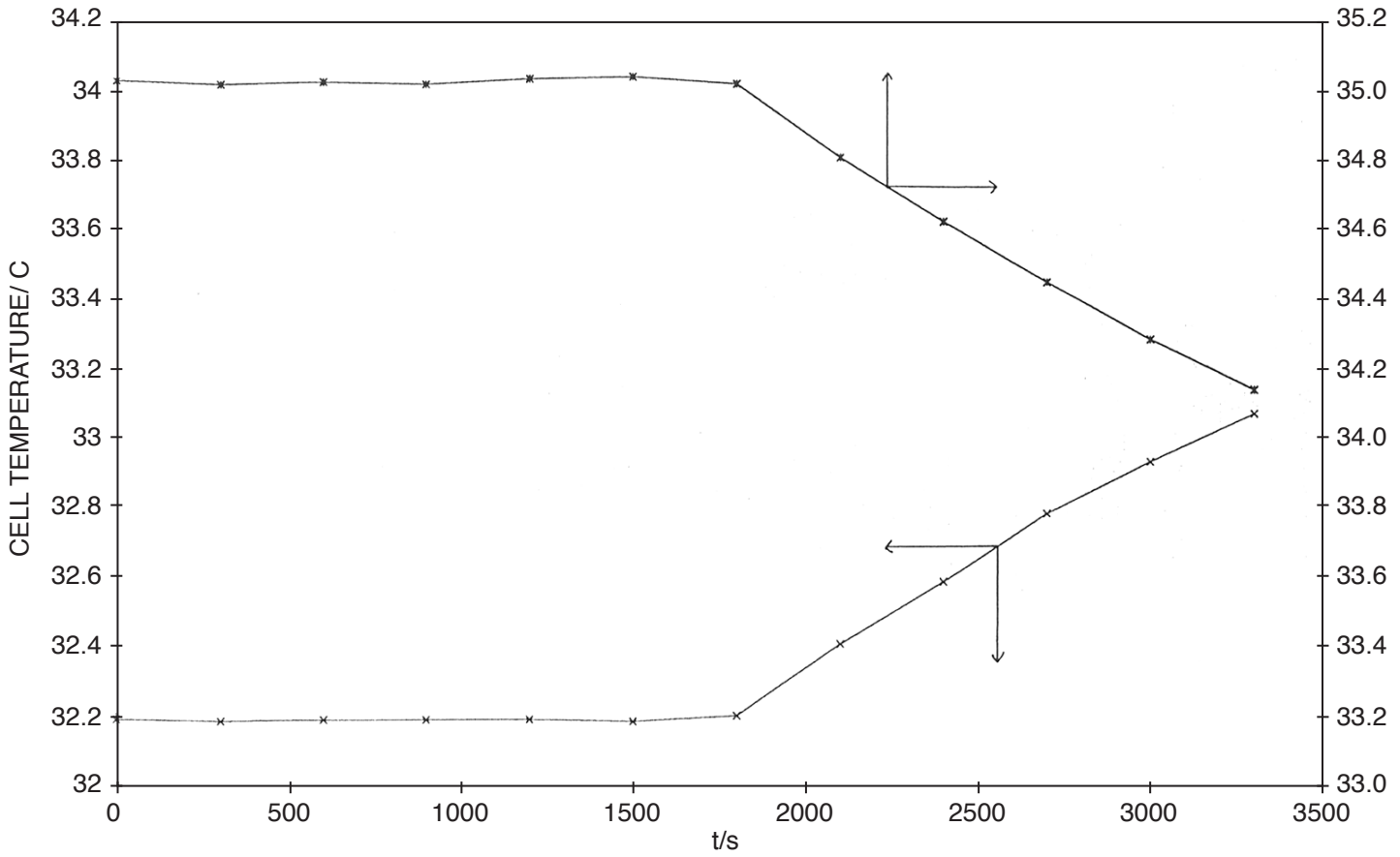

Fig. 39. The Temperature–Time variations in Fig. 38 in the vicinity of t and t on an expanded scale.

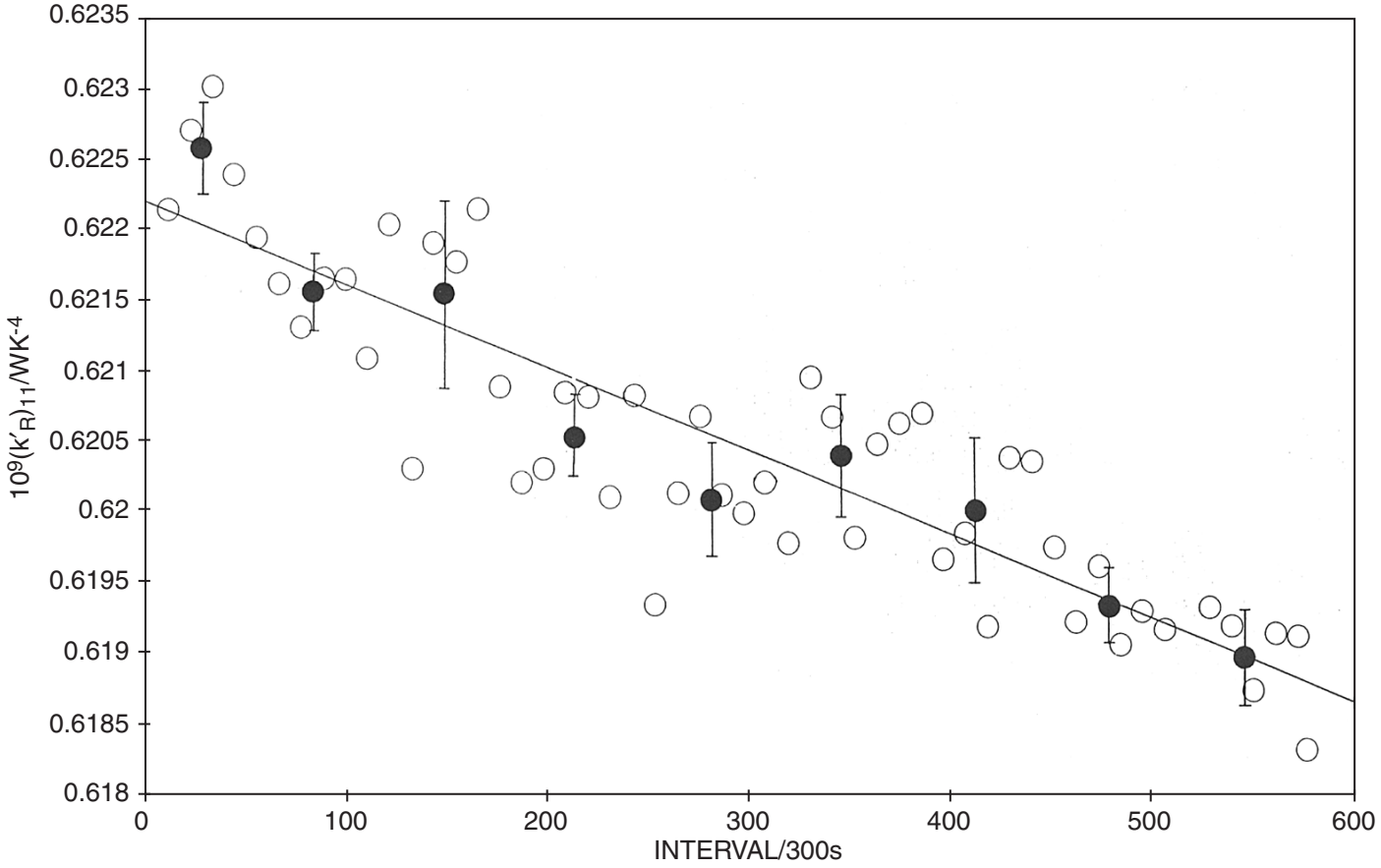

Fig. 40. $(k'_R)_{11}$ for the experiment illustrated in Fig. 38 plotted versus time.

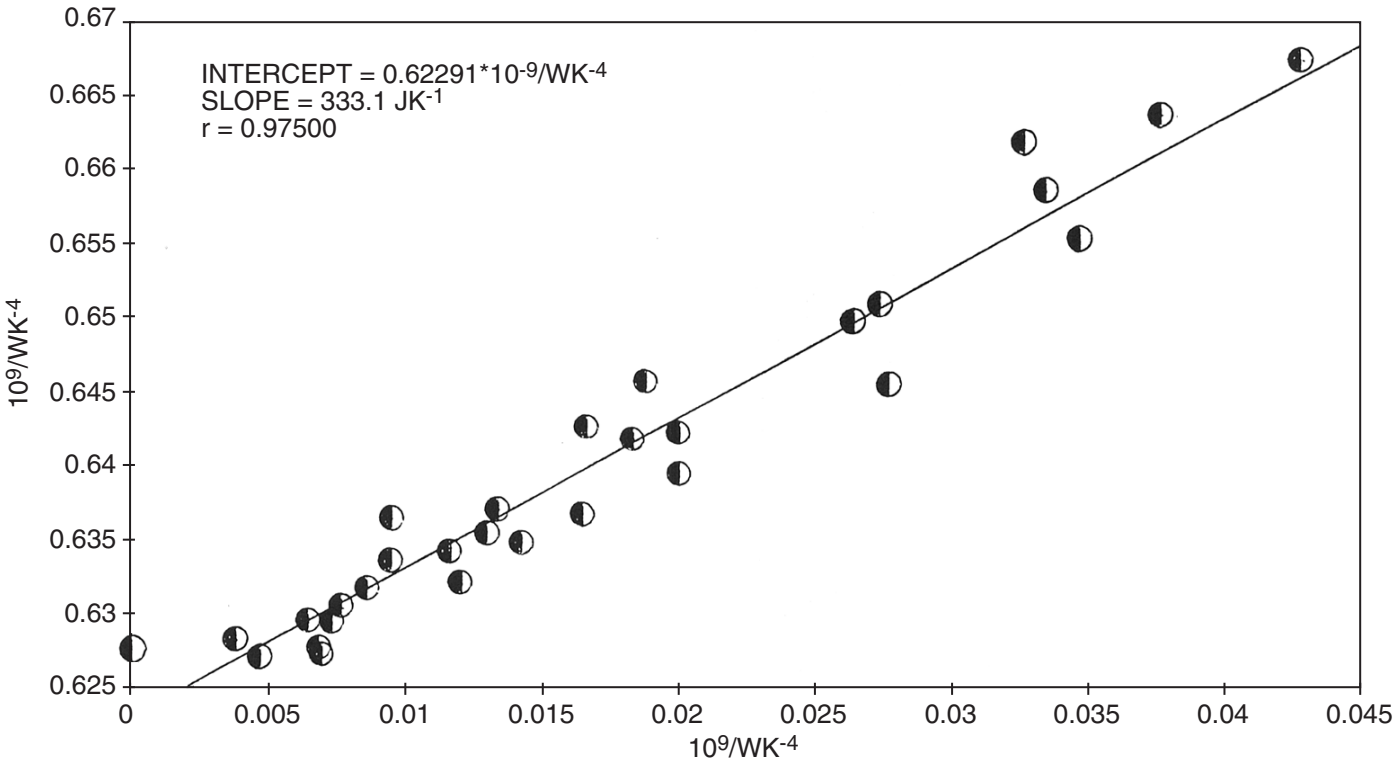

Fig. 41. ICARUS-2. Evaluation of $(k'_R{}^o)_{151}$.

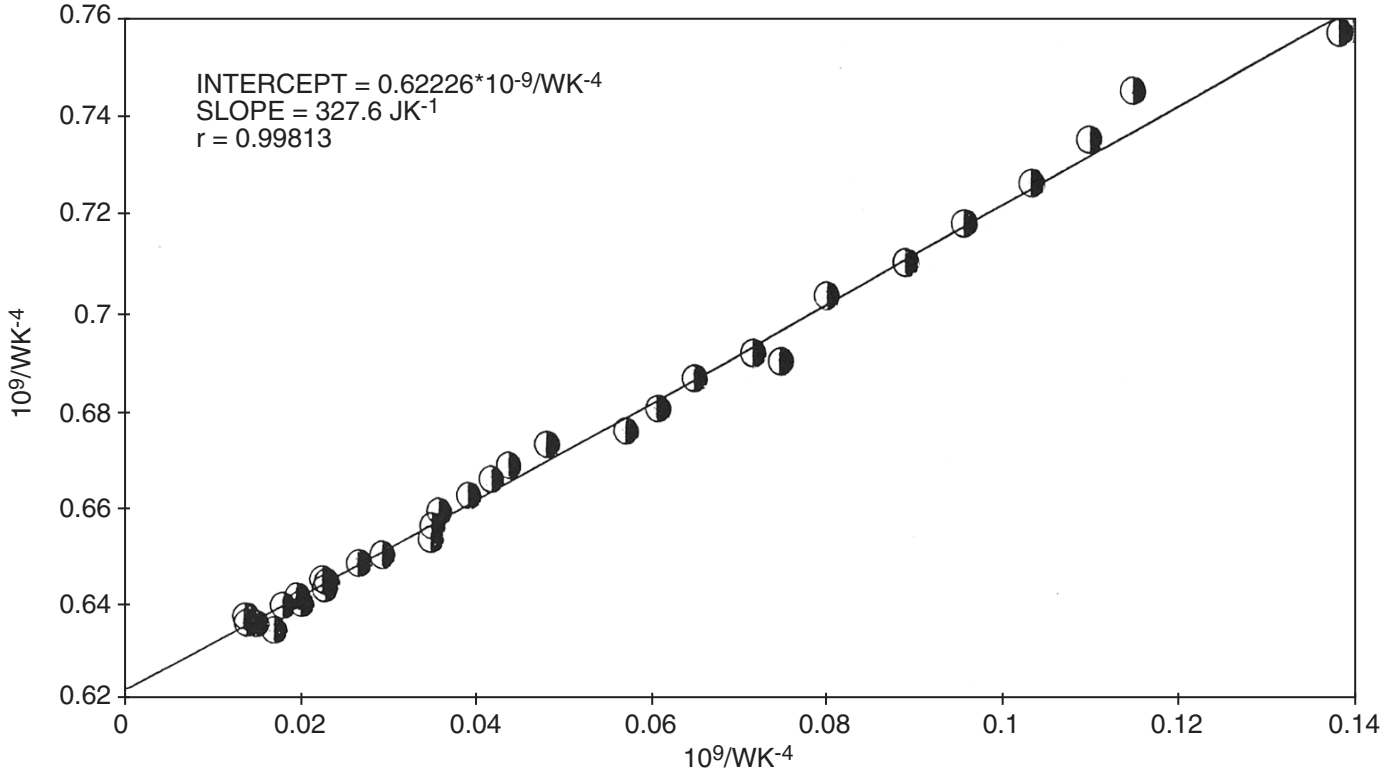

Fig. 42. ICARUS-2. Evaluation of $(k'_R{}^o)_{161}$.

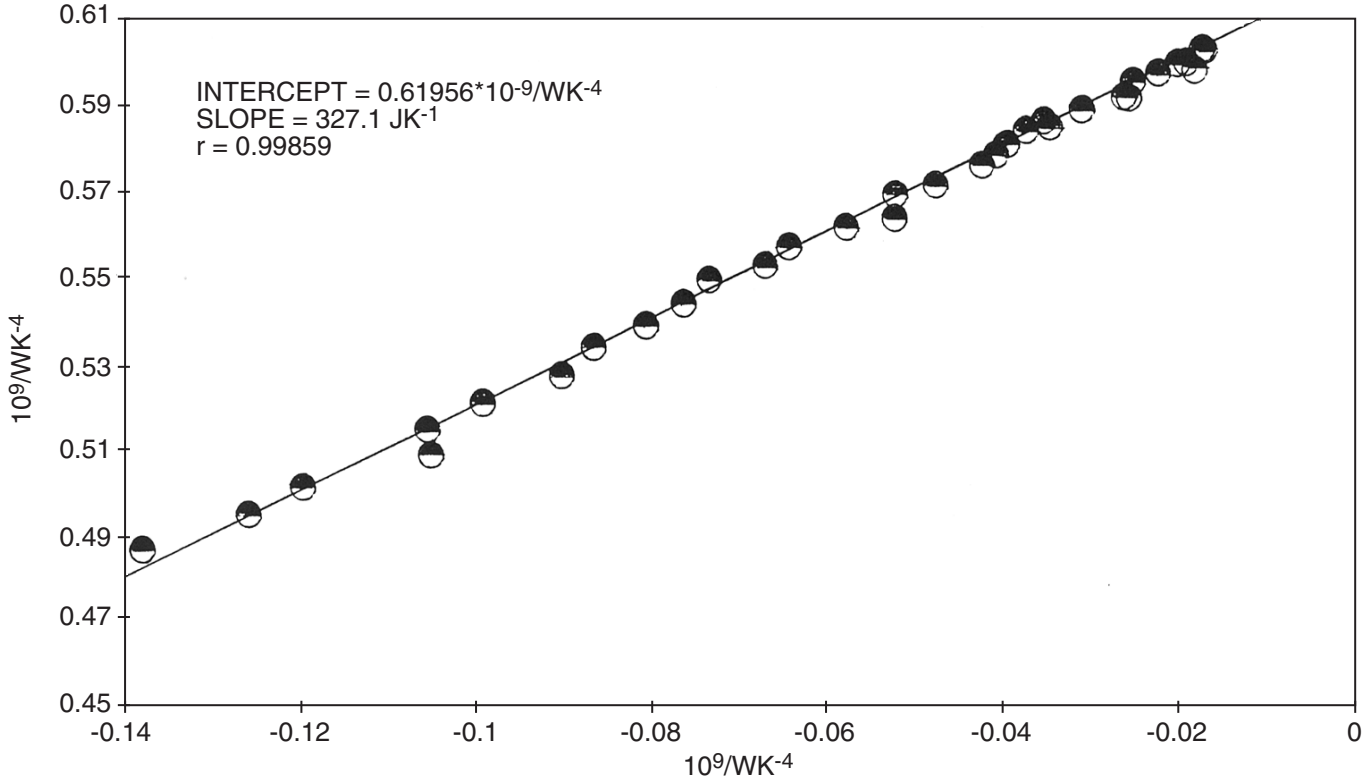

Fig. 43. ICARUS-2. Evaluation of $(k'_R{}^o)_{171}$.

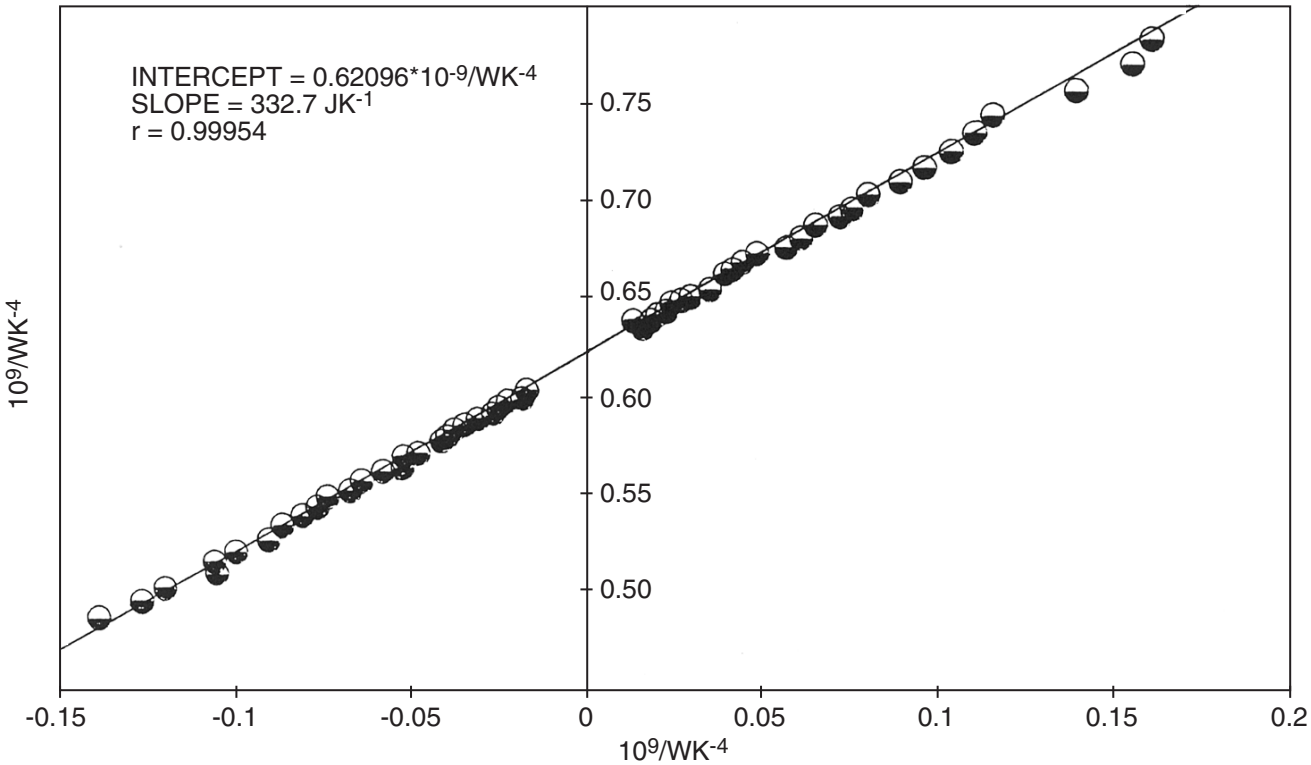

Fig. 44. ICARUS-2. Evaluation of $(k'_R{}^o)_{181}$.

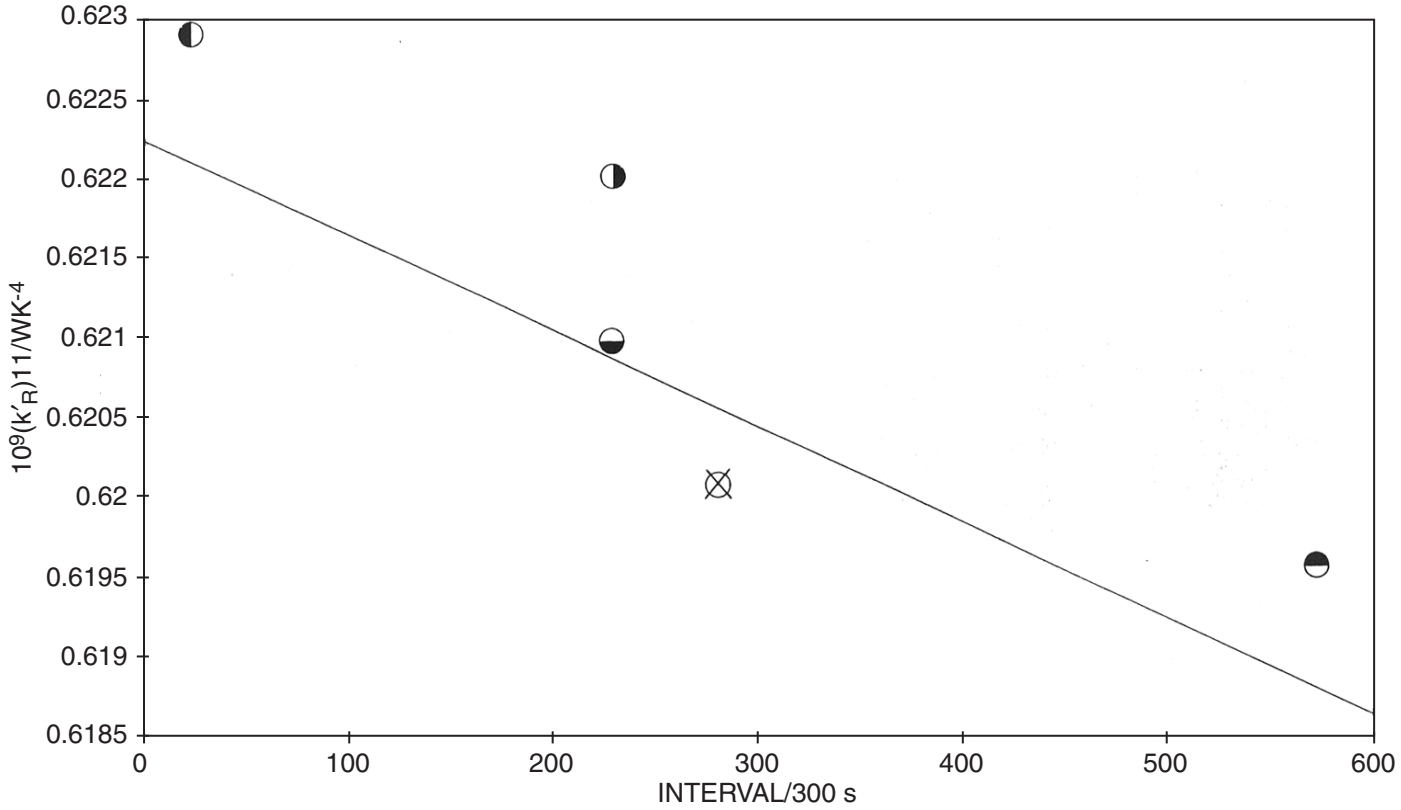

Fig. 45. $(k'_R)_{11}$, $(k'_R{}^o)_{151}$, $(k'_R{}^o)_{161}$, $(k'_R{}^o)_{171}$, and $(k'_R{}^o)_{181}$ for the experiment illustrated in Fig. 38.

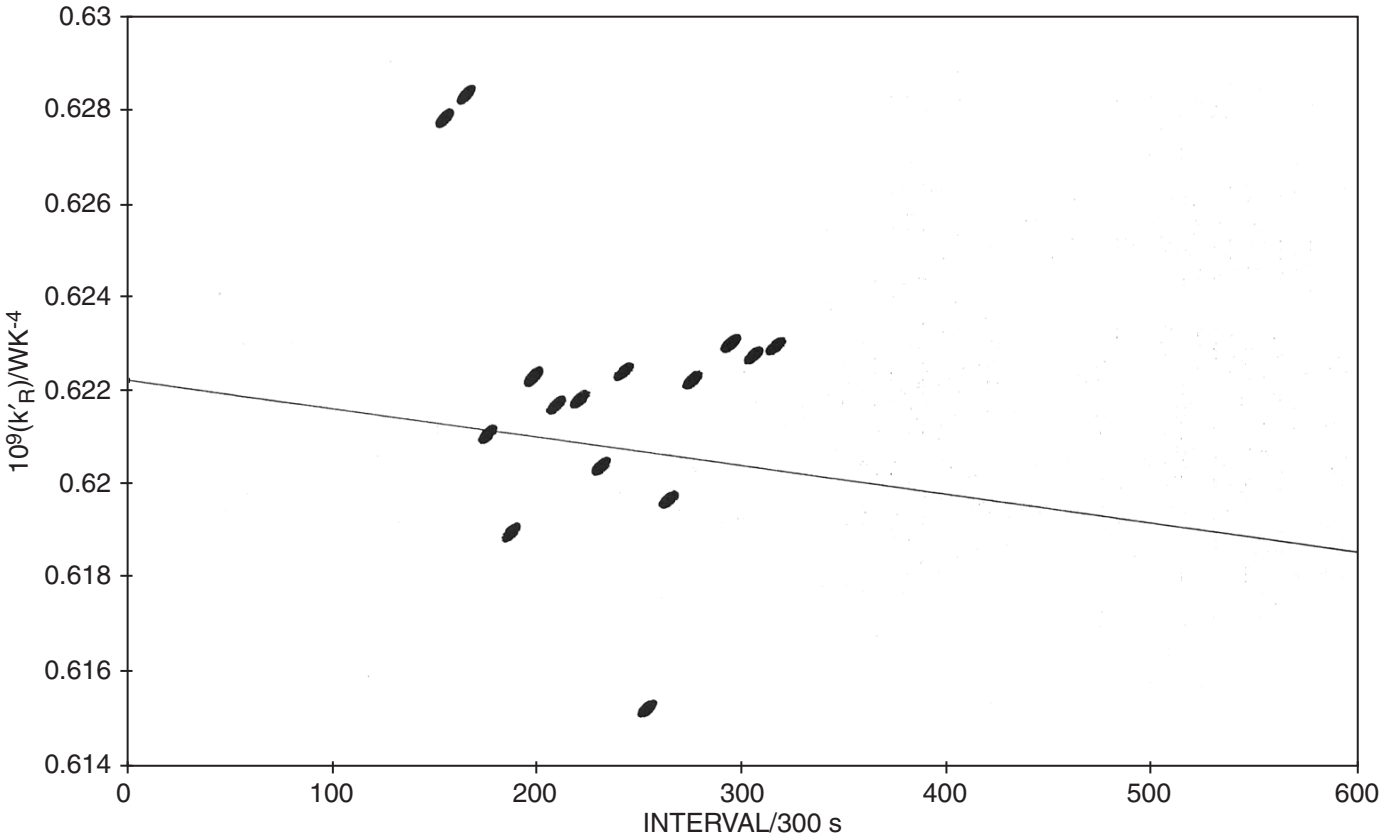

Fig. 46. $(\overline{k'_R})_{12}$ for the experiment illustrated in Fig. 38 versus time.

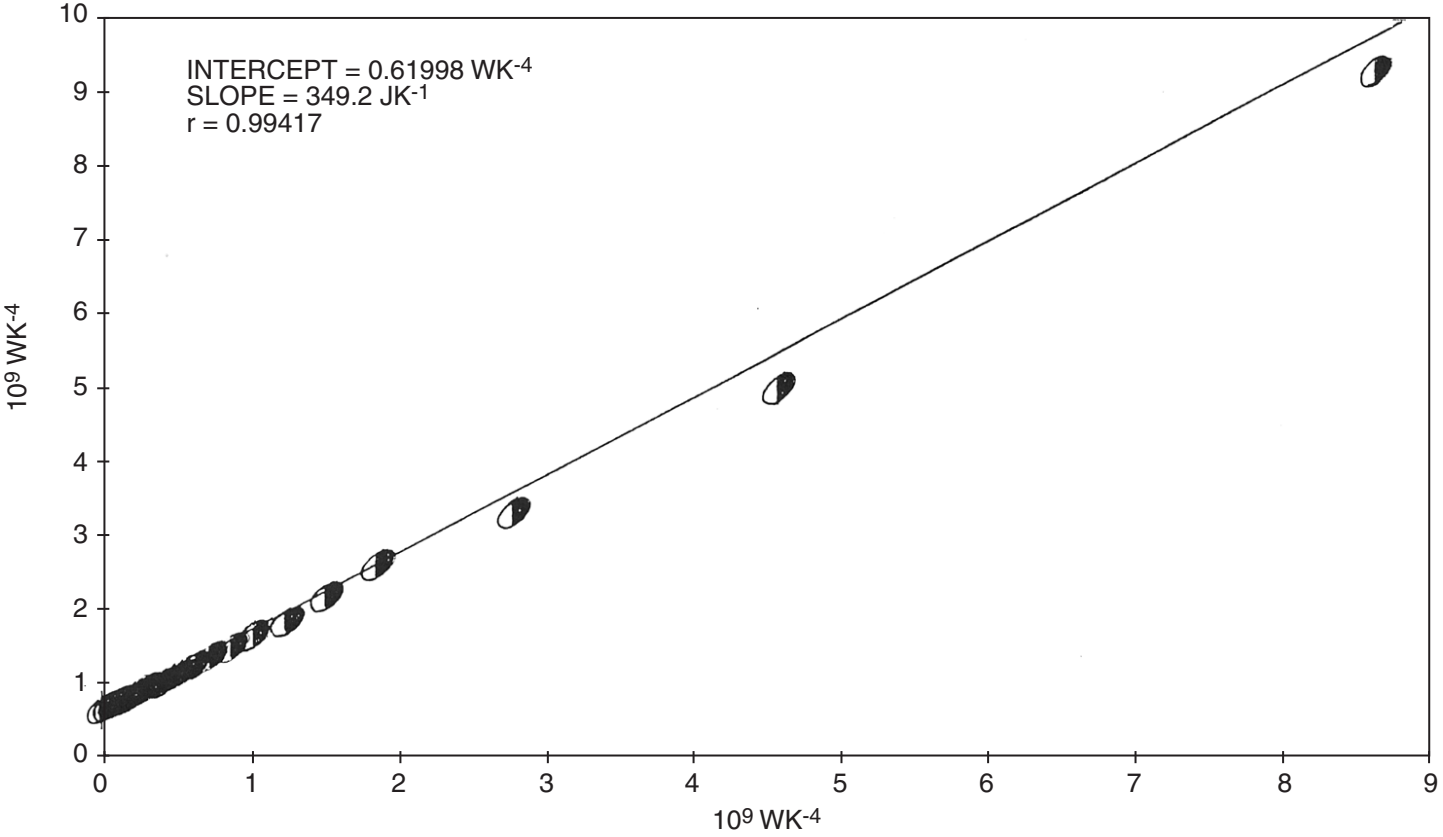

Fig. 47. ICARUS-2. Evaluation of $(k'_R{}^o)_{162}$ for the experiment illustrated in Fig. 38.

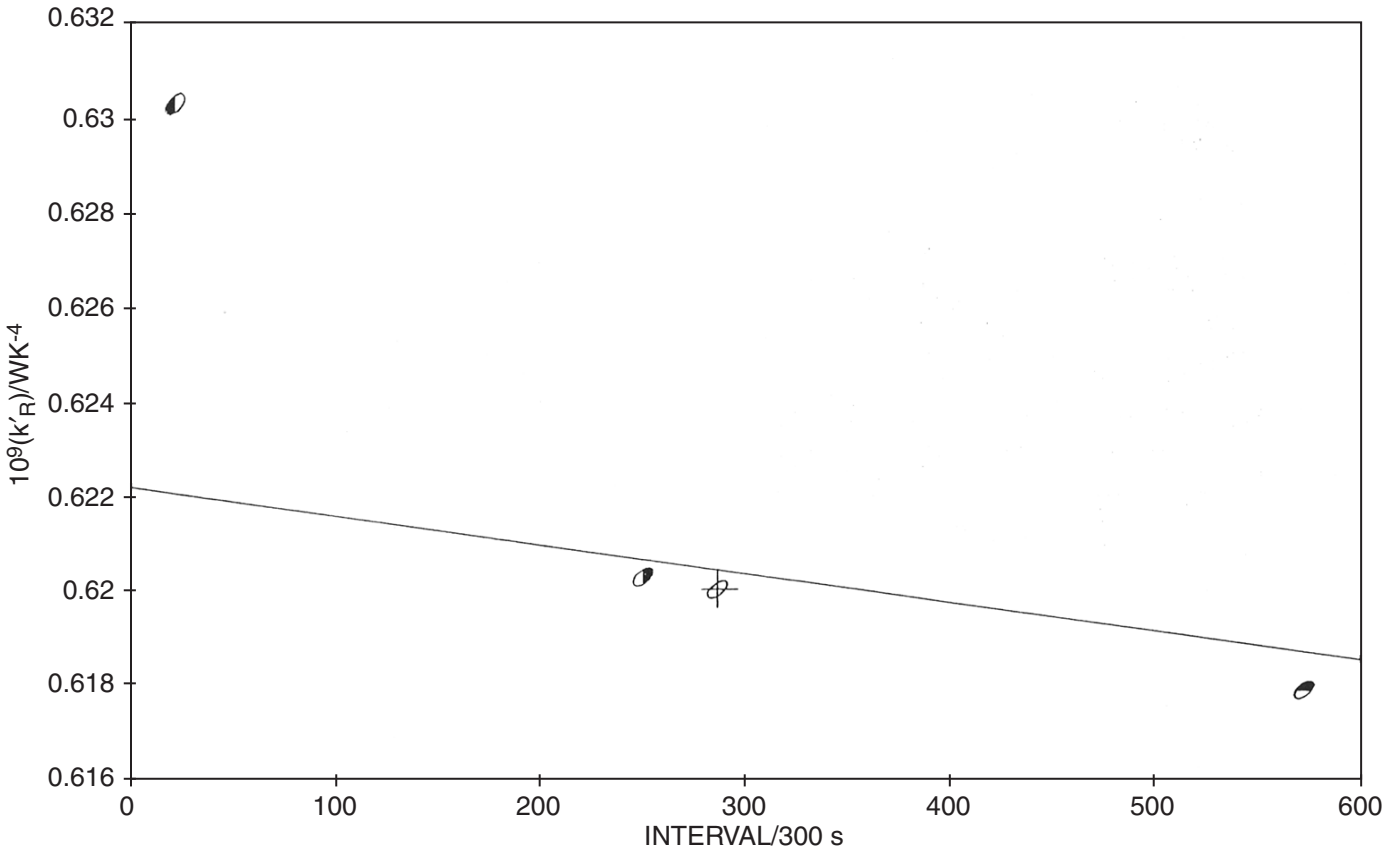

Fig. 48. ICARUS-2. $(k'_R{}^o)_{152}$, $(k'_R{}^o)_{162}$, $(k'_R{}^o)_{172}$, and $(k'_R)_2$ for the experiment illustrated in Fig. 38.

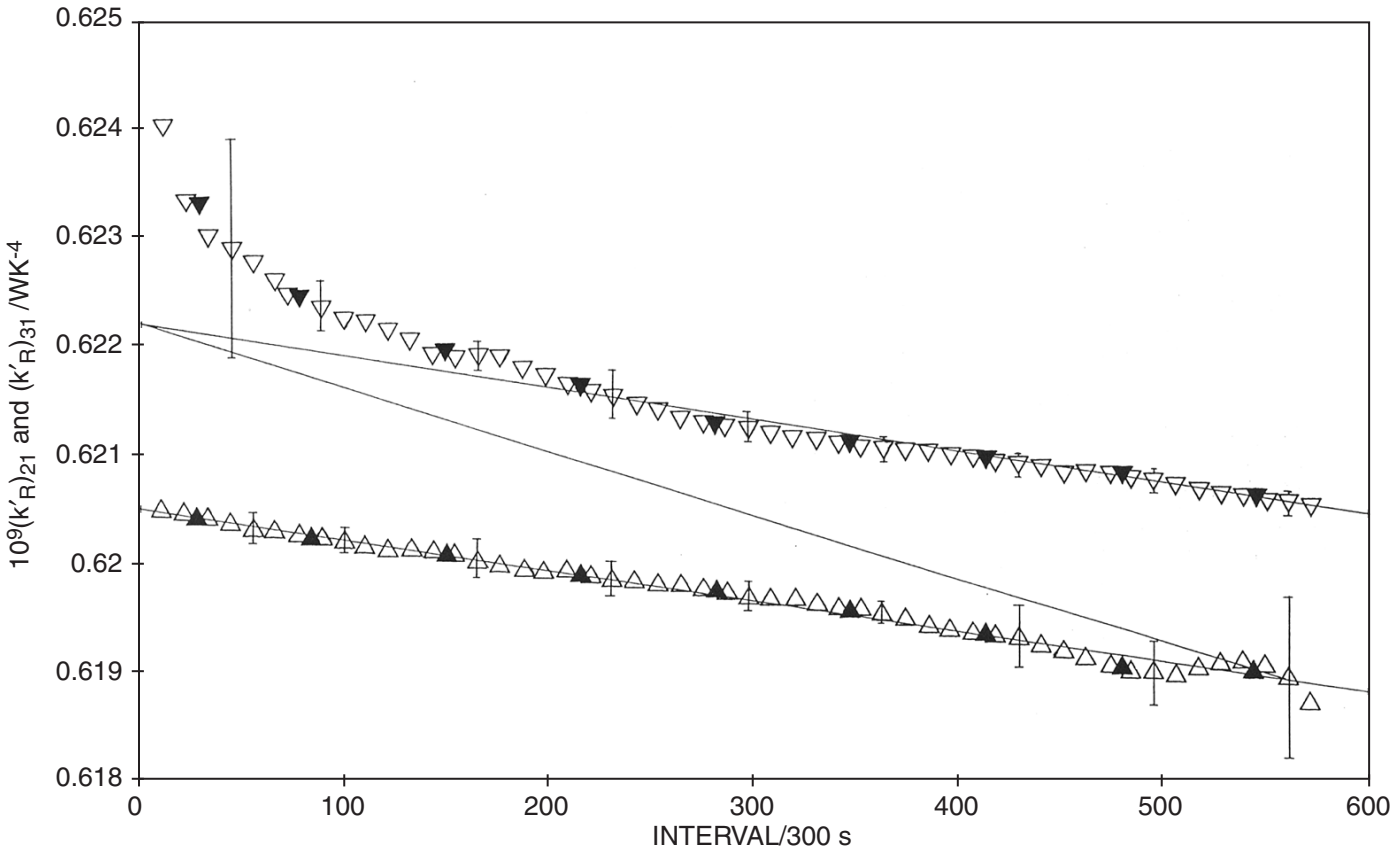

Fig. 49. $(k'_R)_{21}$ and $(k'_R)_{31}$ versus time.

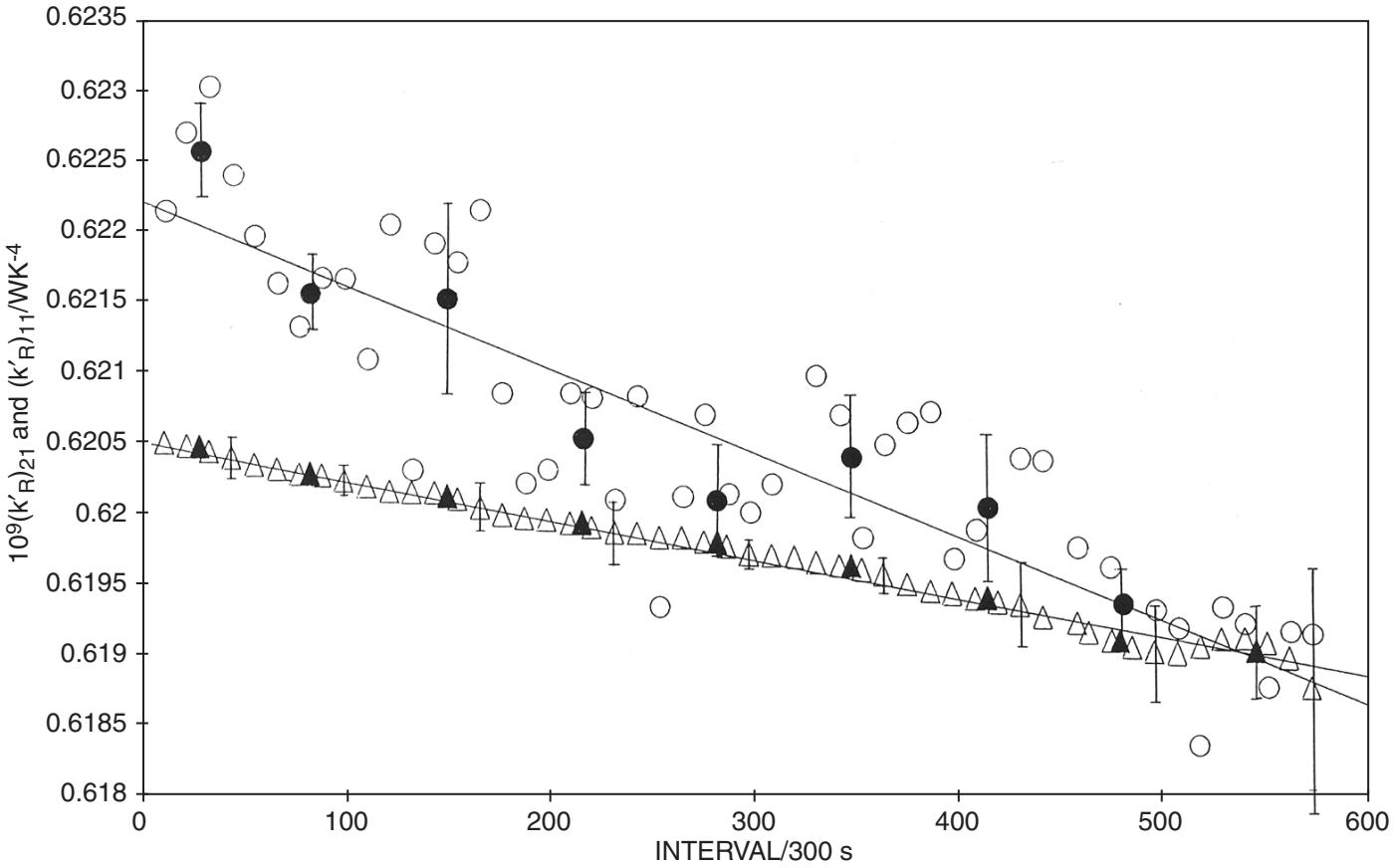

Fig. 50. $(k'_R)_{21}$ and $(k'_R)_{11}$ versus time.

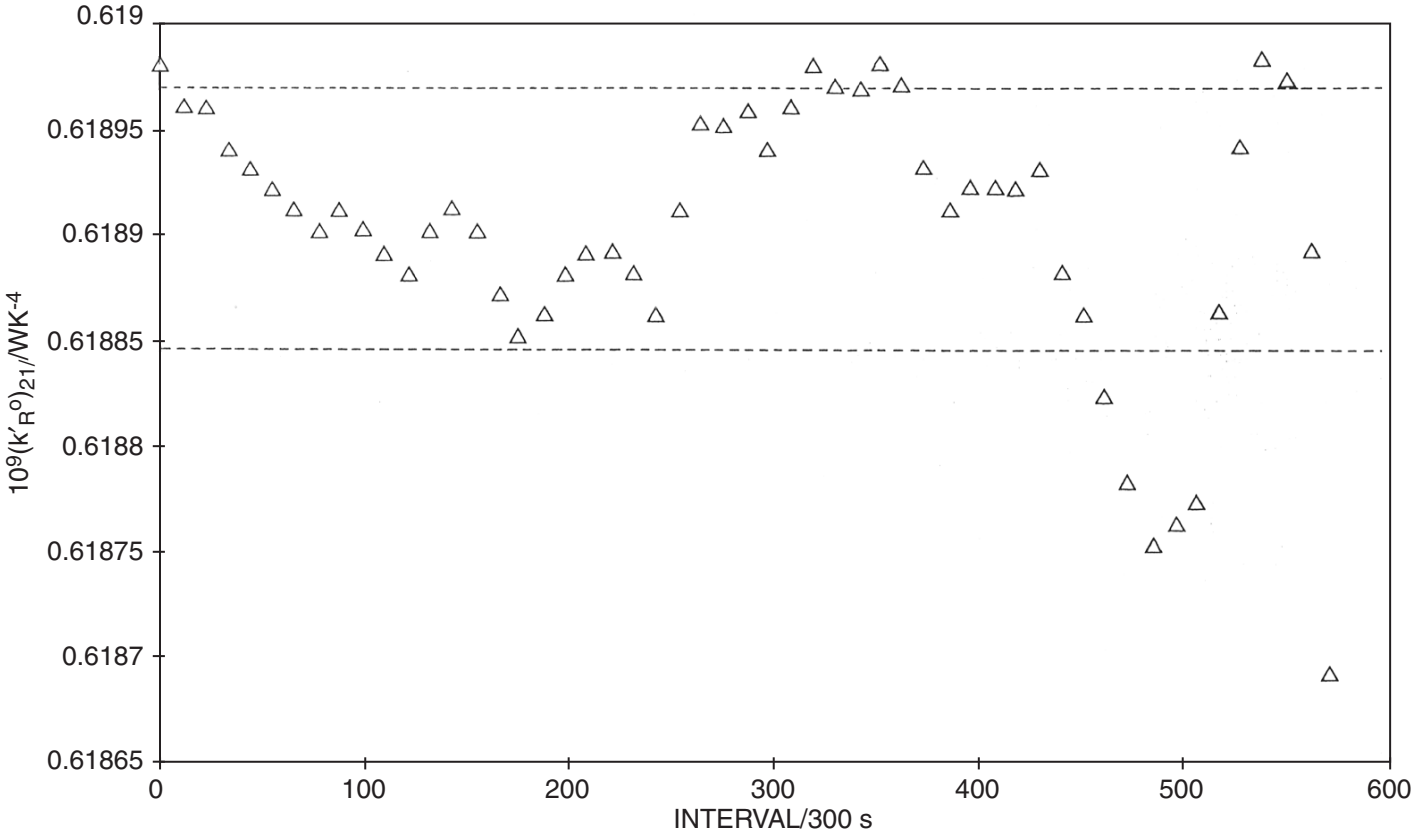

Fig. 51. $(k'_R{}^o)_{21}$ versus time.

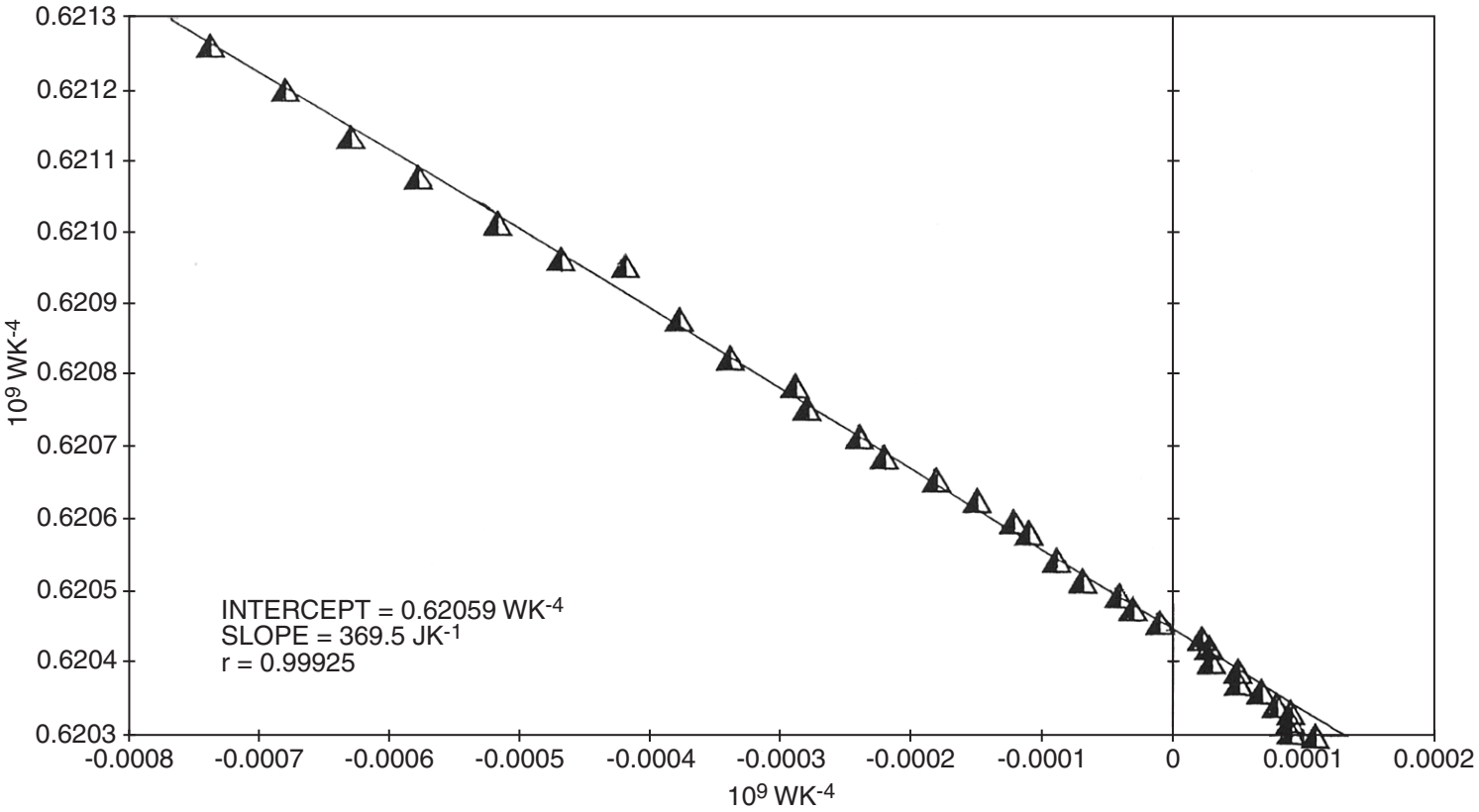

Fig. 52. Evaluation of $(k'_R{}^o)_{251}$.

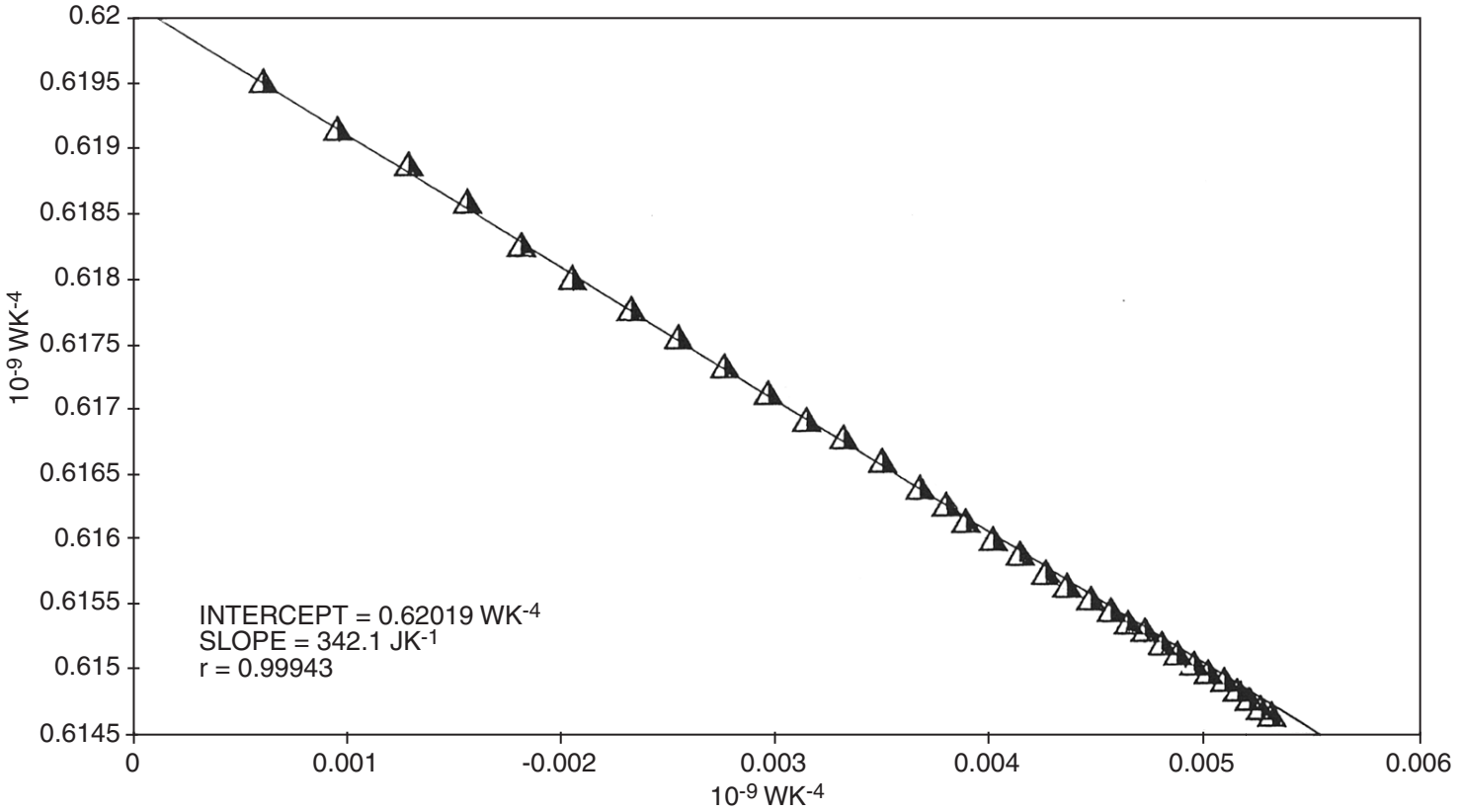

Fig. 53. Evaluation of $(k'_R{}^o)_{261}$.

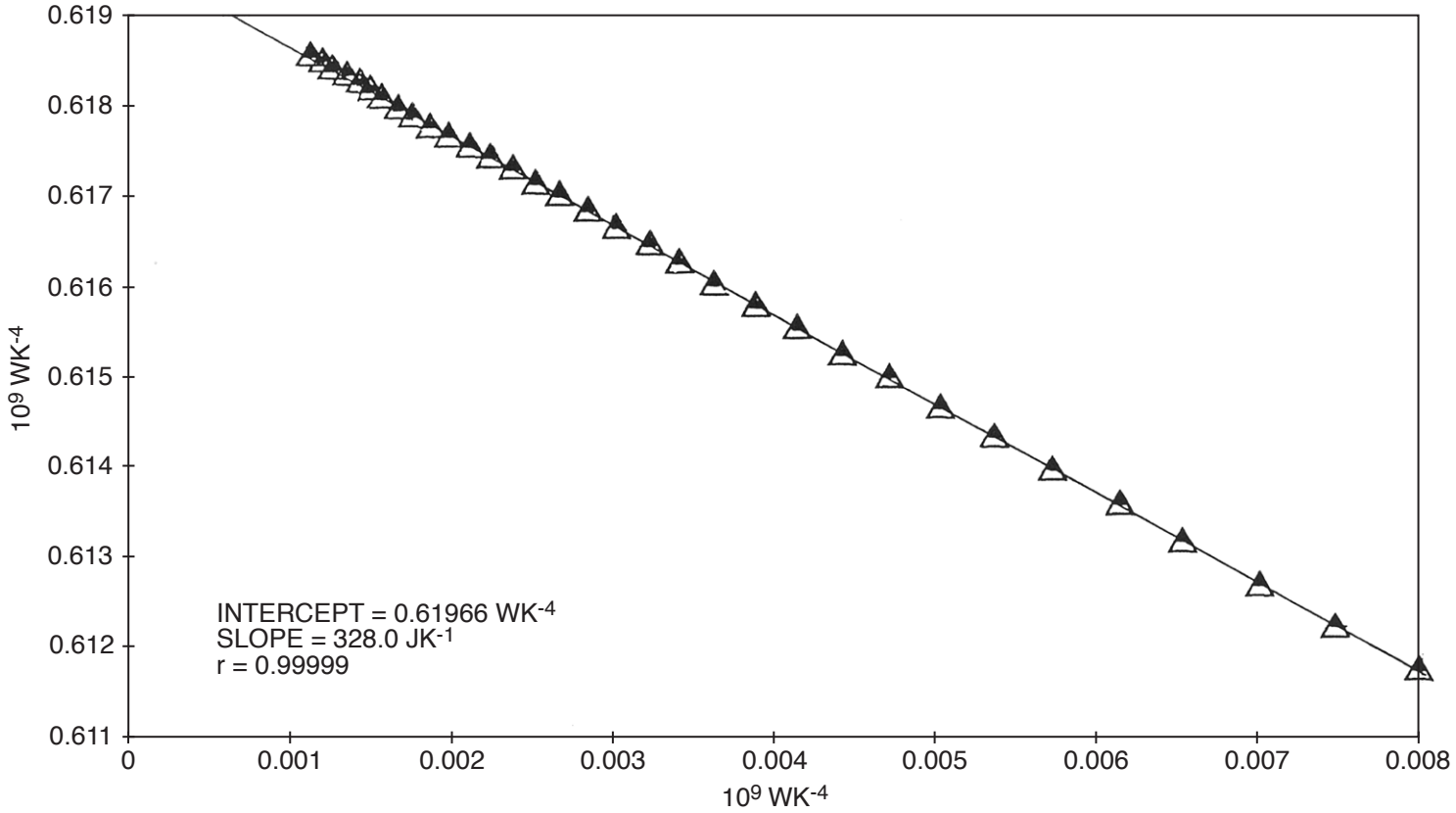

Fig. 54. Evaluation of $(k'_R{}^o)_{271}$.

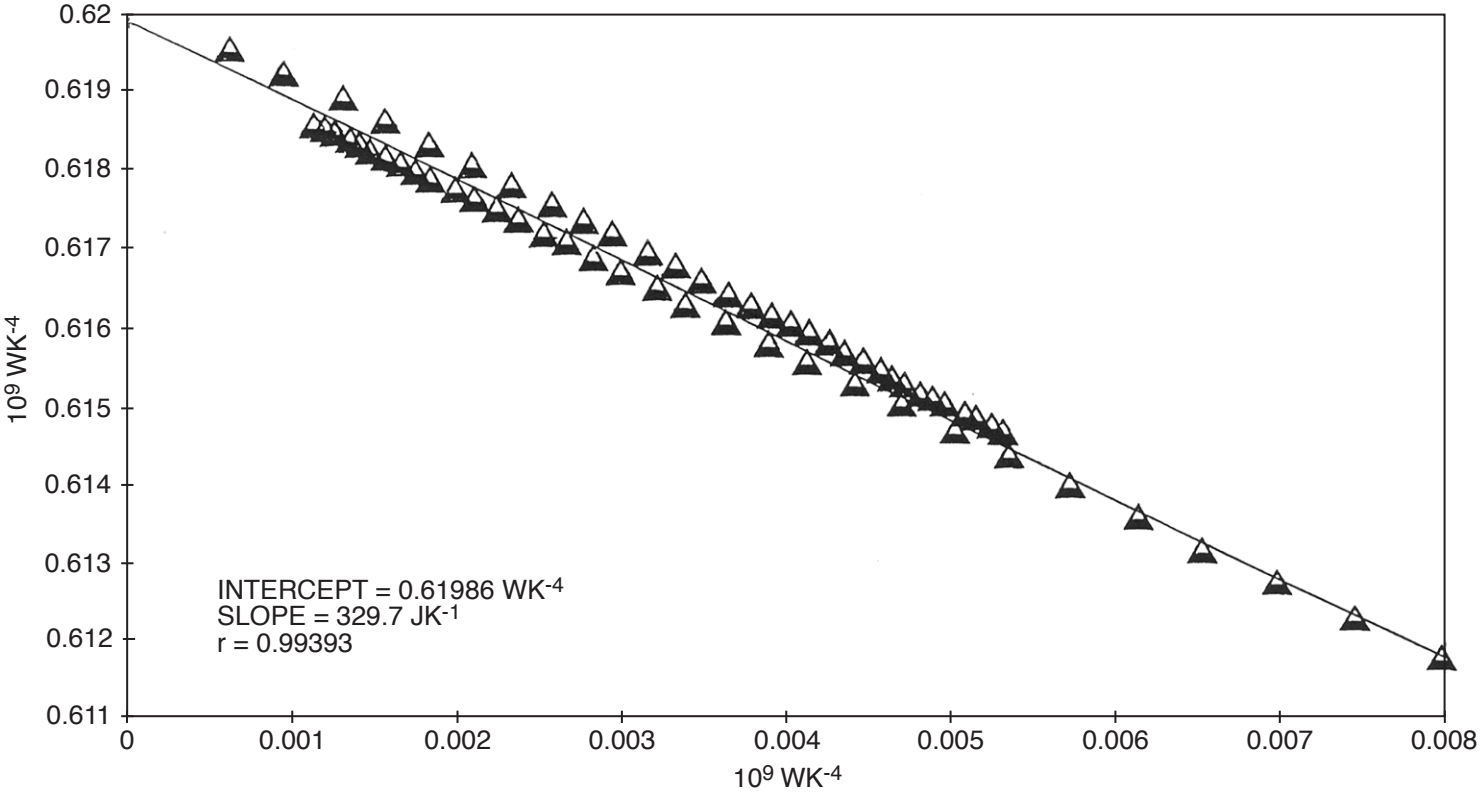

Fig. 55. Evaluation of $(k'_R{}^o)_{281}$.

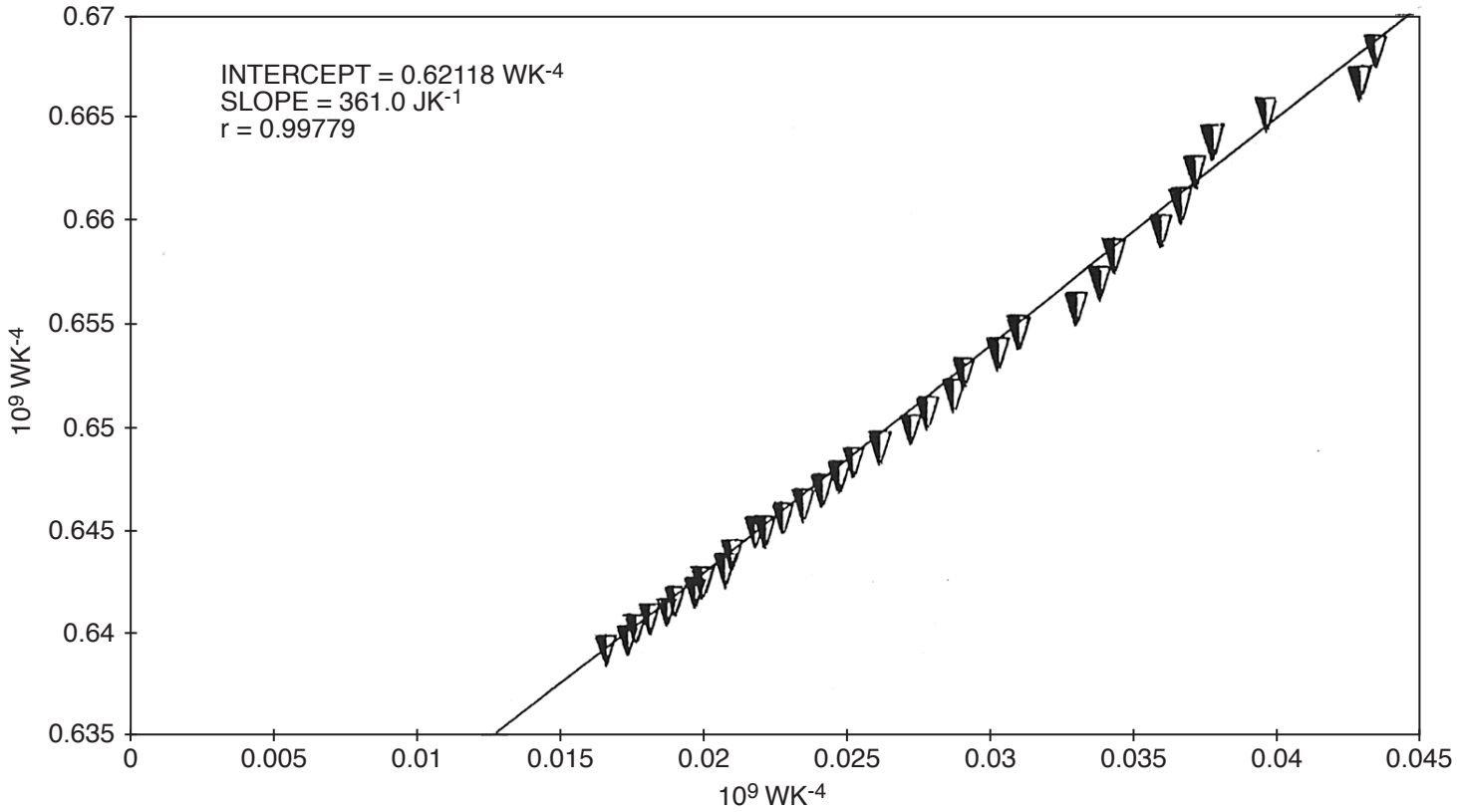

Fig. 56. Evaluation of $(k'_R{}^o)_{351}$.

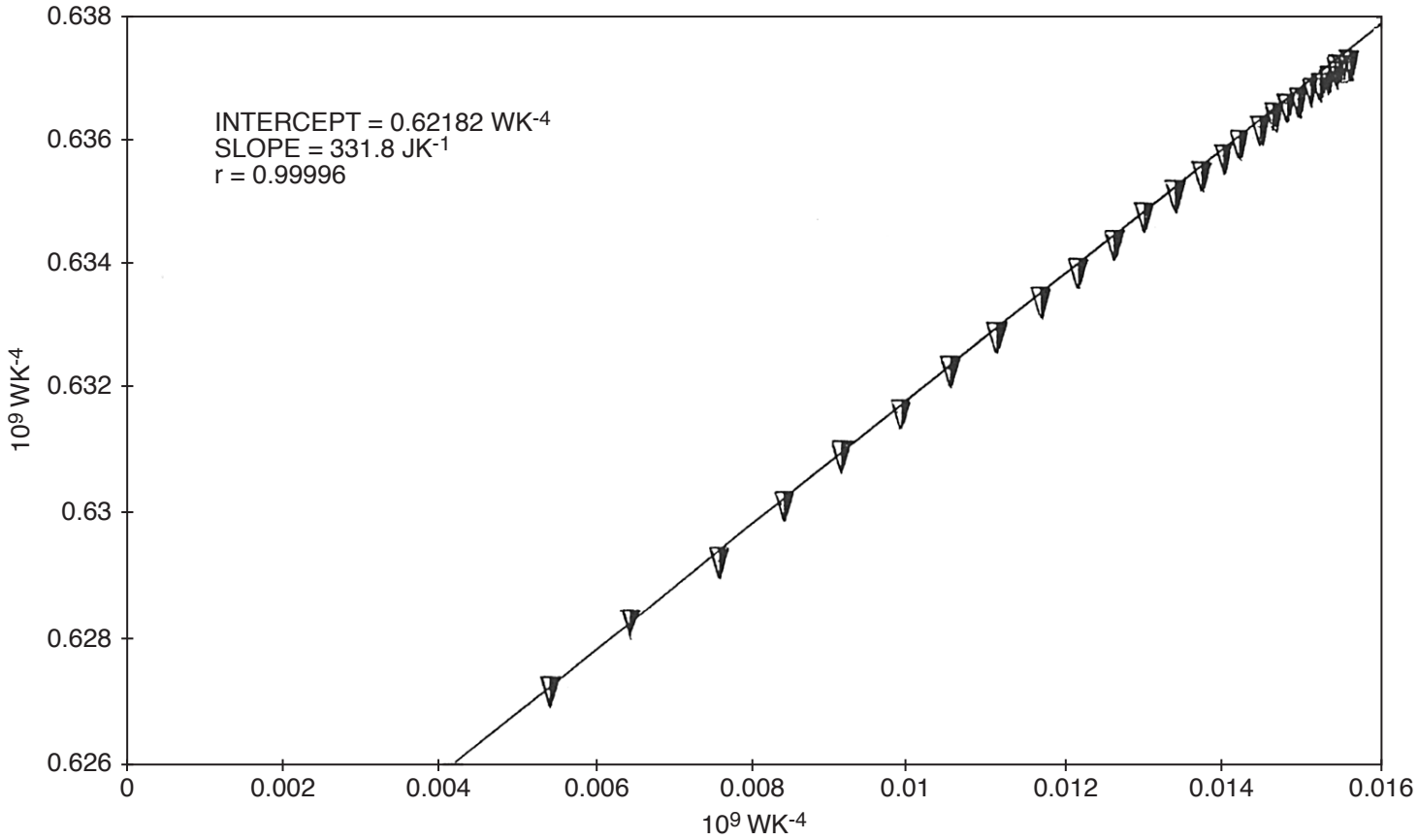

Fig. 57. Evaluation of $(k'_R{}^o)_{361}$.

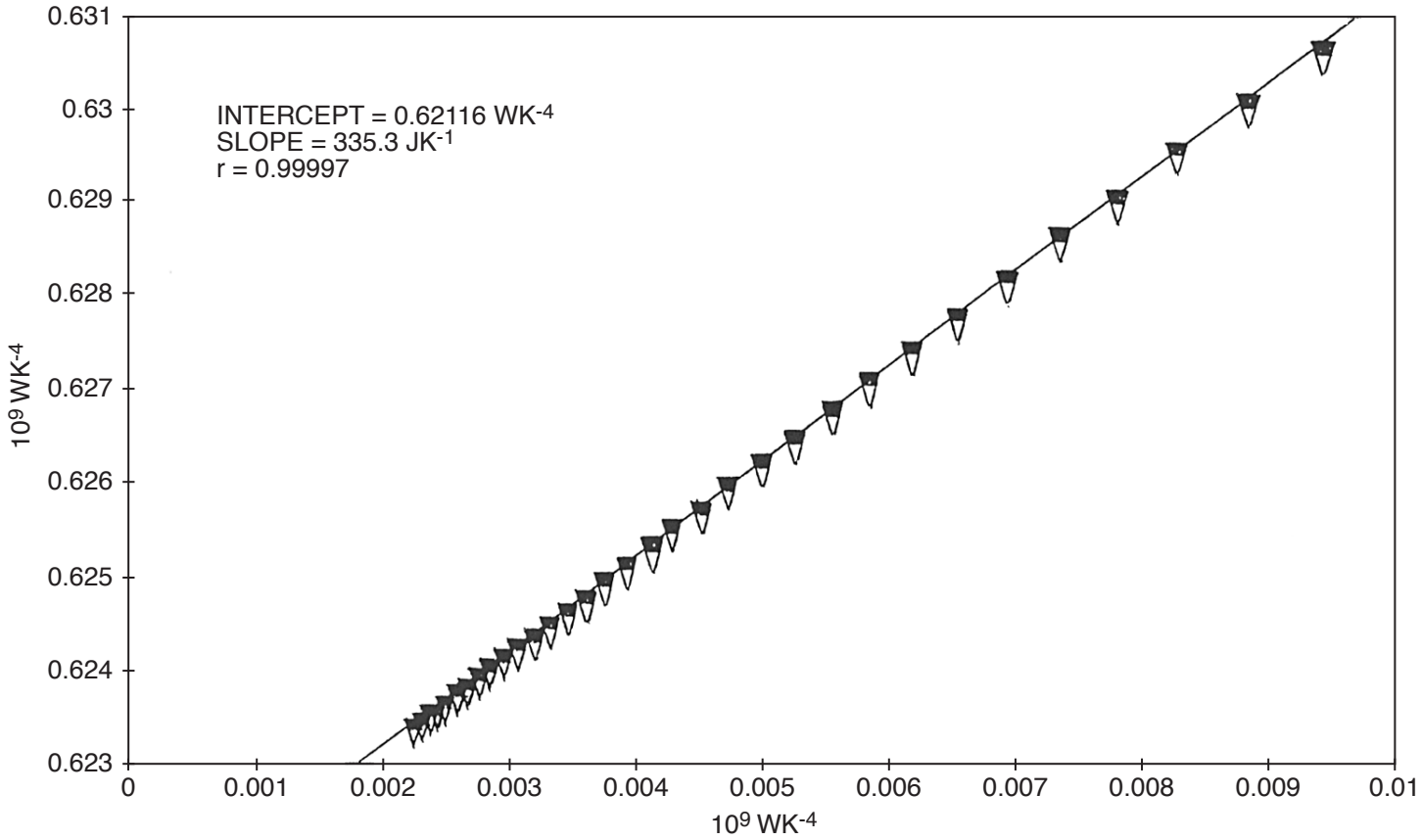

Fig. 58. Evaluation of $(k'_R{}^o)_{371}$.

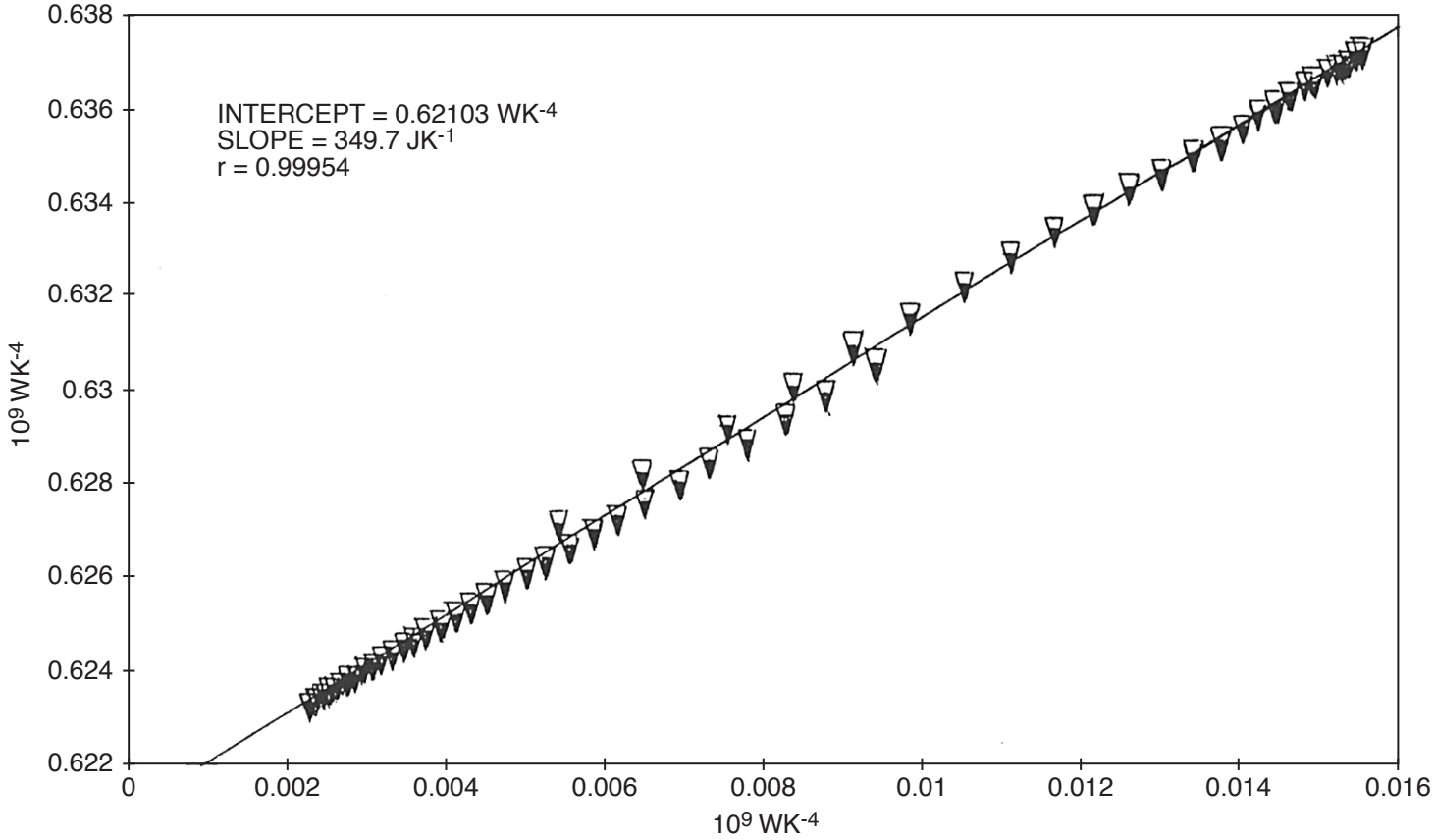

Fig. 59. Evaluation of $(k'_R{}^o)_{381}$.

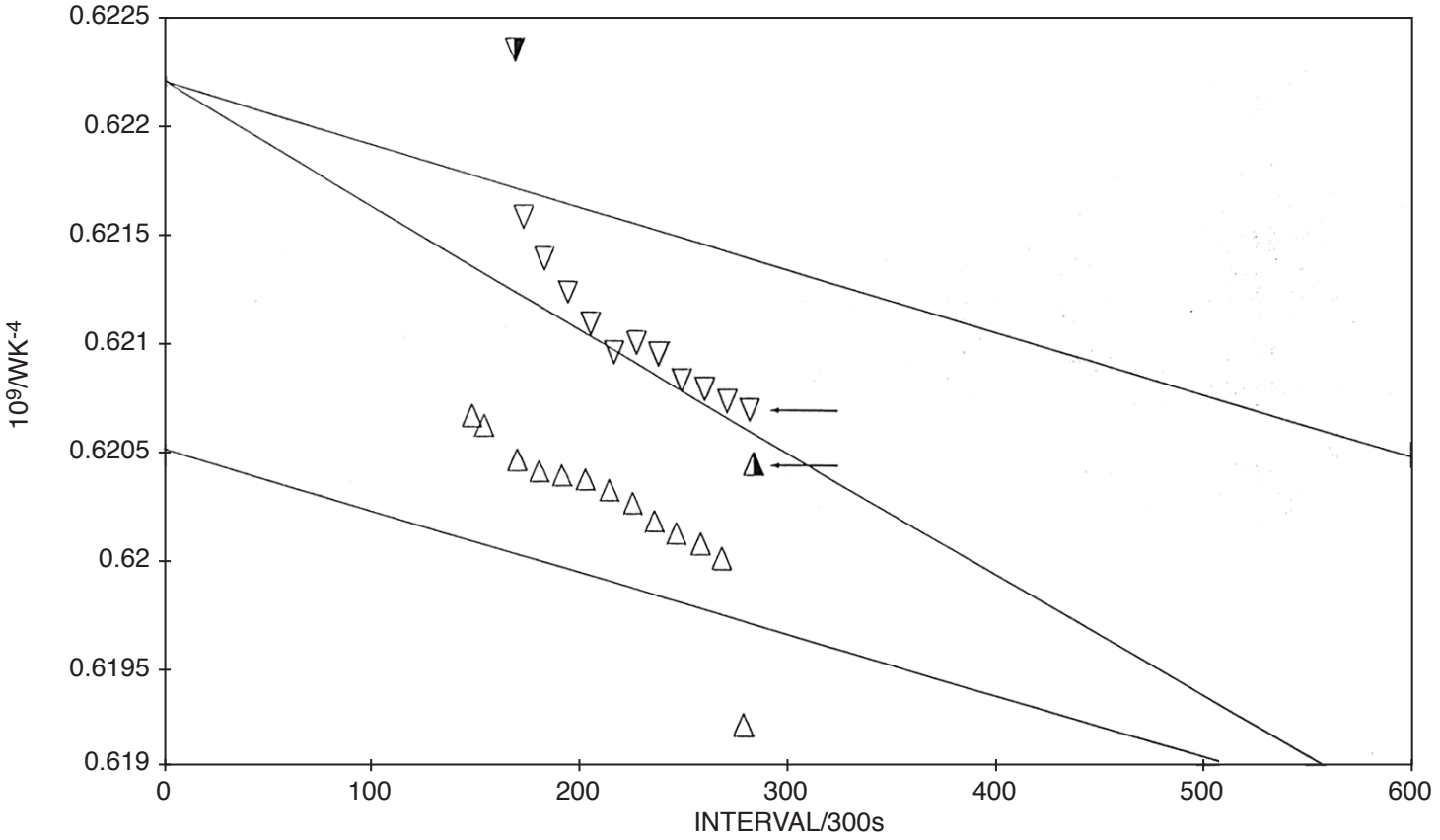

Fig. 60 ICARUS-2. Blank experiment $(k'R)_{21}$, $(k'R_o)_{261}$, and $(k'R)_{31}$ over the range, $t_1<t<t_2$.

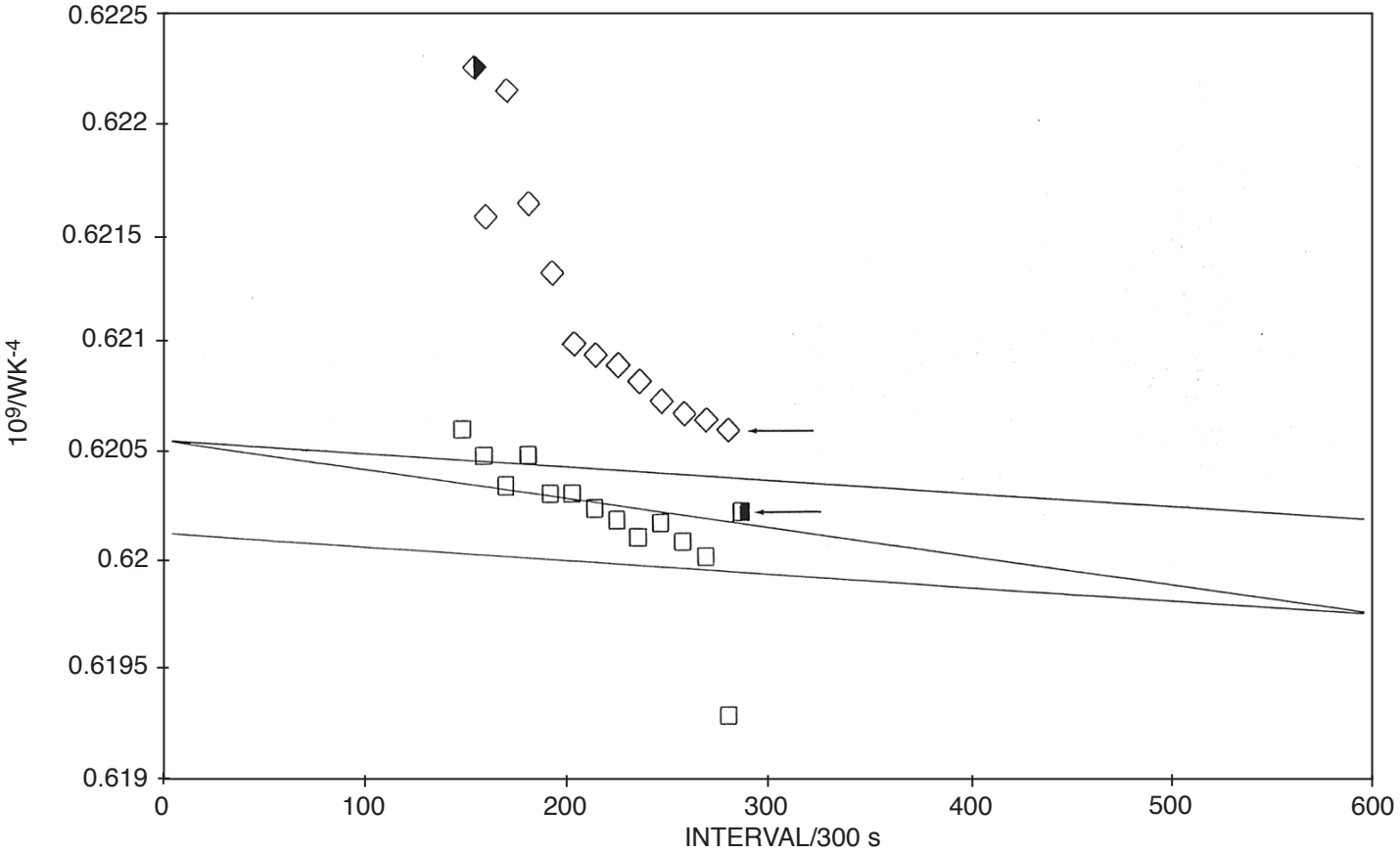

Fig. 61. $(k'_R)_{22}$ and $(k'_R)_{32}$ over the range, $t_1<t<t_2$.

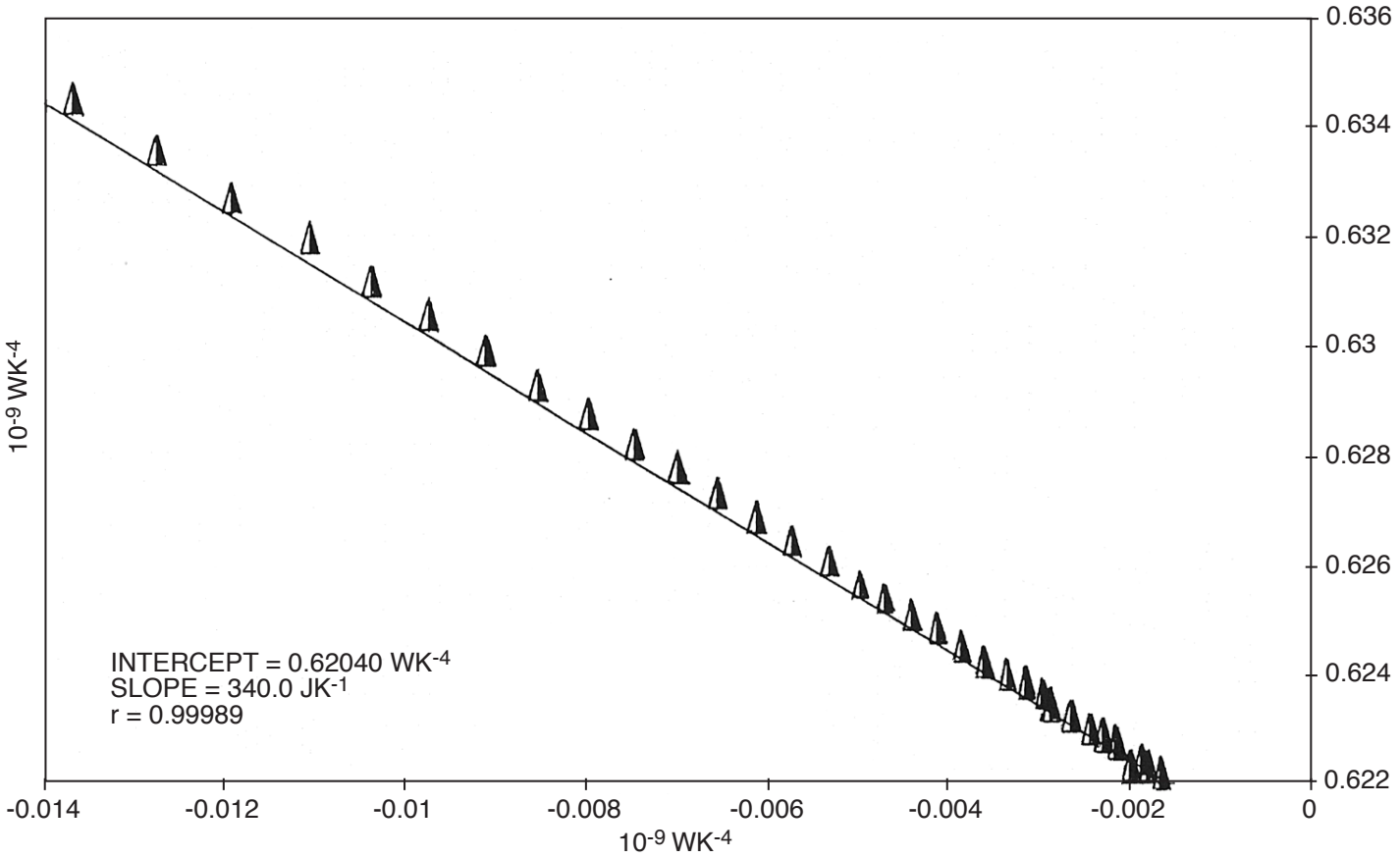

Fig. 62. ICARUS-2. Evaluation of $(k'_R{}^o)_{261}$ using the ICARUS-1 Method.

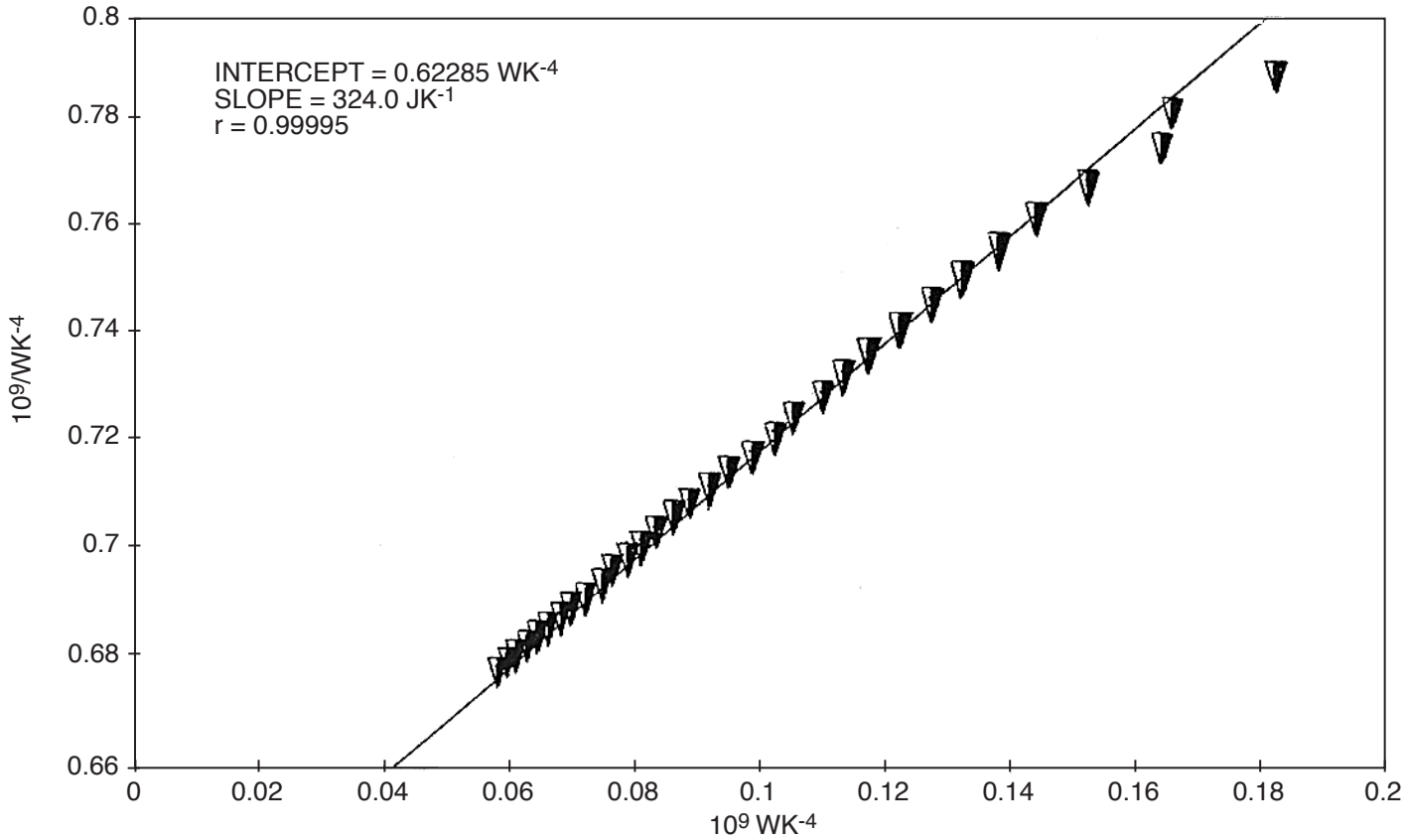

Fig. 63. ICARUS-2. Evaluation of $(k'_R{}^o)_{361}$ using the ICARUS-1 Method.

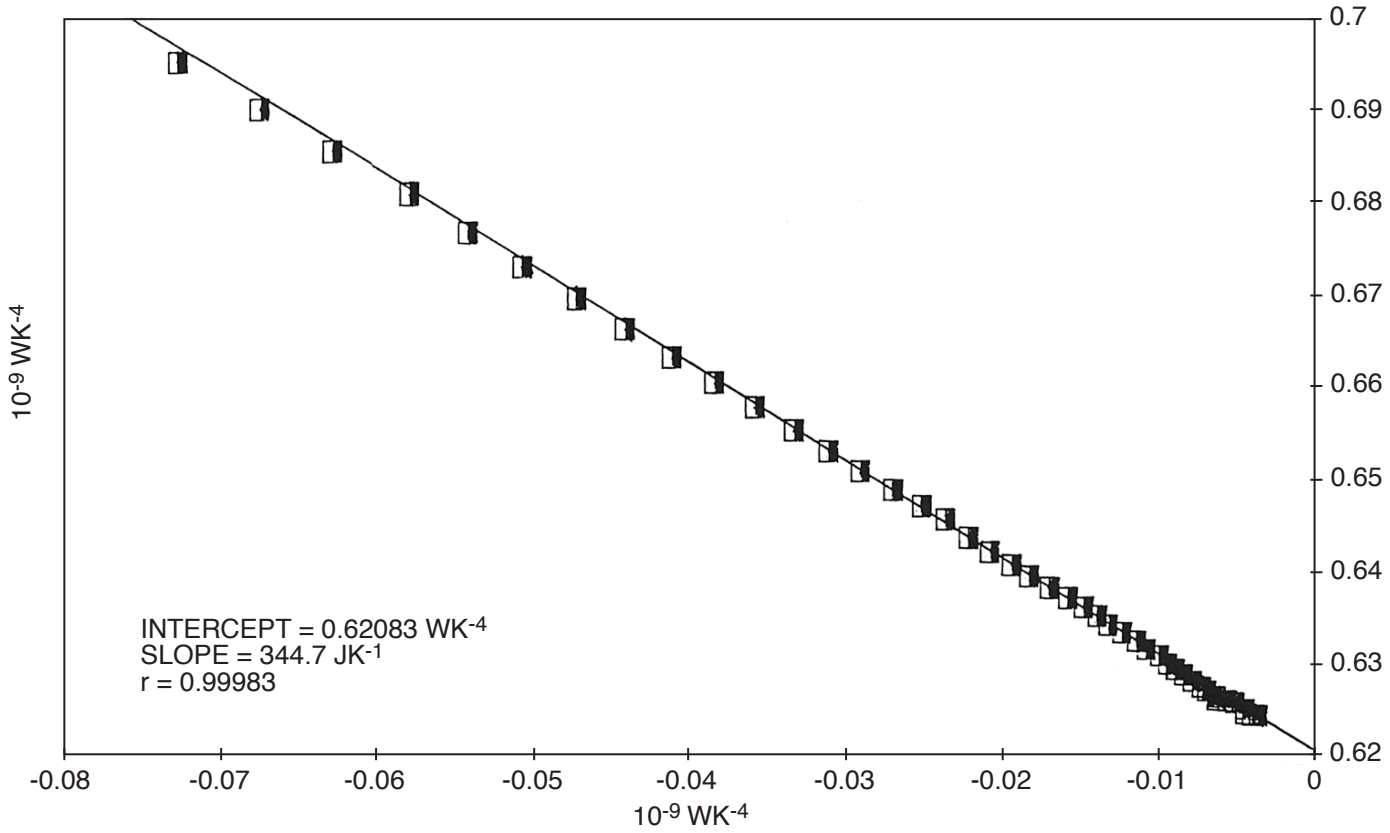

Fig. 64. Evaluation of $(k'_R{}^o)_{262}$ using the ICARUS-1 Method.

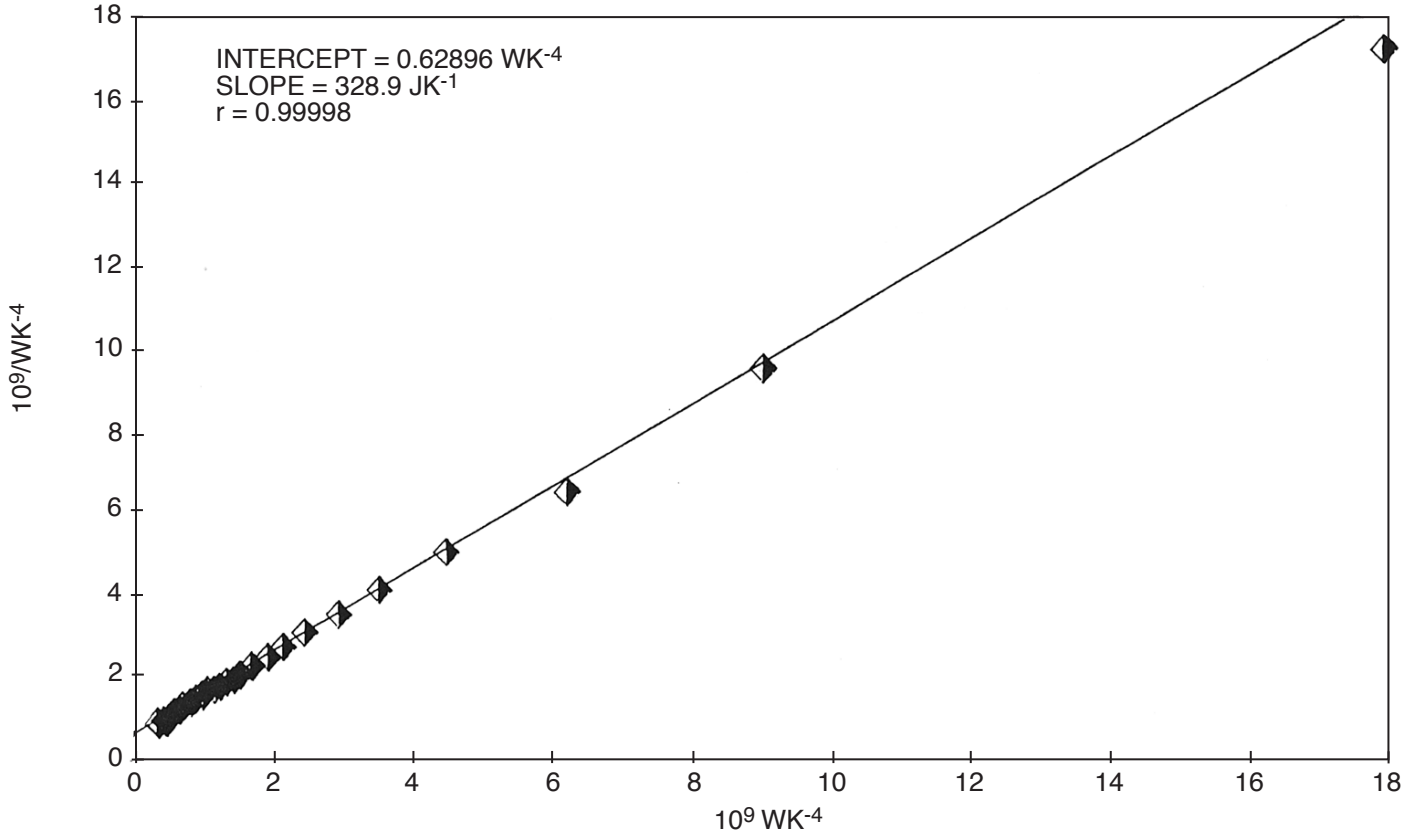

Fig. 65. Evaluation of $(k'_R{}^o)_{362}$ using the ICARUS-1 Method.

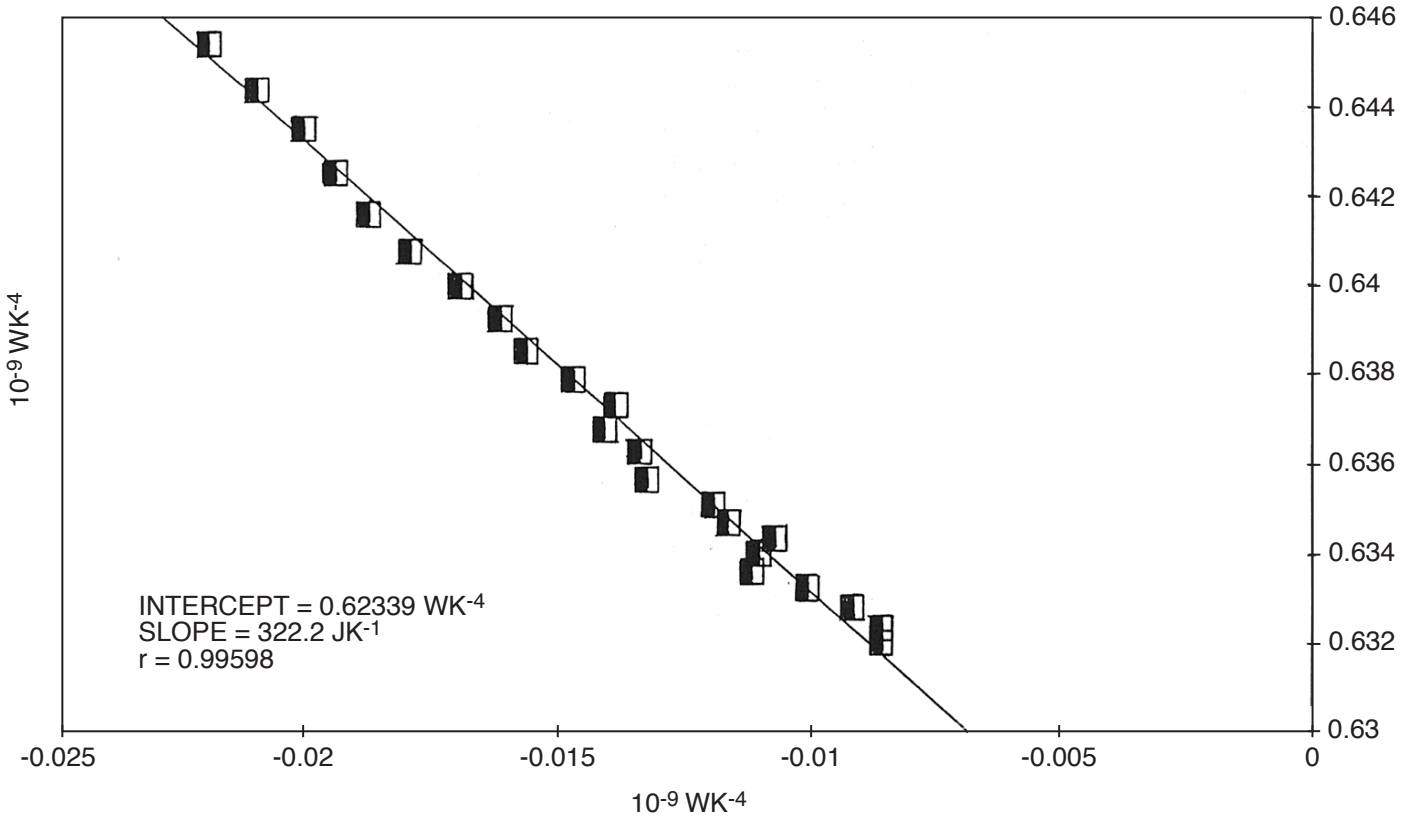

Fig. 66. Evaluation of $(k'_R{}^o)_{252}$ using the ICARUS-1 Method.

TABLES

Spreadsheet 1

Part of the (kc')11 spreadsheet for the region 0< I< T of a simulation of a measurement cycle

Evaluation of $\overline{(kc')}11$, $\overline{(kc')}12$, (kc'o)151, (kc'o)161, (kc'o)171, (kc'o)181 and (kc'o)162

The effects of using the 1st order backward difference for do/dt on the evaluations of (kc')11, (kc')12, (kc'o)151, (kc'o)161, (kc'o)171 and (kc'o)162 (columns 13-20).

1	2	3	4	5	6	7	8	9	10	11	12	13	14	15	16	17	18	19	20
interval 300/s	Δ θ/K	enthalpy input/W	abscissa	ordinate	$\overline{(kc')}11$ / WK^-1	(kc'o)151 / WK^-1	(kc'o)181 / WK^-1	abscissa	ordinate	$\overline{(kc')}12$ / WK^-1	(kc'o)162 / WK^-1	abscissa	ordinate	$\overline{(kc')}11$ / WK^-1	(kc'o)151 / WK^-1	abscissa	ordinate	$\overline{(kc')}12$ / WK^-1	(kc'o)162 / WK^-1
						slope /JK^-1	slope /JK^-1				slope /JK^-1				slope /JK^-1				slope /JK^-1
						r	r				r				r				r
143						(kc'o)161 / WK^-1									(kc'o)161 / WK^-1				
						slope /JK^-1									slope /JK^-1				
						r									r				
144																			
286						(kc'o)171 / WK^-1									(kc'o)171 / WK^-1				
						slope /JK^-1									slope /JK^-1				
						r									r				
287																			
0	11.75	1																	
1	11.87473	0.999509	0.011149	0.084171									0.084171						
2	11.99071	0.998315	0.010266	0.083257		0.073 ↑		-0.08007	-0.007			0.01064	0.083257		0.073 ↑				
3	12.09855	0.99756	0.009461	0.082453		329.7		-0.08007	-0.007			0.009805	0.082453		318.1				
4	12.19883	0.996858	0.008725	0.081718		1		-0.08007	-0.007			0.009043	0.081718		1				
5	12.29207	0.996205	0.008052	0.081045				-0.08008	-0.007			0.008344	0.081045						
6	12.37878	0.995599	0.007435	0.080428				-0.08008	-0.007			0.007705	0.080428						
7	12.4594	0.995034	0.006868	0.079862	0.072994			-0.08007	-0.007	0.073071		0.007118	0.079862	0.072714		-0.08298	-0.007	0.075981	
8	12.53436	0.994509	0.006348	0.079343				-0.08007	-0.007			0.006578	0.079343						
9	12.60407	0.994021	0.00587	0.078865				-0.08008	-0.007			0.006084	0.078865						
10	12.66889	0.993568	0.005431	0.078426				-0.08008	-0.007			0.005628	0.078426						
11	12.72916	0.993146	0.005026	0.078021				-0.08008	-0.007			0.005208	0.078021						
12	12.78521	0.992754	0.004653	0.077649				-0.08008	-0.007			0.004822	0.077649						
13	12.83732	0.992389	0.004309	0.077305		0.073 ↑		-0.08008	-0.007			0.004465	0.077305		0.073 ↑				

14	12.88578	0.99205	0.003991	0.076988		329.7		-0.08007	-0.007			0.004137	0.076988		318.1						
15	12.93083	0.991734	0.003698	0.076695		1		-0.08007	-0.007			0.003832	0.076695		1						
16	12.97273	0.991441	0.003428	0.076425				-0.08008	-0.007			0.003553	0.076425								
17	13.01169	0.991168	0.00318	0.076175				-0.08009	-0.007			0.003294	0.076175								
18	13.04792	0.990915	0.002947	0.075944	0.072997			-0.08008	-0.007	0.07308		0.003054	0.075944	0.07289		-0.083	-0.007	0.075995			
19	13.0816	0.990679	0.002733	0.075731				-0.08007	-0.007			0.002832	0.075731								
20	13.11292	0.99046	0.002535	0.075533				-0.08009	-0.007			0.002627	0.075533								
21	13.14205	0.990256	0.002352	0.07535				-0.08009	-0.007			0.002438	0.07535								
22	13.16913	0.990066	0.002183	0.075181				-0.08007	-0.007			0.002262	0.075181								
23	13.19431	0.98989	0.002026	0.075024				-0.08009	-0.007			0.002099	0.075024								
24	13.21773	0.989726	0.00188	0.074879		0.073	^	-0.08009	-0.007			0.001949	0.074879		0.073	^					
25	13.2395	0.989574	0.001175	0.074744		329.6		-0.08009	-0.007			0.001809	0.074744		318.2						
26	13.25975	0.989432	0.001621	0.074619		0.999999		-0.08009	-0.007			0.00168	0.074619		0.999997						
27	13.27857	0.9893	0.001505	0.074504				-0.08009	-0.007			0.001559	0.074504								
28	13.29608	0.989177	0.001397	0.074396				-0.08009	-0.007			0.001449	0.074396								
29	13.31235	0.989064	0.001298	0.074297	0.072999			-0.08008	-0.007	0.073083		0.001344	0.074297	0.072953		-0.08295	-0.007	0.075951			
30	13.32749	0.988958	0.001205	0.074204				-0.0801	-0.007			0.00125	0.074204								
31	13.34156	0.988859	0.00112	0.074119				-0.08009	-0.007			0.00116	0.074119								
32	13.35465	0.988767	0.00104	0.074039				-0.08011	-0.007			0.001078	0.074039								
33	13.36682	0.988682	0.000966	0.073965				-0.08009	-0.007			0.001002	0.073965								
34	13.37813	0.988603	0.000897	0.073897				-0.08008	-0.007			0.00093	0.073897								
35																					
36																					
37																					
38																					
39	13.42386	0.988283																			
40	13.43117	0.988232	0.000578	0.073578	0.073							0.000599	0.073578	0.072979							
41	13.43797	0.988184																			
42																					
43																					
44																					
45																					
46																					
47																					
48																					
49																					
50	13.48128	0.987881																			
51	13.48561	0.987858	0.000253	0.073253	0.073							0.000353	0.073253	0.072989							
52	13.48762	0.98784																			
53																					
54																					
55																					
56																					
57																					
58																					
59																					
60																					
61	13.50707																				
62	13.50855	0.98769	0.000116	0.073116	0.073							0.000121	0.073116	0.072995							
63	13.50992																				
64																					
65																					
66																					
67																					

68																			
69																			
70																			
71																			
72		13.51867																	
73		13.519	0.987615	0.000052	0.073052	0.073							0.000054	0.073052	0.072998				
74		13.51995																	
75																			
76																			
77																			
78																			
79																			
80																			
81																			
82																			
83		13.52388																	
84		13.52417	0.987581	0.000023	0.073023	0.073							0.000024	0.073023	0.072999				
85		13.52445																	
86																			
87																			
88																			
89																			
90																			
91																			
92																			
93																			
94		13.52662																	
95		13.52635	0.987566	0.00001	0.073011	0.073							0.000011	0.073011	0.073				
96		13.52647																	
97																			
98																			
99																			
100																			
101																			
102																			
103																			
104																			
105		13.52727																	
106		13.52733	0.987559	0.000004	0.073005	0.073							0.000005	0.073005	0.073				
107		13.52738																	
108																			
109																			
110																			
111																			
112																			
113																			
114																			
115																			
116		13.52774																	
117		13.52796	0.987556	0.000002	0.073002	0.073							0.000002	0.073002	0.073				
118		13.52779																	
119																			
120																			
121																			

122																			
123																			
124																			
125																			
126	13.52795																		
127	13.52796	0.987554	0.000001	0.073001	0.073								0.000001	0.073001	0.073				
128	13.52798																		
129																			
130																			
131																			
132																			
133																			
134																			
135																			
136																			
137																			
138	13.52805																		
139	13.52805	0.987554	0	0.073	0.073								0	0.073	0.073				
140	13.52806																		
141																			
142																			
143																			
144	13.52807	1.187554																	
145	13.70344	1.186326	0.013584	0.086571		0.073	0.072998	1.06166	1.13364		0.073002	0.014077	0.086571		0.072999	1.100188	1.13364		0.073002
146	13.86651	1.185184	0.012482	0.085471		329.7	329.8	0.511449	0.583992		329.7	0.012936	0.085471		318.2	0.530058	0.583997		318.1
147	14.01813	1.184123	0.011481	0.084471		1	0.999998	0.328431	0.401138		1	0.011898	0.084471		1	0.340357	0.401138		1
148	14.15913	1.183136	0.01057	0.08356				0.23716	0.309942			0.010954	0.08356			0.245789	0.309942		
149	14.29023	1.182218	0.009737	0.082729				0.18258	0.255422			0.010092	0.082729			0.18922	0.255422		
150	14.41213	1.181365	0.008978	0.08197	0.072992			0.146367	0.219236	0.072869		0.009304	0.08197	0.072666		0.15168	0.219236	0.067556	
151	14.52549	1.180572	0.008283	0.081276				0.120633	0.193524			0.008585	0.081276			0.125022	0.193524		
152	14.63089	1.179834	0.007647	0.08064				0.101448	0.174358			0.007924	0.08064			0.105133	0.17438		
153	14.7289	1.179148	0.007063	0.080057				0.086636	0.159556			0.00732	0.080057			0.089783	0.159556		
154	14.82004	1.17851	0.006527	0.079521				0.074875	0.147806			0.006765	0.079521			0.0776	0.147806		
155	14.90478	1.177917	0.006035	0.079029				0.065336	0.138277			0.006254	0.079029			0.067709	0.138277		
156	14.98358	1.177365	0.005582	0.078577		0.073	0.073	0.057465	0.130412		0.072999	0.005785	0.078577		0.073	0.059554	0.130412		0.072999
157	15.05685	1.176852	0.005165	0.078161		329.7	329.7	0.050872	0.123826		329.7	0.005358	0.078161		318.1	0.052721	0.123826		318.1
158	15.12498	1.176375	0.004781	0.077777		1	1	0.045285	0.118244		1	0.004955	0.077777		0.999999	0.046931	0.118244		1
159	15.18833	1.175932	0.004427	0.077423				0.040502	0.113465			0.004588	0.077423			0.041973	0.113465		
160	15.24724	1.175519	0.004101	0.077097				0.036369	0.109337			0.00425	0.077097			0.037694	0.109337		
161	15.30201	1.175136	0.0038	0.076796	0.072997			0.032775	0.105745	0.07297		0.003937	0.076796	0.072859		0.033963	0.105745	0.071782	
162	15.35295	1.174779	0.003521	0.076518				0.029627	0.102598			0.00365	0.076518			0.030706	0.102598		
163	15.40031	1.174448	0.003264	0.076261				0.026851	0.099826			0.003383	0.076261			0.027826	0.099826		
164	15.44435	1.17414	0.003027	0.076024				0.024394	0.097371			0.003137	0.076024			0.025281	0.097371		
165	15.4853	1.173853	0.002807	0.075804				0.022206	0.095187			0.002909	0.075804			0.023015	0.095187		
166	15.52337	1.173586	0.002603	0.075601				0.020255	0.093237			0.002698	0.075601			0.020988	0.093237		
167	15.55878	1.173339	0.002415	0.075413		0.072999	0.073	0.018507	0.091489		0.073001	0.002503	0.075413		0.072999	0.019181	0.091489		0.073
168	15.5917	1.173108	0.002241	0.075239		329.8	329.7	0.016935	0.089918		329.7	0.002323	0.075239		318.3	0.017548	0.089918		318.1
169	15.62232	1.172894	0.00208	0.075078		0.999998	1	0.015516	0.088501		0.999999	0.002156	0.075078		0.999999	0.016083	0.088501		0.999997
170	15.65078	1.172695	0.00193	0.074929				0.014233	0.087221			0.002	0.074929			0.014748	0.087221		
171	15.67725	1.172509	0.001792	0.07479				0.013072	0.08606			0.001857	0.07479			0.013548	0.08606		
172	15.70186	1.172337	0.001664	0.074662	0.072998			0.012018	0.085006	0.072988		0.001724	0.074662	0.072938		0.012454	0.085006	0.072552	
173	15.72475	1.172177	0.001545	0.074543				0.011059	0.084048			0.001601	0.074543			0.011462	0.084048		
174	15.74603	1.172028	0.001436	0.074433				0.010194	0.083174			0.001487	0.074433			0.010554	0.083174		
175	15.76586	1.171889	0.001332	0.07433				0.009386	0.082375			0.001384	0.07433			0.009748	0.082375		

176	15.78422	1.17176	0.001236	0.074236				0.008647	0.081647			0.00128	0.074236			0.008952	0.081647		
177	15.80133	1.171641	0.001149	0.074148				0.007987	0.080981			0.001191	0.074148			0.008279	0.080981		
178	15.81723																		
179																			
180																			
181																			
182	15.87047																		
183	15.88153	1.171079	0.000739	0.073738	0.072999			0.004987	0.077982	0.072995		0.000766	0.073738	0.072972		0.005169	0.077982	0.072813	
184	15.89181																		
185																			
186																			
187																			
188																			
189																			
190																			
191																			
192																			
193	15.95728																		
194	15.96225	1.170514	0.00033	0.07333	0.073			0.002167	0.075164	0.072997		0.000342	0.07333	0.072988		0.002246	0.075164	0.072918	
195	15.96687																		
196																			
197																			
198																			
199																			
200																			
201																			
202																			
203																			
204	15.99629																		
205	15.99853	1.17026	0.000148	0.073148	0.073			0.00096	0.073957	0.072998		0.000154	0.073148	0.072994		0.000997	0.073957	0.07296	
206	16.0006																		
207																			
208																			
209																			
210																			
211																			
212																			
213																			
214																			
215	16.01382																		
216	16.01483	1.170146	0.000067	0.073066	0.073			0.000429	0.073427	0.072998		0.000069	0.073066	0.072997		0.000447	0.073427	0.07298	
217	16.01576																		
218																			
219																			
220																			
221																			
222																			
223																			
224																			
225																			
226	16.0217																		
227	16.02215	1.170095	0.00003	0.07303	0.073			0.000192	0.073191	0.072999		0.000031	0.07303	0.072999		0.000198	0.073191	0.072993	
228	16.02257																		
229																			

230																				
231																				
232																				
233																				
234																				
235																				
236																				
237	16.02524																			
238	16.02544	1.170072	0.000013	0.073013	0.073			0.000086	0.073085	0.072999		0.000014	0.073013	0.072999		0.000088	0.073085	0.072997		
239	16.02563																			
240																				
241																				
242																				
243																				
244																				
245																				
246																				
247																				
248	16.02683																			
249	16.02692	1.170062	0.000006	0.073006	0.073			0.000037	0.073038	0.073		0.000006	0.073006	0.073		0.00004	0.073038	0.072998		
250	16.027																			
251																				
252																				
253																				
254																				
255																				
256																				
257																				
258																				
259	16.02754																			
260	16.02758	1.170057	0.000003	0.073003	0.073			0.000018	0.073017	0.072999		0.000003	0.073003	0.073		0.000018	0.073017	0.072999		
261	16.02762																			
262																				
263																				
264																				
265																				
266																				
267																				
268																				
269																				
270	16.02788																			
271	16.0279	1.170055	0.000001	0.073001	0.073			0.000007	0.073006	0.073		0.000001	0.073001	0.073		0.000009	0.073006	0.072997		
272	16.02791																			
273																				
274																				
275																				
276																				
277																				
278																				
279																				
280																				
281	16.02802																			
282	16.02802	1.170054	0	0.073001	0.073			0.000002	0.073003	0.073		0	0.073001	0.073001		0	0.073001	0.073001		
283	16.02803																			

284																			
285																			
286																			
287	16.02805	0.970054																	
288	15.85269	0.971281	-0.01174	0.061269		0.073	0.072998	-0.08007	-0.007			-0.01217	0.061269		0.072999				
289	15.68963	0.972423	-0.01103	0.061979		329.1	329.8	-0.08007	-0.007			-0.01143	0.061979		318.1				
290	15.53801	0.973484	-0.01036	0.062652		1	0.999998	-0.08007	-0.007			-0.01073	0.062652		0.999999				
291	15.39703	0.974471	-0.00972	0.06329				-0.08007	-0.007			-0.01007	0.06329						
292	15.26593	0.975388	-0.00912	0.063893				-0.08007	-0.007			-0.00945	0.063893						
293	15.14403	0.976242	-0.00854	0.064464	0.073008			-0.08007	-0.007	0.073069		-0.00885	0.064464	0.073318		-0.08298	-0.007	0.07598	
294	15.03068	0.977035	-0.008	0.065003				-0.08007	-0.007			-0.0083	0.065003						
295	14.92529	0.977773	-0.0075	0.065511				-0.08007	-0.007			-0.00777	0.065511						
296	14.82728	0.978459	-0.00702	0.06599				-0.08007	-0.007			-0.00727	0.06599						
297	14.73615	0.979097	-0.00656	0.066442				-0.08007	-0.007			-0.0068	0.066442						
298	14.63141	0.97964	-0.00614	0.066866				-0.08007	-0.007			-0.00636	0.06687						
299	14.57262	0.980242	-0.00574	0.067266		0.073	0.072998	-0.08007	-0.007			-0.00595	0.067266		0.073001				
300	14.49935	0.980755	-0.00536	0.067641		329.1	330	-0.08006	-0.007			-0.00556	0.067641		318.3				
301	14.43123	0.981231	-0.00501	0.067994		1	0.9999	-0.08006	-0.007			-0.00519	0.067994		0.999999				
302	14.36788	0.981675	-0.00468	0.068324				-0.08006	-0.007			-0.00485	0.068324						
303	14.30897	0.982087	-0.00437	0.068634				-0.08007	-0.007			-0.00453	0.068634						
304	14.2542	0.982471	-0.00408	0.068925	0.073003			-0.08006	-0.007	0.073062		-0.00421	0.068925	0.073131		-0.08297	-0.007	0.075973	
305	14.20327	0.982827	-0.00381	0.069197				-0.08006	-0.007			-0.00394	0.069197						
306	14.15591	0.983159	-0.00356	0.069452				-0.08007	-0.007			-0.00368	0.069452						
307	14.11187	0.983467	-0.00331	0.069691				-0.08006	-0.007			-0.00343	0.069691						
308	14.07093	0.983754	-0.00309	0.069914				-0.08006	-0.007			-0.0032	0.069914						
309	14.03285	0.98402	-0.00288	0.070123				-0.08006	-0.007			-0.00299	0.070123						
310	13.99745	0.984268	-0.00268	0.070318		0.072999	0.073	-0.08006	-0.007			-0.00278	0.070318		0.073				
311	13.96453	0.984498	-0.0025	0.0705		329.6	329.7	-0.08007	-0.007			-0.00259	0.0705		318.2				
312	13.93391	0.984713	-0.00233	0.07067		1	1	-0.08007	-0.007			-0.00242	0.07067		1				
313	13.90545	0.984912	-0.00217	0.070829				-0.08006	-0.007			-0.00225	0.070829						
314	13.87898	0.985097	-0.00202	0.070978				-0.08006	-0.007			-0.0021	0.070978						
315	13.85437	0.985269	-0.00189	0.071116	0.073001			-0.08005	-0.007	0.073046		-0.00195	0.071116	0.07307		-0.08297	-0.007	0.075969	
316	13.83149	0.98543	-0.00176	0.071245				-0.08005	-0.007			-0.00182	0.071245						
317	13.81021	0.985579	-0.00164	0.071366				-0.08006	-0.007			-0.0017	0.071366						
318	13.79042	0.985717	-0.00152	0.071478				-0.08006	-0.007			-0.00158	0.071478						
319	13.77202	0.985846	-0.00142	0.071583				-0.08006	-0.007			-0.00147	0.071583						
320	13.75491	0.985966	-0.00132	0.071681				-0.08004	-0.007			-0.00137	0.071681						
321																			
322																			
323																			
324																			
325	13.68578																		
326	13.67472	0.986527	-0.00086	0.072142	0.073001							-0.00089	0.072142	0.073032					
327	13.66443																		
328																			
329																			
330																			
331																			
332																			
333																			
334																			
335																			
336	13.59896																		
337	13.59399	0.98709	-0.00039	0.072612	0.073							-0.0004	0.072612	0.073014					

338	13.58937																		
339																			
340																			
341																			
342																			
343																			
344																			
345																			
346																			
347	13.55995																		
348	13.55772	0.987346	-0.00017	0.072825	0.073								-0.00018	0.072825	0.073006				
349	13.55565																		
350																			
351																			
352																			
353																			
354																			
355																			
356																			
357																			
358	13.54243																		
359	13.54142	0.98746	-7.9E-05	0.072921	0.073								-8.2E-05	0.072921	0.073003				
360	13.54049																		
361																			
362																			
363																			
364																			
365																			
366																			
367																			
368																			
369	13.53455																		
370	13.5341	0.987511	-3.5E-05	0.072965	0.073								-3.7E-05	0.072965	0.073002				
371	13.53368																		
372																			
373																			
374																			
375																			
376																			
377																			
378																			
379																			
380	13.53101																		
381	13.53081	0.987534	-1.6E-05	0.072984	0.073								-1.6E-05	0.072984	0.073				
382	13.53062																		
383																			
384																			
385																			
386																			
387																			
388																			
389																			
390																			
391	13.52942																		

392	13.52933	0.987545	-7E-06	0.072993	0.073							-7E-06	0.072993	0.073					
393	13.52925																		
394																			
395																			
396																			
397																			
398																			
399																			
400																			
401																			
402	13.52871																		
403	13.52867	0.987549	-3E-06	0.072997	0.073							-3E-06	0.072997	0.073					
404	13.52863																		
405																			
406																			
407																			
408																			
409																			
410																			
411																			
412																			
413	13.52839																		
414	13.52832	0.987551	-2E-06	0.072999	0.073001							-2E-06	0.072999	0.073					
415	13.52835																		
416																			
417																			
418																			
419																			
420																			
421																			
422																			
423																			
424	13.52824																		
425	13.52823	0.987552	0	0.072999	0.073							0	0.072999	0.073					
426	13.52823																		
427																			
428																			
429																			
430																			
431																			
432																			
433																			
434																			
435	13.52818																		
436	13.52817	0.987553	0	0.073	0.073							0	0.073	0.073					
437	13.52817																		
438																			
439																			
440																			
441																			
442																			
443																			
444																			
445																			

446	13.52815																		
447	13.52815	0.987553	0	0.073	0.073							0	0.073	0.073					
448	13.52815																		
449																			
450																			
451																			
452																			
453																			
454																			
455																			
456																			
457	13.52814																		
458	13.52814	0.987553	0	0.073	0.073							0	0.073	0.073					
459	13.52814																		
460																			
461																			
462																			
463																			
464																			
465																			
466																			
467																			
468	13.52813																		
469	13.52813	0.987553	0	0.073	0.073							0	0.073	0.073					
470	13.52813																		
471																			
472																			
473																			
474																			
475																			
476																			
477																			
478																			
479	13.52813																		
480	13.52813	0.987553	0	0.073	0.073							0	0.073	0.073					
481	13.52813																		
482																			
483																			
484																			
485																			
486																			
487																			
488																			
489																			
490	13.52813																		
491	13.52813	0.987553	0	0.073	0.073							0	0.073	0.073					
492	13.52813																		
493																			
494																			
495																			
496																			
497																			
498																			
499																			

500																			
501	13.52813																		
502	13.52813	0.987755	0	0.073	0.073								0	0.073	0.073				
503	13.52813																		
504																			
505																			
506																			
507																			
508																			
509																			
510																			
511																			
512	13.52813																		
513	13.52813	0.987553	0	0.073	0.073								0	0.073	0.073				
514	13.52813																		
515																			
516																			
517																			
518																			
519																			
520																			
521																			
522																			
523	13.52813																		
524	13.52813	0.987553	0	0.073	0.073								0	0.073	0.073				
525	13.52813																		
526																			
527																			
528																			
529																			
530																			
531																			
532																			
533																			
534	13.52813																		
535	13.52813	0.987553	0	0.073	0.073								0	0.073	0.073				
536	13.52813																		
537																			
538																			
539																			
540																			
541																			
542																			
543																			
544																			
545	13.52813																		
546	13.52813	0.987553	0	0.073	0.073								0	0.073	0.073				
547	13.52813																		
548																			
549																			
550																			
551																			
552																			
553																			

554																			
555																			
556	13.52813																		
557	13.52813	0.987553	0	0.073	0.073								0	0.073	0.073				
558	13.52813																		
559																			
560																			
561																			
562																			
563																			
564																			
565																			
566																			
567	13.52813																		
568	13.52813	0.987553	0	0.073	0.073								0	0.073	0.073				
569	13.52813																		
570																			
571																			
572																			
573																			
574																			
575																			
576																			

Spreadsheet 2

Part of the (kc')21 spreadsheet for the time region 0<t<T of a simulation of a measurement cycle

Evaluation of (kc')21 and (kc')31

1	2	3	4	5	6	7	8	9	10	11
interval	$\int f(\theta)d\tau$	$\int inputd\tau$	abscissa	ordinate	(kc')21 /WK^-1	$\int f(\theta)d\tau$	$\int inputd\tau$	abscissa	ordinate	(kc')31 /WK^-1
0	2429452	177937.5	-0.00024	0.073242	0.073					
7	2403971	175843.7	-0.00015	0.073147	0.073	25481.51	2093.86	0.009187	0.082172	0.072985
18	2361757	173567.1	-6.7E-05	0.073067	0.073	67695.62	5370.4	0.006327	0.079332	0.073005
29	2318205	169300.6	-3.1E-05	0.073031	0.073	111247.2	8636.96	0.004635	0.077638	0.073003
40	2274053	166038.2	-1.4E-05	0.073014	0.073	155399.5	11899.32	0.00357	0.076572	0.073002
51	3229630	162777.7	-6E-06	0.073007	0.073001	199822.1	15159.79	0.002866	0.075866	0.073
62	2185086	159518.1	-3E-06	0.073003	0.073	294366.1	18419.41	0.002375	0.075376	0.073001
73	2140488	156258.9	-1E-06	0.073002	0.073	288964.4	21678.65	0.002021	0.075022	0.073001
84	2095865	152999.8	0	0.073001	0.073	333587.2	24937.71	0.001755	0.074756	0.073001
95	2051231	149740.8	0	0.073	0.073	378221.1	28196.7	0.00155	0.074551	0.073001
106	2006592	146481.9	0	0.073	0.073	422859.9	31455.65	0.001387	0.074388	0.073001
117	1961951	143212.9	0	0.073	0.073	467500.9	34714.59	0.001255	0.074256	0.073001
128	1917309	139964	0	0.073001	0.073	512142.9	37973.52	0.001146	0.074146	0.073001
139	1872667	136705.1	0	0.073	0.073	556785.3	41232.45	0.001054	0.074054	0.073001
150	1827173	133092.1	0.00016	0.07284	0.073	602279.7	44845.42	0.001459	0.074459	0.073001
161	1777952	129205.2	0.000329	0.072671	0.073	651500.1	48732.3	0.001799	0.0748	0.073001
172	1726709	125332.4	0.000415	0.072585	0.073	702742.8	52605.15	0.001856	0.074857	0.073001
183	1674558	121466	0.000464	0.072536	0.073	754894.2	56471.52	0.001806	0.074807	0.073001
194	1621998	117602.5	0.000495	0.072505	0.073	807453.9	60335.03	0.001722	0.074723	0.073001
205	1569255	113740.3	0.00052	0.07248	0.073	860197	64197.25	0.00163	0.074631	0.073001
216	1516429	109878.6	0.000541	0.072459	0.073	913023.6	68058.9	0.001541	0.074542	0.073001
227	1463567	106017.2	0.000562	0.072438	0.073	965885.1	71920.28	0.00146	0.07446	0.073001
238	1410687	102156	0.000584	0.072416	0.073	1018764	75781.55	0.001385	0.074386	0.073001
249	1357801	98294.74	0.000607	0.072393	0.073	1071651	79642.77	0.001317	0.074318	0.073001
260	1304911	94433.54	0.000632	0.072368	0.073	1124541	83503.97	0.001255	0.074256	0.073001
271	1252020	90572.36	0.000659	0.072341	0.073	1177433	87365.15	0.001199	0.0742	0.073001
282	1199127	86711.18	0.000688	0.072312	0.073	1230325	91226.33	0.001147	0.074148	0.073001
293	1147086	83204.04	0.000465	0.072535	0.073	1282366	94733.47	0.000873	0.073874	0.073001
304	1098775	79970.82	0.000218	0.072782	0.073	1330678	97966.69	0.000621	0.073622	0.073001
315	1052482	76723.45	0.000102	0.072898	0.073	1376970	101214.1	0.000504	0.073505	0.073001
326	1007098	73469.71	0.000048	0.072952	0.073	1422355	104467.8	0.000447	0.073447	0.073
337	962121.7	70213.12	0.000023	0.072977	0.073	1467331	107724.4	0.000415	0.073415	0.073
348	917329.2	66955.24	0.000011	0.072989	0.073	1512123	110982.3	0.000395	0.073395	0.073
359	872619.1	63696.79	0.000005	0.072995	0.073	1556833	114240.7	0.00038	0.07338	0.073
370	827946.1	60438.08	0.000002	0.072998	0.073	1601506	117499.4	0.000368	0.073368	0.073
381	783289.7	57179.25	0.000001	0.072999	0.073	1646163	120758.3	0.000357	0.073357	0.073
392	738640.8	53920.36	1E-07	0.072999	0.073	1690812	124017.2	0.000347	0.073348	0.073001
403	693995.2	50661.46	0	0.073	0.073	1735457	127276.1	0.000338	0.073339	0.073
414	649351.2	47402.54	0	0.073	0.073	1780101	130535	0.00033	0.07333	0.073
425	604707.8	44143.62	0	0.073	0.073	1824744	133793.9	0.000322	0.073322	0.073
436	560064.7	40884.69	0	0.073	0.073	1869388	137052.8	0.000314	0.073314	0.073
447	515421.8	37625.77	0	0.073	0.073	1914030	140311.7	0.000307	0.073307	0.073

458	470778.9	34366.84	0	0.073	0.073	1958673	143570.7	0.0003	0.0733	0.073
469	426136.1	31107.92	0	0.073	0.073	2003316	146829.6	0.000293	0.073293	0.073
480	381493.3	27848.99	0	0.073	0.073	2047959	150088.5	0.000287	0.073287	0.073
491	336850.4	24590.07	0	0.073	0.073	2092602	153347.4	0.00028	0.073281	0.073001
502	292207.6	21331.14	0	0.073	0.073	2137245	156606.4	0.000275	0.073275	0.073
513	247564.8	18072.22	0	0.073	0.073	2181887	159865.3	0.000269	0.073269	0.073
524	202922	14813.3	0	0.073	0.073	2226530	163124.2	0.000264	0.073264	0.073
535	158279.1	11554.37	0	0.073	0.073	2271173	166383.1	0.000258	0.073259	0.073001
546	113636.3	8295.45	0	0.073	0.073	2315816	169642.1	0.000253	0.073254	0.073001
557	68993.46	5036.52	0	0.073	0.073	2360459	172901	0.000249	0.073249	0.073
567	24350.63	1777.6	0	0.073	0.073	2405102	176159.9	0.000244	0.073244	0.073
574						2429452	177937.5	0.000242	0.073242	0.073

Spreadsheet 3

Part of the (kc')21 spreadsheet for the time region t1< t < t2 of a simulation of a measurement cycle

Evaluation of (kc')21, (kc')22, (kc'o)261, (kc'o)262, (kc')31, (kc')32, (kc'o)361 and (kc'o)362

1	2	3	4	5	6	7	8	9	10	11	12	13	14	15	16	17	18	19
interval 300/s	$\int f(\theta)d\tau$	$\int inputd\tau$	abscissa	ordinate	(kc')21 / WK^-1	(kc'o)261 / WK^-1 slope /JK^-1 r	abscissa	ordinate	(kc')22 / WK^-1	(kc'o)262 / WK^-1 slope /JK^-1 r	abscissa	ordinate	(kc')31 / WK^-1	(kc'o)361 / WK^-1 slope /JK^-1 r	abscissa	ordinate	(kc')32 / WK^-1	(kc'o)362 / WK^-1 slope /JK^-1 r
143	676539.7	50227.74	-0.00122	0.074242														
144	672481.3	49916.48	-0.00123	0.074227														
145	668396.6	49560.4	-0.00115	0.074148	0.073	0.073	-0.00798	0.08098	0.073002	0.072999	0.014168	0.087173	0.073006	0.073001	2.20046	2.274295	0.073835	0.072984
146	664261.1	49204.67	-0.00107	0.074074		330.1	-0.00742	0.080426		330.1	0.013587	0.086593		330.1	1.080755	1.154228		330.1
147	660078.4	48849.27	-0.00101	0.074005		0.999999	-0.00691	0.079914		1	0.013039	0.086045		1	0.71045	0.78378		1
148	655857.8	48494.18	-0.00094	0.073941			-0.00644	0.07994			0.012523	0.085529			0.526162	0.599398		
149	651584.4	48139.38	-0.00088	0.073881			-0.006	0.079002			0.012036	0.085041			0.415889	0.48907		
150	647279.1	47784.97	-0.00082	0.073824	0.073		-0.00559	0.078596	0.073002		0.011576	0.084576	0.073005		0.342546	0.415548	0.073001	
151	642938.4	47430.55	-0.00077	0.073772			-0.00522	0.078218			0.011141	0.084146			0.29028	0.363407		
152	638564.9	47076.49	-0.00072	0.073722			-0.00487	0.077868			0.01073	0.083735			0.251174	0.324284		
153	634161	46722.65	-0.00068	0.073676			-0.00454	0.077543			0.010341	0.083346			0.220832	0.293924		
154	629728.6	46369	-0.00063	0.073633			-0.00424	0.077241			0.009972	0.082977			0.196622	0.269705		
155	625269.9	46015.53	-0.00059	0.073593			-0.00396	0.07696			0.009623	0.082627			0.176868	0.249944		
156	620786.6	45662.24	-0.00056	0.073555		0.073	-0.0037	0.076699		0.072999	0.009291	0.082296		0.073	0.160454	0.233523		0.073006
157	616280.6	45309.11	-0.00052	0.07352		330.1	-0.00346	0.076456		330.1	0.008972	0.081981		330.2	0.146608	0.21967		330.1
158	611753.3	44956.12	-0.00049	0.073487		0.999999	-0.00323	0.07623		1	0.008678	0.081682		1	0.134779	0.207837		0.999998
159	607206.3	44603.28	-0.00046	0.073457			-0.00302	0.076019			0.008394	0.081397			0.124561	0.197613		
160	602641	44250.56	-0.00043	0.073428			-0.00282	0.075823			0.008123	0.081127			0.115652	0.188701		
161	598058.6	43898.09	-0.0004	0.073401	0.073		-0.00264	0.075642	0.073002		0.007866	0.080868	0.073004		0.10782	0.180843	0.073022	
162	593460.3	43545.47	-0.00038	0.073376			-0.00247	0.075469			0.007621	0.080624			0.100886	0.173929		
163	588847.3	43193.09	-0.00035	0.073352			-0.00231	0.07531			0.007387	0.080391			0.094706	0.167746		
164	584220.6	42840.8	-0.00033	0.07333			-0.00216	0.075162			0.007165	0.080168			0.089167	0.162204		
165	579581.2	42488.6	-0.00031	0.073309			-0.00202	0.075023			0.006952	0.079956			0.084167	0.157195		
166	574929.9	42136.49	-0.00029	0.07329			-0.00189	0.074894			0.00675	0.079753			0.079658	0.152691		
167	570267.6	41784.45	-0.00027	0.073272		0.073	-0.00177	0.074773		0.073	0.006556	0.079559		0.72999	0.075552	0.148584		0.072998
168	565595	41432.48	-0.00026	0.073255		329.3	-0.00166	0.074661		330	0.006371	0.079374		330.2	0.071806	0.144836		330.1
169	560912.8	41080.58	-0.00024	0.073239		0.99998	-0.00156	0.074555		0.99999	0.006194	0.079197		0.999998	0.068374	0.141403		1
170	556221.9	40728.74	-0.00022	0.073224			-0.00146	0.074457			0.006025	0.079028			0.065222	0.138249		
171	551522.7	40376.96	-0.00021	0.07321			-0.00137	0.074365			0.005863	0.078886			0.062317	0.135315		
172	546815.9	40025.24	-0.0002	0.073197	0.073		-0.00128	0.074279	0.073		0.005708	0.078711	0.073002		0.059633	0.132658	0.073032	
173	542101.9	39673.56	-0.00019	0.073185			-0.0012	0.074198			0.00556	0.078562			0.057147	0.13017		
174	537381.3	39321.93	-0.00017	0.073173			-0.00112	0.074123			0.005418	0.07842			0.054838	0.12786		
175	532654.5	38970.34	-0.00016	0.073163			-0.00105	0.074053			0.005281	0.078284			0.05269	0.12571		
176	527922	38618.79	-0.00015	0.073152			-0.00099	0.073987			0.00515	0.078153			0.050684	0.123705		
177	523184.1	38267.28	-0.00014	0.073143			-0.00093	0.073925			0.005025	0.078027			0.048811	0.121831		
178																		

179																
180																
181																
182																
183	494664.5	36158.87	-9.8E-05	0.073098	0.073		-0.00063	0.07363	0.072999		0.004368	0.07737	0.073002		0.03975	0.112766	0.073016	
184																
185																
186																
187																
188																
189																
190																
191																
192																
193																
194	442104.8	32295.36	-4.9E-05	0.073049	0.073		-0.00032	0.073315	0.072999		0.003487	0.076488	0.073002		0.029258	0.10227	0.073012	
195																
196																
197																
198																
199																
200																
201																
202																
203																
204																
205	389361.7	28433.14	-2.5E-05	0.073025	0.073		-0.00016	0.07316	0.072999		0.00288	0.075881	0.073001		0.022929	0.094526	0	
206																
207																
208																
209																
210																
211																
212																
213																
214																
215																
216																
217																
218																
219																
220																
221																
222																
223																
224																
225																
226																
227	283673.6	20710.11	-7E-06	0.073007	0.073		-4.4E-05	0.073043	0.072999		0.002117	0.075118	0.073001		0.015841	0.088846	0.073006	
228																
229																
230																
231																
232																

233																	
234																	
235																	
236																	
237																	
238	230794.3	16848.84	-4E-06	0.073004	0.073		-2.4E-05	0.073023	0.072999		0.001866	0.074867	0.073001		0.013691	0.086696	0.073005
239																	
240																	
241																	
242																	
243																	
244																	
245																	
246																	
247																	
248																	
249	177907.6	12987.62	-2E-06	0.073002	0.073		-1.3E-05	0.073012	0.072999		0.001667	0.074668	0.073001		0.012049	0.085053	0.073004
250																	
251																	
252																	
253																	
254																	
255																	
256																	
257																	
258																	
259																	
260	125017.5	9126.42	-1E-06	0.073001	0.073		-8E-06	0.073006	0.072998		0.001507	0.074507	0.073001		0.010756	0.08376	0.073004
261																	
262																	
263																	
264																	
265																	
266																	
267																	
268																	
269																	
270																	
271	72125.95	5265.24	-1E-06	0.073001	0.073		-4E-06	0.073003	0.072999		0.001374	0.074375	0.073001		0.009713	0.082716	0.073003
272																	
273																	
274																	
275																	
276																	
277																	
278																	
279																	
280																	
281	19233.65	1404.06	-1E-06	0.073001	0.072999		-3E-06	0.073	0.072997		0.001263	0.074263	0.073001		0.008484	0.081487	0.073003
282																	
283																	
284																	
285																	
286											0.001227	0.074227	0.073001		0.008577	0.08158	0.073003

Spreadsheet 4

Part of the (kc')21 spreadsheet for the time region t1 > t > t2 of a simulation of a measurement cycle

Effects of errors of +30J (columns 2-9) and -30J (columns10-17) on the evaluation of (kc')21, (kc')22, (kc'o)261 and (kc'o)262

1	2	3	4	5	6	7	8	9	10	11	12	13	14	15	16	17
interval 300/s	abscissa	ordinate	(kc')21 / WK^-1	(kc'o)261 / WK^-1 slope /JK^-1 r	abscissa	ordinate	(kc')22 / WK^-1	(kc'o)262 / WK^-1 slope /JK^-1 r	abscissa	ordinate	(kc')21 / WK^-1	(kc'o)261 / WK^-1 slope /JK^-1 r	abscissa	ordinate	(kc')22 / WK^-1	(kc'o)262 / WK^-1 slope /JK^-1 r
143	-0.00122	0.074286							-0.00122	0.074198						
144	-0.00123	0.074272							-0.00123	0.074183						
145	-0.00115	0.074193	0.073045	0.073058	-0.00798	0.081292	0.073314	0.073359	-0.00115	0.074103	0.072955	0.072944	-0.00798	0.080668	0.07269	0.072639
146	-0.00107	0.074119		326.3	-0.00742	0.080738		327.6	-0.00107	0.074029		333.9	-0.00742	0.080114		332.8
147	-0.00101	0.074051		0.99999	-0.00691	0.080227		0.999991	-0.00101	0.07396		0.999988	-0.00691	0.079602		0.999992
148	-0.00094	0.073987			-0.00644	0.079754			-0.00094	0.073895			-0.00644	0.079127		
149	-0.00088	0.073927			-0.006	0.079315			-0.00088	0.073834			-0.006	0.078688		
150	-0.00082	0.073871			-0.00559	0.078911			-0.00082	0.073778			-0.00559	0.078282		
151	-0.00077	0.073818			-0.00522	0.078533			-0.00077	0.073725			-0.00522	0.077902		
152	-0.00072	0.073769			-0.00487	0.078185			-0.00072	0.073675			-0.00487	0.077551		
153	-0.00068	0.073724			-0.00454	0.077861			-0.00068	0.073629			-0.00454	0.077225		
154	-0.00063	0.073681			-0.00424	0.07756			-0.00063	0.073586			-0.00424	0.076922		
155	-0.00059	0.073641			-0.00396	0.077281			-0.00059	0.073545			-0.00396	0.07664		
156	-0.00056	0.073604	0.073049	0.073059	-0.0037	0.077021	0.073322	0.073378	-0.00056	0.073507	0.072952	0.072942	-0.0037	0.076377	0.072678	0.072621
157	-0.00052	0.073569		323.3	-0.00346	0.07678		324.4	-0.00052	0.073472		336.7	-0.00346	0.076133		335.8
158	-0.00049	0.073536		0.999976	-0.00323	0.076555		0.999987	-0.00049	0.073438		0.999958	-0.00323	0.075905		0.999987
159	-0.00046	0.073506			-0.00302	0.076346			-0.00046	0.073407			-0.00302	0.075693		
160	-0.00043	0.073478			-0.00282	0.076152			-0.00043	0.073378			-0.00282	0.075494		
161	-0.0004	0.073451			-0.00264	0.075972			-0.0004	0.073351			-0.00264	0.075311		
162	-0.00038	0.073426			-0.00247	0.075802			-0.00038	0.073325			-0.00247	0.075137		
163	-0.00035	0.073403			-0.00231	0.075645			-0.00035	0.073301			-0.00231	0.074976		
164	-0.00033	0.073381			-0.00216	0.075499			-0.00033	0.073278			-0.00216	0.074825		
165	-0.00031	0.073361			-0.00202	0.075362			-0.00031	0.073257			-0.00202	0.074684		
166	-0.00029	0.073342			-0.00189	0.075235			-0.00029	0.073238			-0.00189	0.074553		
167	-0.00027	0.073324	0.073052	0.073063	-0.00177	0.075117	0.073343	0.073398	-0.00027	0.073219	0.072947	0.07294	-0.00177	0.07443	0.072656	0.0726
168	-0.00026	0.073308		316.5	-0.00166	0.075007		319.5	-0.00026	0.073202		339.4	-0.00166	0.074315		340.8
169	-0.00024	0.073292		0.999968	-0.00156	0.074904		0.999992	-0.00024	0.073185		0.99934	-0.00156	0.074207		0.999989
170	-0.00022	0.073278			-0.00146	0.074808			-0.00022	0.07317			-0.00146	0.074106		
171	-0.00021	0.073264			-0.00137	0.074718			-0.00021	0.073156			-0.00137	0.074011		
172	-0.0002	0.073252			-0.00128	0.074635			-0.0002	0.073142			-0.00128	0.073922		
173	-0.00019	0.07324			-0.0012	0.074558			-0.00019	0.073129			-0.0012	0.073839		
174	-0.00017	0.073229			-0.00112	0.074485			-0.00017	0.073117			-0.00112	0.073761		
175	-0.00016	0.073219			-0.00105	0.074418			-0.00016	0.073106			-0.00105	0.073688		
176	-0.00015	0.073209			-0.00099	0.074355			-0.00015	0.073096			-0.00099	0.073619		
177	-0.00014	0.0732			-0.00093	0.074296			-0.00014	0.073086			-0.00093	0.073554		

227	-7E-06	0.073113	0.073106		-4.4E-05	0.073812	0.073768		-7E-06	0.072901	0.072894		-4.4E-05	0.012365	0.072321
281	-1E-06	0.07456	0.074559		-3E-06	0.082999	0.082996		-1E-06	0.07144	0.071439		-3E-06	0.062998	0.62995

Spreadsheet 5

Part of the (kc')21 spreadsheet for the time region t1 < t < t2 of a simulation of a measurement cycle

Effects of errors of +30J (columns 2-9) and -30J (columns 10-17) on the evaluation of (kc')31, (kc')32, (kc'o)361 and (kc'o)362

1	2	3	4	5	6	7	8	9	10	11	12	13	14	15	16	17
interval 300/s	abscissa	ordinate	(kc')31 / WK^-1	(kc'o)361 / WK^-1	abscissa	ordinate	(kc')32 / WK^-1	(kc'o)362 / WK^-1	abscissa	ordinate	(kc')31 / WK^-1	(kc'o)361 / WK^-1	abscissa	ordinate	(kc')32 / WK^-1	(kc'o)362 / WK^-1
				slope /JK^-1				slope /JK^-1				slope /JK^-1				slope /JK^-1
				r				r				r				r
145	0.014168	0.094518	0.08035	0.070712	2.20046	3.414829	1.21437	0.013085	0.014168	0.079829	0.065661	0.075284	2.20046	1.13346	-1.067	0.132932
146	0.013587	0.090242		453.9	1.080755	1.444552		484.2	0.013587	0.082943		206.4	1.080755	0.863944		176
147	0.013039	0.088464		0.970213	0.71045	0.915565		0.995012	0.013039	0.083626		0.876513	0.71045	0.651979		0.963945
148	0.012523	0.087333			0.526162	0.675207			0.012523	0.083725			0.526162	0.523611		
149	0.012036	0.086477			0.415889	0.538577			0.012036	0.083606			0.415889	0.439464		
150	0.011576	0.085767			0.342546	0.450768			0.011576	0.083386			0.342546	0.380319		
151	0.011141	0.085162			0.29028	0.389867			0.011141	0.083131			0.29028	0.336952		
152	0.01073	0.08462			0.251174	0.344988			0.01073	0.082851			0.251174	0.303578		
153	0.010341	0.084128			0.220832	0.310645			0.010341	0.082563			0.220832	0.277209		
154	0.009972	0.083679			0.196622	0.28354			0.009972	0.082275			0.196622	0.25587		
155	0.009623	0.083263			0.176868	0.261622			0.009623	0.081992			0.176868	0.238263		
156	0.009291	0.082876	0.072755	0.072755	0.160454	0.243545	0.083091	0.071239	0.009291	0.081715	0.072424	0.073245	0.160454	0.223502	0.063048	0.07475
157	0.008977	0.082514		357.9	0.146608	0.228388		353.2	0.008977	0.081447		302.3	0.146608	0.210952		307.1
158	0.008678	0.082176		0.999929	0.134779	0.215511		0.999979	0.008678	0.081188		0.999903	0.134779	0.200165		0.999973
159	0.008394	0.081857			0.124561	0.204434			0.008394	0.080938			0.124561	0.190793		
160	0.008123	0.081556			0.115652	0.194816			0.008123	0.080697			0.115652	0.182585		
161	0.007866	0.081271			0.10782	0.186369			0.007866	0.080465			0.10782	0.175318		
162	0.007621	0.081004			0.100886	0.178955			0.007621	0.080245			0.100886	0.168903		
163	0.007387	0.080749			0.094706	0.172345			0.007387	0.080032			0.094706	0.163148		
164	0.007165	0.080508			0.089167	0.166434			0.007165	0.079828			0.089167	0.157974		
165	0.006952	0.080278			0.084167	0.161104			0.006952	0.079632			0.084167	0.153285		
166	0.00675	0.08006			0.079658	0.156321			0.00675	0.079445			0.079658	0.149062		
167	0.006556	0.079853	0.073297	0.072895	0.075552	0.151966	0.076414	0.072328	0.006556	0.079266	0.07271	0.073102	0.075552	0.145201	0.069649	0.073672
168	0.006371	0.079655		350.1	0.071806	0.147998		347.7	0.006371	0.079093		310.3	0.071806	0.141672		312.5
169	0.006194	0.079466		0.999994	0.068374	0.144371		0.999998	0.006194	0.078928		0.999996	0.068374	0.138435		0.999999
170	0.006025	0.079286			0.065222	0.141042			0.006025	0.07877			0.065222	0.135456		
171	0.005863	0.079111			0.062317	0.137952			0.005863	0.078615			0.062317	0.13268		
172	0.005708	0.07895			0.059633	0.135152			0.005708	0.078472			0.059633	0.130164		
173	0.00556	0.078793			0.057147	0.132535			0.00556	0.078332			0.057147	0.127805		
174	0.005418	0.078642			0.054838	0.130108			0.005418	0.078198			0.054838	0.125613		
175	0.005281	0.078498			0.05269	0.127851			0.005281	0.078069			0.05269	0.12357		
176	0.00515	0.07836			0.050684	0.125748			0.00515	0.077945			0.050684	0.121663		
177	0.005025	0.078228			0.048811	0.123783			0.005025	0.077826			0.048811	0.119879		

227	0.002117	0.075195	0.073078		0.015841	0.089424	0.073583		0.002117	0.075041	0.072924		0.015841	0.088269	0.072428
286	0.001227	0.074272	0.073045		0.008577	0.081892	0.073315		0.001227	0.074183	0.072956		0.008577	0.081268	0.072691

Spreadsheet 6

Part of the (kR')11 spreadsheet for the region 0<t<T of a measurement cycle for a "blank" experiment (Pt cathode polarised in 0.1M LioD / D_2O

Evaluation of $\overline{(kR')}11$, $\overline{\overline{(kR')}}11$, $\overline{(kR')}12$, $\overline{\overline{(kR')}}12$, (kR'o)151, (kR'o)161, (kR'o)171, (kR'o)181 and (kR'o)162

1	2	3	4	5	6	7	8	9	10	11	12	13	14	15	16
interval / 300s	θ cell / °C	E cell / V	abscissa	ordinate	10^9(kR'o) 151/WK^-4	10^9 (kR'o) 181/WK^-4	0^9 $\overline{(kR')}$ 11/WK^-4	10^9 $\overline{\overline{(kR')}}$ 11/WK^-4	abscissa	ordinate	10^9(kR'o) 162/WK^-4	10^9$\overline{(kR')}$ 12/WK^-4	10^9$\overline{\overline{(kR')}}$ 12/WK^-4		
					slope / JK^-1	slope / JK^-1	10^9 σ /WK^-4	10^9 σ / WK^-4			slope JK^-1	10^9 σ /WK^-4	10^9 σ / WK^-4		
					r	r	σ / (kR')11 / %	σ / (kR')11 / %			r	σ/(kR')12 / %	σ / (kR')12 / %		
141					10^9(kR'o) 161 / JK^-1										
					slope / JK^-1										
					r										
142															
285					10^9(kR'o) 171 / WK^-4										
					slope / JK^-1										
					r										
286															
0	31.492	5.5515													
1	31.54	5.5543	0.04282	0.66737	0.62291				-0.67634	-0.08636					
2	31.587	5.5493	0.03771	0.66364	333.1				-0.64272	-0.0807					
3	31.624	5.5519	0.03265	0.66175	0.975				-0.59316	-0.09376					
4	31.66	5.5442	0.03342	0.65835					-0.64853	-0.07564					
5	31.699	5.5392	0.03466	0.65523					-0.72568	-0.06443					
6	31.738	5.5386	0.03275	0.65279					-0.78472	-0.06832		0.64177			
7	31.733	5.5345	0.02736	0.6508					-0.80264	-0.07181		0.09391			
8	31.8	5.5428	0.02641	0.64974					-0.71637	-0.08254		14.63			
9	31.833	5.5287	0.02765	0.64545					-0.75294	-0.10371					
10	31.863	5.5408	0.01881	0.64571	0.62391		0.62214		-0.85804	-0.04402					
11	31.876	5.5252	0.01662	0.64263	302.5		0.00268		-0.53757	-0.02786					
12	31.901	5.5303	0.01832	0.64186	0.91543		0.43		-0.64122	-0.05955					
13	31.918	5.5384	0.02003	0.64213					-0.74268	-0.11202					
14	31.947	5.5326	0.01997	0.63947					-0.82265	-0.08634					
15	31.964	5.5215	0.01648	0.63676					-0.72607	-0.01482					

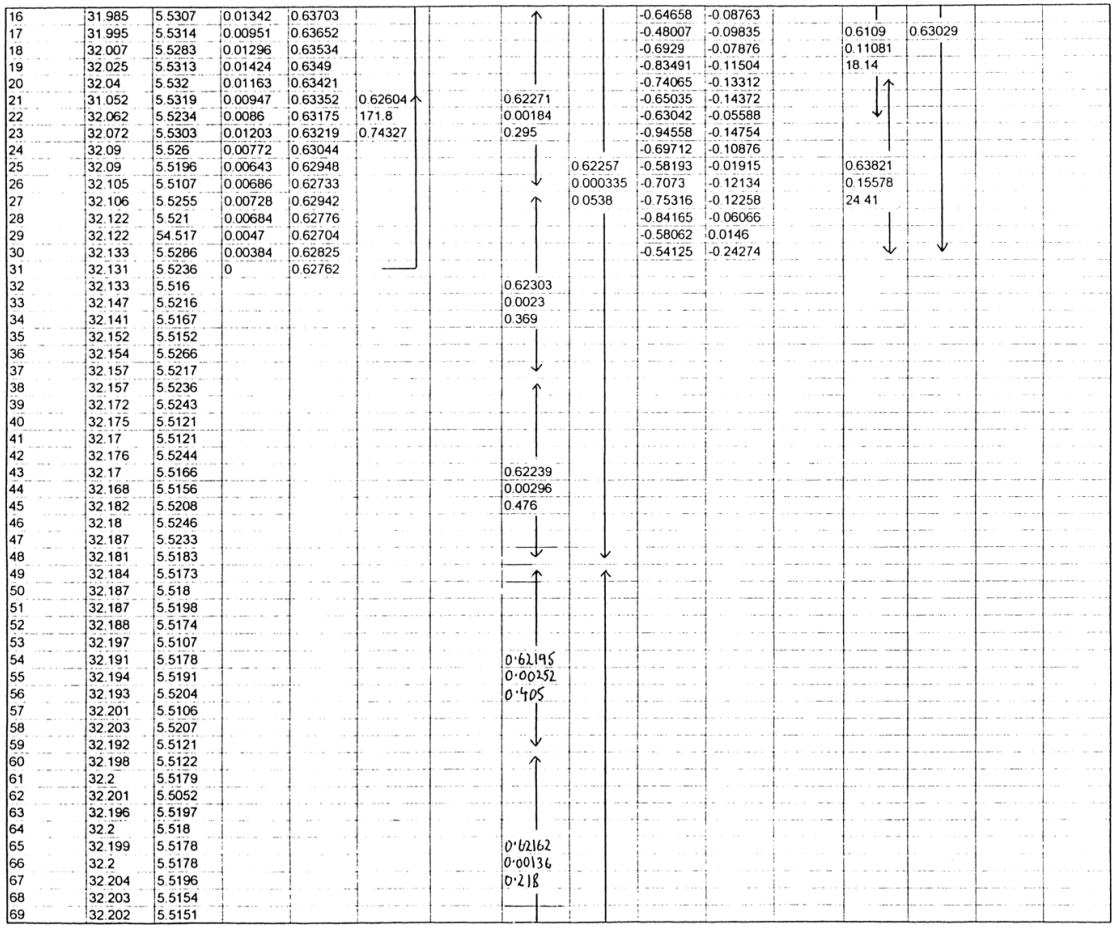
16 31.985 5.5307 0.01342 0.63703
17 31.995 5.5314 0.00951 0.63652
18 32.007 5.5283 0.01296 0.63534
19 32.025 5.5313 0.01424 0.6349
20 32.04 5.532 0.01163 0.63421
21 31.052 5.5319 0.00947 0.63352 0.62604
22 32.062 5.5234 0.0086 0.63175 171.8
23 32.072 5.5303 0.01203 0.63219 0.74327
24 32.09 5.526 0.00772 0.63044
25 32.09 5.5196 0.00643 0.62948
26 32.105 5.5107 0.00686 0.62733
27 32.106 5.5255 0.00728 0.62942
28 32.122 5.521 0.00684 0.62776
29 32.122 54.517 0.0047 0.62704
30 32.133 5.5286 0.00384 0.62825
31 32.131 5.5236 0 0.62762
32 32.133 5.516
33 32.147 5.5216
34 32.141 5.5167
35 32.152 5.5152
36 32.154 5.5266
37 32.157 5.5217
38 32.157 5.5236
39 32.172 5.5243
40 32.175 5.5121
41 32.17 5.5121
42 32.176 5.5244
43 32.17 5.5166
44 32.168 5.5156
45 32.182 5.5208
46 32.18 5.5246
47 32.187 5.5233
48 32.181 5.5183
49 32.184 5.5173
50 32.187 5.518
51 32.187 5.5198
52 32.188 5.5174
53 32.197 5.5107
54 32.191 5.5178
55 32.194 5.5191
56 32.193 5.5204
57 32.201 5.5106
58 32.203 5.5207
59 32.192 5.5121
60 32.198 5.5122
61 32.2 5.5179
62 32.201 5.5052
63 32.196 5.5197
64 32.2 5.518
65 32.199 5.5178
66 32.2 5.5178
67 32.204 5.5196
68 32.203 5.5154
69 32.202 5.5151
0.62271
0.00184
0.295
0.62303
0.0023
0.369
0.62239
0.00296
0.476
0·62195
0·00252
0·405
0·62162
0·00136
0·218
0.62257
0.000335
0.0538
-0.64658 -0.08763
-0.48007 -0.09835
-0.6929 -0.07876
-0.83491 -0.11504
-0.74065 -0.13312
-0.65035 -0.14372
-0.63042 -0.05588
-0.94558 -0.14754
-0.69712 -0.10876
-0.58193 -0.01915
-0.7073 -0.12134
-0.75316 -0.12258
-0.84165 -0.06066
-0.58062 0.0146
-0.54125 -0.24274
0.6109
0.11081
18.14
0.63821
0.15578
24.41
0.63029

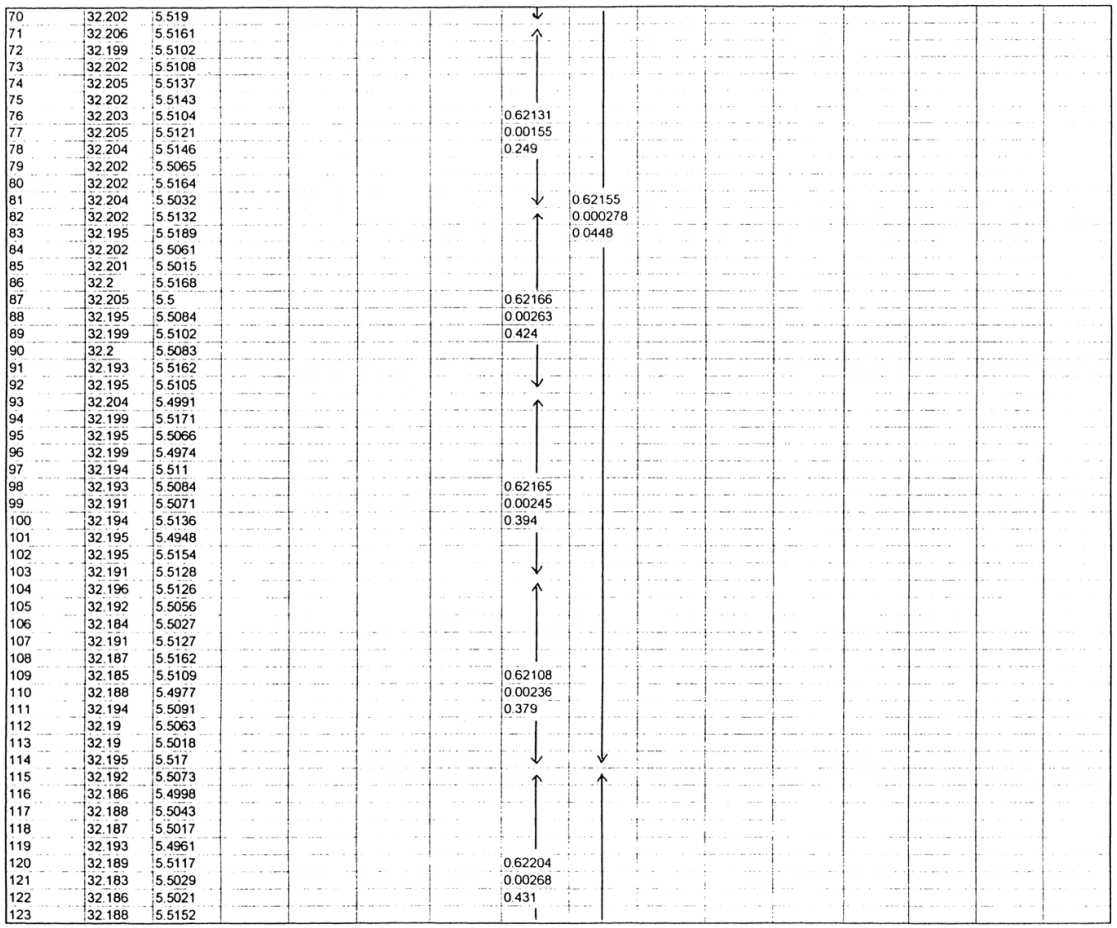
70 32.202 5.519
71 32.206 5.5161
72 32.199 5.5102
73 32.202 5.5108
74 32.205 5.5137
75 32.202 5.5143
76 32.203 5.5104
77 32.205 5.5121
78 32.204 5.5146
79 32.202 5.5065
80 32.202 5.5164
81 32.204 5.5032
82 32.202 5.5132
83 32.195 5.5189
84 32.202 5.5061
85 32.201 5.5015
86 32.2 5.5168
87 32.205 5.5
88 32.195 5.5084
89 32.199 5.5102
90 32.2 5.5083
91 32.193 5.5162
92 32.195 5.5105
93 32.204 5.4991
94 32.199 5.5171
95 32.195 5.5066
96 32.199 5.4974
97 32.194 5.511
98 32.193 5.5084
99 32.191 5.5071
100 32.194 5.5136
101 32.195 5.4948
102 32.195 5.5154
103 32.191 5.5128
104 32.196 5.5126
105 32.192 5.5056
106 32.184 5.5027
107 32.191 5.5127
108 32.187 5.5162
109 32.185 5.5109
110 32.188 5.4977
111 32.194 5.5091
112 32.19 5.5063
113 32.19 5.5018
114 32.195 5.517
115 32.192 5.5073
116 32.186 5.4998
117 32.188 5.5043
118 32.187 5.5017
119 32.193 5.4961
120 32.189 5.5117
121 32.183 5.5029
122 32.186 5.5021
123 32.188 5.5152
0.62131
0.00155
0.249
0.62155
0.000278
0.0448
0.62166
0.00263
0.424
0.62165
0.00245
0.394
0.62108
0.00236
0.379
0.62204
0.00268
0.431

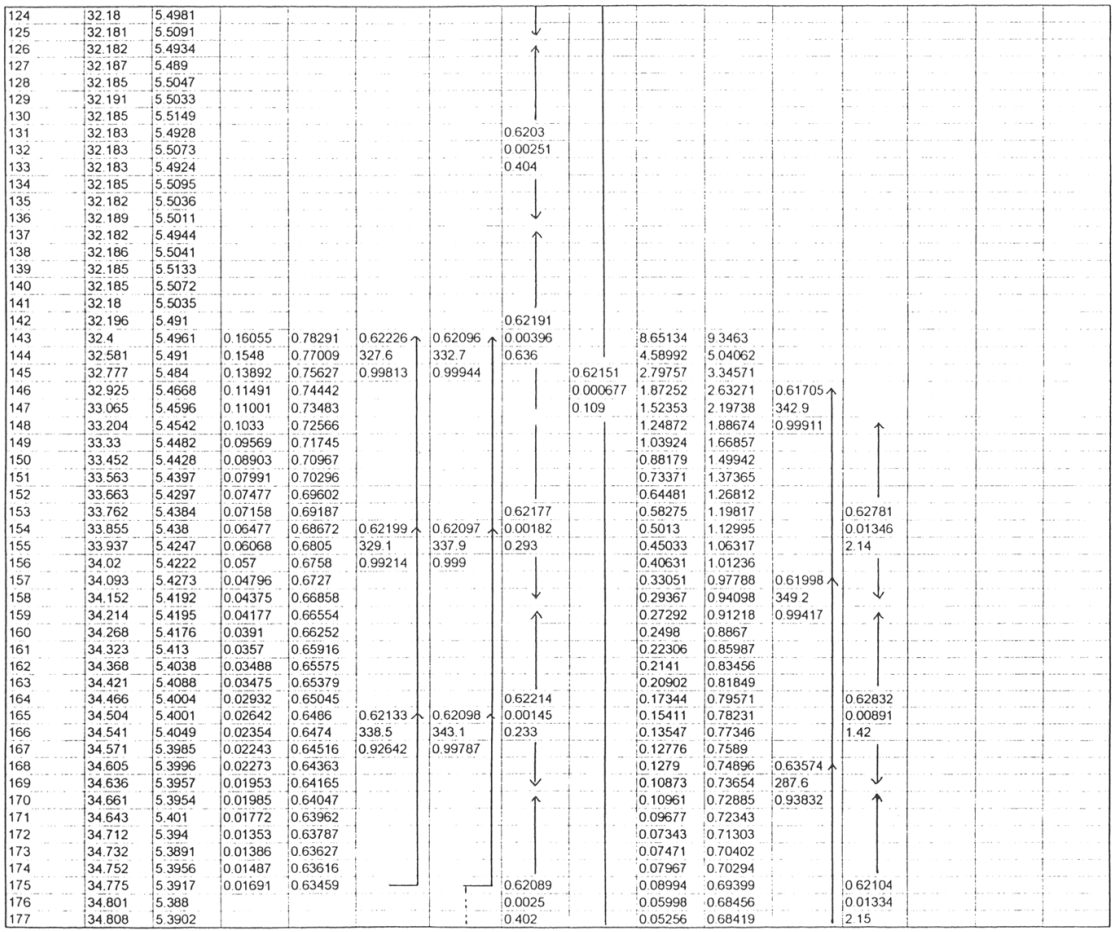

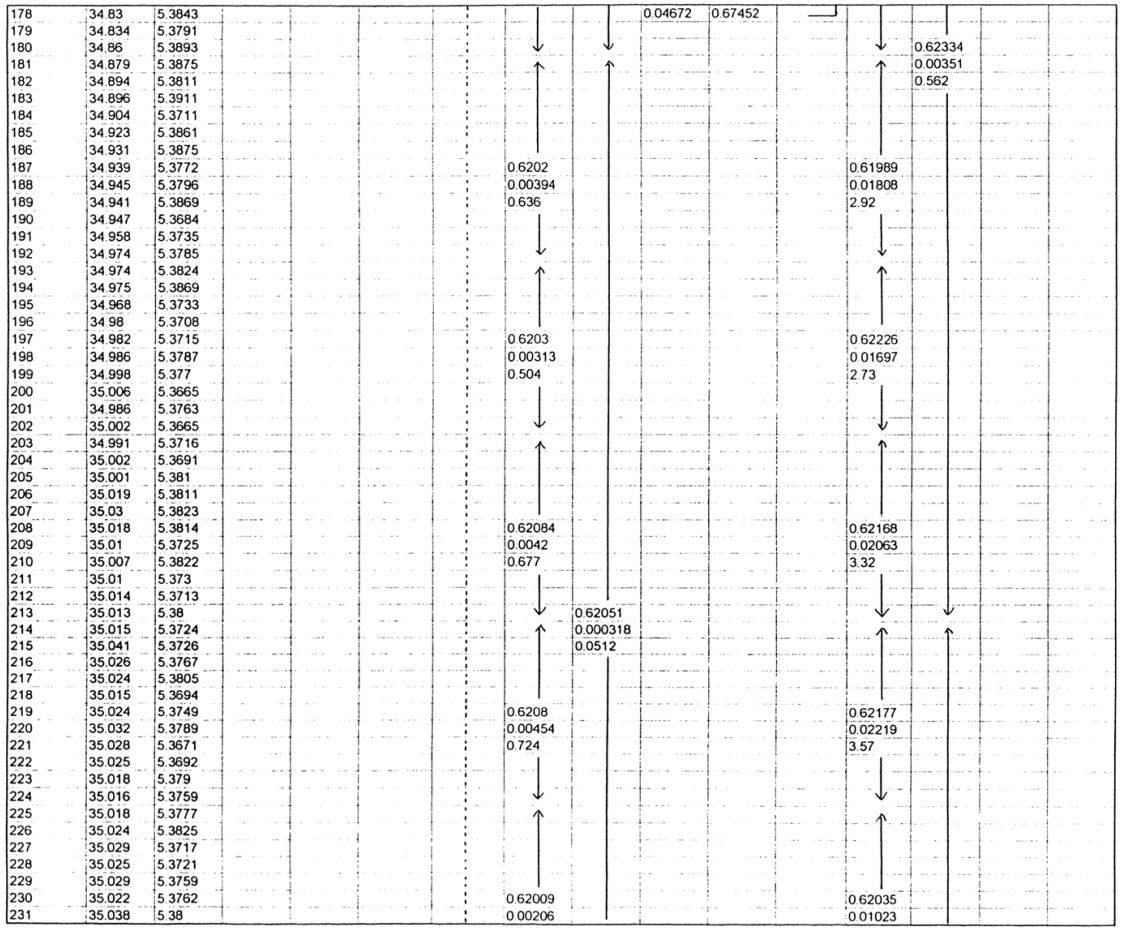
178 34.83 5.3843
179 34.834 5.3791
180 34.86 5.3893
181 34.879 5.3875
182 34.894 5.3811
183 34.896 5.3911
184 34.904 5.3711
185 34.923 5.3861
186 34.931 5.3875
187 34.939 5.3772
188 34.945 5.3796
189 34.941 5.3869
190 34.947 5.3684
191 34.958 5.3735
192 34.974 5.3785
193 34.974 5.3824
194 34.975 5.3869
195 34.968 5.3733
196 34.98 5.3708
197 34.982 5.3715
198 34.986 5.3787
199 34.998 5.377
200 35.006 5.3665
201 34.986 5.3763
202 35.002 5.3665
203 34.991 5.3716
204 35.002 5.3691
205 35.001 5.381
206 35.019 5.3811
207 35.03 5.3823
208 35.018 5.3814
209 35.01 5.3725
210 35.007 5.3822
211 35.01 5.373
212 35.014 5.3713
213 35.013 5.38
214 35.015 5.3724
215 35.041 5.3726
216 35.026 5.3767
217 35.024 5.3805
218 35.015 5.3694
219 35.024 5.3749
220 35.032 5.3789
221 35.028 5.3671
222 35.025 5.3692
223 35.018 5.379
224 35.016 5.3759
225 35.018 5.3777
226 35.024 5.3825
227 35.029 5.3717
228 35.025 5.3721
229 35.029 5.3759
230 35.022 5.3762
231 35.038 5.38
0.6202
0.00394
0.636
0.6203
0.00313
0.504
0.62084
0.0042
0.677
0.6208
0.00454
0.724
0.62009
0.00206
0.04672
0.67452
0.62051
0.000318
0.0512
0.62334
0.00351
0.562
0.61989
0.01808
2.92
0.62226
0.01697
2.73
0.62168
0.02063
3.32
0.62177
0.02219
3.57
0.62035
0.01023

232	35.027	5.3726					0.333					1.65			
233	35.025	5.3624													
234	35.029	5.374													
235	35.022	5.3604													
236	35.034	5.3745													
237	35.026	5.3741													
238	35.028	5.3794													
239	35.03	5.365													
240	35.027	5.379													
241	35.043	5.3707					0.62082					0.62239			
242	35.045	5.3721					0.00461					0.02272			
243	35.042	5.372					0.743					3.65			
244	35.029	5.3698													
245	35.053	5.3643													
246	35.017	5.3733											0.62026		
247	35.022	5.3649											0.00246		
248	35.03	5.3748											0.397		
249	35.023	5.3677													
250	35.026	5.3672													
251	35.022	5.3584													
252	35.027	5.3759					0.61933					0.61521			
253	35.028	5.3693					0.00263					0.01289			
254	35.031	5.36					0.42					2.09			
255	35.021	5.3646													
256	35.019	5.3686													
257	35.028	5.3754													
258	35.039	5.3673													
259	35.04	5.3761													
260	35.03	5.3645													
261	35.026	5.3758													
262	35.019	5.3622													
263	35.045	5.3718					0.62011					0.61965			
264	35.025	5.3701					0.00441					0.02075			
265	35.024	5.3677					0.711					3.35			
266	35.024	5.3686													
267	35.023	5.3705													
268	35.04	5.3713													
269	35.03	5.3687													
270	35.032	5.3747													
271	35.019	5.3649													
272	35.029	5.3755													
273	35.034	5.3571													
274	35.017	5.373					0.62068					0.62219			
275	35.039	5.3641					0.00375					0.01823			
276	35.035	5.361					0.604					2.93			
277	35.022	5.3625													
278	35.023	5.3679													
279	35.014	5.3561						0.62007							
280	35.031	5.3643						0.000397							
281	35.018	5.3705						0.064							
282	35.026	5.3692													
283	35.018	5.3689													
284	35.033	5.3572													
285	35.039	5.3559					0.62011								

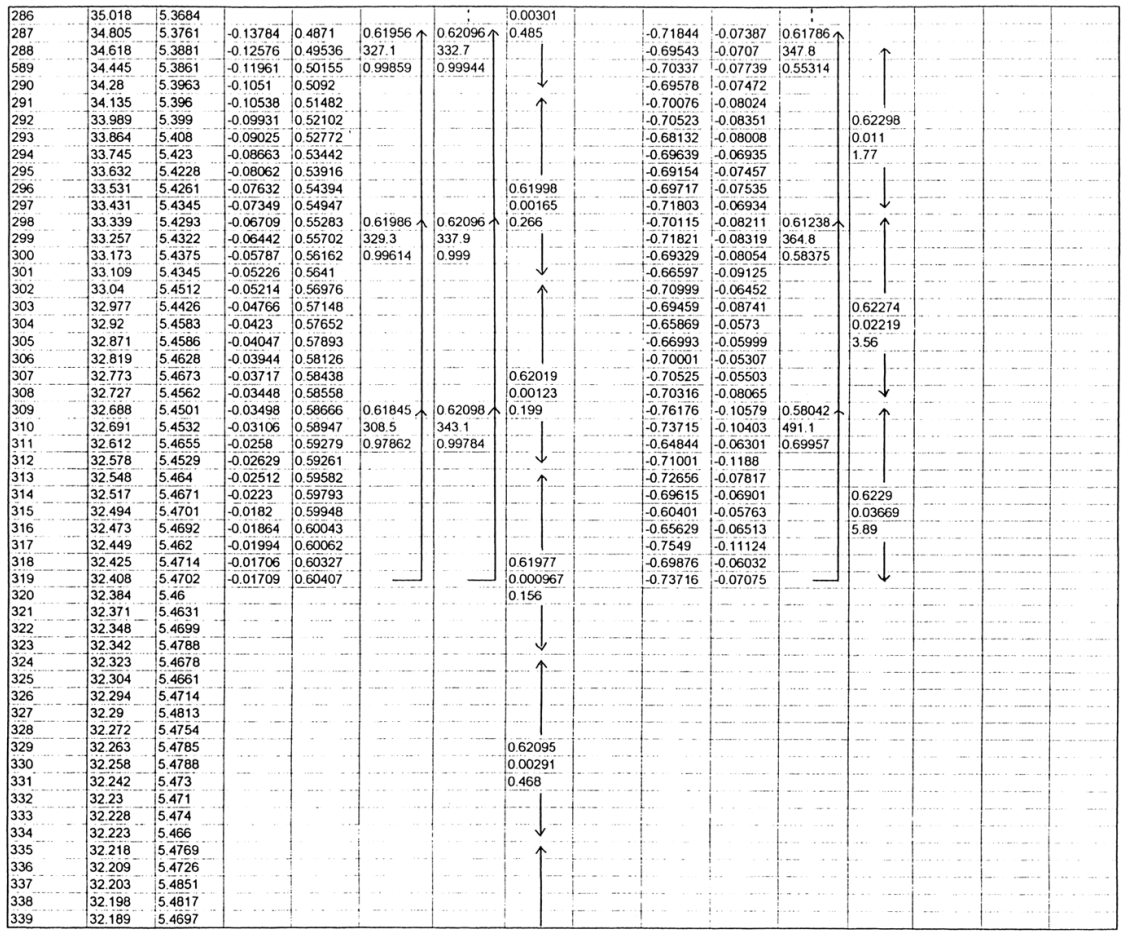

340	32.191	5.4676					0.62067											
341	32.187	5.4698					0.00241											
342	32.182	5.4822					0.388											
343	32.176	5.4659																
344	32.176	5.4732																
345	32.17	5.4815						0.62038										
346	32.161	5.4662						0.000444										
347	32.166	5.4795						0.0715										
348	32.161	5.4686																
349	32.16	5.4738																
350	32.159	5.4771																
351	32.153	5.4772					0.6198											
352	32.154	5.4742					0.00126											
353	32.153	5.4719					0.203											
354	32.148	5.4725																
355	32.145	5.4717																
356	32.146	5.4801																
357	32.142	5.482																
358	32.141	5.4799																
359	32.139	5.4804																
360	32.136	5.4742																
361	32.136	5.47																
362	32.133	5.4687					0.62046											
363	32.136	5.4771					0.00135											
364	32.136	5.472					0.218											
365	32.135	5.4765																
366	32.13	5.476																
367	32.132	5.4806																
368	32.131	5.4792																
369	32.131	5.4811																
370	32.127	5.4686																
371	32.125	5.4764																
372	32.118	5.4806																
373	32.124	5.4671					0.62062											
374	32.126	5.4625					0.00259											
375	32.118	5.477					0.417											
376	32.118	5.479																
377	32.119	5.474																
378	32.121	5.4727																
379	32.124	5.4607																
380	32.119	5.4807																
381	32.12	5.4766																
382	32.12	5.4709																
383	32.123	5.4803																
384	32.121	5.472																
385	32.118	5.4737					0.62069											
386	32.115	5.476					0.00187											
387	32.117	5.469					0.301											
388	32.117	5.4759																
389	32.119	5.463																
390	32.118	5.4739																
391	32.114	5.4667																
392	32.124	5.4734																
393	32.124	5.4712																

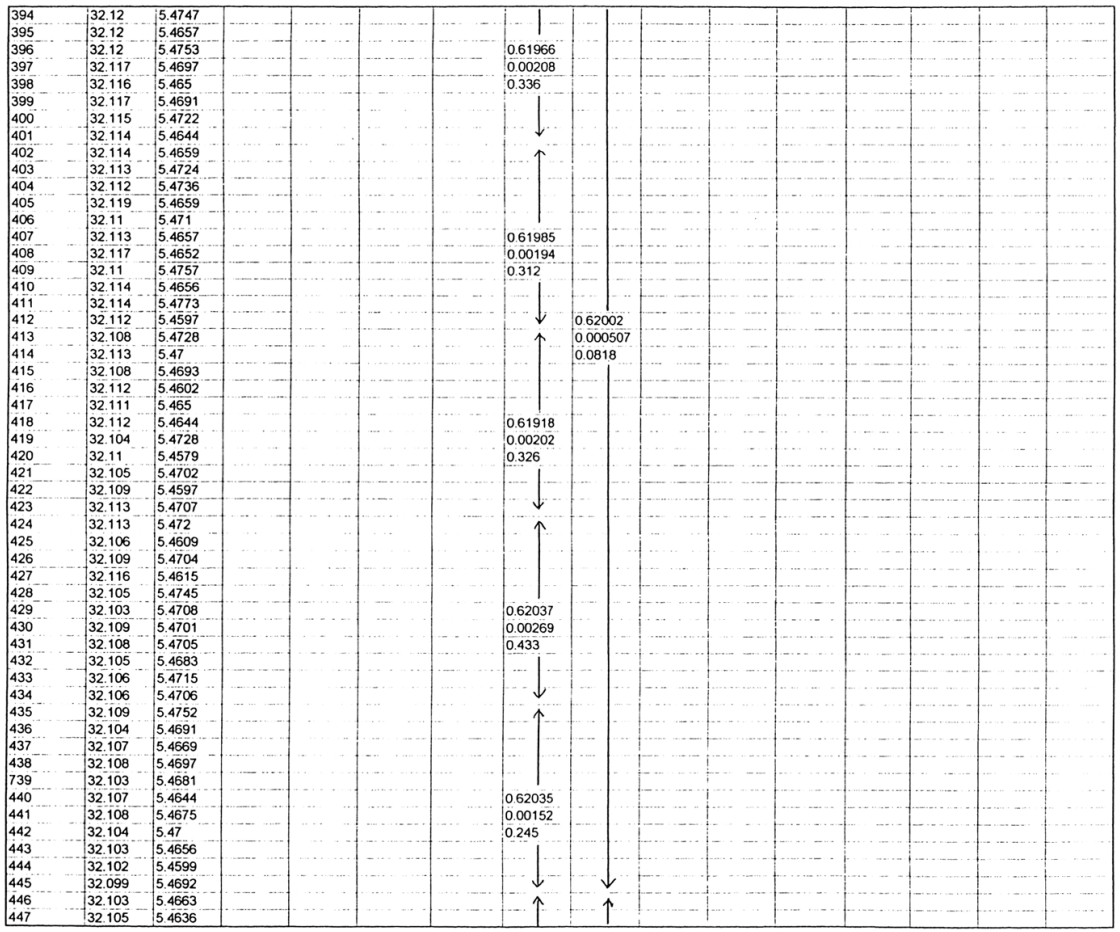
394 32.12 5.4747
395 32.12 5.4657
396 32.12 5.4753
397 32.117 5.4697
398 32.116 5.465
399 32.117 5.4691
400 32.115 5.4722
401 32.114 5.4644
402 32.114 5.4659
403 32.113 5.4724
404 32.112 5.4736
405 32.119 5.4659
406 32.11 5.471
407 32.113 5.4657
408 32.117 5.4652
409 32.11 5.4757
410 32.114 5.4656
411 32.114 5.4773
412 32.112 5.4597
413 32.108 5.4728
414 32.113 5.47
415 32.108 5.4693
416 32.112 5.4602
417 32.111 5.465
418 32.112 5.4644
419 32.104 5.4728
420 32.11 5.4579
421 32.105 5.4702
422 32.109 5.4597
423 32.113 5.4707
424 32.113 5.472
425 32.106 5.4609
426 32.109 5.4704
427 32.116 5.4615
428 32.105 5.4745
429 32.103 5.4708
430 32.109 5.4701
431 32.108 5.4705
432 32.105 5.4683
433 32.106 5.4715
434 32.106 5.4706
435 32.109 5.4752
436 32.104 5.4691
437 32.107 5.4669
438 32.108 5.4697
739 32.103 5.4681
440 32.107 5.4644
441 32.108 5.4675
442 32.104 5.47
443 32.103 5.4656
444 32.102 5.4599
445 32.099 5.4692
446 32.103 5.4663
447 32.105 5.4636
0.61966
0.00208
0.336
0.61985
0.00194
0.312
0.62002
0.000507
0.0818
0.61918
0.00202
0.326
0.62037
0.00269
0.433
0.62035
0.00152
0.245

448	32.106	5.4701			
449	32.103	5.4679			
450	32.099	5.4554			
451	32.1	5.4696	0.61974		
452	32.1	5.4581	0.00187		
453	32.1	5.4638	0.303		
454	32.098	5.4691			
455	32.103	5.4521			
456	32.096	5.4726			
457	32.1	5.4554			
458	32.097	5.4543			
459	32.086	5.4468			
460	32.1	5.4704			
461	32.093	5.4724			
462	32.097	5.4713	0.61922		
463	32.097	5.4649	0.00215		
464	32.094	5.4672	0.347		
465	32.094	5.4612			
466	32.094	5.4662			
467	32.095	5.4576			
468	32.098	5.4606			
469	32.092	5.4649			
470	32.092	5.4667			
471	32.096	5.4566			
472	32.091	5.4533			
473	32.096	5.4578	0.6196		
474	32.095	5.466	0.00206		
475	32.089	5.4603	0.332		
476	32.094	5.4518			
477	32.091	5.4658			
478	32.089	5.4665		0.61934	
479	32.094	5.465		0.000245	
480	32.09	5.471		0.0396	
481	32.095	5.4657			
482	32.09	5.4579			
483	32.096	5.4625			
484	32.094	5.4541	0.61905		
485	32.09	5.4603	0.00173		
486	32.089	5.4629	0.28		
487	32.1	5.4635			
488	32.092	5.465			
489	32.101	5.4589			
490	32.096	5.4617			
491	32.097	5.4547			
492	32.094	5.4518			
493	32.095	5.4662			
494	32.093	5.456			
495	32.09	5.4632	0.61929		
496	32.097	5.4509	0.00172		
497	32.089	5.4536	0.278		
498	32.088	5.4624			
499	32.092	5.4616			
500	32.095	5.4616			
501	32.093	5.4534			

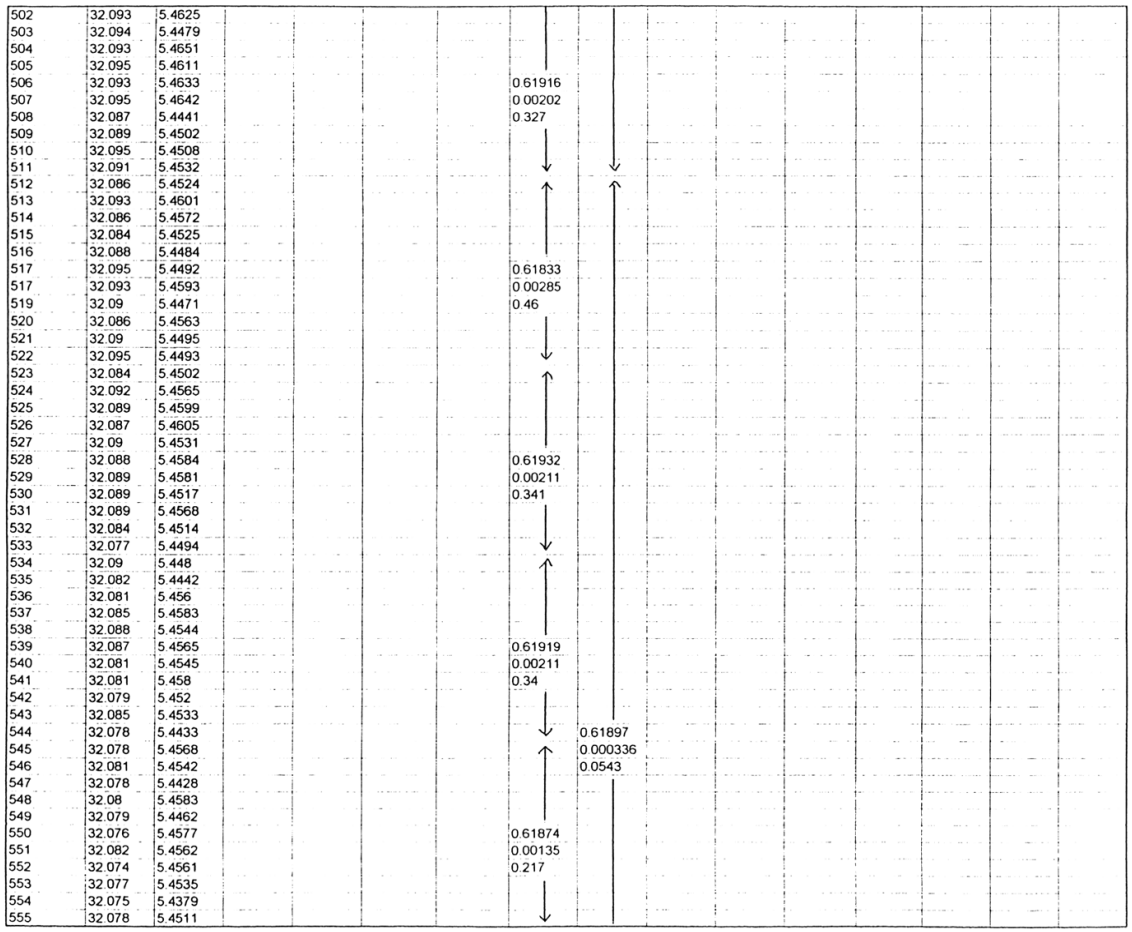
502 32.093 5.4625
503 32.094 5.4479
504 32.093 5.4651
505 32.095 5.4611
506 32.093 5.4633
507 32.095 5.4642
508 32.087 5.4441
509 32.089 5.4502
510 32.095 5.4508
511 32.091 5.4532
512 32.086 5.4524
513 32.093 5.4601
514 32.086 5.4572
515 32.084 5.4525
516 32.088 5.4484
517 32.095 5.4492
517 32.093 5.4593
519 32.09 5.4471
520 32.086 5.4563
521 32.09 5.4495
522 32.095 5.4493
523 32.084 5.4502
524 32.092 5.4565
525 32.089 5.4599
526 32.087 5.4605
527 32.09 5.4531
528 32.088 5.4584
529 32.089 5.4581
530 32.089 5.4517
531 32.089 5.4568
532 32.084 5.4514
533 32.077 5.4494
534 32.09 5.448
535 32.082 5.4442
536 32.081 5.456
537 32.085 5.4583
538 32.088 5.4544
539 32.087 5.4565
540 32.081 5.4545
541 32.081 5.458
542 32.079 5.452
543 32.085 5.4533
544 32.078 5.4433
545 32.078 5.4568
546 32.081 5.4542
547 32.078 5.4428
548 32.08 5.4583
549 32.079 5.4462
550 32.076 5.4577
551 32.082 5.4562
552 32.074 5.4561
553 32.077 5.4535
554 32.075 5.4379
555 32.078 5.4511
0.61916
0.00202
0.327
0.61833
0.00285
0.46
0.61932
0.00211
0.341
0.61919
0.00211
0.34
0.61897
0.000336
0.0543
0.61874
0.00135
0.217

556	32.077	5.4464																
557	32.07	5.4486																
558	32.068	5.4553																
559	32.07	5.4488																
560	32.079	5.4584																
561	32.072	5.4517									0.61913							
562	32.075	5.4423									0.00279							
563	32.071	5.4526									0.451							
564	32.067	5.4577																
565	32.072	5.4432																
566	32.073	5.4437																
567	32.075	5.4562																
568	32.078	5.4491																
569	32.068	5.4532																
570	32.071	5.4524																
571	32.072	5.4458																
572	32.074	5.4501									0.61911							
573	32.069	5.4529									0.0024							
574	32.068	5.4411									0.388							
575	32.074	5.4429																
576	32.064	5.452																
577	32.069	5.455																
578	32.073	5.4534																

Spreadsheet 7

Part of the (kR')21 spreadsheet for the region 0< t< T of a measurement cycle for a "blank" experiment (Pt cathode polarised in 0.1M LiOD/D_2O)

Evaluation of (kR')21, (kR')21, (kR')31, (kR')31, (kR'o)251, (kR'o)261, (kR'o)271, (kR'o)281, (kR'o)351, (kR'o)361, (kR'o)371 and (kR'o)381

1	2	3	4	5	6	7	8	9	10	11	12	13	14	15
interval 300 /s	$\int$input dτ	$\int$f(0)dτ	abscissa	ordinate	10^9(kR'o) 251/ WK^-4	10^9(kR'o) 281/ WK^-4	10^9($\overline{kR'}$) 21/ WK^-4	10^9($\overline{\overline{kR'}}$) 21/ WK^-4	abscissa	ordinate	10^9(kR'o) 351/ WK^-4	10^9(kR'o) 281/ WK^-4	10^9($\overline{kR'}$) 31/ WK^-4	10^9($\overline{\overline{kR'}}$) 31/ WK^-4
					slope /JK-1	slope /JK-1	10^9σ / WK^-4	10^9σ / WK^-4			slope /JK^-1	slope /JK^-1	10^9σ / WK^-4	10^9σ / WK^-4
					r	r	σ/(kR')21 /%	σ/(kR')21 /%			r	r	σ/(kR')31 /%	σ/(kR')31 /%
141					10^9(kR'o) 261/ WK^-4						10^9(kR'o) 361/ WK^-4			
					slope /JK^-1						slope /JK^-1			
					r						r			
142														
285					10^9(kR'o) 271/ WK^-4						10^9(kR'o) 371/ WK^-4			
					slope /JK^-1						slope /JK^-1			
					r						r			
0	147378.4	237194.2	-0.00081	0.62134										
1	147134.2	236829	-0.00074	0.62126	0.62059				0.04337	0.66865				
2	146890	236462.1	-0.00068	0.6212	369.5				0.04282	0.66707	0.6118			
3	196646	236093.8	-0.00063	0.62113	0.99925				0.039959	0.66561	361			
4	146402.1	235724.3	-0.00058	0.62107					0.03772	0.66421	0.99779			
5	146158.6	235353.5	-0.00052	0.62101					0.03711	0.66271				
6	145915.2	234981.5	-0.00047	0.62096					0.03669	0.66125				
7	145671.9	234608.1	-0.00042	0.62095					0.03586	0.65988				
8	145428.4	234233.7	-0.00038	0.62087					0.03433	0.65867				
9	145185.2	233858.2	-0.00034	0.62082					0.03373	0.65742				
10	144942.2	233481.7	-0.00029	0.62078			0.62048		0.03298	0.65622			0.62403	
11	144699.2	233104.5	-0.00028	0.62075			0.0000108		0.03099	0.65511			0.000626	
12	144456.5	232726.7	-0.00024	0.62071	0.62059		0.00175		0.03021	0.065402			0.1	
13	144213.5	232348.1	-0.00022	0.62068	390.5				0.02901	0.65308	0.62205			
14	143970.4	321968.7	-0.00018	0.62065	0.99724				0.02873	0.65219	347.7			
15	143727.8	231588.5	-0.00015	0.62062					0.02779	0.65123	0.99881			

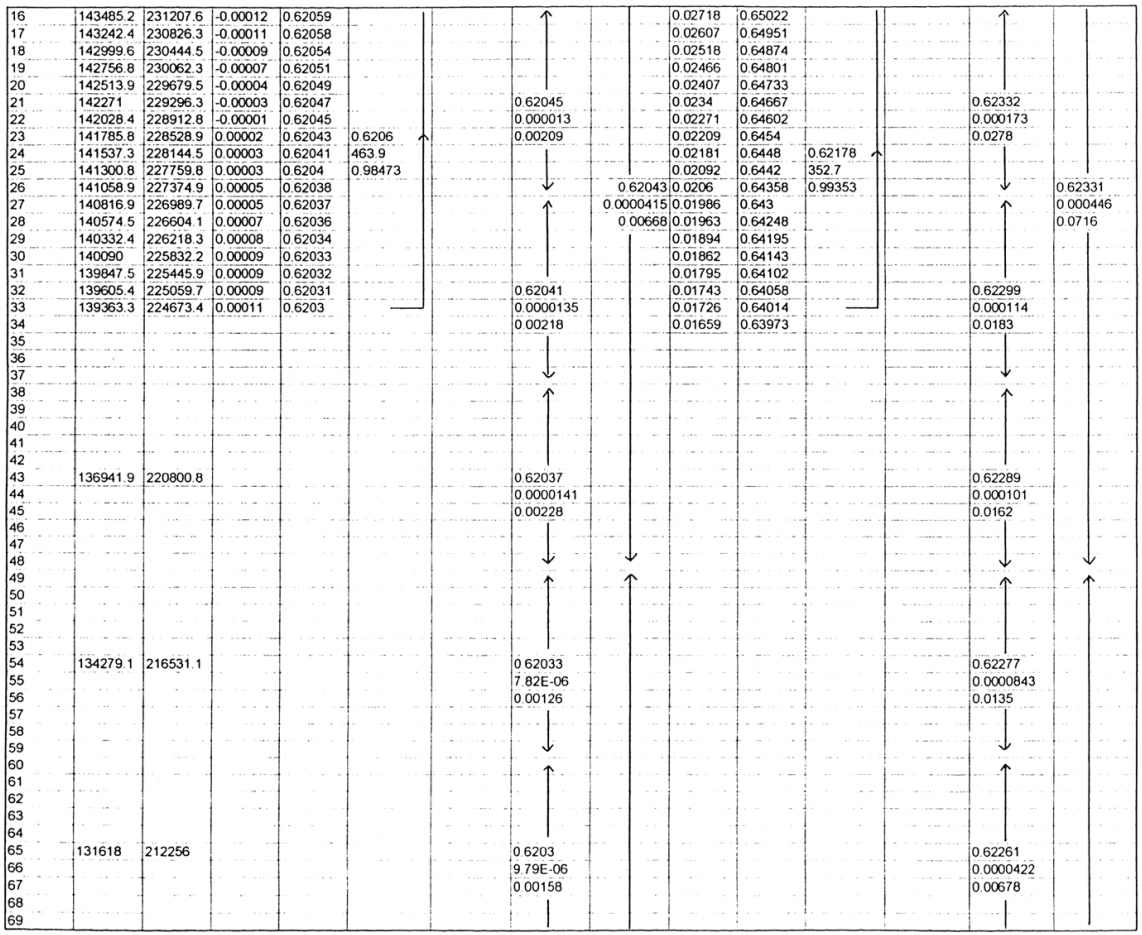
16 143485.2 231207.6 -0.00012 0.62059
17 143242.4 230826.3 -0.00011 0.62058
18 142999.6 230444.5 -0.00009 0.62054
19 142756.8 230062.3 -0.00007 0.62051
20 142513.9 229679.5 -0.00004 0.62049
21 142271 229296.3 -0.00003 0.62047
22 142028.4 228912.8 -0.00001 0.62045
23 141785.8 228528.9 0.00002 0.62043 0.6206
24 141537.3 228144.5 0.00003 0.62041 463.9
25 141300.8 227759.8 0.00003 0.6204 0.98473
26 141058.9 227374.9 0.00005 0.62038
27 140816.9 226989.7 0.00005 0.62037
28 140574.5 226604.1 0.00007 0.62036
29 140332.4 226218.3 0.00008 0.62034
30 140090 225832.2 0.00009 0.62033
31 139847.5 225445.9 0.00009 0.62032
32 139605.4 225059.7 0.00009 0.62031
33 139363.3 224673.4 0.00011 0.6203
43 136941.9 220800.8
54 134279.1 216531.1
65 131618 212256
0.62045
0.000013
0.00209
0.62041
0.0000135
0.00218
0.62037
0.0000141
0.00228
0.62033
7.82E-06
0.00126
0.6203
9.79E-06
0.00158
0.62043
0.0000415
0.00668
0.02718 0.65022
0.02607 0.64951
0.02518 0.64874
0.02466 0.64801
0.02407 0.64733
0.0234 0.64667
0.02271 0.64602
0.02209 0.6454
0.02181 0.6448 0.62178
0.02092 0.6442 352.7
0.0206 0.64358 0.99353
0.01986 0.643
0.01963 0.64248
0.01894 0.64195
0.01862 0.64143
0.01795 0.64102
0.01743 0.64058
0.01726 0.64014
0.01659 0.63973
0.62332
0.000173
0.0278
0.62299
0.000114
0.0183
0.62289
0.000101
0.0162
0.62277
0.0000843
0.0135
0.62261
0.0000422
0.00678
0.62331
0.000446
0.0716

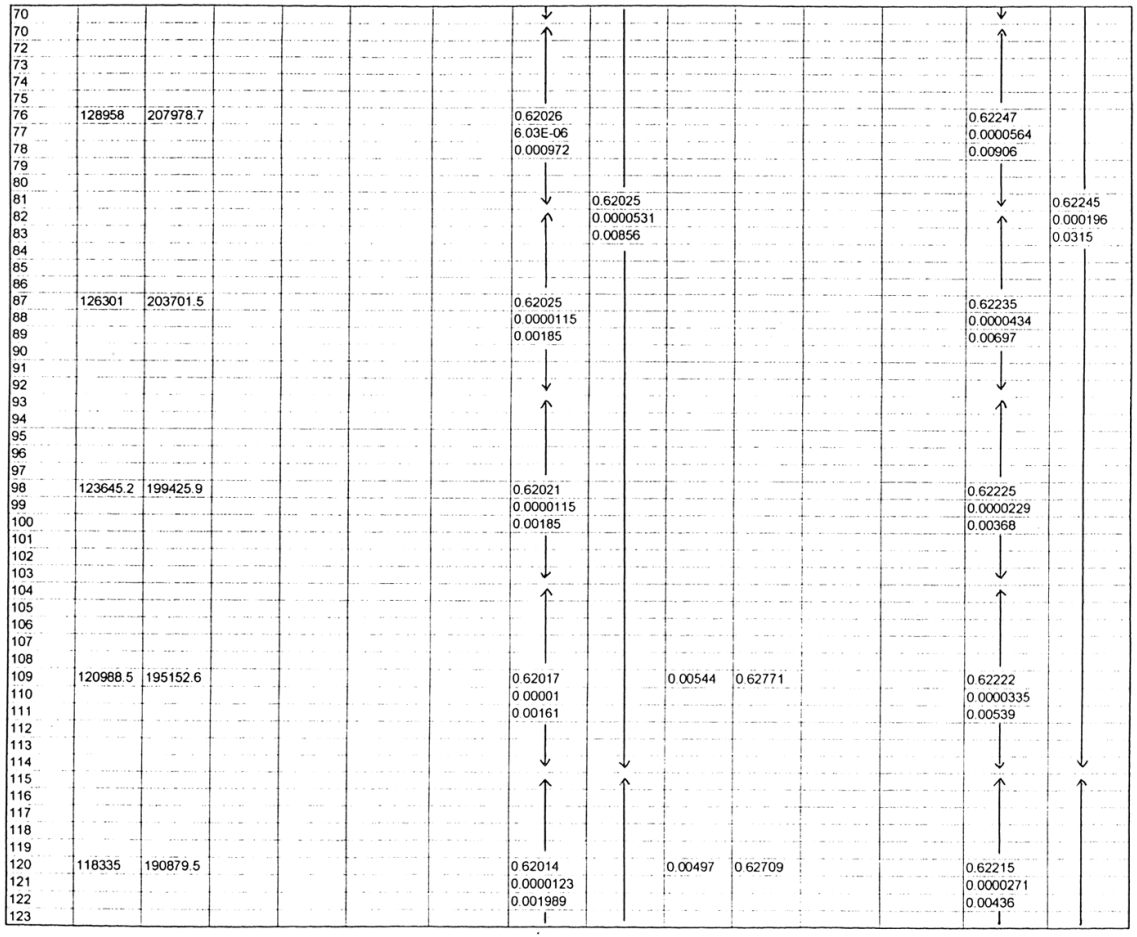
128958
207978.7
126301
203701.5
123645.2
199425.9
120988.5
195152.6
118335
190879.5
0.62026
6.03E-06
0.000972
0.62025
0.0000115
0.00185
0.62021
0.0000115
0.00185
0.62017
0.00001
0.00161
0.62014
0.0000123
0.001989
0.62025
0.0000531
0.00856
0.00544
0.62771
0.00497
0.62709
0.62247
0.0000564
0.00906
0.62235
0.0000434
0.00697
0.62225
0.0000229
0.00368
0.62222
0.0000335
0.00539
0.62215
0.0000271
0.00436
0.62245
0.000196
0.0315

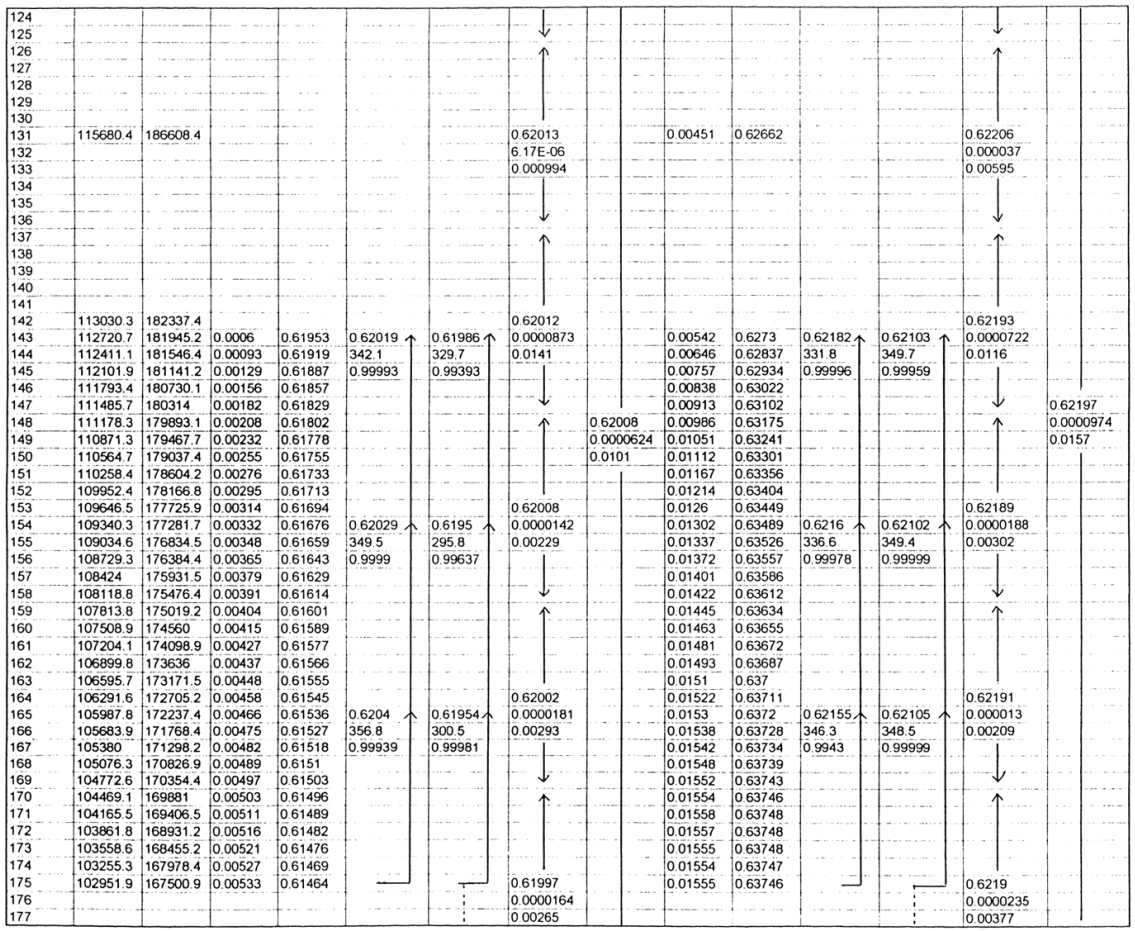

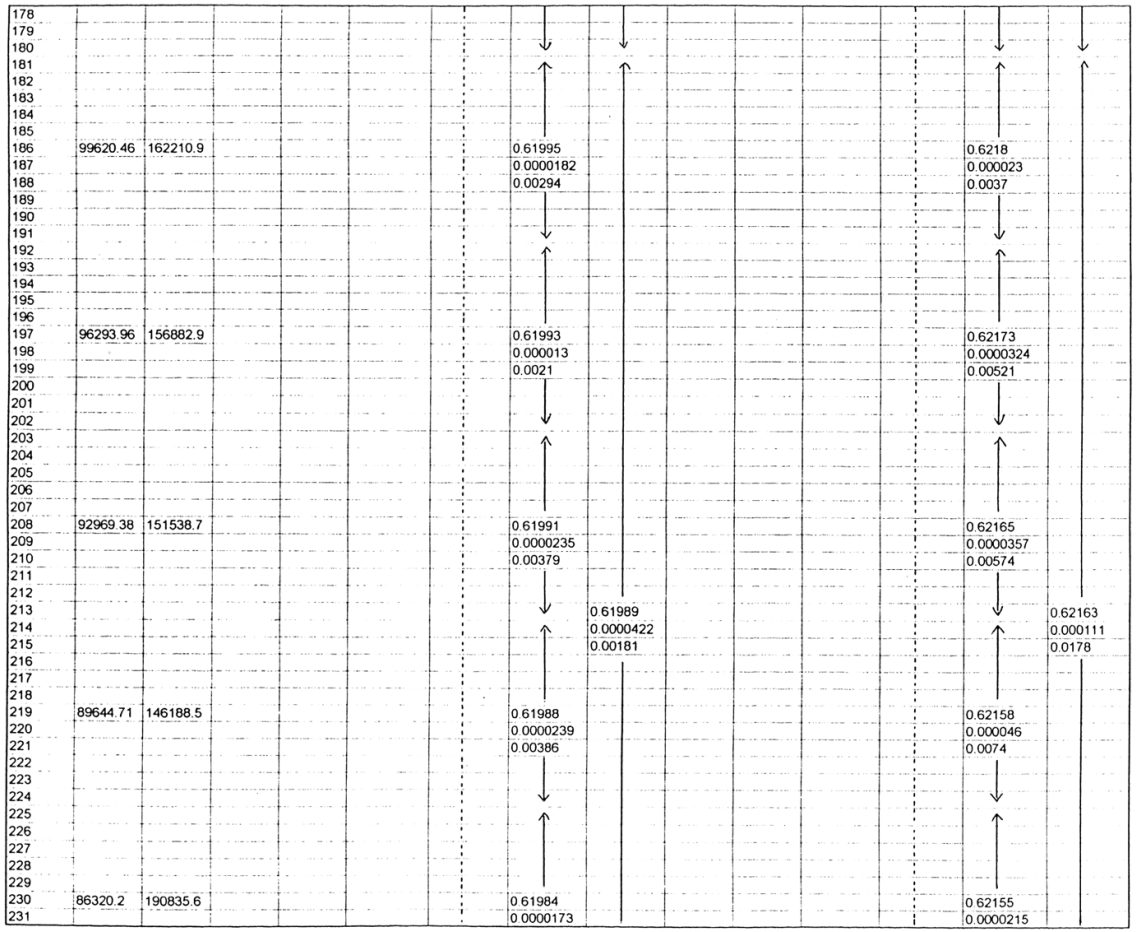
99620.46
162210.9
96293.96
156882.9
92969.38
151538.7
89644.71
146188.5
86320.2
190835.6
0.61995
0.0000182
0.00294
0.61993
0.000013
0.0021
0.61991
0.0000235
0.00379
0.61989
0.0000422
0.00181
0.61988
0.0000239
0.00386
0.61984
0.0000173
0.6218
0.000023
0.0037
0.62173
0.0000324
0.00521
0.62165
0.0000357
0.00574
0.62163
0.000111
0.0178
0.62158
0.000046
0.0074
0.62155
0.0000215

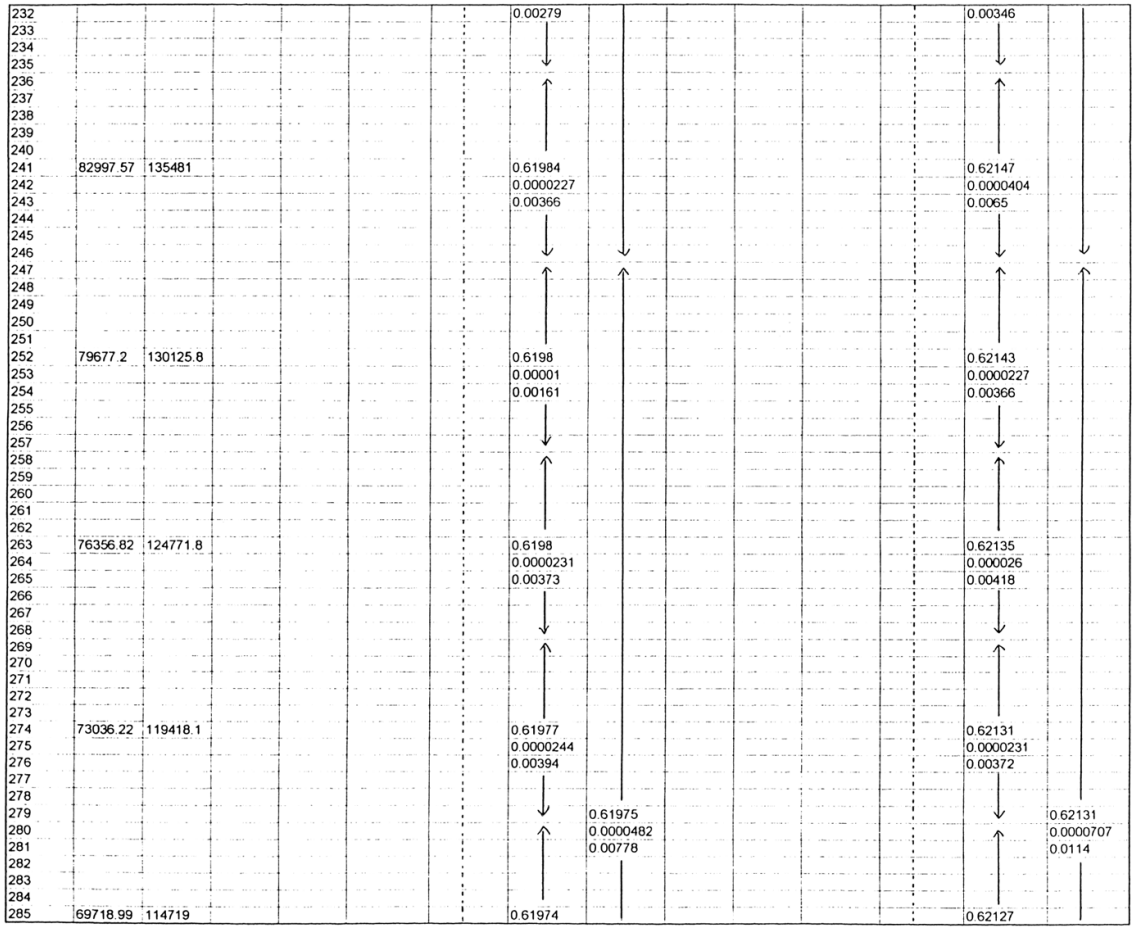
232
233
234
235
236
237
238
239
240
241
242
243
244
245
246
247
248
249
250
251
252
253
254
255
256
257
258
259
260
261
262
263
264
265
266
267
268
269
270
271
272
273
274
275
276
277
278
279
280
281
282
283
284
285
82997.57
135481
79677.2
130125.8
76356.82
124771.8
73036.22
119418.1
69718.99
114719
0.00279
0.61984
0.0000227
0.00366
0.6198
0.00001
0.00161
0.6198
0.0000231
0.00373
0.61977
0.0000244
0.00394
0.61975
0.0000482
0.00778
0.61974
0.00346
0.62147
0.0000404
0.0065
0.62143
0.0000227
0.00366
0.62135
0.000026
0.00418
0.62131
0.0000231
0.00372
0.62131
0.0000707
0.0114
0.62127

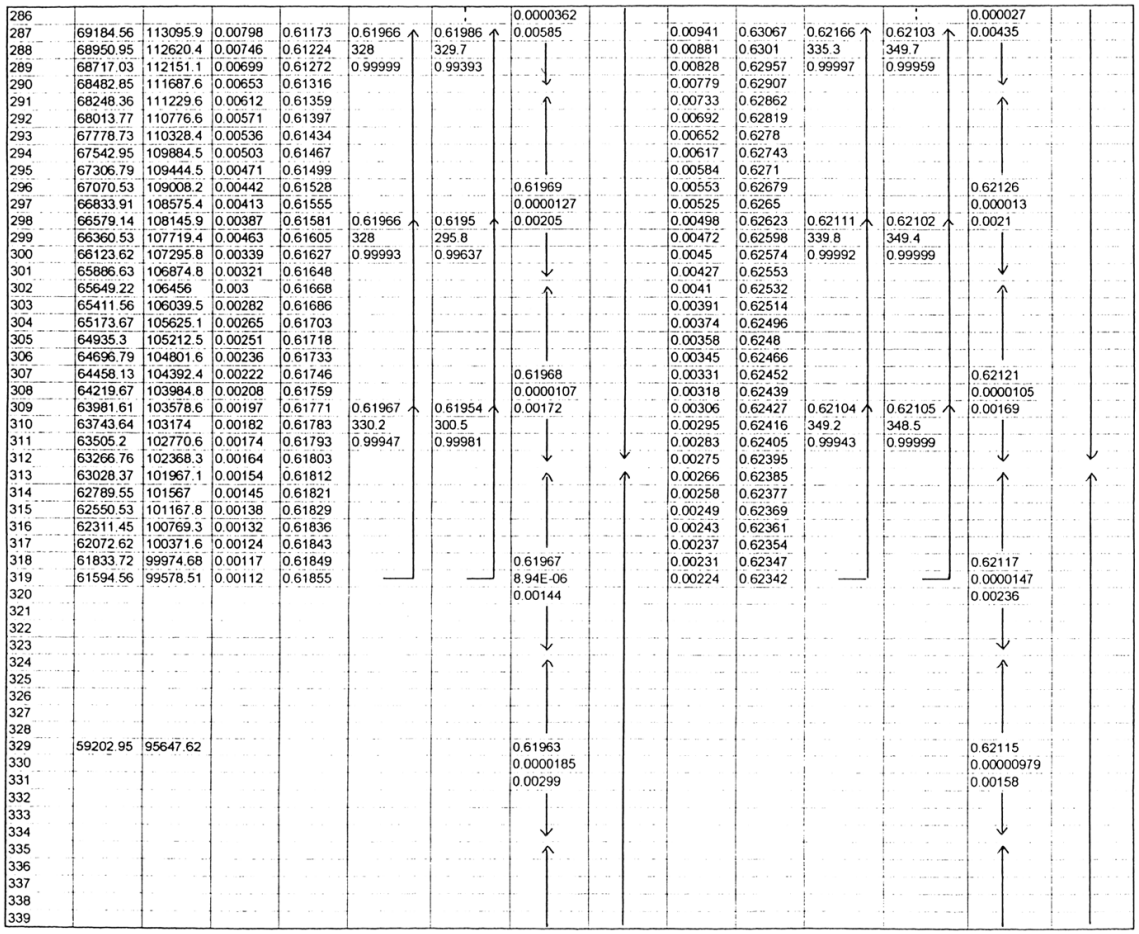

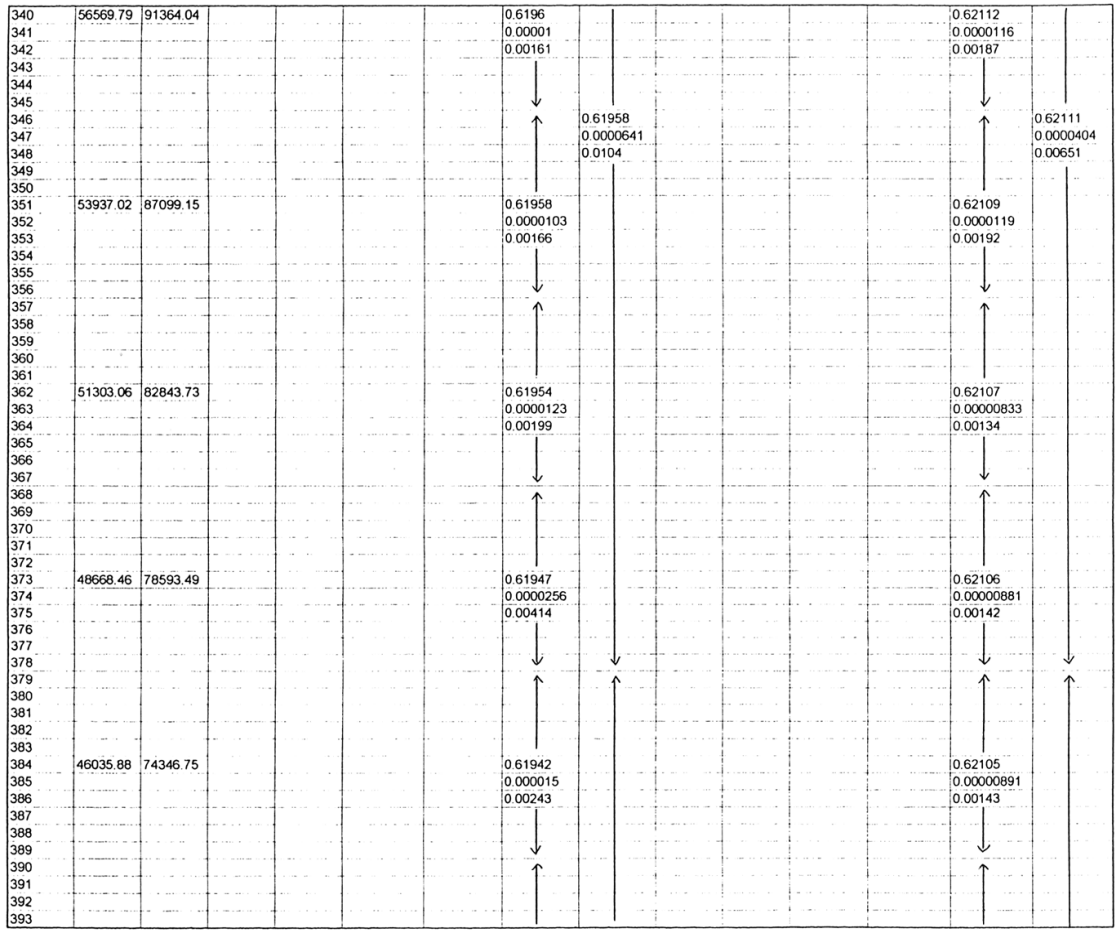
340
341
342
343
344
345
346
347
348
349
350
351
352
353
354
355
356
357
358
359
360
361
362
363
364
365
366
367
368
369
370
371
372
373
374
375
376
377
378
379
380
381
382
383
384
385
386
387
388
389
390
391
392
393
56569.79
91364.04
53937.02
87099.15
51303.06
82843.73
48668.46
78593.49
46035.88
74346.75
0.6196
0.00001
0.00161
0.61958
0.0000103
0.00166
0.61954
0.0000123
0.00199
0.61947
0.0000256
0.00414
0.61942
0.000015
0.00243
0.61958
0.0000641
0.0104
0.62112
0.0000116
0.00187
0.62109
0.0000119
0.00192
0.62107
0.00000833
0.00134
0.62106
0.00000881
0.00142
0.62105
0.00000891
0.00143
0.62111
0.0000404
0.00651

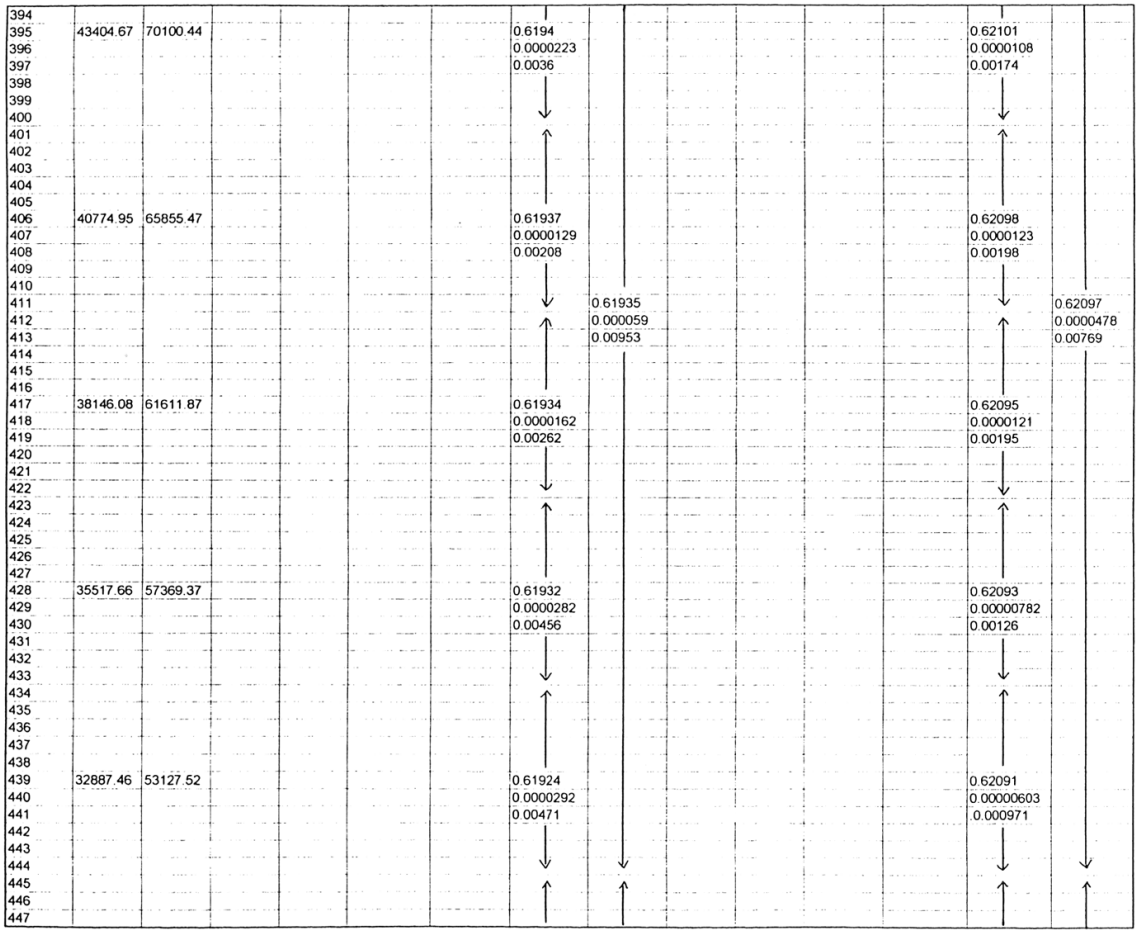
43404.67
70100.44
40774.95
65855.47
38146.08
61611.87
35517.66
57369.37
32887.46
53127.52
0.6194
0.0000223
0.0036
0.61937
0.0000129
0.00208
0.61934
0.0000162
0.00262
0.61932
0.0000282
0.00456
0.61924
0.0000292
0.00471
0.61935
0.000059
0.00953
0.62101
0.0000108
0.00174
0.62098
0.0000123
0.00198
0.62095
0.0000121
0.00195
0.62093
0.00000782
0.00126
0.62091
0.00000603
0.000971
0.62097
0.0000478
0.00769

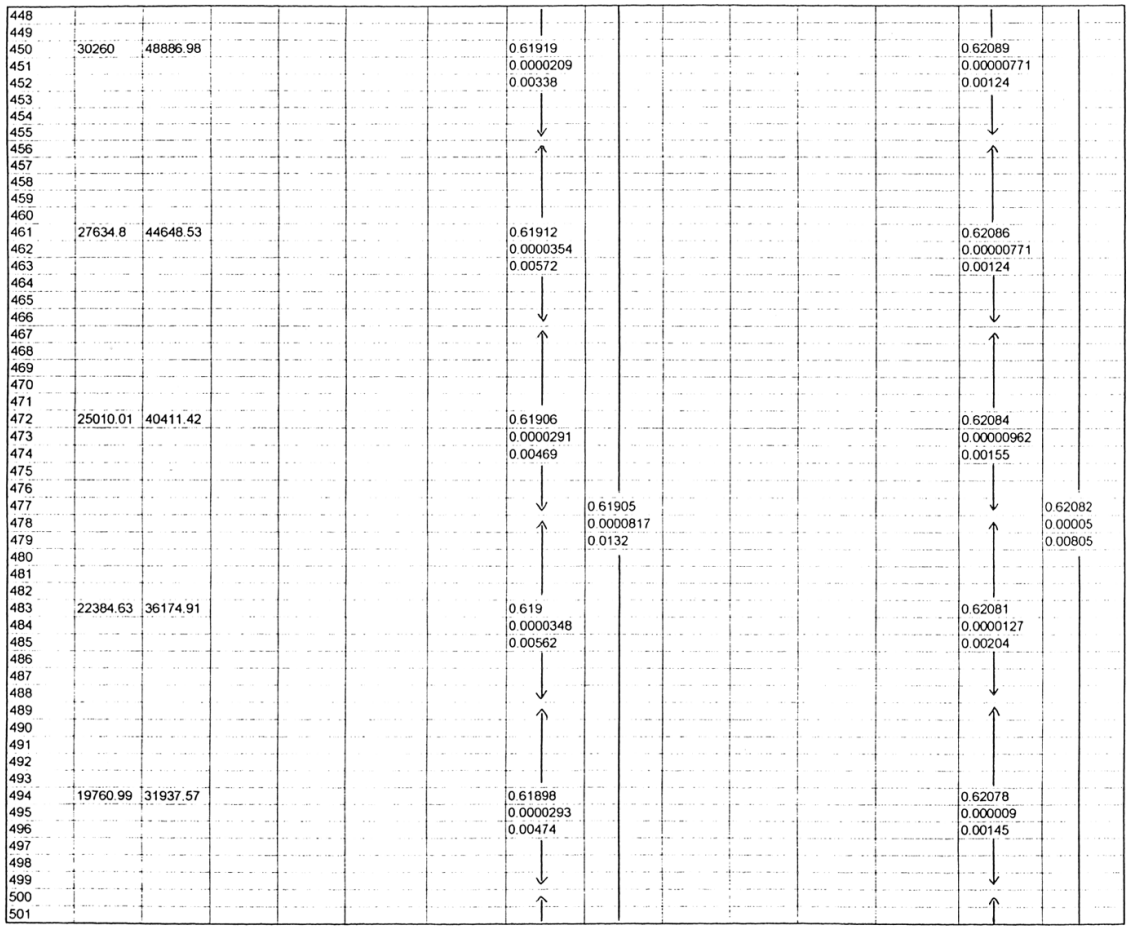
30260
48886.98
27634.8
44648.53
25010.01
40411.42
22384.63
36174.91
19760.99
31937.57
0.61919
0.0000209
0.00338
0.61912
0.0000354
0.00572
0.61906
0.0000291
0.00469
0.619
0.0000348
0.00562
0.61898
0.0000293
0.00474
0.61905
0.0000817
0.0132
0.62089
0.00000771
0.00124
0.62086
0.00000771
0.00124
0.62084
0.00000962
0.00155
0.62081
0.0000127
0.00204
0.62078
0.000009
0.00145
0.62082
0.00005
0.00805

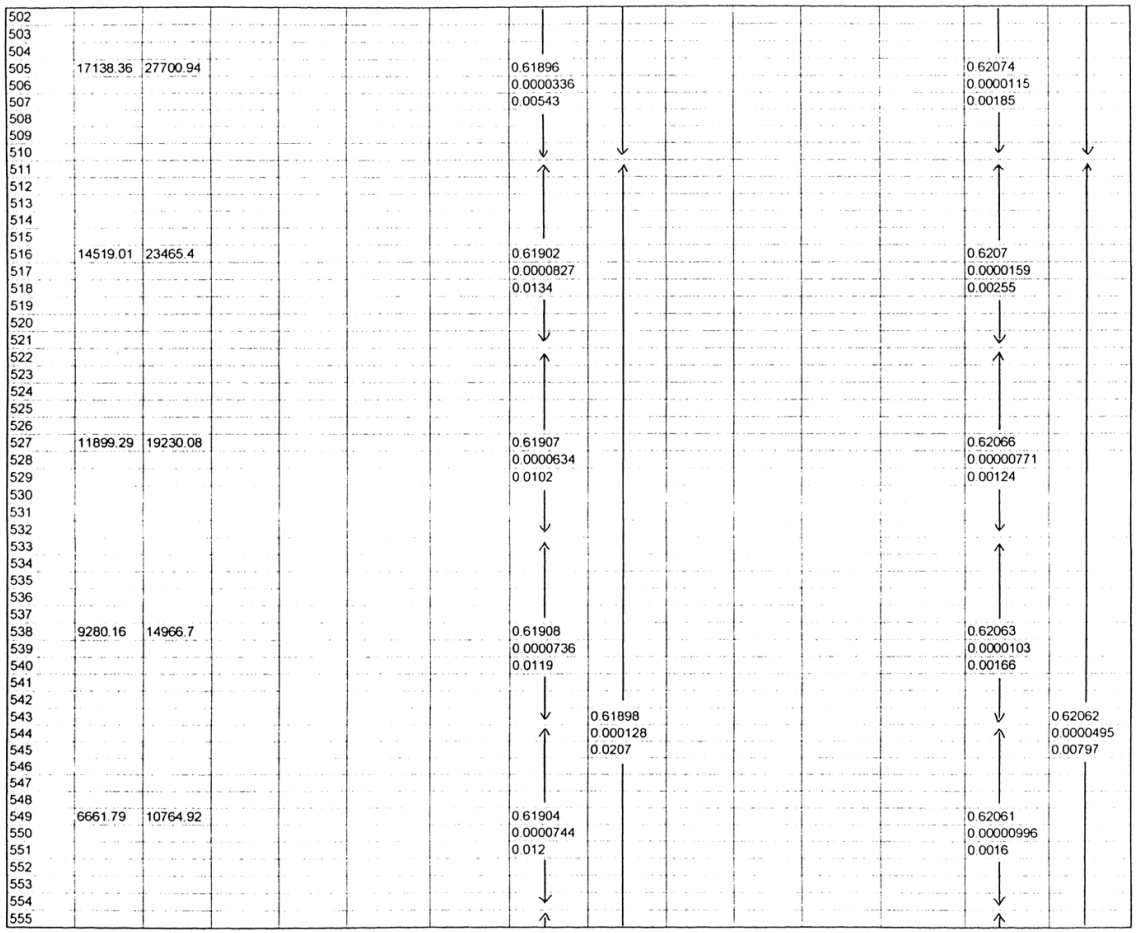
17138.36
27700.94
14519.01
23465.4
11899.29
19230.08
9280.16
14966.7
6661.79
10764.92
0.61896
0.0000336
0.00543
0.61902
0.0000827
0.0134
0.61907
0.0000634
0.0102
0.61908
0.0000736
0.0119
0.61904
0.0000744
0.012
0.61898
0.000128
0.0207
0.62074
0.0000115
0.00185
0.6207
0.0000159
0.00255
0.62066
0.00000771
0.00124
0.62063
0.0000103
0.00166
0.62061
0.00000996
0.0016
0.62062
0.0000495
0.00797

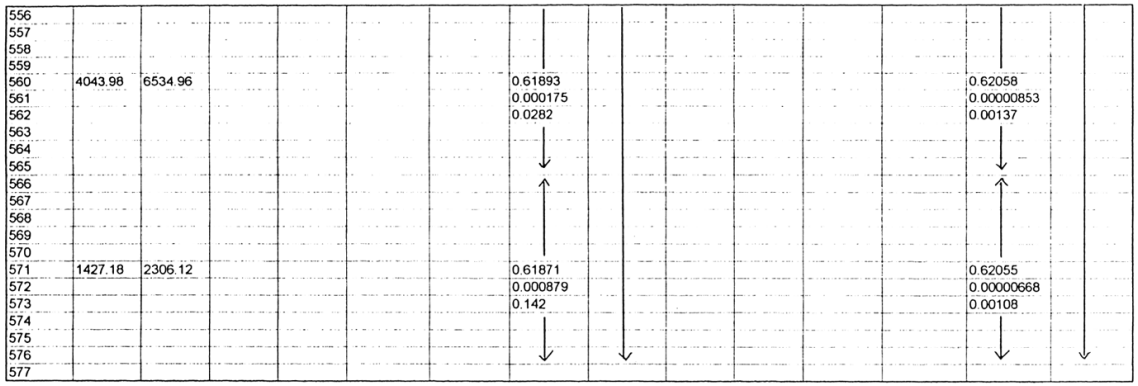
556
557
558
559
560
561
562
563
564
565
566
567
568
569
570
571
572
573
574
575
576
577
4043.98
6534.96
1427.18
2306.12
0.61893
0.000175
0.0282
0.61871
0.000879
0.142
0.62058
0.00000853
0.00137
0.62055
0.00000668
0.00108

Spreadsheet 8

Part of the (kR')21 spreadsheet for the region t1 < t < t2 of a measurement cycle for a "blank" experiment (Pt cathode polarised in 0.1M LiOD / D_2O)

Evaluation of $\overline{(kR')}21$, $\overline{(kR')21}$, $\overline{(kR')}31$, $\overline{(kR')31}$, (kR'o)261 and (kR'o)361

1	2	3	4	5	6	7	8	9	10	11	12	13	14	15	16
interval / 300s	$\int$input dτ	$\int$f(θ)dτ	abscissa	ordinate	10^9(kR'o) 261/WK^-4	10^9$\overline{(kR')}$ 21/WK^-4	10^9$\overline{\overline{(kR')}}$ 21/WK^-4	abscissa	ordinate	10^9(kR'o) 361/WK^-4	10^9$\overline{(kR')}$ 31/ WK^-4	10^9$\overline{\overline{(kR')}}$ 31/WK^-4			
					slope /JK^-1	10^9σ / WK^-4	10^9σ / WK^-4			slope / JK^-1	10^9σ / WK^-4	10^9σ / WK^-4			
					r	σ/(kR')21 / %	σ/(kR')21 / %			r	σ/(kR')31 / %	σ/(kR')31 / %			
142	43311.34	68272.2	-0.01368	0.63439	0.6204										
143	43001.72	67880.02	-0.01277	0.6335	340			0.18184	0.78948						
144	42692.11	67481.27	-0.01196	0.63265	0.9989			0.16568	0.78291	0.62505					
145	42382.88	67076.05	-0.01107	0.63186				0.16363	0.77621	315.2					
146	42074.4	66664.92	-0.01041	0.63113				0.15216	0.76959	0.9993					
147	41766.67	66248.84	-0.00977	0.63045		0.62069		0.1437	0.76342						
148	41459.33	65827.95	-0.00914	0.62981		4.38E-05		0.13772	0.7577		0.61884				
149	41152.34	65402.5	-0.00856	0.62922		0.00705		0.1318	0.75234		0.00256				
150	40845.72	64972.77	-0.008	0.62866				0.12683	0.74729		0.414				
151	40539.36	64539.02	-0.00749	0.62814				0.12191	0.74253						
152	40233.41	64101.61	-0.00702	0.62765				0.11704	0.73801						
153	39927.48	63660.76	-0.00656	0.62719	0.6203			0.11293	0.7338						
154	39621.31	63216.57	-0.00612	0.62676	349.5			0.10908	0.72989	0.62285					
155	39315.58	62769.33	-0.00635	0.62635	0.9997			0.10513	0.72612	324					
156	39010.34	62319.21	-0.00533	0.62598				0.10178	0.72249	0.99995					
157	38705.01	61866.38	-0.00498	0.62562				0.09835	0.71909						
158	38399.79	61411.25	-0.0047	0.62529		0.62058		0.09466	0.71587		0.62117				
159	38094.81	60954.04	-0.0044	0.62498		5.29E-05		0.09154	0.71282		0.000341				
160	37789.88	60494.83	-0.00414	0.62468		0.00853		0.08843	0.70994		0.0549				
161	37485.15	60033.7	-0.00387	0.6244				0.08568	0.70719						
162	37180.84	59570.84	-0.00365	0.62415				0.08283	0.70455						
163	36876.67	59106.3	-0.00338	0.6239				0.08054	0.70202						
164	36572.6	58640.02	-0.00316	0.62368	0.62029			0.07819	0.69961						
165	36268.8	58172.29	-0.00297	0.62347	349.4			0.07581	0.69729						
166	35964.86	57703.25	-0.00293	0.62327	0.99616			0.0736	0.6951	0.62237					
167	35660.98	57233.05	-0.00263	0.62308				0.07136	0.69302	326.3					
168	35357.26	56761.72	-0.00245	0.62291				0.06941	0.69103	0.99995					
169	35053.63	56289.24	-0.00229	0.62274		0.62043		0.06753	0.68912		0.6216				
170	34750.12	55815.8	-0.00216	0.62259		5.42E-05		0.06562	0.6873		0.0001				
171	34446.46	55341.36	-0.00199	0.62244		0.00873		0.06403	0.68556		0.161				
172	34142.84	54866.02	-0.0019	0.6223				0.06223	0.6839						
173	33839.59	54390.01	-0.00179	0.62217				0.06057	0.6823						
174	33536.29	53913.27	-0.00168	0.62204			0.62046	0.05902	0.68077			0.62089			
175							0.00013	0.05763	0.6793			0.000933			
176							0.0209					0.15			

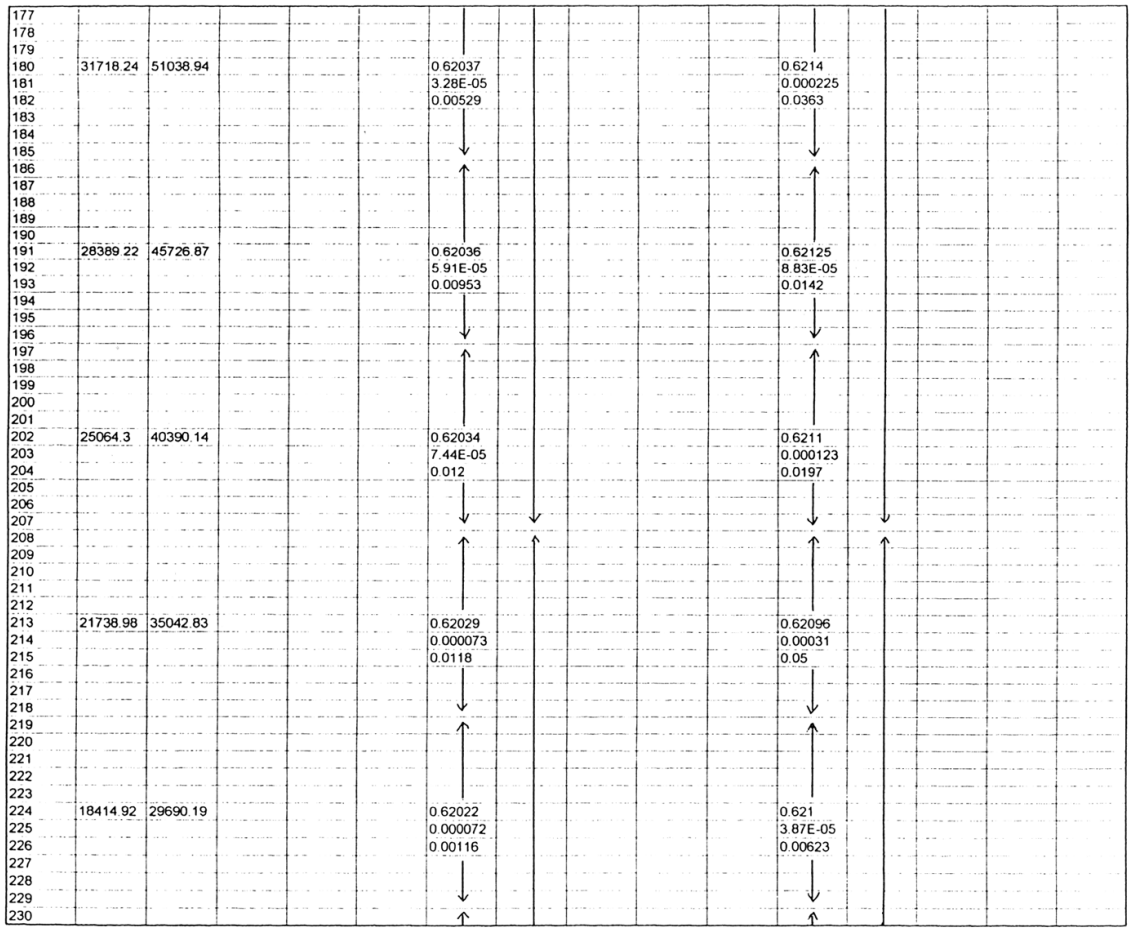
177
178
179
180 31718.24 51038.94 0.62037 3.28E-05 0.00529 0.6214 0.000225 0.0363
181
182
183
184
185
186
187
188
189
190
191 28389.22 45726.87 0.62036 5.91E-05 0.00953 0.62125 8.83E-05 0.0142
192
193
194
195
196
197
198
199
200
201
202 25064.3 40390.14 0.62034 7.44E-05 0.012 0.6211 0.000123 0.0197
203
204
205
206
207
208
209
210
211
212
213 21738.98 35042.83 0.62029 0.000073 0.0118 0.62096 0.00031 0.05
214
215
216
217
218
219
220
221
222
223
224 18414.92 29690.19 0.62022 0.000072 0.00116 0.621 3.87E-05 0.00623
225
226
227
228
229
230

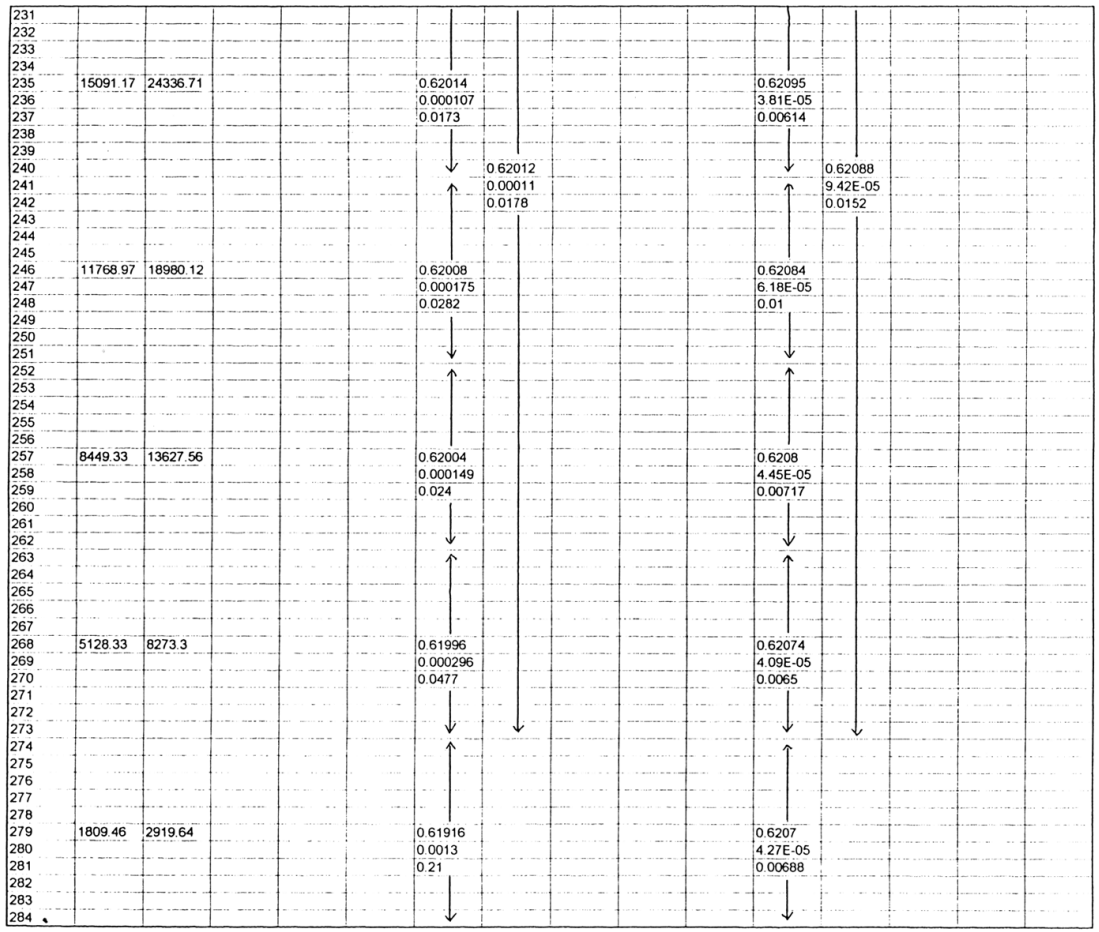
15091.17
24336.71
11768.97
18980.12
8449.33
13627.56
5128.33
8273.3
1809.46
2919.64
0.62014
0.000107
0.0173
0.62012
0.00011
0.0178
0.62008
0.000175
0.0282
0.62004
0.000149
0.024
0.61996
0.000296
0.0477
0.61916
0.0013
0.21
0.62095
3.81E-05
0.00614
0.62088
9.42E-05
0.0152
0.62084
6.18E-05
0.01
0.6208
4.45E-05
0.00717
0.62074
4.09E-05
0.0065
0.6207
4.27E-05
0.00688

Spreadsheet 9

Part of the (kR')21 spreadsheet for the region $t_1 < t < t_2$ of a measurement cycle for a "blank" experiment (Pt cathode polarised in 0.1M LiOD / D_2O)

Evaluation of $\overline{(kR')22}$, $\overline{(kR')22}$, $\overline{(kR')32}$, $\overline{\overline{(kR')32}}$, (kR'o)262 and (kR'o)362

1	2	3	4	5	6	7	8	9	10	11	12	13	14	15
interval / 300s	∫input dτ	∫f(θ)dτ	abscissa	ordinate	10^9(kR'o) 262/WK^-4	10^9$\overline{(kR')}$ 22/WK^-4	10^9$\overline{\overline{(kR')}}$ 22/WK^-4	abscissa	ordinate	10^9(kR'o) 362/WK^-4	10^9$\overline{(kR')}$ 32/WK^-4	10^9$\overline{\overline{(kR')}}$ 32/WK^-4		
					slope /JK^-1	10^9σ / WK^-4	10^9σ / WK^-4			slope /JK^-1	10^9σ / WK^-4	10^9σ / WK^-4		
					r	σ/$\overline{(kR')}$22 /%	σ/$\overline{\overline{(kR')}}$22 /%			r	σ/$\overline{(kR')}$32 /%	σ/$\overline{\overline{(kR')}}$32 /%		
142	8932.73	12849.29	-0.07271	0.69519	0.62106									
143	8864.407	12845.31	-0.06749	0.69006	338.8			17.9171	17.2513	0.68596				
144	8795.4	12834.75	-0.06289	0.68528	0.99993			9.0124	9.445	309.6				
145	8727.1	12817.71	-0.05793	0.68086				6.1976	6.5114	0.99966				
146	8659.55	12794.75	-0.05422	0.67681				4.484	5.0088					
147	8592.74	12766.84	-0.05072	0.67305		0.6224		3.5265	4.1236					
148	8526.32	12734.1	-0.04725	0.66957		0.000223		2.9224	3.5282		0.44654			
149	8460.23	12696.8	-0.04411	0.66633		0.0359		2.4802	3.0986		0.36445			
150	8394.51	12655.2	-0.04107	0.66333				2.1561	2.773		81.62			
151	8329.04	12609.58	-0.03832	0.66.53				1.89854	2.51842					
152	8263.97	12560.28	-0.03584	0.65794				1.68893	2.31405					
153	8198.91	12507.55	-0.03338	0.65552	0.62083			1.52388	2.14731					
154	8133.61	12451.46	-0.03106	0.65323	344.7			1.38617	2.0087	0.62896				
155	8068.74	12392.31	-0.02903	0.65111	0.99983			1.26596	1.89065	328.4				
156	8004.35	12330.28	-0.02695	0.64916				1.16743	1.78875	0.99998				
157	7939.87	12265.52	-0.02513	0.64733				1.07919	1.70077					
158	7875.4	12198.46	-0.02367	0.64561		0.62189		0.99791	1.62459					
159	7811.33	12129.3	-0.02212	0.64401		0.000272		0.93047	1.55752		0.62622			
160	7747.22	12058.14	-0.02077	0.64249		0.0438		0.8693	1.49846		0.00307			
161	7683.31	11985.05	-0.01939	0.64107				0.81679	1.44569		0.49			
162	7619.8	11910.22	-0.01826	0.63977				0.76752	1.39812					
163	7556.43	11833.7	-0.0169	0.63855				0.72691	1.35517					
164	7493.15	11755.44	-0.01575	0.63742	0.62086			0.68848	1.31607					
165	7430.14	11675.71	-0.01479	0.63638	343.4			0.65239	1.28035	0.62353				
166	7366.97	11594.67	-0.01384	0.63538	0.99884			0.61998	1.248	333				
167	7303.86	11512.45	-0.01307	0.63443				0.58926	1.21845	0.99996				
168	7204.9	11429.1	-0.01219	0.63355				0.56257	1.19127					
169	7178.02	11344.59	-0.01138	0.63273		0.62132		0.53778	1.16615					
170	7115.25	11259.11	-0.01073	0.63196		0.00021		0.51406	1.14294		0.62854			
171	7052.34	11172.62	-0.00987	0.63122		0.0338		0.49384	1.1215		0.00047			
172	6989.45	11085.23	-0.00938	0.63052				0.47293	1.1016		0.0748			
173	6926.92	10997.15	-0.00886	0.62988				0.454	1.08297					
174	6864.33	10908.34	-0.00832	0.62927			0.62151	0.43663	1.06566					
175	6801.65	10818.77	-0.00769	0.62869	0.62149		0.0477	0.4211	1.04952					
176	6739.21	10728.34	-0.00695	0.62817	305.7		0.0768	0.4072	1.03422					

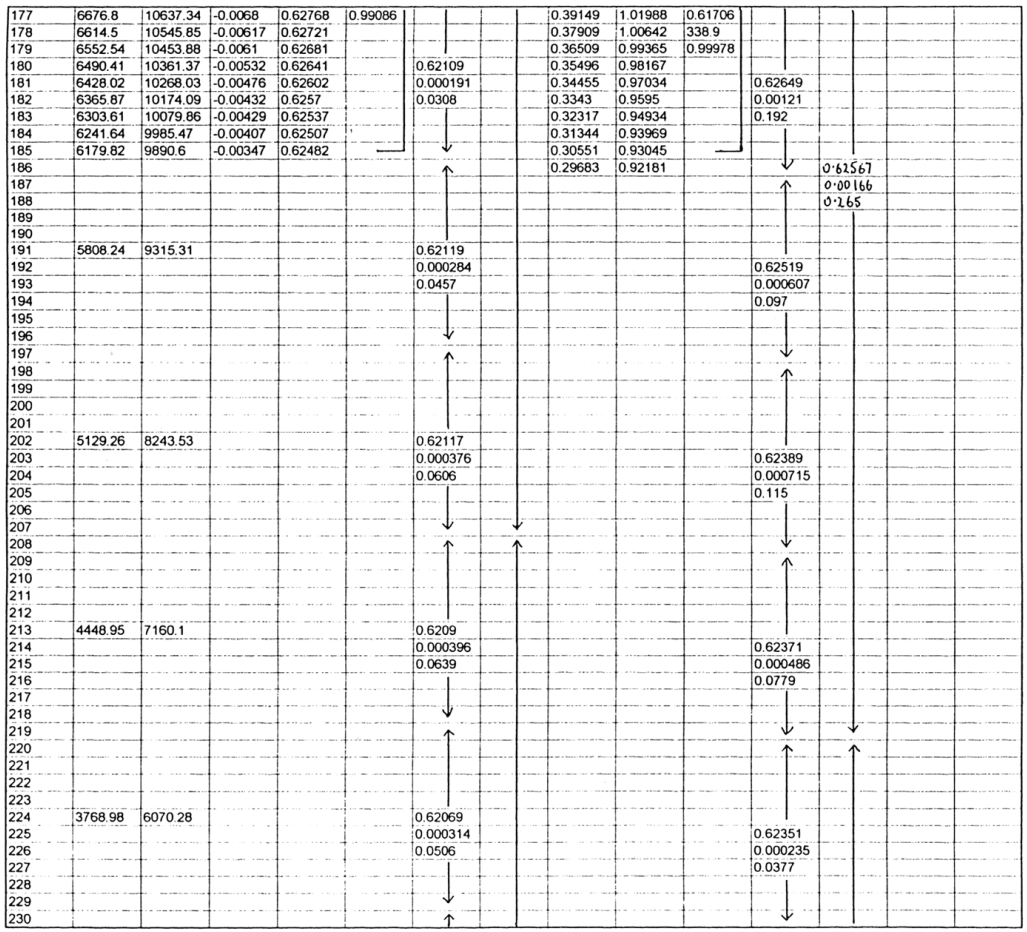

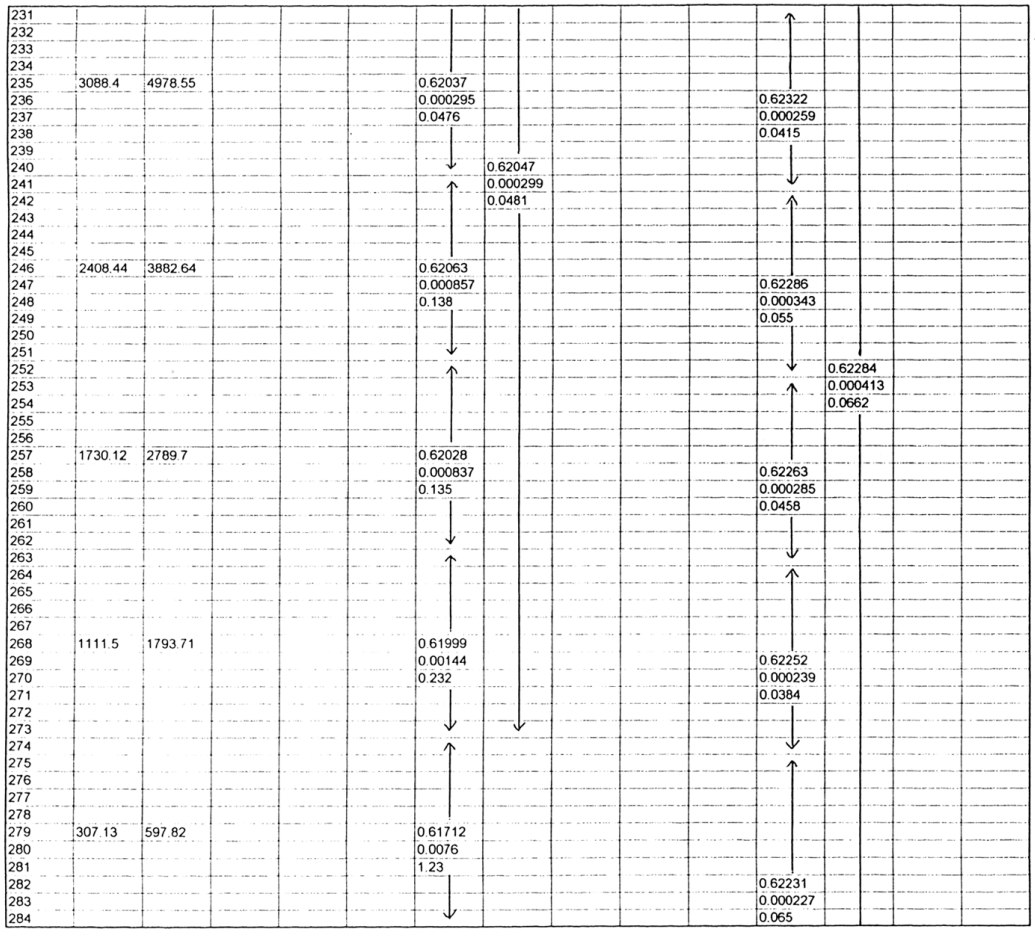
3088.4
4978.55
0.62037
0.000295
0.0476
0.62047
0.000299
0.0481
0.62322
0.000259
0.0415
2408.44
3882.64
0.62063
0.000857
0.138
0.62286
0.000343
0.055
0.62284
0.000413
0.0662
1730.12
2789.7
0.62028
0.000837
0.135
0.62263
0.000285
0.0458
1111.5
1793.71
0.61999
0.00144
0.232
0.62252
0.000239
0.0384
307.13
597.82
0.61712
0.0076
1.23
0.62231
0.000227
0.065

INITIAL DISTRIBUTION

Defense Technical Information Center
Fort Belvoir, VA 22060–6218 (4)

SSC San Diego Liaison Office
C/O PEO-SCS
Arlington, VA 22202–4804

Center for Naval Analyses
Alexandria, VA 22302–0268

Office of Naval Research
ATTN: NARDIC (Code 362)
Arlington, VA 22217–5660

Government-Industry Data Exchange
Program Operations Center
Corona, CA 91718–8000

Naval Air Warfare Center,
Weapons Division
China Lake, CA 93555–6001 (15)

Naval Research Laboratory
Washington, DC 20375–5320 (13)

Office of Naval Research
Arlington, VA 22217–5660

Professor J. O'M. Bockris
College Station, TX 77845

Research Systems, Inc.
Arlington, VA 22207

Portland State University
Portland, OR 97207–0751

Massachusetts Institute of Technology
Cambridge, MA 02139

New Energy Research Laboratory
Concord, NH 03302–2816

SRI International
Menlo Park, CA 94025

Dr. Michael Melich
Niceville, FL 32578–3018

University of Illinois
Urbana, IL 61801

The George Washington University
Washington, DC 20052

Defense Advanced Research Projects Agency
Arlington, VA 22203–1714

University of Minnesota
Minneapolis, MN 55455

U.S. Department of Energy
Germantown, MD 20874–1290

Massachusetts Institute of Technology
Cambridge, MA 02139

Stanford University
Stanford, CA 94305–6010